NUREG/CR-3391, Vol. 3
HEDL-TME 83-23

LWR PRESSURE VESSEL SURVEILLANCE DOSIMETRY IMPROVEMENT PROGRAM

1983 ANNUAL REPORT
(OCTOBER 1, 1982 - SEPTEMBER 30, 1983)

Hanford Engineering Development Laboratory

Prepared by
W.N. McElroy (HEDL)
F.B.K. Kam (ORNL)
J.A. Grundl and E.D. McGarry (NBS)
A. Fabry (CEN/SCK)

Prepared for the U.S. Nuclear Regulatory Commission

GPO Printed copy price: $6.00

NUREG/CR-3391, Vol. 3
HEDL-TME 83-23
R5

LWR PRESSURE VESSEL SURVEILLANCE DOSIMETRY IMPROVEMENT PROGRAM

1983 ANNUAL REPORT
(OCTOBER 1, 1982 - SEPTEMBER 30, 1983)

Hanford Engineering Development Laboratory

Operated by Westinghouse Hanford Company
P.O. Box 1970 Richland, WA 99352
A Subsidiary of Westinghouse Electric Corporation

Prepared by
W.N. McElroy (HEDL)
F.B.K. Kam (ORNL)
J.A. Grundl and E.D. McGarry (NBS)
A. Fabry (CEN/SCK)

Manuscript Completed: December 1983
Date Published: June 1984

Prepared for Division of Engineering Technology
Office of Nuclear Regulatory Research
U.S. Nuclear Regulatory Commission
Washington, DC 20555
NRC FIN No. B5988-7

PREVIOUS REPORTS IN LWR-PV-SDIP SERIES

NUREG/CR-0038	HEDL-TME 78-4	July 1977 - September 1977
NUREG/CR-0127	HEDL-TME 78-5	October 1977 - December 1977
NUREG/CR-0285	HEDL-TME 78-6	January 1978 - March 1978
NUREG/CR-0050	HEDL-TME 78-7	April 1978 - June 1978
NUREG/CR-0551	HEDL-TME 78-8	July 1978 - September 1978
NUREG/CR-0720	HEDL-TME 79-18	October 1978 - December 1978
NUREG/CR-1240, Vol. 1	HEDL-TME 79-41	January 1979 - March 1979
NUREG/CR-1240, Vol. 2	HEDL-TME 80-1	April 1979 - June 1979
NUREG/CR-1240, Vol. 3	HEDL-TME 80-2	July 1979 - September 1979
NUREG/CR-1240, Vol. 4	HEDL-TME 80-3	October 1979 - December 1979
NUREG/CR-1291	HEDL-SA-1949	October 1978 - September 1979*
NUREG/CR-1241, Vol. 1	HEDL-TME 80-4	January 1980 - March 1980
NUREG/CR-1241, Vol. 2	HEDL-TME 80-5	April 1980 - June 1980
NUREG/CR-1241, Vol. 3	HEDL-TME 80-6	October 1980 - December 1980
NUREG/CR-1747	HEDL-TME 80-73	October 1979 - September 1980*
NUREG/CR-2345, Vol. 1	HEDL-TME 81-33	January 1981 - March 1981
NUREG/CR-2345, Vol. 2	HEDL-TME 81-34	April 1981 - June 1981
NUREG/CP-0029	HEDL-SA-2546	October 1980 - September 1981*
NUREG/CR-2345, Vol. 4	HEDL-TME 81-36	October 1981 - December 1981
NUREG/CR-2805, Vol. 1	HEDL-TME 82-18	January 1982 - March 1982
NUREG/CR-2805, Vol. 2	HEDL-TME 82-19	April 1982 - June 1982
NUREG/CR-2805, Vol. 3	HEDL-TME 82-20	October 1981 - September 1982*
NUREG/CR-2805, Vol. 4	HEDL-TME 82-21	October 1982 - December 1982
NUREG/CR-3391, Vol. 1	HEDL-TME 83-21	January 1983 - March 1983
NUREG/CR-3391, Vol. 2	HEDL-TME 83-22	April 1983 - June 1983

*Annual Reports

FOREWORD

The Light Water Reactor Pressure Vessel Surveillance Dosimetry Improvement Program (LWR-PV-SDIP) has been established by NRC to improve, test, verify, and standardize the physics-dosimetry-metallurgy, damage correlation, and associated reactor analysis methods, procedures and data used to predict the integrated effect of neutron exposure to LWR pressure vessels and their support structures. A vigorous research effort attacking the same measurement and analysis problems exists worldwide, and strong cooperative links between the US NRC-supported activities at HEDL, ORNL, NBS, and MEA-ENSA and those supported by CEN/SCK (Mol, Belgium), EPRI (Palo Alto, USA), KFA (Jülich, Germany), and several UK laboratories have been extended to a number of other countries and laboratories. These cooperative links are strengthened by the active membership of the scientific staff from many participating countries and laboratories in the ASTM E10 Committee on Nuclear Technology and Applications. Several subcommittees of ASTM E10 are responsible for the preparation of LWR surveillance standards.

The primary objective of this multilaboratory program is to prepare an updated and improved set of physics-dosimetry-metallurgy, damage correlation, and associated reactor analysis ASTM standards for LWR pressure vessel and support structure irradiation surveillance programs. Supporting this objective are a series of analytical and experimental validation and calibration studies in "Standard, Reference, and Controlled Environment Benchmark Fields," research reactor "Test Regions," and operating power reactor "Surveillance Positions."

These studies will establish and certify the precision and accuracy of the measurement and predictive methods recommended in the ASTM Standards and used for the assessment and control of the present and end-of-life (EOL) condition of pressure vessel and support structure steels. Consistent and accurate measurement and data analysis techniques and methods, therefore, will be developed, tested and verified along with guidelines for required neutron field calculations used to correlate changes in material properties with the characteristics of the neutron radiation field. Application of established ASTM standards is expected to permit the reporting of measured materials property changes and neutron exposures to an accuracy and precision within bounds of 10 to 30%, depending on the measured metallurgical variable and neutron environment.

The assessment of the radiation-induced degradation of material properties in a power reactor requires accurate definition of the neutron field from the outer region of the reactor core to the outer boundaries of the pressure vessel. The accuracy of measurements on neutron flux and spectrum is associated with two distinct components of LWR irradiation surveillance procedures 1) proper application of calculational estimates of the neutron exposure at in- and ex-vessel surveillance positions, various locations in the vessel wall and ex-vessel support structures, and 2) understanding the relationship between material property changes in reactor vessels and their support structures, and in metallurgical test specimens irradiated in test reactors and at accelerated neutron flux positions in operating power reactors.

The first component requires verification and calibration experiments in a variety of neutron irradiation test facilities including LWR-PV mockups, power reactor surveillance positions, and related benchmark neutron fields. The benchmarks serve as a permanent reference measurement for neutron flux and fluence detection techniques, which are continually under development and widely applied by laboratories with different levels of capability. The second component requires a serious extrapolation of an observed neutron-induced mechanical property change from research reactor "Test Regions" and operating power reactor "Surveillance Positions" to locations inside the body of the pressure vessel wall and to ex-vessel support structures. The neutron flux at the vessel inner wall is up to one order of magnitude lower than at surveillance specimen positions and up to two orders of magnitude lower than for test reactor positions. At the vessel outer wall, the neutron flux is one order of magnitude or more lower than at the vessel inner wall. Further, the neutron spectrum at, within, and leaving the vessel is substantially different.

To meet reactor pressure vessel radiation monitoring requirements, a variety of neutron flux and fluence detectors are employed, most of which are passive. Each detector must be validated for application to the higher flux and harder neutron spectrum of the research reactor "Test Region" and to the lower flux and degraded neutron spectrum at "Surveillance Positions." Required detectors must respond to neutrons of various energies so that multigroup spectra can be determined with accuracy sufficient for adequate damage response estimates. Detectors being used, developed, and tested for the program include radiometric (RM) sensors, helium accumulation fluence monitor (HAFM) sensors, solid state track recorder (SSTR) sensors, and damage monitor (DM) sensors.

The necessity for pressure vessel mockup facilities for physics-dosimetry investigations and for irradiation of metallurgical specimens was recognized early in the formation of the NRC program. Experimental studies associated with high- and low-flux versions of a pressurized water reactor (PWR) pressure vessel mockup are in progress in the US, Belgium, France, and United Kingdom. The US low-flux version is known as the ORNL Poolside Critical Assembly (PCA) and the high-flux version is known as the Oak Ridge Research Reactor (ORR) Poolside Facility (PSF), both located at Oak Ridge, Tennessee. As specialized benchmarks, these facilities provide well-characterized neutron environments where active and passive neutron dosimetry, various types of LWR-PV and support structure neutron field calculations, and temperature-controlled metallurgical specimen exposures are brought together.

The two key low-flux pressure vessel mockups in Europe are known as the Mol-Belgium-VENUS and Winfrith-United Kingdom-NESDIP facilities. The VENUS Facility is being used for PWR core source and azimuthal lead factor studies, while NESDIP is being used for PWR cavity and azimuthal lead factor studies. A third and important low-fluence pressure vessel mockup in Europe is identified with a French PV-simulator at the periphery of the Triton reactor. It served as the irradiation facility for the DOMPAC dosimetry experiment for studying surveillance capsule perturbations and through-PV-wall radial fluence and damage profiles (gradients) for PWRs of the Fessenheim 1 type.

- Results of measurement and calculational strategies outlined here will be made available for use by the nuclear industry as ASTM standards. Federal Regulation 10 CFR 50 (Cf83) already requires adherence to several ASTM standards that establish a surveillance program for each power reactor and incorporate metallurgical specimens, physics-dosimetry flux-fluence monitors, and neutron field evaluation. Revised and new standards in preparation will be carefully updated, flexible, and, above all, consistent.

CONTRIBUTORS LWR-PV-SDIP 1983 ANNUAL REPORT

Prepared by W. N. McElroy, F. B. K. Kam, J. A. Grundl, E. D. McGarry, and A. Fabry with reference to and/or use of selected contributions from the following participants and laboratories:

W. N. McElroy, L. D. Blackburn, R. Gold, G. L. Guthrie,
L. S. Kellogg, E. P. Lippincott, W. Y. Matsumoto,
J. P. McNeese, C. C. Preston, J. H. Roberts, F. H. Ruddy,
J. M. Ruggles, F. A. Schmittroth, R. L. Simons, and J. A. Ulseth
Hanford Engineering Development Laboratory (HEDL), USA

E. D. McGarry, C. M. Eisenhauer, D. M. Gilliam,
J. A. Grundl, and G. P. Lamaze,
National Bureau of Standards (NBS), USA

F. B. K. Kam, C. A. Baldwin, R. E. Maerker, F. W. Stallmann, and M. Williams
Oak Ridge National Laboratory (ORNL), USA

A. Fabry, J. Debrue, G. DeLeeuw, S. DeLeeuw, G. Minsart,
H. Tourwé, and Ph. Van Asbroeck
Centre d'Etudes de l'Energie Nucleaire,
Studiecentrum voor Kernenergie (CEN/SCK), Mol, Belgium

W. Schneider, D. Packur, and L. Weise
Kernforschungsanlage (KFA) Jülich, Federal Republic of Germany

M. Austin, A. F. Thomas, and T. J. Williams
Rolls-Royce & Associates Limited (RR&A), Derby, UK

A. J. Fudge (Harwell) and J. Butler (Winfrith)
Atomic Energy Research Establishment (AERE), Harwell, UK

A. A. Alberman and J. P. Genthon (Saclay) and P. Mas (Grenoble)
Commissariat a l'Energie Atomique,
Centre d'Etudes Nucleaires (CEA/CEN), France

H. Farrar IV and B. L. Oliver
Rockwell International (RI), USA

W. H. Zimmer
EG&G ORTEC, USA

G. R. Odette and G. Lucas
University of California at Santa Barbara (UCSB), USA

P. D. Hedgecock
APTECH Engineering Services, USA

J. S. Perrin and R. A. Wullaert
Fracture Control Corporation (FCC), USA

B. A. Magurno and J. F. Carew
Brookhaven National Laboratory (BNL), USA

T. U. Marston, O. Ozer, T. Passell, and R. Shaw
Electric Power Research Institute (EPRI), USA

C. O. Cogburn, L. West, and J. Williams
University of Arkansas (UA), USA

W. C. Hopkins
Bechtel Power Corporation, USA

M. Haas
Engineering Services Associates (ENSA), USA

J. R. Hawthorne
Materials Engineering Associates (MEA), USA

E. B. Norris
Southwest Research Institute (SWRI), USA

M. P. Manahan
Battelle Memorial Institute (BMI) Columbus Laboratory, USA

S. L. Anderson, T. R. Mager, and S. E. Yanichko
Westinghouse Electric Corporation (W), USA

A. A. Lowe Jr, R. H. Lewis, and C. L. Whitmarsh
Babcock & Wilcox Company (B&W), USA

G. C. Martin Jr
General Electric Company (GE), USA

G. P. Cavanaugh, S. T. Byrnes, and J. J. Koziol
Combustion Engineering, Inc. (CE), USA

N. Tsoulfanidis and D. R. Edwards
University of Missouri, Rolla (UMR), USA

S. Grant
Carolina Power and Light Company, USA

H. F. Jones
Maine Yankee Atomic Power Company, USA

F. Hegedus
Swiss Federal Institute for Reactor Research (EIR),
Wuerenlingen, Switzerland

NUREG/CR-3391, Vol. 3
HEDL-TME 83-23
R5

LWR PRESSURE VESSEL SURVEILLANCE DOSIMETRY IMPROVEMENT PROGRAM

1983 ANNUAL REPORT

W. N. McElroy (HEDL)
J. A. Grundl (NBS)
E. D. McGarry (NBS)
F. B. Kam (ORNL)
A. Fabry (CEN/SCK)

ABSTRACT

This report describes progress made in the Light Water Reactor Pressure Vessel Surveillance Dosimetry Improvement Program (LWR-PV-SDIP) during FY 1983. The primary concern of this program is to improve, test, verify, and standardize the physics-dosimetry-metallurgy and the associated reactor and damage analysis procedures and data used for predicting the integrated effects of neutron exposure to LWR pressure vessels and support structures. These procedures and data are being recommended in a new and updated set of ASTM standards being prepared, tested, and verified by program participants. These standards, together with parts of the US Code of Federal Regulations and ASME codes, are needed and used for the assessment and control of the condition of LWR pressure vessels and support structures during the 30- to 60-year lifetime of a nuclear power plant.

ACKNOWLEDGMENTS

The success of the LWR Pressure Vessel Surveillance Dosimetry Improvement Program (LWR-PV-SDIP) continues to depend on the efforts and the free exchange of ideas and views by representatives of a large number of research, service, regulatory, vendor, architect/engineer, and utility organizations. The information reported herein could not have been developed without the continuing support of the respective funding organizations and their management and technical staffs. Special acknowledgment is due to C. Z. Serpan of NRC for having identified the need for an international program such as the LWR-PV-SDIP and for making it possible by taking a strong overall support and management lead.

Additional acknowledgment is due to D. G. Doran, B. R. Hayward, R. L. Knecht, W. F. Sheely, and H. H. Yoshikawa of HEDL for their constructive comments and help in the preparation and review of program documentation. Very special acknowledgment is given to N. E. Kenny and J. M. Dahlke who edited this document, and to the HEDL Publications Services, Word Processing, Graphics, and Duplicating personnel who contributed to its preparation.

CONTENTS

CONTENTS (Cont'd)

CONTENTS (Cont'd)

CONTENTS (Cont'd)

FIGURES

FIGURES (Cont'd)

FIGURES (Cont'd)

FIGURES (Cont'd)

FIGURES (Cont'd)

TABLES

TABLES (Cont'd)

ACRONYMS

ADC	Analog-Digital Converter
AEEW	Atomic Energy Establishment (Winfrith, UK)
AERE	Atomic Energy Research Establishment
ANO-1,-2	Arkansas Nuclear One, Units 1 and 2 PWR Nuclear Power Plants
AOTS	Argonne Optical Track Scanner
ASEM	Automated Scanning Electron Microscope
ASME	American Society of Mechanical Engineers
ASPIS	Generic LWR Benchmark "Cave" Facility (Winfrith, UK)
ASTM	American Society for Testing and Materials
B&W	Babcock & Wilcox
BMI	Battelle Memorial Institute
BNL	Brookhaven National Laboratory
BR-2	Belgium Test Reactor
BR-3	Belgium PWR Nuclear Power Plant
BSR	Bulk Shielding Reactor
BWR	Boiling Water Reactor
C/E	Calculated to Experimental
CE	Combustion Engineering
CEA/CEN	Centre d'Etudes Nucleaires (Saclay and Grenoble, France)
CEN/SCK	Centre d'Etudes de l'Energie Nucleaire (Mol, Belgium)
CFR	Code of Federal Regulation
CR	Crystal River PWR Nuclear Power Plant
DB	Davis-Besse PWR Nuclear Power Plant
DBTT	Ductile-Brittle Transition Temperature
DIDO	UK Test Reactor
DM	Damage Monitor
DMA	Direct Memory Access
DOMPAC	Triton Reactor Thermal Shield and Pressure Vessel Mockup
DPA	Displacements Per Atom
EBR-II	Experimental Breeder Reactor II
EFPY	Effective Full-Power Years
ENDF	Evaluated Nuclear Data File

ACRONYMS (Cont'd)

ENSA	Engineering Services Associates
EOL	End of Life
EPRI	Electric Power Research Institute
ESP	Emulsion Scanning Processor
ETZ	Extrapolation to Zero
EWGRD	EURATOM Working Group on Reactor Dosimetry
FBR	Fast Breeder Reactor
FC	Fission Chamber
FCC	Fracture Control Corporation
FRJ 1	German Test Reactor
FRJ 2	German Test Reactor
FSAR	Final Safety Analysis Report
GE	General Electric
HAFM	Helium Accumulation Fluence Monitor
HEDL	Hanford Engineering Development Laboratory
HERALD	UK Test Reactor
HOTS	Hanford Optical Track Scanner
HSST	Heavy Section Steel Technology (Program)
IAEA	International Atomic Energy Agency
KFA	Kernforschungsanlage (Jülich, Germany)
LWR	Light Water Reactor
MATSURV	NRC Computerized Reactor Pressure Vessel Materials Information System
MEA	Materials Engineering Associates, Inc.
MFR	Magnetic Fusion Reactor
MPC	Materials Property Council, Subcommittee 6 on Nuclear Materials
MTR	Materials Test Reactor
NBS	National Bureau of Standards
NDTT	Nil Ductility Transition Temperature
NESDIP	NESTOR Dosimetry Improvement Program
NESSUS	Facility (Winfrith, UK)
NESTOR	PWR Mockup Reactor (Winfrith, UK)

NRC	Nuclear Regulatory Commission
NRE	Nuclear Research Emulsion
NSTF	Nuclear Science and Technology Facilities (Buffalo, NY)
NUREG	Nuclear Regulatory Report Prefix
OCA	Overcooling Accident
ORNL	Oak Ridge National Laboratory
ORR	Oak Ridge Research Reactor (ORNL)
PCA	Poolside Critical Assembly (ORNL)
PCBT	PV-Simulator, "Emplacement Special" Position in Melusine Reactor (Grenoble, France)
PSF	Poolside Facility (ORNL)
PTS	Pressurized Thermal Shock
PV	Pressure Vessel
PVF	Pressure Vessel Front
PVS	Pressure Vessel Simulator (includes both SPVC and SVBC)
PWR	Pressurized Water Reactor
QA	Quality Assurance
RI	Rockwell International
RIL	Research Information Letter
RM	Radiometric Monitors
RPV	Reactor Pressure Vessel
RR&A	Rolls-Royce & Associates Limited (UK)
RT_{NDT}	Reference Nil Ductility Transition Temperature
RT_{NDT}	Initial Unirradiated Value of RT_{NDT}
SDIP	Surveillance Dosimetry Improvement Program
SDMF	Simulated Dosimetry Measurement Facility
SEM	Scanning Electron Microscope
SPVC	Simulated Pressure Vessel Capsule
SRM	Standard Reference Material
SS	Stainless Steel
SSC	Simulated Surveillance Capsule
SSTR	Solid State Track Recorder

ACRONYMS (Cont'd)

SUNY-NSTF	State University of New York-Nuclear Science Technology Facilities (Buffalo, NY)
SVBC	Simulated Void Box Capsule
TLD	Thermoluminescent Dosimeter
TM	Temperature Monitor
TSB	Thermal Shield Back
UA	University of Arkansas
UCSB	University of California (Santa Barbara, CA)
UK	United Kingdom
UMR	University of Missouri (Rolla, MO)
VENUS	PWR Critical Mockup Facility (Mol, Belgium)
WEC (or W)	Westinghouse Electric Corporation
WRSR	Water Reactor Safety Research

LWR PRESSURE VESSEL SURVEILLANCE DOSIMETRY IMPROVEMENT PROGRAM
1983 ANNUAL REPORT

1.0 INTRODUCTION

Light water reactor pressure vessels (LWR-PV) are accumulating significant neutron fluence exposures, with consequent changes in their steel fracture toughness and embrittlement characteristics. Recognizing that accurate and validated measurement and data analysis procedures are needed to periodically evaluate the metallurgical condition of these reactor vessels, the US Nuclear Regulatory Commission (NRC) has established the LWR Pressure Vessel Surveillance Dosimetry Improvement Program (LWR-PV-SDIP). The primary concerns of this program are to improve, test, verify, and standardize: 1) physics-dosimetry-metallurgy, 2) damage correlation, and 3) associated reactor analysis methods, procedures and data used for predicting the integrated effects of neutron exposure to LWR pressure vessels and support structures, see Figure 1.1.

A vigorous research effort attacking the same measurement and analysis problems exists worldwide, and strong cooperative links between the US NRC-supported activities at HEDL, ORNL, NBS and MEA-ENSA and those supported by CEN/SCK (Mol, Belgium), EPRI (Palo Alto, USA), KFA (Jülich, Germany) and several UK laboratories have been extended to a number of other countries and laboratories. (A current listing to the literature of documents most relevent to LWR-PV-SDIP interlaboratory efforts up to early 1984 is provided in Section 3.0, Bibliography.) These cooperative links have been strengthened by the active membership of the scientific staff of many of the participating countries and laboratories in the ASTM E10 Committee on Nuclear Technology and Applications (He82). Several subcommittees of ASTM E10 are responsible for the preparation of LWR pressure vessel and support structure surveillance standards. Figures 1.2 and 1.3 summarize the status of the preparation of LWR-ASTM standards and their supporting documentation. Summary information on LWR-PV-SDIP FY 1983 research results is provided in Section 2.0.

The major benefit of this program will be a significant improvement in the accuracy of the assessment and control of the present and end-of-life (EOL) condition of light water reactor pressure vessels and their support structures. A primary objective of this multilaboratory program is to prepare an updated and improved set of physics-dosimetry-metallurgy, damage correlation, and the associated reactor analysis ASTM standards for LWR pressure vessel and support structure surveillance programs, as described in Section 2.1.1. Supporting this objective are a series of analytical and experimental verification and calibration studies in "Benchmark Neutron Fields," research reactor "Test Regions," and operating power reactor "Surveillance Positions." As discussed in Sections 2.2 through 2.6, these studies will establish and certify the precision and accuracy of the measurement and predictive methods recommended for use in the ASTM standards. Consistent and accurate measurement and data analysis techniques and methods, therefore, will have been developed, tested, and verified along with guidelines for required neutron

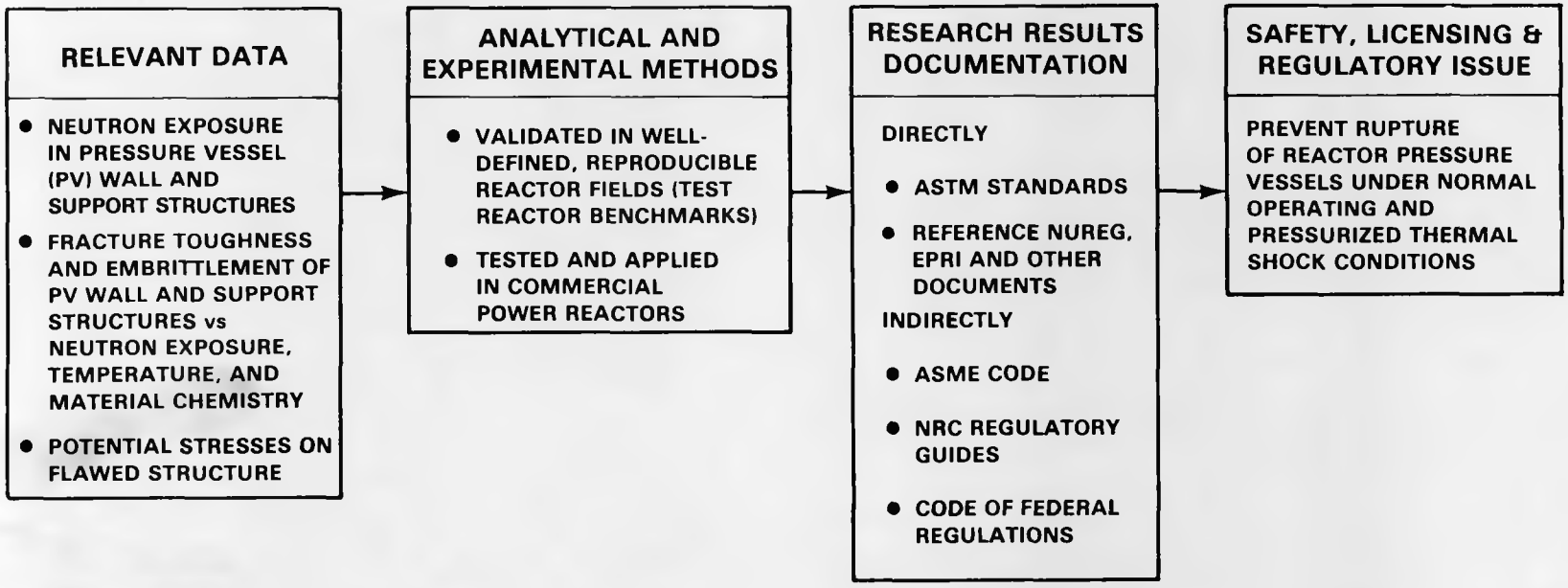

FIGURE 1.1. Relationship of Physics-Dosimetry-Metallurgy Aspects of the LWR-PV-SDIP to the Assessment of the Integrity of Reactor Pressure Vessels and Their Support Structures.

FIGURE 1.2. Status of ASTM Surveillance Standards for Pressure Vessels and Their Support Structures.

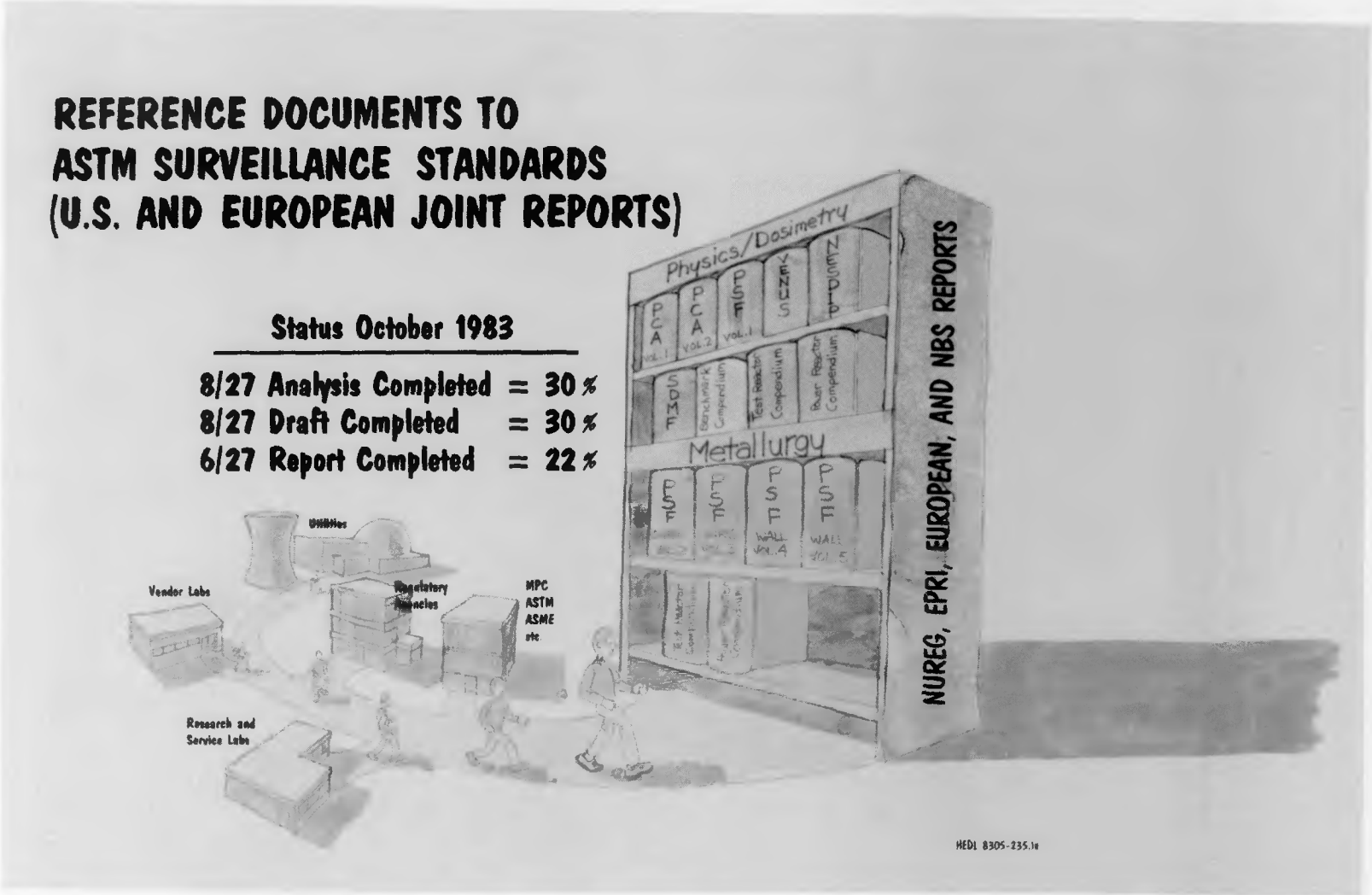

FIGURE 1.3. Reference Documents to ASTM Surveillance Standards (U.S. and European Joint Reports). Neg 8308980-1

field physics-dosimetry-metallurgy calculations. Based on nuclear power plant operational, safety, licensing, and regulatory requirements, these calculations are then used 1) to correlate changes in material properties with the characteristics of the neutron radiation field and 2) to predict the present and EOL condition of pressure vessel and support structure steels from both power and research reactor data.

2.0 SUMMARY OF FY 1983 RESEARCH PROGRESS

To account for neutron radiation damage in setting pressure-temperature limits and making fracture analyses (see appropriate references in Section 3.0) neutron-induced changes in reactor pressure vessel (PV) steel fracture toughness and embrittlement must be predicted, then checked by extrapolation of surveillance program data during the vessel's service life. Uncertainties in the predicting methodology can be significant. The main variables of concern are associated with:

- Steel chemical composition and microstructure
- Steel irradiation temperature
- Power plant configurations and dimensions - core edge to surveillance to vessel wall to support structure positions
- Core power distribution
- Reactor operating history
- Reactor physics computations
- Selection of neutron exposure units
- Dosimetry measurements
- Neutron spectral effects
- Neutron dose rate effects

Variables associated with the physical measurements of PV steel property changes are not considered here and are addressed separately in Appendices G and H of 10 CFR Part 50 (Cf83), in ASTM Standards, and appropriate references in Section 3.0.

The US NRC has estimated that without remedial action, there are a number of operating early-generation US pressurized water reactors (PWR) that could have beltline materials with marginal toughness, relative to the existing requirements of Appendices G and H and Regulatory Guide 1.99 (Re77), sometime within their presently licensed service life (Nr80); i.e., in the range up to about 32 years. This is of particular concern for safety, licensing, and regulatory issues related to pressurized thermal shock (PTS) (Di82).

As older vessels become more highly irradiated, the predictive capability for changes in fracture toughness and embrittlement must improve, particularly for plants operated beyond their current design service life, i.e., in the range above about 32 years. Since during the vessel's service life an increasing amount of information will be available from research reactor tests and power reactor surveillance programs, better procedures to evaluate and use this information can and must be developed. The most appropriate way to make information available on these procedures is through voluntary consensus standards, such as those now being developed by ASTM Committee E10 on Nuclear Technology and Applications (As82,As83,He82) discussed here and in Section 2.1.

Important summary highlights of FY 1983 research activities of this multilaboratory program are:

- The completion of first, revised, or final drafts (Figures 2.1 and 2.2) of 18 of 21 ASTM standards that focus on the physics-dosimetry-metallurgy, damage correlation, and the associated reactor analysis and interpretation aspects of the problem of guaranteeing the safety and integrity of the pressure vessel boundary and its support structures for LWR power reactors (see Section 2.1.1) (As82,As83).

- The initiation and completion of important supporting verification and calibration benchmark studies, reviews, as well as neutron and gamma field experimental and calculational work (see Tables 2.26 and 2.27 and Sections 2.2, 2.3, and 2.4), which demonstrate and verify the direct applicability of the recommended procedures and data in the 21 ASTM standards (1 "master matrix," 9 "practices," 6 "guides," and 5 "methods"), see Sections 2.2, 2.3, 2.4, and 2.5. Of particular interest here was 1) the continuation of studies on fuel management effects and neutron exposure parameters and their impact relative to the assessment and control of the present and EOL condition of pressure vessel and support structure steels (Au83,Ch82,Ch83,Di82,Gu82,Gu82a, Nr82) and 2) the continued planning and implementation of verification tests in H. B. Robinson, Maine Yankee, Crystal River (or Davis Besse), Arkansas-1 and Arkansas-2 (see Table 2.2).

- The completion of the analysis of key experimental physics-dosimetry studies associated with the ORNL-PCA low-flux version of a PWR pressure vessel mockup and the continuation of work associated with the VENUS and NESDIP mockups (Table 2.26), in Belgium and the UK, respectively (see Sections 2.2, 2.4.4, 2.5.1.1, and 2.5.1.2).

- The successful completion of the 2 years of irradiations and preliminary testing and analyses for the Oak Ridge Research Reactor (ORR) simulated surveillance capsule (SSC), simulated pressure vessel capsule (SPVC) and simulated void box capsule (SVBC) LWR power plant physics-dosimetry-metallurgy experiments (see Section 2.3). Associated with this was the successful implementation of an international physics-dosimetry-metallurgy "PSF Blind Test."

- The completion of required studies associated with the evaluation and reevaluation of exposure units and values for existing and new metallurgical data bases (NRC, MPC, EPRI, ASTM, and others), see Section 2.4.1. The initial power reactor studies have involved the reanalysis of data from 42 PWR surveillance capsule reports for Westinghouse, Babcock and Wilcox, and Combustion Engineering power plants. Using a consistent set of auxiliary data and dosimetry-adjusted reactor physics results, the revised fluence values for $E > 1$ MeV averaged 27% higher than the originally reported values. The range of fluence values (new/old) was from a low of 0.80 to a high of 2.38, see Table 2.11, and Reference (Si82a). The research reactor studies have involved the reanalysis of data originally reported by NRL and HEDL, see Section 2.4.2, and the analysis of the results of a new test reactor (SUNY-NSTF) "chemical variables" experiment by MEA-ENSA and HEDL.

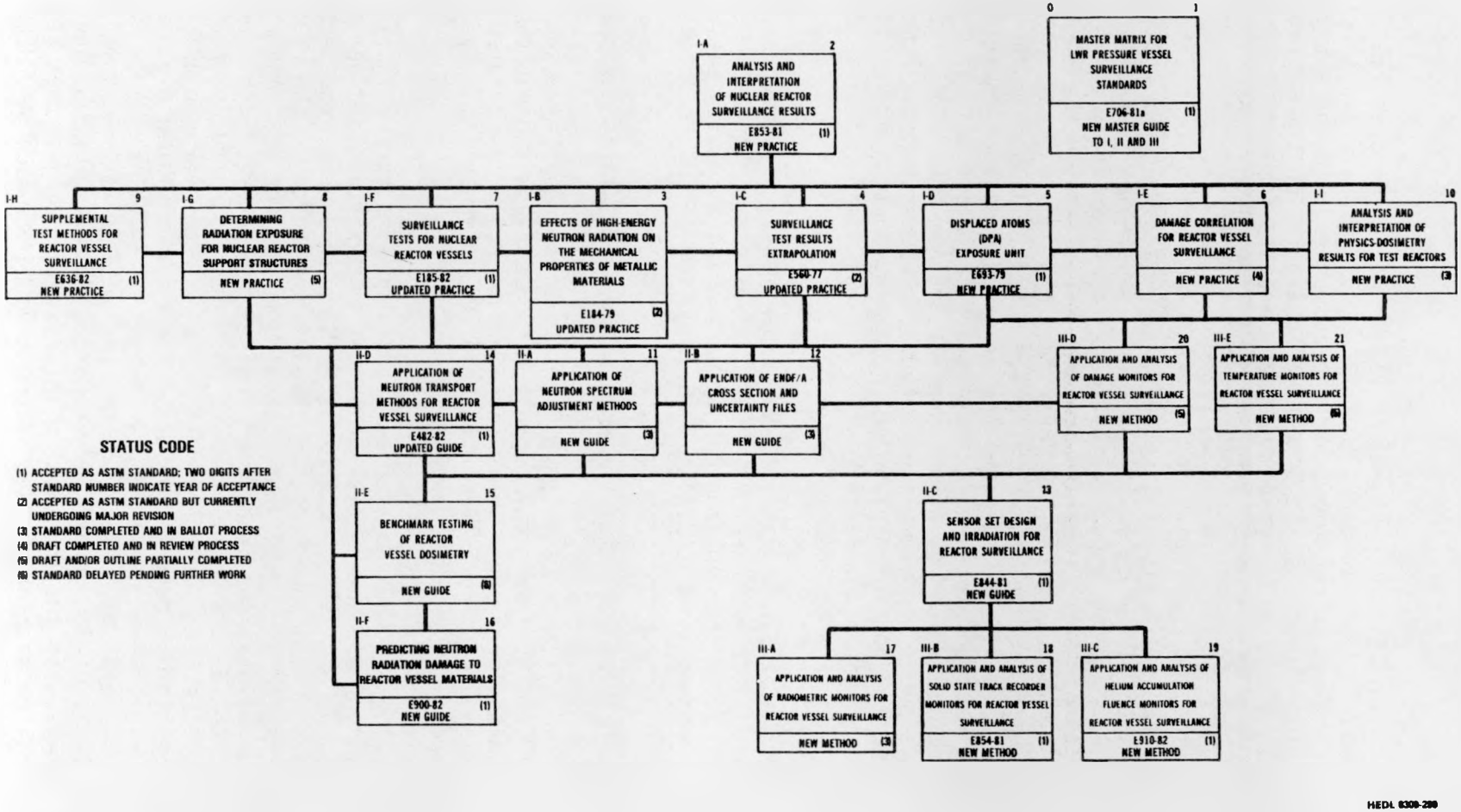

FIGURE 2.1. ASTM Standards for Surveillance of LWR Nuclear Reactor Pressure Vessels and Their Support Structures.

FIGURE 2.2. Preparation, Validation, and Calibration Schedule for LWR Nuclear Reactor Pressure Vessels and Their Support Structure Surveillance Standards.

- The completion of required studies associated with the data development and testing for new trend curves for the ΔRT_{NDT} shift versus neutron exposure (fluence E > 1.0 MeV and dpa) for an NRC selected power reactor surveillance capsule data base of up to 177 points, see Section 2.4.1 and References (Gu82,Gu82b,Gu82c,Gu83,Gu83a,Gu84). The status of EPRI-supported program work related to physics-dosimetry-metallurgy data development and testing is provided in References (Mc82c,Od78,Od79,Od83, Pe84,Va81,Va82,Va83).

  Of particular interest here is the establishment and application of new ΔRT_{NDT} versus fluence and dpa curves for use by R. Randall of NRC in the issuance of a 1984 Revision of Regulatory Guide 1.99 (Re77).

- A new development is the establishment of a trend curve that contains a term to account for possible thermal neutron effects; the implications of this are discussed in Sections 2.4.1.1 through 2.4.1.3 and in References (Gu84a,Mc84e). The impact of this work could be quite important for future revisions of Reg. Guide 1.99 and licensing and regulatory issues and actions related to the new NRC screening criteria requirements associated with pressurized thermal shock.

- The completion of the planning work and preparation of abstracts of papers for the Fifth ASTM-EURATOM International Symposium on Reactor Dosimetry to be held at Geesthacht, Republic of West Germany in September 1984 and the preparation and presentation of a series of LWR-PV-SDIP-related papers at the NRC 11th WRSR Information Meeting in October 1983.

2.1 ASTM STANDARDS AND PROGRAM DOCUMENTATION

2.1.1 ASTM Standards

Figures 2.1 and 2.2 provide information on the interrelationships and current schedule for the preparation and acceptance of the set of 21 ASTM standards. Results of ASTM balloting for these standards were discussed at the June 1983 Colorado Springs, CO and the January 1984 San Diego, CA ASTM E10 meetings. Figures 2.1 and 2.2 will be updated next at the June 1984 Williamsburg, VA meeting and will be reviewed by the ASTM E10.05 Nuclear Radiation Metrology and E10.02 Metallurgy Subcommittee members to coordinate the preparation, balloting, testing, and acceptance of the entire set of standards. Reference (As83) provides additional information related to the scope, content, and preparation of most of these standards. More detailed, but summary information on the status of the preparation of the individual standards follows:

E706(0) Master Matrix Guide

Lead Authors	W. McElroy (E10.05)* and P. Hedgecock (E10.02)*
Participants	Lead authors of all Practices (I), Guides (II), and Methods (III)
Status	This standard is in place in the 1983 Annual Book of Standards as E706-81a. The entire standard, scope, and discussion sections have been reviewed and updated. The revised standard was successfully balloted at the E10 level.

E706(IA) Analysis and Interpretation of Reactor Surveillance Results

Lead Authors	S. Anderson and W. McElroy (E10.05)
Status	This standard has been reviewed and updated and was successfully balloted at the E10 level.

E706(IB) Effects of High-Energy Neutron Radiation on the Mechanical Properties of Metallic Materials

Lead Authors	J. Beeston (E10.02); E. Norris, and H. Farrar (E10.05)
Status	E184-79 is on the books. E. Norris and W. McElroy updated the physics-dosimetry parts of the standard for the San Diego meeting. A title change for the standard to "Recommended Physics-Dosimetry-Metallurgy Interface Standard for LWR, FBR, and MFR Development Programs," as well as some revisions to the text were balloted at the E10.02 and E10.05 levels. As a result of this ballot and discussions at San Diego, it is now planned to reballot the standard for removal since specific users of the standard could not be identified.

*P. D. Hedgecock and W. N. McElroy are the current chairmen of the E10.02 and E10.05 Subcommittees, respectively, of the ASTM E10 Committee. The current chairman of the ASTM E10 Committee is J. Perrin.

E706(IC) Surveillance Test Results Extrapolation

Lead Authors: G. Guthrie and W. N. McElroy (E10.05); S. Byrne (E10.02)

Status: This standard has been reviewed and updated and was successfully balloted at the E10 level. This practice has been given the number E560 by ASTM, which is the number of the present standard (E560-77) that it will replace. Information on physics-dosimetry-metallurgy studies from test and power reactor benchmark studies supporting the preparation of this standard are provided in subsequent sections of the annual report.

E706(ID) Displaced Atom (dpa) Exposure Unit

Lead Authors: D. Doran, E. Lippincott, and W. N. McElroy (E10.05)

Status: This standard appears in the 1983 Annual Book of Standards as E693-79. The need exists to update the basic nuclear data, i.e., using ENDF/B-V data and comparing the results with those obtained using ENDF/B-IV data. More complete and detailed information on the testing and application of the dpa exposure unit is provided in a Research Information Letter (RIL) on "An Improved Damage Exposure Unit, dpa, for LWR Pressure Vessel and Support Structure Surveillance," which was prepared for NRC in August 1982 [see Reference (Mc82a)]. An ASTM news release on the results of an MPC ad hoc task group meeting on the use of dpa as an exposure unit for PV surveillance stated: "Task group members have concluded that both fluence (E > 1.0 MeV) and dpa can and should be used for the foreseeable future, until such time as the fluence (E > 1.0 MeV) is totally outmoded and no longer necessary because of appropriate standards for dpa."

E706(IE) Damage Correlation for Reactor Vessel Surveillance

Lead Authors: G. Guthrie (E10.05) and P. Hedgecock (E10.02)

Status: A draft of this standard has been prepared and requires further revision, which is dependent on the analysis of physics-dosimetry-metallurgy results from test and power reactor benchmarking studies in progress and discussed in subsequent sections of the annual report.

E706(IF) Surveillance Tests for Nuclear Reactor Vessels

Lead Authors: P. Hedgecock (E10.02) and C. Whitmarsh (E10.05)

Status: This standard appears in the 1983 Annual Book of Standards as E185-82. An update on physics-dosimetry is needed in 1984. The reader is referred to ASTM E853-81 for information on needed changes in this key ASTM standard, which is used for establishing a physics-dosimetry-metallurgy surveillance program for each operating LWR nuclear power plant.

E706(IG) Determining Radiation Exposure for Nuclear Reactor Support Structures

Lead Authors W. Hopkins (E10.05) and P. Hedgecock (E10.02)
Status A draft of the standard was distributed for discussion at the San Diego meeting. Appropriate revisions were made, and the standard will be balloted at the E10.05 and E10.02 levels for the June 1984 meeting in Williamsburg, VA.

E706(IH) Supplemental Test Methods for Reactor Vessel Surveillance

Lead Authors R. Hawthorne (E10.02) and E. Norris (E10.05)
Status This standard appears in the 1983 Annual Book of Standards as E636-83.

E706(II) Analysis and Interpretation of Physics Dosimetry Results for Test Reactors

Lead Authors F. Kam, F. Stallmann, and M. Williams (E10.05)
Status This standard was successfully balloted at the E10 level. Summary information on NRC-supported US test reactor physics-dosimetry-metallurgy program studies is provided in Sections 2.2, 2.3, and 2.4 of the annual report. Information on other program studies is provided in appropriate references in Section 3.0.

E706(IIA) Application of Spectrum Adjustment Methods

Lead Author F. Stallman (E10.05)
Status This standard appears in the 1983 Annual Book of Standards as E944-83.

E706(IIB) Application of ENDF/A Cross-Section and Uncertainty File

Lead Authors E. Lippincott and W. McElroy (E10.05)
Status This standard was successfully balloted, with appropriate editorial changes, at the E10 level.

It is anticipated that the first version of the ENDF/A file will be issued in 1984. It is apparent that the ENDF/B format may not be the most appropriate for tabulation of all the covariance data, so it may be desirable to put the data in a more appropriate format and supply a simple processing code to read the file. This will depend on the amount of covariance data to be included.

A paper on the ENDF/A file and ASTM Standard was presented for the Fourth ASTM-EURATOM Symposium (Li82); another paper (Sc83) discusses the benefits and limitations of using adjusted (or benchmarked) cross sections in neutron spectrum unfolding; and Reference (As82) provides additional information on the scope of the E706(IIB) Standard.

E706(IIC) Sensor Set Design and Irradiation for Reactor Surveillance

Lead Authors: G. Martin and E. Lippincott (E10.05)
Status: This standard appears in the 1983 Annual Book of Standards as E844-81.

E706(IID) Application of Neutron Transport Methods for Reactor Vessel Surveillance

Lead Authors: L. Miller and R. Maerker (E10.05)
Status: This standard appears in the 1983 Annual Book of Standards as E482-82.

E706(IIE) Benchmark Testing of Reactor Vessel Dosimetry

Lead Authors: E. McGarry and G. Grundl (E10.05)
Status: A first draft of this standard is to be submitted at the June 1984 ASTM meeting. The NBS Compendium of Benchmark Neutron Fields for Reactor Dosimetry was completed by J. Grundl of NBS and will be distributed as an NBS publication.

E706E(IIF) Predicting Neutron Radiation Damage to Reactor Vessel Materials

Lead Authors: P. Hedgecock and S. Byrne (E10.02); G. Guthrie (E10.05)
Status: This standard appears in the 1983 Annual Book of Standards as E900-82. This standard is expected to be further revised to provide new trend curves based on LWR power plant surveillance results; i.e., only power reactor data will be used to establish the curves that will be recommended for assessing and controlling the condition of pressure vessels for BWR and PWR nuclear power plants. Information on existing NRC-MPC-EPRI-ASTM and other metallurgical data bases is provided in the Section 3.0, Bibliography. Information on reevaluated exposure parameter values (flux and fluence: total, thermal, $E > 1.0$ MeV; and dpa) for PWR power plant surveillance capsules is provided in (Si82a). (See Section 2.4.1 and Table 2.11.)

E706(IIIA) Analysis of Radiometric Monitors for Reactor Vessel Surveillance

Lead Authors: L. Kellogg, F. Ruddy, and W. Matsumoto (E10.05)
Status: This standard was successfully balloted at the E10 level. It makes reference to a series of other ASTM standards for the measurement of individual fission and non-fission reaction rates. The EURATOM Working Group on Reactor Dosimetry (EWGRD) is preparing a new ASTM standard for the measurement of reaction rates for the $^{93}Nb(n,n')^{93}Nb^{m}$ sensor. Results of the testing and verification of the procedures, data, and the accuracy of RM results being obtained by service laboratories in the US and Europe are presented in References (Ke82,To82,To82a).

E706(IIIB) Application and Analysis of Solid State Track Recorder (SSTR) Monitors for Reactor Vessel Surveillance

Lead Authors: R. Gold, F. Ruddy, and J. Roberts (E10.05)
Status: This standard appears in the 1983 Annual Book of Standards as E854-81. The increased application of SSTR, RM, HAFM, and DM sensors for in- and ex-vessel physics-dosimetry surveillance programs in support of the determination of the effects of old and new fuel management schemes on the present and EOL condition of pressure vessels and their support structures is discussed elsewhere (Mc82a).

E706(IIIC) Application and Analysis of Helium Accumulation Fluence Monitors (HAFM) for Reactor Vessel Surveillance

Lead Authors: H. Farrar and B. Oliver (E10.05)
Status: This standard appears in the 1983 Annual Book of Standards as E910-82.

E706(IIID) Application and Analysis of Damage Monitors (DM) for Reactor Vessel Surveillance

Lead Authors: A. Fudge, A. Fabry, and G. Guthrie (E10.05)
Status: A draft outline was submitted. The first draft of this standard has yet to be prepared, and it is expected to concentrate on the initial use of sapphire and surveillance capsule steel correlation monitor materials. This and other candidate sensor materials for test and power reactor applications are discussed in References (Al82,Au82a,De82,Fa82,Ma82b,Pe82).

E706(IIIE) Application and Analysis of Temperature Monitors for Reactor Vessel Surveillance

Lead Authors: B. Seidel (E10.02) and G. Guthrie (E10.05)
Status: A first draft of this standard has been prepared for ballot. It concentrates on the use of melt wires for PWR and BWR surveillance capsules.

2.1.2 Program Documentation

The following list of planned NRC NUREG reports is provided for reference purposes. Each document will have LWR Pressure Vessel Surveillance Dosimetry Improvement as the main title followed by individual subtitles. These documents are expected to be completed during the period September 1982 to September 1987 with subsequent annual updating of the loose-leaf documents, as required.

2.1.2.1 NUREG/CR-1861 (Issue Date: July 1981)

PCA Experiments and Blind Test
W. N. McElroy, Editor

This document provides the results of calculations and active and passive physics-dosimetry measurements for the PCA 8/7 and 12/13 configurations [X/Y: Water gaps (in cm) from the core edge to the thermal shield (X) and from the thermal shield to the vessel wall (Y)]. The focus of the document is on an international Blind Test of transport theory methods in LWR-PV applications involving eleven laboratories, including reactor vendors.

2.1.2.2 NUREG/CR-3295 (Issue Date: May 1984)

Notch Ductility and Fracture Toughness Degradation of A302-B and A533-B Reference Plate from PSF Simulated Surveillance and Through-Wall Irradiation Capsules
R. Hawthorne, Editor

Beyond scope of title, this document will support analysis of the PSF Blind Test and provide as-built documentation and final PSF A302-B and A533-B reference plate metallurgical results for SSC and SPVC.

2.1.2.3 NUREG/CR-3318 (Issue Date: May 1984)

PCA Dosimetry in Support of the PSF Physics-Dosimetry-Metallurgy Experiments (4/12, 4/12 SSC configurations and update of 8/7 and 12/13 configurations)
W. N. McElroy, Editor

Beyond scope of title, this document will support analysis of the PSF Blind Test and updates NUREG/CR-1861, "PCA Experiments and Blind Test," July 1981.

2.1.2.4 NUREG/CR-3319 (Issue Date: May 1984)

LWR Power Reactor Surveillance Physics-Dosimetry Data Base Compendium
W. N. McElroy, Editor

In loose-leaf form this document will provide new or reevaluated exposure parameter values [total, thermal, and fast (E > 1.0 MeV) fluences, dpa, etc.] for individual surveillance capsules removed from operating PWR and BWR power plants. As surveillance reports are reevaluated with FERRET-SAND, this document will be revised annually. The corresponding metallurgical data base is provided in the loose-leaf EPRI NP-2428, "Irradiated Nuclear Pressure Vessel Steel Data Base" (Mc82c).

2.1.2.5 NUREG/CR-3220
PSF Physics-Dosimetry-Metallurgy Experiments:

Vol. 1 (Issue Date: February 1985)
PSF Blind Test
W. N. McElroy and F. B. K. Kam, Editors

This document will provide summary information on the comparison of measured and predicted physics-dosimetry-metallurgy results for the PSF experiment. This document will also contain summary results of each participants' final report published in NUREG/CR-3320, Vol. 6.

Vol. 2 (Issue Date: November 1984)
PSF Startup and Simulated Surveillance Capsule (SSC) Physics-Dosimetry Program
W. N. McElroy and F. B. K. Kam, Editors

Beyond scope of title, this document will support analysis of the PSF Blind Test and provide experimental conditions, as-built documentation,and final PSF physics-dosimetry results for SSC-1 and SSC-2.

Vol. 3 (Issue Date: January 1985)
PSF Simulated Pressure Vessel Capsule (SPVC) and Simulated Void Box Capsule (SVBC) Physics-Dosimetery Program
W. N. McElroy and F. B. K. Kam, Editors

Beyond scope of title, this document will support analysis of the PSF Blind Test and provide experimental conditions, as-built documentation, and final PSF physics-dosimetry results for SPVC and SVBC.

Vol. 4 (Issue Date: June 1985)
PSF Simulated Surveillance Capsules (SCC-1 and SCC-2), Simulated Pressure Vessel Capsule (SPVC) and Simulated Void Box Capsule (SVBC) Metallurgy Program
W. N. McElroy and F. B. K. Kam, Editors

Beyond scope of title, this document will support analysis of the PSF Blind Test and provide experimental conditions, as-built documentation, and final metallurgical data on measured property changes in different pressure vessel steels for SSC-1 and -2 positions, and the (SPVC) simulated PV locations at the inner surface, 1/4 T, and 1/2 T positions of the 4/12 PWR PV wall mockup. The corresponding SSC-1, SSC-2, and SPVC locations' neutron exposures are $\sim 2 \times 10^{19}$, $\sim 4 \times 10^{19}$, $\sim 4 \times 10^{19}$,$\sim 2 \times 10^{19}$, and $\sim 1 \times 10^{19}$ n/cm^2, respectively, for a ~550°F irradiation temperature.

Vol. 5 (Issue Date: September 1984)
PSF Simulated Surveillance Capsule (SSC) Results-CEN/SCK/MEA
Ph. Van Asbroeck, A. Fabry, and R. Hawthorne, Editors

This document, to be issued by CEN/SCK, will provide CEN/SCK/MEA metallurgical data and results from the Mol, Belgium PV steel irradiated in the SSC position for the ORR-PSF physics-dosimetry-metallurgy experiments.

Vol. 6 (Issue Date: September 1986)
PSF Experiment - Recommended Physics-Dosimetry-Metallurgy Data Base and Blind Test Participants' Final Analyses
W. N. McElroy and F. B. K. Kam, Editors

This document will provide a compilation of participants' final camera-ready reports on PSF physics-dosimetry-metallurgy experiments for the PSF Blind Test.

Vol. 7 (Issue Date: January 1985)
PSF Simulated Void Box Capsule (SVBC) Charpy and Tensile Metallurgical Test Results
J. S. Perrin and T. U. Marston, Editors

Beyond scope of title, this document will provide experimental conditions, as-built documentation, and final Charpy and tensile specimen measured property changes in PV support structure and reference steels for the SVBC simulated ex-vessel cavity (void box) neutron exposure of $\sim 5 \times 10^{17}$ n/cm^2 (E > 1.0 MeV)* for ~95°F irradiation temperature.

Vol. 8 (Issue Date: January 1986)
PSF Simulated Void Box Capsule (SVBC) Physics-Dosimetry-Metallurgy Program Results
W. N. McElroy, F. B. K. Kam, G. L. Guthrie, J. S. Perrin, and T. U. Marston, Editors

Beyond scope of title, this document will provide small specimen measured property changes in PV support structure and reference steels for the SVBC simulated ex-vessel cavity (void box) neutron exposure of $\sim 5 \times 10^{17}$ n/cm^2 (E > 1.0 MeV)* for ~95°F irradiation temperature. The report will analyze and summarize combined physics-dosimetry-metallurgy results of NUREG/CR-3320, Vols. 3 and 7, including an assessment of thermal neutron effects, which are expected to be small.

2.1.2.6 NUREG/CR-3321 (Issue Date: June 1986)
PSF Surveillance Dosimetry Measurement Facility (SDMF)
W. N. McElroy, F. B. K. Kam, J. Grundl, and E. D. McGarry, Editors

This loose-leaf volume will provide results to certify the accuracy of exposure parameter and perturbation effects for surveillance capsules removed from PWR and BWR power plants.

2.1.2.7 NUREG/CR-3322 (Issue Date: September 1986)
LWR Test Reactor Physics-Dosimetry Data Base Compendium
W. N. McElroy and F. B. K. Kam, Editors

This loose-leaf volume will present results from FERRET-SAND, LSL, and other least-squares-type code analyses of physics-dosimetry for US (BSR, PSF, SUNY-NSTF [Buffalo], Virginia, etc.), UK (DIDO, HERALD, etc.), Belgium (BR-2,

*This estimate is based on preliminary ORNL calculations, as yet unsubstantiated by measurements.

etc.), France (Melusine, etc.), Germany (FRJ1, FRJ2, etc.), and other participating countries. It will provide needed and consistent exposure parameter values [total, thermal, and fast (E > 1.0 MeV) fluences, dpa, etc.] and uncertainties for correlating test reactor property change data with those obtained from PWR and BWR power plant surveillance capsules. NUREG/CR-3319 and -3322 will serve as reference physics-dosimetry data bases for correlating and applying power and research reactor-derived steel irradiation effects data. These latter metallurgical data are provided in EPRI NP-2428 (Mc82c) and in NUREG/CR-3326.

2.1.2.8 NUREG/CR-3323
VENUS PWR Core Source and Azimuthal Lead Factor Experiments and Calculational Tests:

Vol. 1 (Issue Date: September 1984)
Preliminary Results
A. Fabry, W. N. McElroy, and E. D. McGarry, Editors

Vol. 2 (Issue Date: September 1985)
Final Results
A. Fabry, W. N. McElroy, and E. D. McGarry, Editors

These two documents, to be prepared by CEN/SCK and other participants, will provide VENUS-derived reference physics-dosimetry data on active, passive, and calculational dosimetry studies involving CEN/SCK, HEDL, NBS, ORNL, and other LWR program participants.

2.1.2.9 NUREG/CR-3324
NESDIP PWR Cavity and Azimuthal Lead Factor Experiments and Calculational Tests:

Vol. 1 (Issue Date: April 1984)
PCA Replica Results: Preliminary Results
J. Butler, M. Austin, and W. N. McElroy, Editors

Vol. 2 (Issue Date: September 1985)
PCA Replica Results: Final Results
J. Butler, M. Austin, and W. N. McElroy, Editors

These two documents, to be prepared by Winfrith-RR&A and other participants, will provide NESDIP-PCA replica-derived reference physics-dosimetry data on active, passive, and calculational dosimetry studies involving Winfrith, CEN/SCK, HEDL, NBS, and other LWR program participants.

Vol. 3 (Issue Date: September 1986)
Zero- and Twenty-Centimeter Cavity Results
J. Butler, M. Austin, and W. N. McElroy, Editors

This document will provide NESDIP zero- and twenty-centimeter cavity-derived reference physics-dosimetry data on active, passive, and calculational dosimetry studies involving Winfrith, RR&A, HEDL, ORNL, NBS, CEN/SCK, and other LWR program participants.

Vol. 4 (Issue Date: September 1987)
Hundred-Centimeter Cavity Results
J. Butler, M. Austin, and W. N. McElroy, Editors

This document will provide NESDIP hundred-centimeter cavity-derived reference physics-dosimetry data on active, passive, and calculational dosimetry studies involving Winfrith, RR&A, HEDL, ORNL, NBS, CEN/SCK, and other LWR program participants. Results of zero-centimeter cavity studies will also be discussed and reported, as appropriate.

Vol. 5 (Issue Date: September 1988)
Other Configuration Cavity Results
J. Butler, M. Austin, and W. N. McElroy, Editors

This document will provide NESDIP "other" configuration cavity-derived results similar to those indicated for Vols. 3 and 4, above.

2.1.2.10 NUREG/CR-3325 (Issue Date: September 1987)
Gundremmingen Physics-Dosimetry-Metallurgy Program:

These documents will provide results that support the NRC fracture mechanics analysis of pressure vessel base metal using Charpy, tensile, compact tension, and full-wall thickness metallurgical specimens for Gundremmingen. HEDL compression and micro-hardness metallurgical and dosimetry specimens will be obtained as a function of distance through the PV wall. Previous surveillance capsule and cavity physic-dosimetry-metallurgy results will be correlated with new in-wall vessel results. Appropriate PSF results will be used to help NRC obtain the best possible overall data correlations.

Vol. 1 (Issue Date: June 1984)
Reactor Physics Calculational and Preliminary Dosimetry Results
W. N. McElroy and R. Gold, Editors

This document will provide the results of the W-NTD physics calculations and comparisons to previously available reactor cavity, concrete wall/steel liner, and surveillance capsule results. The calculations will provide information on both neutron and gamma components of the radiation field as well as best estimates of PV wall temperature profiles during full-power operation.

Vol. 2 (Issue Date: September 1985)
Program Description
W. N. McElroy and R. Gold, Editors

This document will provide relevant as-built and operated plant reference information and trepan metallurgical and dosimetry specimen experimental conditions, locations, etc. Information on previous reactor cavity and surveillance capsule physics-dosimetry-metallurgy results will be discussed and referenced, as well as results of radiometric [Si(Li)] and [Ge(Li)] measurements on PV wall trepans, concrete wall/steel liner trepans, PV wall, and other components, as appropriate.

Vol. 3 (Issue Date: January 1986)
Final Physics-Dosimetry Results
W. N. McElroy and R. Gold, Editors

This document will provide the final results of estimated surveillance capsule and PV (r,θ,z) wall neutron exposure parameter values [total, thermal, and fast (E > 1.0 MeV) fluences, dpa, etc.]; all in support of the data analysis of the trepan and surveillance capsule metallurgical specimens results.

Vol. 4 (Issue Date: September 1986)
Final Metallurgical and Data Correlation Results
W. N. McElroy and R. Gold, Editors

This document will provide the final results of the physics-dosimetry-metallurgy data correlation studies performed by HEDL/W-NTD of the surveillance capsule and PV wall metallurgical results. As appropriate, the results will be used to help in developing improved trend curves for future revisions of the E706 (IIF), E900, ΔNTT versus fluence and Reg. Guide 1.99 trend curves. The physics-dosimetry results will, similarly, be used to help in the final 1987 and 1988 revisions of the set of 21 LWR ASTM standards.

2.1.2.11 NUREG/CR-3326 (Issue Date: September 1987)
LWR Test Reactor Irradiated Nuclear Pressure Vessel and Support Structure Steel Data Base Compendium
W. N. McElroy and F. B. K. Kam, Editors

This loose-leaf volume will present data and results for selected metallurgical experiments performed in the US (BSR, PSF, SUNY-NSTF [Buffalo], Virginia, etc.), UK (DIDO, HERALD, etc.), Belgium (BR-2, etc.), France (Melusine, etc.), Germany (FRJ1, FRJ2, etc.), and other participating countries. It will provide needed and consistent Charpy, upper shelf energy, tensile, compact tension, compression, hardness, etc. property change values and uncertainties. With NUREG/CR-3322 physics-dosimetry data, NUREG/CR-3326 provides: 1) a more precisely defined and representative research reactor physics-dosimetry-metallurgy data base, 2) a better understanding of the mechanisms causing neutron damage, and 3) tested and verified exposure data and physical damage correlation models, all of which are needed to support the preparation and acceptance of the ASTM E706(IE) Damage Correlation and ASTM E706(IIF) ΔNDTT with fluence standards and future revisions of Reg. Guide 1.99.

2.1.2.12 NUREG/CR-3457 (Issue Date: May 1984)
Postirradiation Notch Ductility and Tensile Strength Determination for PSF Simulated Surveillance and Through-Wall Specimen Tests
R. Hawthorne, Editor

Beyond scope of title, this document will support analysis of the PSF Blind Test and provide as-built documentation and final PSF EPRI, RR&A, CEN/SCK, and KFA steel metallurgical results generated by MEA for SSC and SPVC.

2.2 LWR PHYSICS-DOSIMETRY TESTING IN THE ORNL POOL CRITICAL ASSEMBLY PRESSURE VESSEL BENCHMARK FACILITY (ORNL-PCA)

The pressure vessel benchmark facility at the PCA has afforded investigation of the following variables: 1) Plant Dimensions - Core Edge to Surveillance to Vessel Wall to Support Structures Positions; 2) Core Power Distribution: 3) Reactor Physics Computations; 4) Selection of Neutron Exposure Units; 5) Neutron Spectral Effects; and 6) Dosimetry Measurements.

In this regard, the ORNL-PCA Pressure Vessel Benchmark Facility, Figures 2.3 and 2.4, has and is being used primarily in support of the development and validation of the following ASTM Standards (see Figures 2.1 and 2.2):

- Analysis and Interpretation of Nuclear Reactor Surveillance Results (IA)
- Surveillance Test Results Extrapolation (IC)
- Damage Correlation for Reactor Vessel Surveillance (IE)
- Surveillance Tests for Nuclear Reactor Vessels (IF)
- Surveillance Tests for Nuclear Reactor Support Structures (IG)
- Application of Neutron Spectrum Adjustment Methods (IIA)
- Application of Neutron Transport Methods (IID)
- Benchmark Testing of Reactor Vessel Dosimetry (IIE)
- Correlation of ΔNDTT with Fluence (IIF)

Results of studies completed to date indicate that routine LWR power plant calculations of flux, fluence and spectrum, using current S_n transport methods can be as accurate as ±15% (1σ) for a criterion of $E > 1.0$ MeV if properly modeled and subjected to benchmark neutron field validation. Otherwise, errors can be a factor of two or more (Mc81). Summary information on the status of PCA program work is provided in Sections 2.2.1, 2.2.2, and 2.2.3.

2.2.1 Experimental Program

Analysis of passive dosimetry data collected during 10/81 - 12/81 has gone forward. These passive dosimetry analyses have emphasized 1) HEDL nuclear research emulsion measurements in the 8/7 and 12/13 configurations; 2) HEDL-SSTR and -RM measurements to fill in and supplement former (1979-1980) measurements in the 8/7 and 12/13 configurations; 3) HEDL active gamma spectrometry measurements with the Janus probe in the 8/7, 12/13, and 4/12 SSC configurations as well as measurements of the perturbation effects of the probe with a miniature HEDL ionization chamber; and 4) confirmation of NBS power and run-to-run normalization monitor measurements.

2.2.1.1 PCA Passive Dosimetry Measurements

NRE Measurements

Nuclear research emulsions (NRE) irradiated in the 1981 PCA experiments have now been scanned in the integral mode. These results, which are summarized

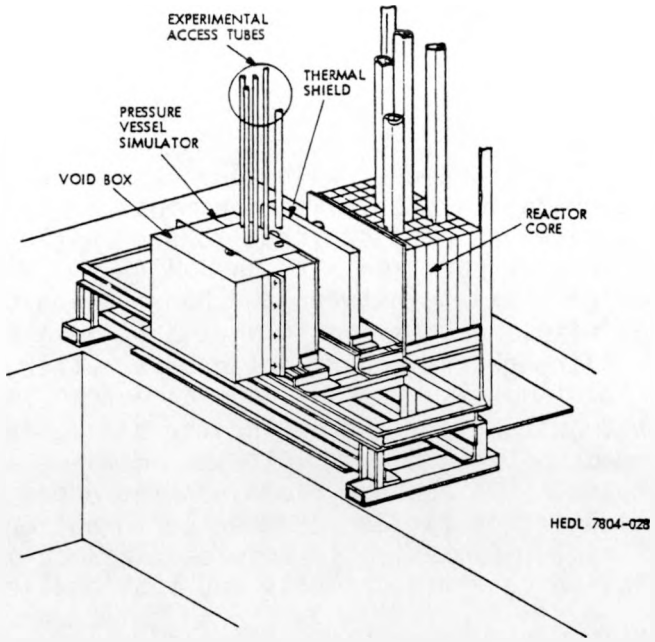

FIGURE 2.3. PV Wall Mockup Schematic of Two Equivalent ORNL Facilities. The high-flux version at ORR (PSF) includes damage exposure of metallurgical test specimens; the low-flux version near a low-power critical assembly (PCA) focuses on active and passive physics-dosimetry measurements. P05788-2

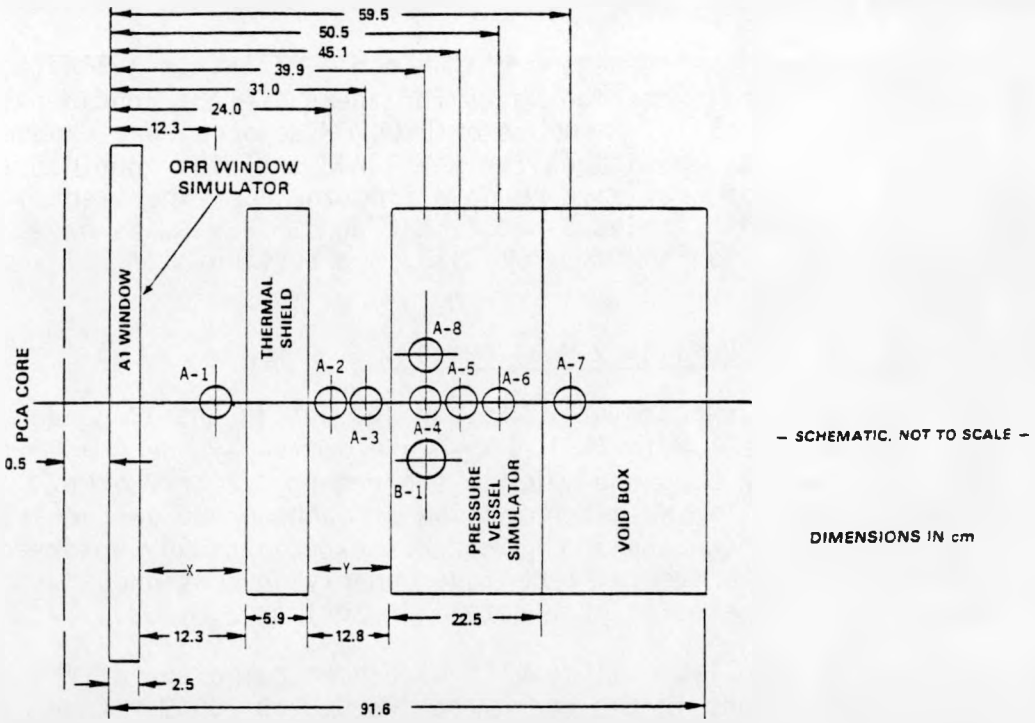

FIGURE 2.4. PCA Experimental Configuration: Locations A1, A2, A3, A4, A5, A6, A7, A8, and B1 in the PCA 12/13 Configuration. Representative for other configurations except for different X and Y dimensions.

in Table 2.1, are recommended as the absolute proton recoil integral rates to use for comparison with calculational results.

SSTR Measurements

Absolute fission rate measurements with mica SSTR were carried out for ^{235}U, ^{238}U, and ^{237}Np during the 1981 experiments at the PCA. SSTR from these irradiations have now been scanned. Based on the recent remeasurement of the optical efficiency for mica SSTR, n=0.9875 ± 0.0085, a consistent difference of about 10% exists between the NBS fission chamber (FC) and HEDL-SSTR-observed fission rates for ^{237}Np and ^{238}U in the PCA steel simulator block. Although the uncertainties are rather high, the CEN/SCK-FC and HEDL-SSTR 12/13 ^{237}Np results show good agreement in the water and void box positions, just before and behind the block, respectively. In view of the good agreement between the NBS fission chambers and the SSTR observations in the standard ^{252}Cf neutron field, on the order of 1% as shown in Table 2.2, re-evaluation of fission chamber perturbation in the PCA is essential. Additional information is provided in Section 2.4.3.1 on the comparisons of fission rate measurements and fissionable deposit masses.

The recommended ^{237}Np, ^{238}U, and ^{232}Th PCA 8/7, 12/13, and 4/12 SSC configuration fission reaction data to be used for comparison with calculational results are summarized in Table 2.3. The steel block values carry a large (~10%) uncertainty because of the existing differences between the FC and SSTR results.

RM Measurement

The recommended non-fission sensor [$^{103}Rh(n,n')$,$^{115}In(n,n')$,$^{58}Ni(n,p)$, and $^{27}Al(n,p)$] PCA integral reaction rates for the different configurations are given in Reference (Mc81). A number of HEDL RM sensors were exposed at the PCA in 1981 in selected positions for the 12/13 and other configurations to complete the matrix of available RM data from the PCA experiments. The final RM, together with Tables 3 and 4, NRE and SSTR results have been documented for inclusion in NUREG/CR-3318, see Sections 2.1.2.1 and 2.1.2.3 and Reference (Mc81).

2.2.1.2 PCA Active Dosimetry Measurements

Continuous gamma-ray spectrometry was carried out in the 12/13 and 4/12 SSC configurations at the PCA in 1981. Absolute gamma-ray spectra from these measurements have now been analyzed in the region 0.2 to 2.5 MeV. Of particular significance is the determination of Janus probe perturbation factors, which have been applied to correct experimentally observed gamma-ray spectra. The experimental technique underlying continuous gamma-ray spectrometry is discussed in more detail in Section 2.5.2.2.

Experimental and calculational results have been compared for the 12/13 and 4/12 SSC configurations in the energy region 0.2 to 2.5 MeV (see Figures 2.5 through 2.10). For the 12/13 configuration, ORNL calculations are roughly a

TABLE 2.1

RECOMMENDED I- AND J-INTEGRAL REACTION RATES FOR THE 1981 NRE EXPOSURES IN THE PCA

Emul No./ Config-uration	Location/ Distance from Core Center (cm)	I-Integral [protons/(MeV)(at.)(W-s)]				J-Integral [protons/(at.)(W-s)]			
		Energy (MeV)	Integral	Statistical Uncertainty (%)	Total* Uncertainty (%)	Energy (MeV)	Integral	Statistical Uncertainty (%)	Total* Uncertainty (%)
W9	TSB	0.4467	1.81×10^{-19}	6.61	8.10	0.4073	1.18×10^{-19}	3.19	5.67
		0.5198	1.73×10^{-19}	5.82	7.48	0.4837	1.05×10^{-19}	3.40	5.79
12/13	23.8	0.5877	1.59×10^{-19}	5.19	7.00	0.5540	9.37×10^{-20}	3.58	5.90
		0.6515	1.42×10^{-19}	5.36	7.12	0.6197	8.52×10^{-20}	3.76	6.01
		0.7119	1.21×10^{-19}	7.42	8.78	0.6197			
K4A	1/4 T	0.4467	4.58×10^{-20}	6.79	8.25	0.4073	2.15×10^{-20}	3.11	5.63
		0.5198	4.18×10^{-20}	4.55	6.53	0.4837	1.78×10^{-20}	3.41	5.80
12/13	39.5	0.5877	3.63×10^{-20}	5.17	6.98	0.5540	1.47×10^{-20}	3.77	6.02
		0.6515	2.96×10^{-20}	6.72	8.19	0.6197	1.27×10^{-20}	4.06	6.20
		0.7119	2.19×10^{-20}	7.47	8.82				
K5A	1/2 T	0.4467	3.31×10^{-20}	5.80	7.46	0.4073	1.21×10^{-20}	3.11	5.63
		0.5198	2.61×10^{-20}	4.42	6.44	0.4837	9.64×10^{-20}	3.50	5.85
12/13	44.7	0.5877	1.96×10^{-20}	5.39	7.14	0.5540	7.81×10^{-21}	3.88	6.09
		0.6515	1.47×10^{-20}	7.42	8.78	0.6197	6.53×10^{-21}	4.25	6.33
		0.7119	1.15×10^{-20}	7.94	9.22				
K6A	3/4 T	0.4467	1.99×10^{-20}	4.99	6.85	0.4073	6.61×10^{-21}	3.15	5.65
		0.5198	1.61×10^{-20}	4.00	6.17	0.4837	5.08×10^{-21}	3.59	5.91
12/13	50.1	0.5877	1.25×10^{-20}	5.50	7.23	0.5540	3.96×10^{-21}	4.07	6.21
		0.6511	9.40×10^{-21}	5.51	7.23	0.6197	3.14×10^{-21}	4.58	6.55
		0.7119	7.08×10^{-21}	7.00	8.43				
K7A	VB	0.4467	6.18×10^{-21}	5.23	7.02	0.4073	2.28×10^{-21}	4.21	6.30
		0.5198	5.62×10^{-21}	4.89	6.78	0.4837	1.81×10^{-21}	4.88	6.77
12/13	59.1	0.5877	4.87×10^{-21}	4.63	6.59	0.5540	1.41×10^{-21}	5.80	7.46
		0.6511	3.93×10^{-21}	4.62	6.58	0.6197	1.08×10^{-21}	6.74	8.21
		0.7119	2.84×10^{-21}	4.86	6.75				
K4B	1/4 T	0.4467	2.82×10^{-19}	6.60	8.10	0.4073	1.24×10^{-19}	3.11	5.63
		0.5198	2.47×10^{-19}	4.55	6.53	0.4837	1.01×10^{-19}	3.45	5.82
8/7	39.5	0.5877	2.09×10^{-19}	5.31	7.08	0.5540	8.48×10^{-20}	3.77	6.02
		0.6511	1.72×10^{-19}	6.86	8.31	0.6197	7.19×10^{-20}	4.10	6.23
		0.7119	1.36×10^{-19}	7.26	8.64				

*Does not include an estimated 4.1% for power normalization.

TABLE 2.2

^{242}Cf BENCHMARK FIELD COMPARISON OF NBS FISSION CHAMBER AND SSTR

Experiment ID No.*	FC Results	SSTR Results	FC/SSTR
TR-U-2a	35056	34160	1.026
TR-U-3a	37120	36211	1.025
TR-U-2b	21178	21347	0.992
TR-U-3b	25295	25168	1.005
TR-Pu-2a	36290	36159	1.004
TR-Pu-3a	26398	26069	1.013
TR-Pu-2b	33497	33083	1.013
TR-Pu-3b	35121	35309	0.995

Average of Overall Experiments

$$\langle FC/SSTR \rangle = 1.009 \pm 0.013$$

$$\langle |FC/SSTR-1| \rangle = 0.0124 \pm 0.009$$

Average Omitting Experiments TR-U-2a and TR-U-3a:**

$$\langle FC/SSTR \rangle = 1.004 \pm 0.009$$

$$\langle |FC/SSTR-1| \rangle = 0.008 \pm 0.004$$

---

*The U denotes that ^{235}U vacuum evaporated deposits were used, whereas the Pu denotes that ^{240}Pu vacuum evaporated deposits were used.

**Experiments TR-U-2a and TR-U-2b used an aluminum backed deposit, whereas all other experiments utilized deposits on polished stainless steel backings. The larger FC/SSTR ratios for these two experiments could be due to surface roughness effects.

TABLE 2.3

RECOMMENDED VALUES FOR ^{237}Np, ^{238}U, and ^{232}Th

Location	Midplane Position	Distance from Core (cm)	Equivalent Fission Fluxes [(flux/atom/core neutron) x 10^{8}] ^{237}Np		^{238}U	
			8/7 CONFIGURATION			
TSF	(A1)	7.9	1460.	(±6.2%)[a]	---	
PVF	(A3)	19.7	164.	(±6.3%)[a]	---	
1/4 T	(A4)	29.5	55.6	(±10.8%)	31.2	(±10.8%)
1/2 T	(A5)	34.7	31.1	(±11.1%)	13.8	(±10.9%)
3/4 T	(A6)	40.1	15.7	(±10.8%)	5.5	(±11.1%)
			12/13 CONFIGURATION			
TSB	(A2)	23.8	54.7	(±5.3%)[b]	---	
PVF	(A3)	29.7	22.9	(±5.8%)[c]	19.2	(±5.8%)[b]
1/4 T	(A4)	39.5	9.0	(±10.5%)	5.80	(±11.0%)
1/2 T	(A5)	44.7	4.92	(±11.2%)	2.56	(±10.9%)
3/4 T	(A6)	50.1	2.60	(±10.6%)	1.06	(±11.1%)
VB	(A7)	59.1	0.72	(±7.3%)[c]	0.281	(±4.9%)
			4/12 SSC CONFIGURATION			
SSC	(A2)	15.6	626.	(±4.8%)[b]	364.	(±4.8%)[b]
1/4 T	(A4)	30.5	48.6	(±11.2%)	23.0	(±10.0%)
1/2 T	(A5)	35.7	26.8	(±10.2%)	10.3	(±10.1%)
3/4 T	(A6)	41.1	14.7	(±5.6%)[d]	4.28	(±10.3%)[d]
VB	(A7)	50.1	4.01	(±5.8%)[a]	1.02	(±5.8%)[a]

Location	Midplane Position	Distance from Core (cm)	Fission Rates in ^{232}Th [(fissions/atom/core neutron) x 10^{34}]	
		8/7 CONFIGURATION		
1/4 T	(A4)	29.5	215.	(±4.8%)
1/2 T	(A5)	34.7	92.4	(±4.8%)
3/4 T	(A6)	40.1	34.6	(±4.8%)
VB	(A7)	49.1	7.82	(±5.0%)
		12/13 CONFIGURATION		
1/4 T	(A4)	39.5	35.6	(±4.9%)
1/2 T	(A5)	44.2	15.5	(±5.1%)
3/5 T	(A6)	50.1	5.95	(±4.9%)
VB	(A7)	59.1	1.32	(±4.7%)

[a]Only CEN/SCK fission chamber measurements were made at these locations.
[b]Only SSTR measurements were made at these locations.
[c]These were averaged CEN/SCK fission chamber and SSTR measurements (no detectable bias exists between the two measurements).
[d]Only NBS fission chamber measurements were made at these locations.

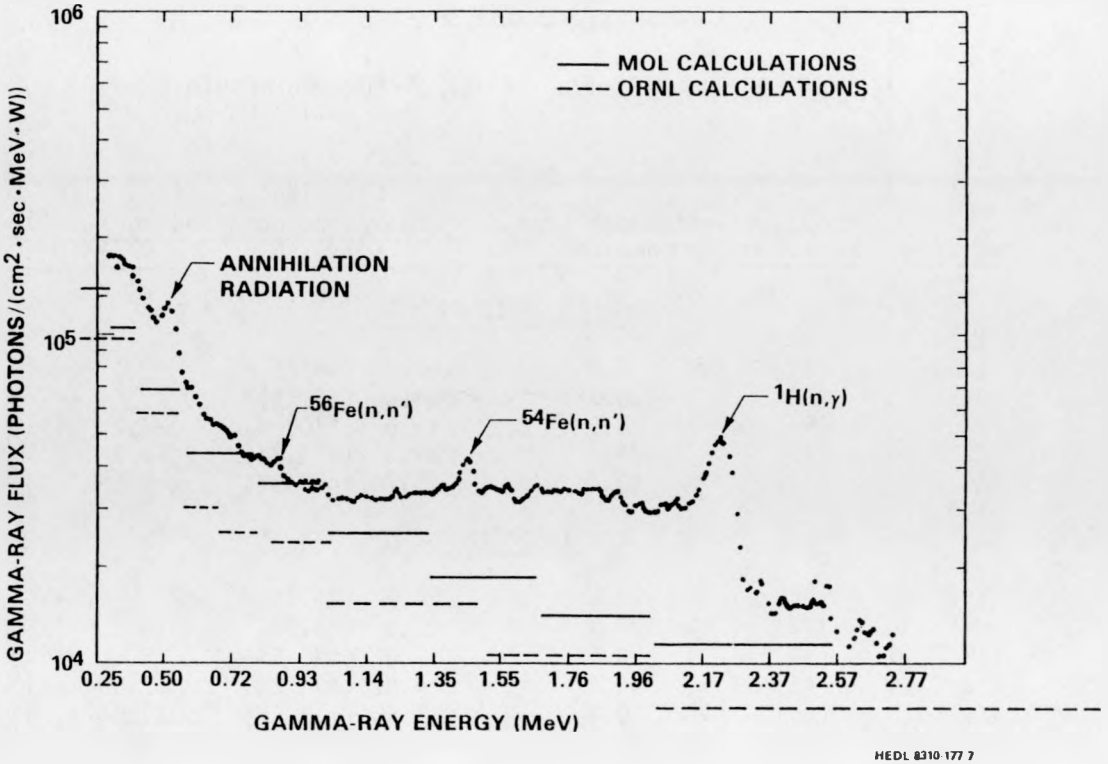

FIGURE 2.5. Measured and Calculated Gamma Spectra for the LWR-PV Mockup in the PCA 12/13 Configuration; 1/4 T Location. Neg 8307649-7

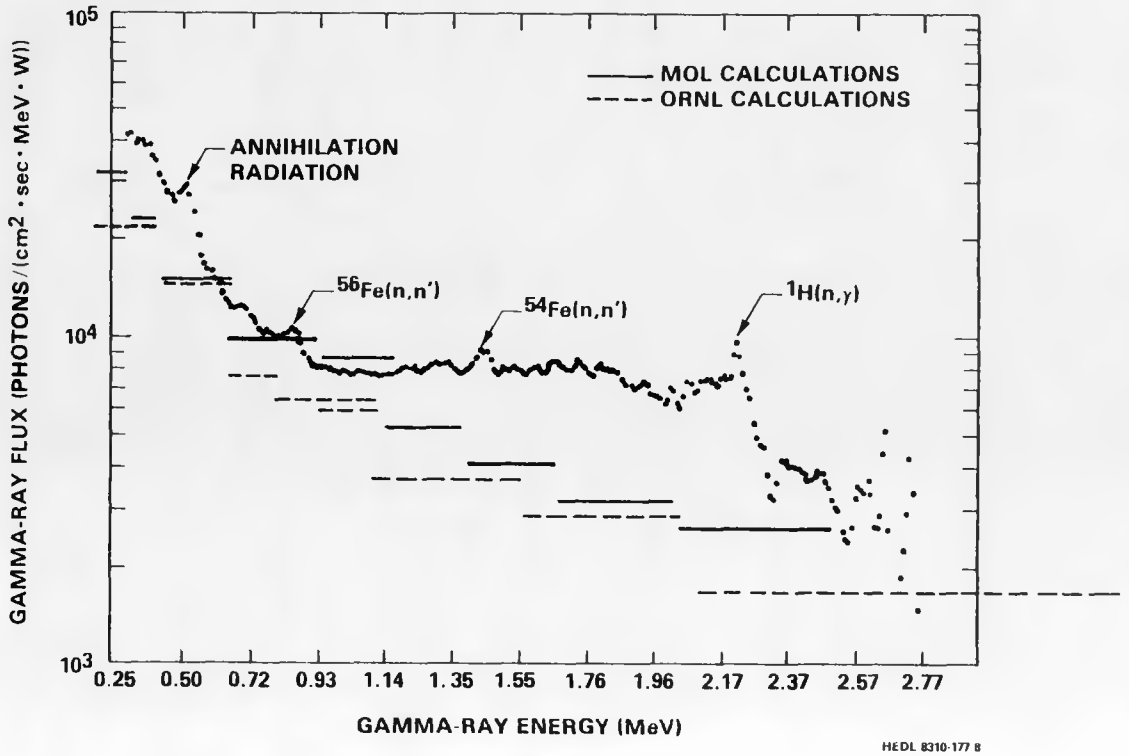

FIGURE 2.6. Measured and Calculated Gamma Spectra for the LWR-PV Mockup in the PCA 12/13 Configuration; 1/2 T Location. Neg 8307649-8

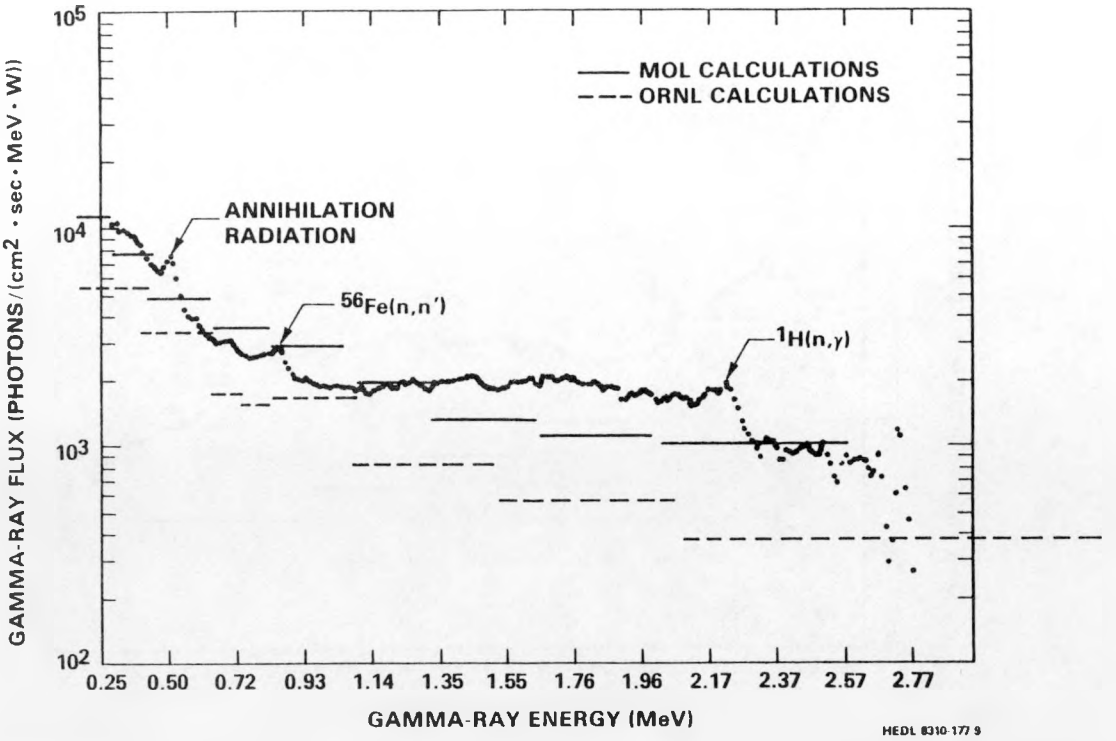

FIGURE 2.7. Measured and Calculated Gamma Spectra for the LWR-PV Mockup in the PCA 12/13 Configuration; 3/4 T Location. Neg 8307649-9

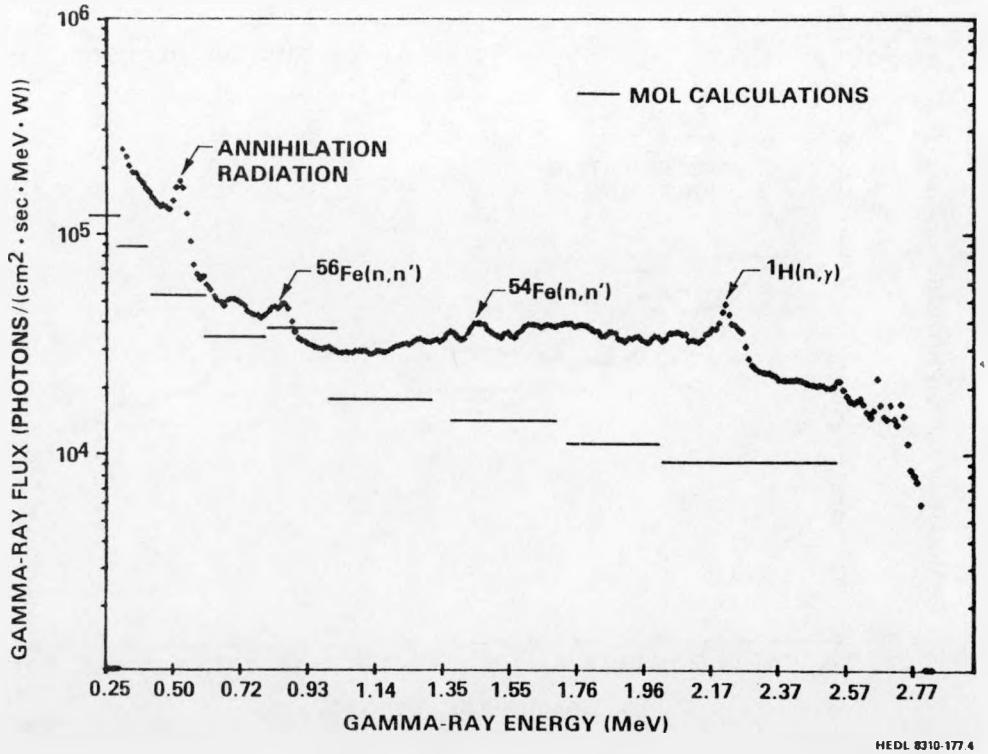

FIGURE 2.8. Measured and Calculated Gamma Spectra for the LWR-PV Mockup in the PCA 4/12 SSC Configuration; 1/4 T Location. Neg 8307649-4

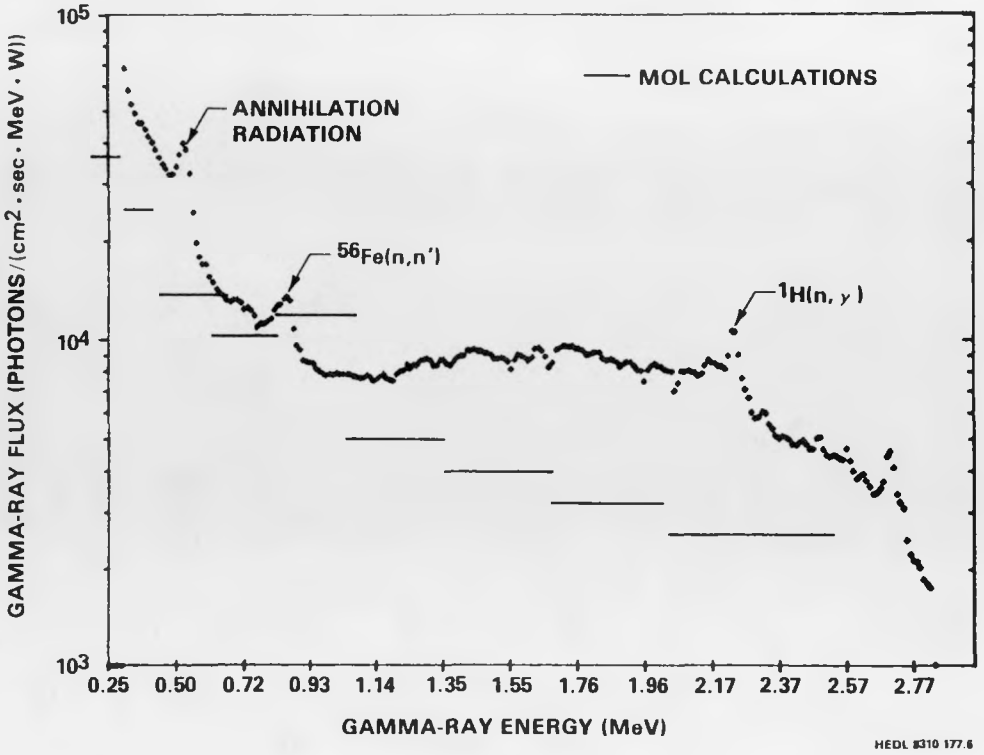

FIGURE 2.9. Measured and Calculated Gamma Spectra for the LWR-PV Mockup in the PCA 4/12 SSC Configuration; 1/2 T Location. Neg 8307649-6

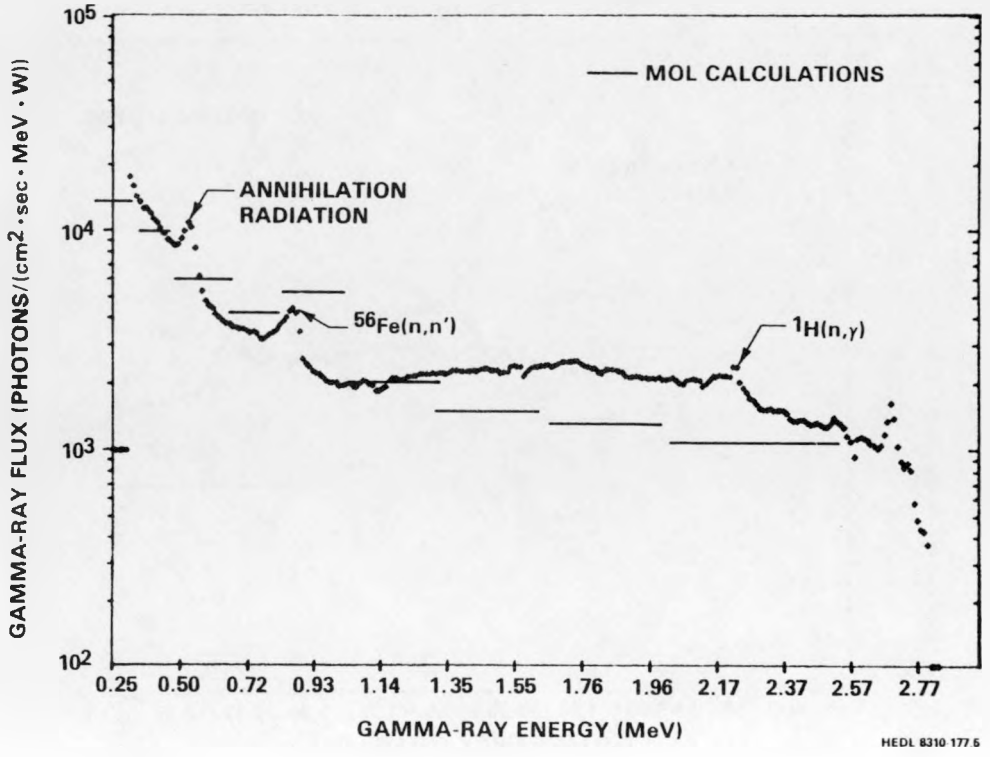

FIGURE 2.10. Measured and Calculated Gamma Spectra for the LWR-PV Mockup in the PCA 4/12 SSC Configuration; 3/4 T Location. Neg 8307649-5

factor of two lower than experimental gamma-ray spectra, whereas CEN/SCK calculations occupy an intermediate position. It is surprising to see that comparisons between theory and experiment generally improve with increasing penetration into the PV. However, calculations generally decrease more rapidly than experiment with increasing gamma-ray energy.

Work has continued on extending the Janus probe response matrix to higher energy. Measurements have been completed with the gamma-rays from $^{12}C^*$ ($\sim$4.4 MeV) and ^{16}O ($\sim$6.1 MeV). Analyses of these data are underway with the goal of providing PCA experimental gamma-ray spectra up to roughly 6 MeV.

2.2.1.3 Run-to-Run Monitoring and Absolute Normalization of Experiments

Although satisfactory from the safety and general user's view points, the accuracy, precision, and linearity of the PCA reactor control instrumentation in the nominal core power range of 1 W to 10 kW are not sufficient for an adequate normalization, on a permanent basis, of the high-accuracy LWR-PV-SDIP experiments (Mc81). For the PCA 8/7 and 12/13 configurations and the period September 1978 to January 1981, the precision of the NBS/CEN-SCK run-to-run power normalization for any given PCA exposure was in the 0.5% to 1.0% range. Data for the 4/12 SSC in the period September 1979 to November 1980 were found to be in this same range. Further, the run-to-run monitor data in both periods tend to substantiate that the accuracy of the reactor instrumentation at powers exceeding 10 W is, on the average, consistent with the accuracy of the integral measurements. This is important because it has not been possible to always have a permanently positioned run-to-run monitor.

2.2.2 Calculational Program

2.2.2.1 Neutron Calculations

Neutron transport calculations for the PCA 4/12 and the PCA 4/12 SSC configurations have been completed in support of the PSF metallurgical irradiation experiment. All neutronics calculations are performed with the DOT (Rh79) computer program and the VITAMIN-C (Ro82) cross-section library. The ORNL methodology utilizes a flux density synthesis technique described by Maerker and Williams (Ma82e). The purpose of these calculations is to verify that the calculations can predict the perturbation effect due to the insertion of a surveillance capsule. The perturbation effect is defined here to be the ratio of the ^{237}Np reaction rate with the SSC to the ^{237}Np reaction rate without the SSC. Table 2.4 illustrates that the calculations predict well the axial shape and the perturbation effect for the ^{237}Np reaction. Only relative measurements are available so that absolute comparisons cannot be made.

2.2.2.2 Gamma Calculations for the PCA 12/13 Configuration

Significant discrepancies exist in the gamma calculations between ORNL and CEN/SCK (Table 2.5). The source of these discrepancies has been identified

TABLE 2.4

COMPARISON OF ORNL-CALCULATED DATA WITH CEN/SCK EXPERIMENTAL MEASUREMENTS FOR THE ^{237}Np REACTION

Axial traverse at the 1/4 T location (mm)	PCA-PVF 4/12 SSC				PCA-PVF 4/12				Perturbation effect		
	ORNL calc.	ORNL calc. norm.	CEN/SCK exp. values norm.	C/E	ORNL calc.	ORNL calc. norm.	CEN/SCK exp. values norm.	C/E	ORNL calc. values	CEN/SCK exp. values	C/E
-101	6.258-31	0.959	0.953	1.01	5.361-31	0.959	0.967	0.99	1.167	1.219	0.96
- 25	6.526-31	1.0	1.0	1.00	5.592-31	1.0	1.0	1.00	1.167	1.238	0.94
+ 52	6.191-31	0.949	0.952	1.00	5.343-31	0.955	0.973	0.98	1.159	1.211	0.96
+102	5.660-31	0.867	0.854	1.01	4.929-31	0.881	0.884	1.00	1.148	1.195	0.96
+153	4.887-31	0.749	0.727	1.03	4.321-31	0.773	0.775	1.00	1.131	1.161	0.97
+204	3.913-31	0.600	0.599	1.00	3.547-31	0.634	0.647	0.98	1.103	1.146	0.96
+240	3.126-31	0.479	0.487	0.98	2.918-31	0.522	0.539	0.97	1.071	1.117	0.96
+280	2.176-31	0.333	0.389	0.86	2.153-31	0.385	0.432	0.89	1.011	1.114	0.91

TABLE 2.5

COMPARISON OF CALCULATED GAMMA FLUXES FOR THE PCA 12/13 CONFIGURATION
(Photons•cm^{-2}•s^{-1}•MeV^{-1}•W^{-1})

Energy boundaries (MeV) lower-upper	1/4 T			1/2 T			3/4 T		
	ORNL	CEN/SCK	Ratio	ORNL	CEN/SCK	Ratio	ORNL	CEN/SCK	Ratio
10.0 -14.0	3.84-2	3.58-2	1.07	9.74-3	9.11-3	1.07	2.36-3	2.40-3	0.98
8.0 -10.0	1.78+2	3.04+2	0.59	4.00+1	7.16+1	0.59	9.02+0	3.85+1	0.23
5.0 - 8.0	1.14+3	1.47+3	0.78	2.89+2	3.68+2	0.79	6.74+1	3.54+2	0.19
4.0 - 5.0	1.71+3	1.84+3	0.93	4.53+2	4.95+2	0.92	5.08+2	3.04+2	0.36
3.0 - 4.0	2.76+3	3.49+3	0.79	7.31+2	9.10+2	0.80	1.74+2	4.30+2	0.40
2.0 - 3.0	7.24+3	9.13+3	0.79	1.65+3	2.07+3	0.80	3.61+2	8.75+2	0.41
1.0 - 2.0	1.31+4	1.91+4	0.69	3.09+3	4.27+3	0.72	6.86+2	1.52+3	0.45
0.8 - 1.0	2.38+4	3.58+4	0.66	6.02+3	8.46+3	0.71	1.51+3	3.01+3	0.50
0.6 - 0.8	2.90+4	4.52+4	0.64	6.80+3	9.77+3	0.70	1.55+3	3.34+3	0.46
0.4 - 0.6	5.93+4	6.66+4	0.89	1.40+4	1.41+4	1.00	3.19+3	4.82+3	0.66
0.2 - 0.4	9.74+4	1.29+5	0.76	2.28+4	2.73+4	0.84	5.17+3	9.77+3	0.53
0.1 - 0.2	1.19+5	1.43+5	0.83	2.78+4	2.98+4	0.93	6.32+3	1.08+4	0.59
0.02- 0.1	1.18+4	2.39+4	0.49	2.76+3	4.88+3	0.57	6.29+2	1.78+3	0.35

to be in the cross-section input. The gamma cross-section set used by CEN/SCK consisted of contributions from prompt, secondary, and fission product gammas. The ORNL gamma cross-section set included the prompt and secondary gammas, but not the fission product gammas. When the effect of the fission product gammas was included in the ORNL set, the agreement between CEN/SCK and ORNL was good. However, significant discrepancies between calculations and measurements still exist as discussed in Section 2.2.1.2 and shown in Figures 2.5 through 2.10.

2.2.3 Documentation

NUREG/CR-3318 of Section 2.1.2.3 on the "PCA Dosimetry in Support of the PSF Physics-Dosimetry-Metallurgy Experiments," which updates the information presented in Reference (Mc81) and incorporates the data from the PCA physics-dosimetry experiments and calculations (for the 8/7, 12/13, 4/12 and 4/12 SCC configurations) is scheduled for completion in May 1984.

British results for the "PCA Replica," NUREG/CR-3324, Volume 1 of Section 2.1.2.9, is scheduled for completion in April 1984. LWR-PV-SDIP participants and final results will be documented in Volume 2 of NUREG/CR-3324, which is scheduled for completion in September 1985.

2.3 LWR STEEL PHYSICS-DOSIMETRY-METALLURGY TESTING IN THE ORR-PSF, ORR-SDMF, BSR-HSST AND SUNY-NSTF

Higher flux/fluence physics-dosimetry-metallurgy benchmark fields have afforded study of the following variables: 1) Steel Chemical Composition and Microstructure; 2) Steel Irradiation Temperature; 3) Reactor Operating History; 4) Reactor Physics Computations; 5) Selection of Neutron Exposure Units; 6) Dosimetry Measurements; and 7) Neutron Spectral and Dose Rate Effects.

In this regard, the LWR Metallurgical Pressure Vessel Benchmark Facility (ORR-PSF) Figures 2.11 through 2.17, is being used primarily in support of the development and validation of the following ASTM Standards (See Figures 2.1 and 2.2):

- Analysis and Interpretation of Nuclear Reactor Surveillance Results (IA)
- Surveillance Dosimetry Extrapolation (IC)
- Displaced Atom (dpa) Exposure Unit (ID)
- Damage Correlation (IE)
- Surveillance Tests for Nuclear Reactor Vessels (IF)
- Surveillance Tests for Nuclear Reactor Support STructures (IG)
- Application of Neutron Spectrum Adjustment Methods (IIA)
- Sensor Set Design (IIC)
- Correlation of ΔNDTT with Fluence (IIF)
- Five Method Standards, IIIA, IIIB, IIIC, IIID and IIIE

A number of metallurgical programs and studies have been established to determine the fracture toughness and Charpy properties of irradiated materials as a function of chemistry, microstructure, and irradiation conditions. The ORR-PSF multilaboratory physics-dosimetry-metallurgy program is expected to provide key irradiation effects data, under well controlled conditions, to help in 1) the verification and calibration of exposure units and values and 2) the analysis and correlation of property change data obtained from this and other program work. Summary information on the status of the ORR-PSF and other program work is provided in Sections 2.3.1, 2.3.2 and 2.3.3. Further use of benchmark fields is elaborated upon in Sections 2.4.3, 2.4.4, and 2.5.1.

2.3.1 Experimental Program

For neutron dosimetry in these higher flux/fluence benchmark fields, just as for commercial LWR power plants, it is extremely advantageous to use time-integrating in addition to radiometric (RM) dosimeters, such as very long half-life radiometric (RM), solid-state track recorders (SSTR), helium accumulation fluence monitors (HAFM), and damage monitors (DM). This advantage is underscored by recent PSF calculations that show as much as 40% cycle-to-cycle variation in the saturated activities of RM dosimeters.

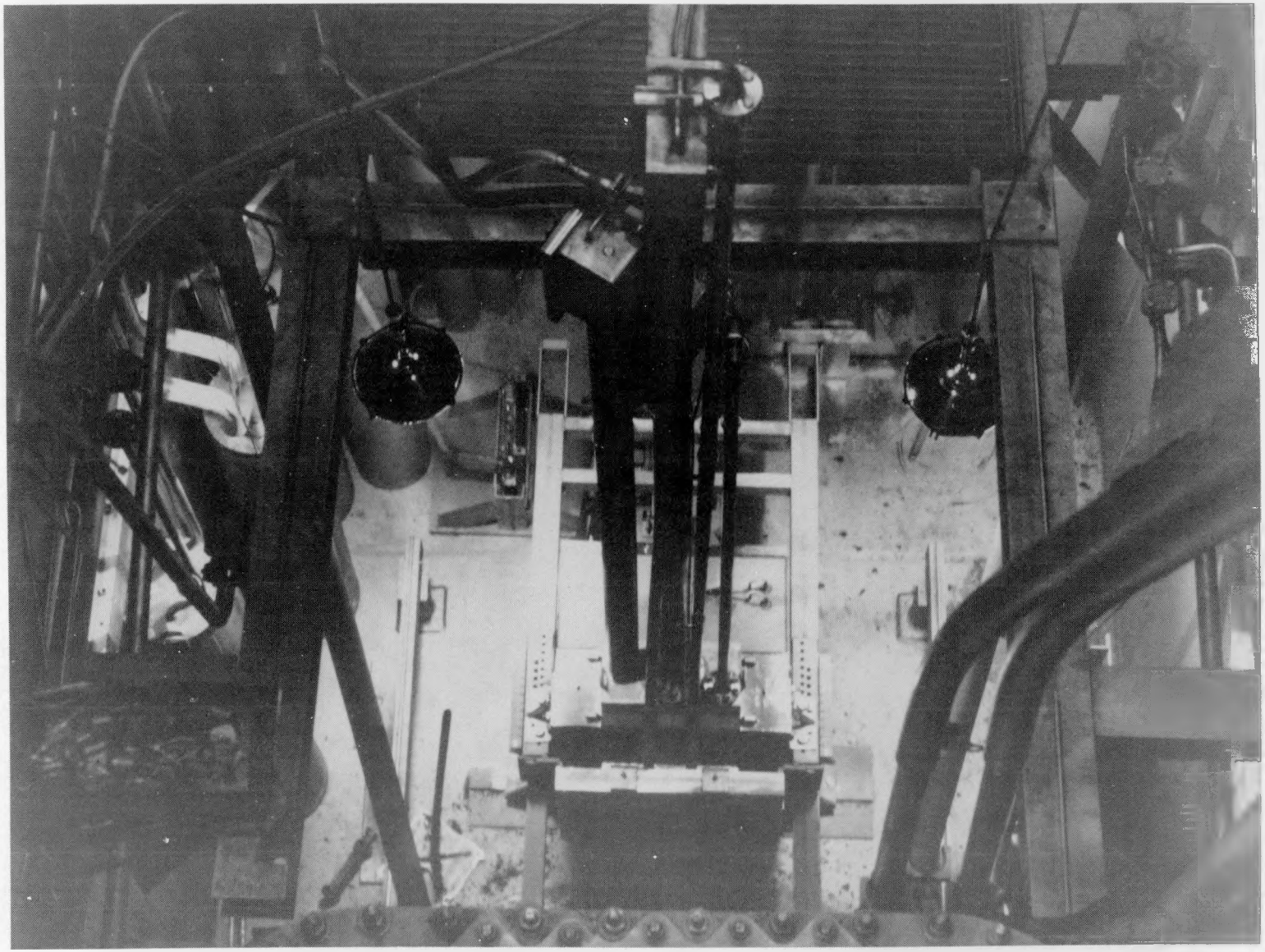

FIGURE 2.11. LWR Metallurgical Pressure Vessel Benchmark Facility. Neg 8010270-19

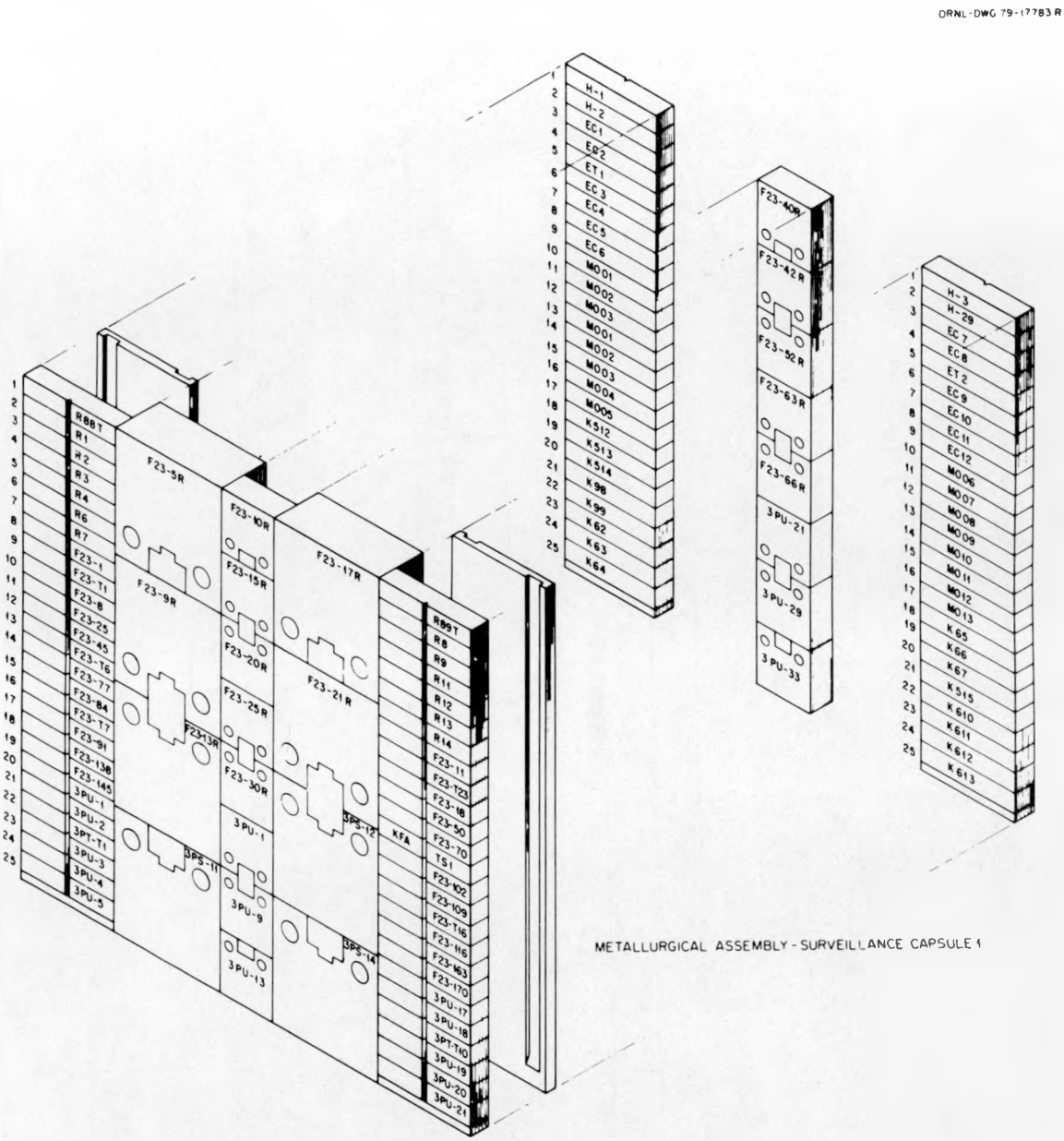

FIGURE 2.12. Metallurgical Assembly Located in the Surveillance Capsule.
Neg 810270-10

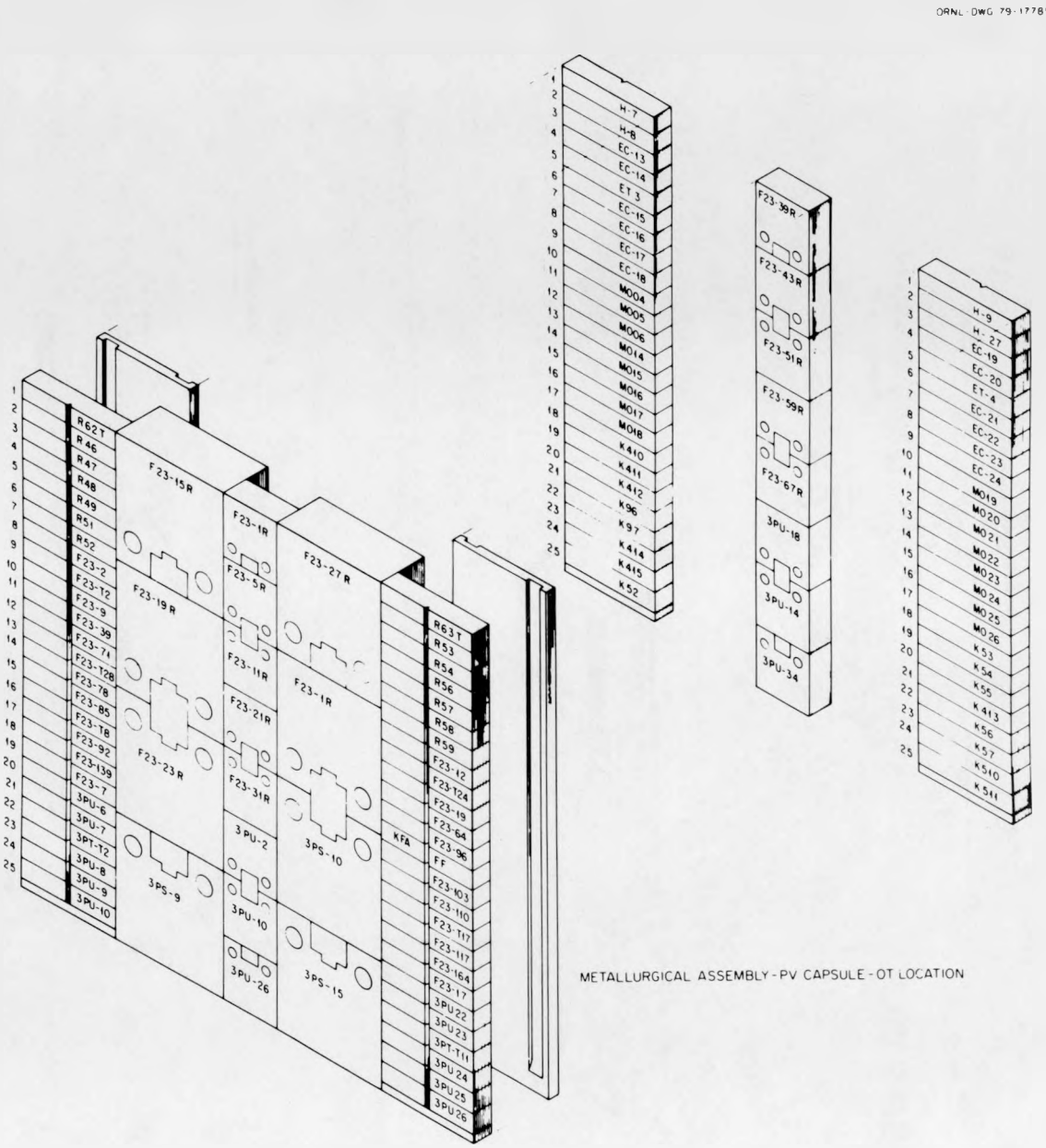

FIGURE 2.13. Metallurgical Assembly at the OT Location (Inside Surface) of the SPVC. Neg 8010270-9

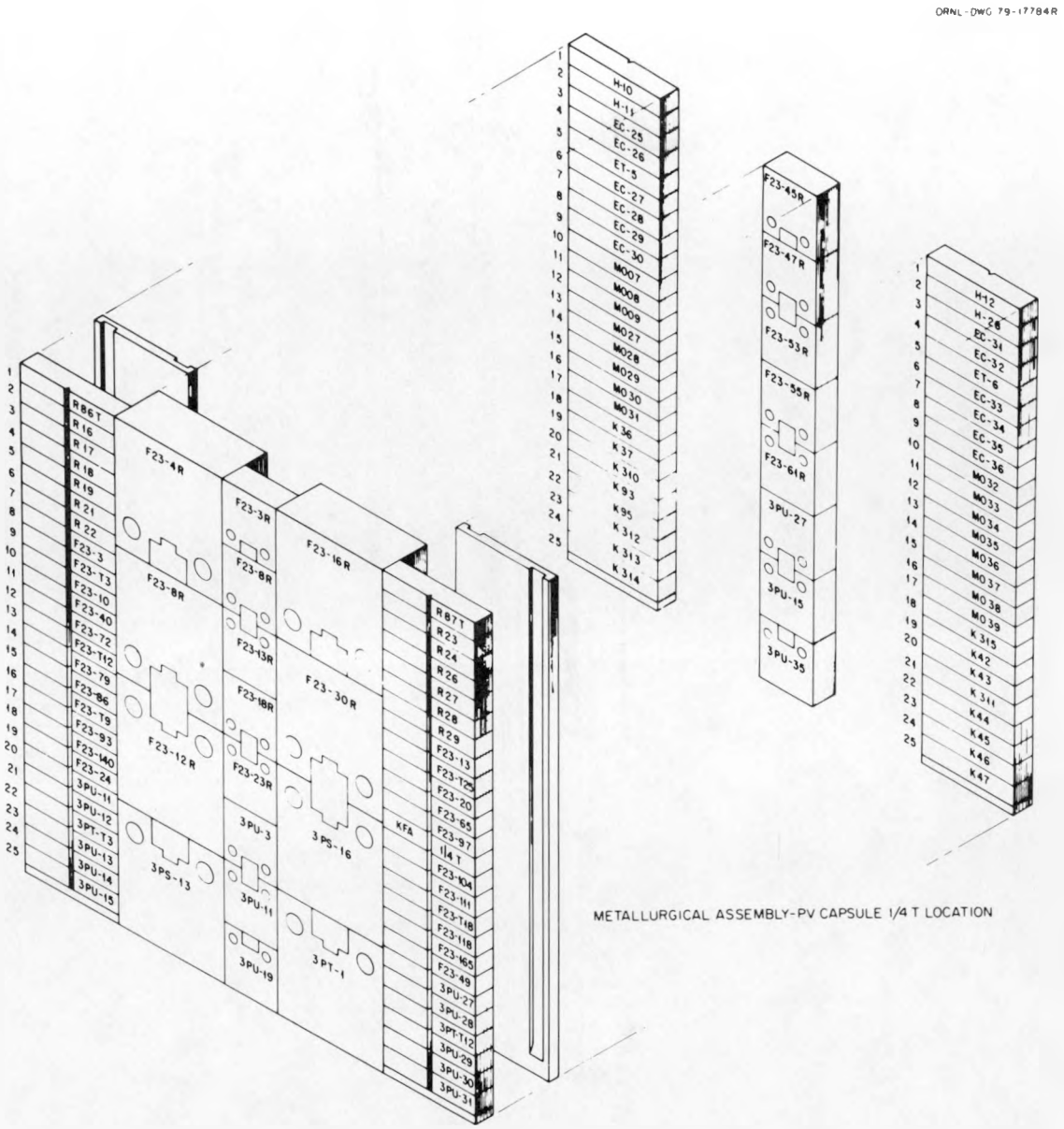

FIGURE 2.14. Metallurgical Assembly at the 1/4 T Location of the SPVC. Neg 8010270-8

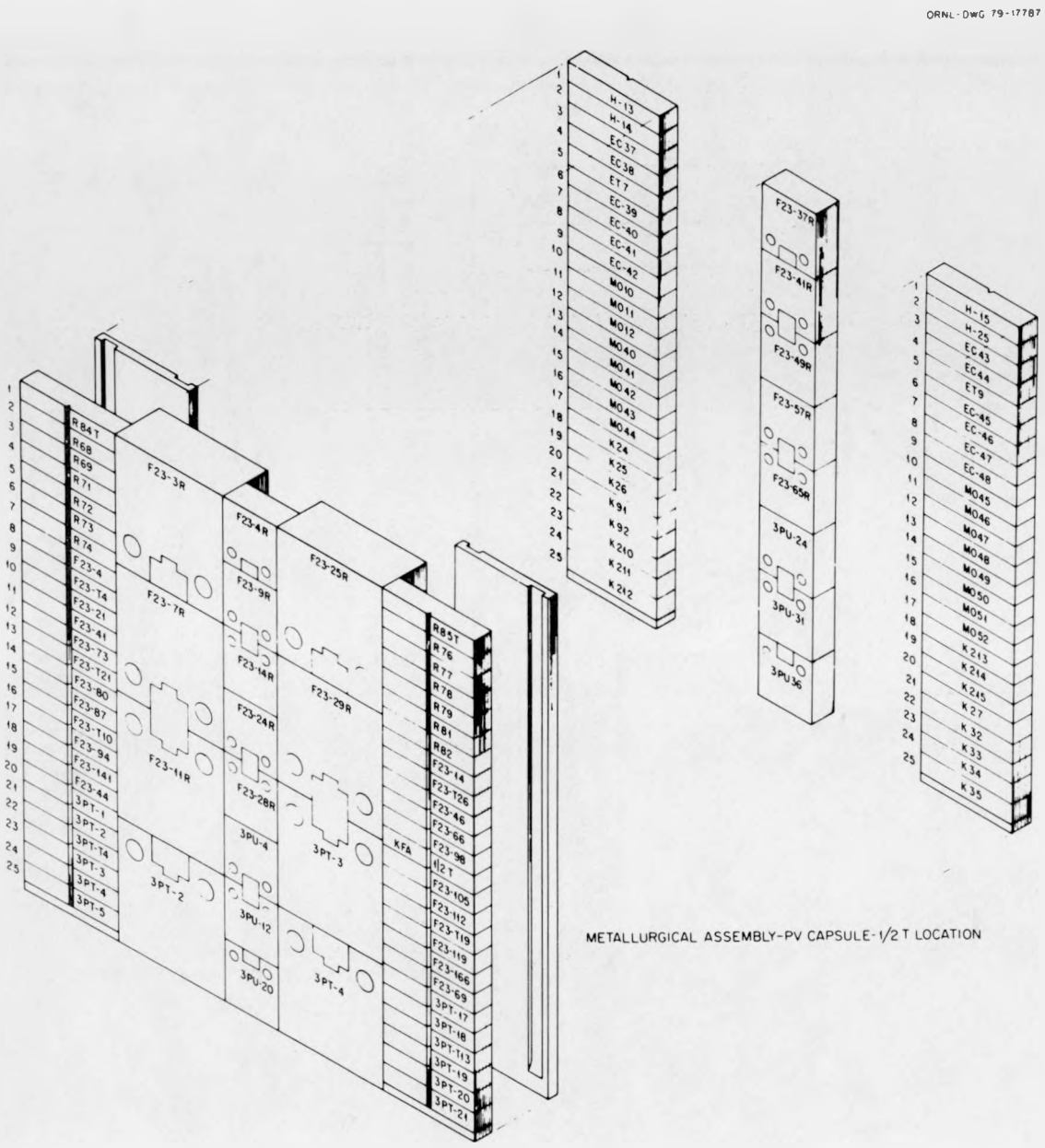

FIGURE 2.15. Metallurgical Assembly at the 1/2 T Location of the SPVC. Neg 8010270-7

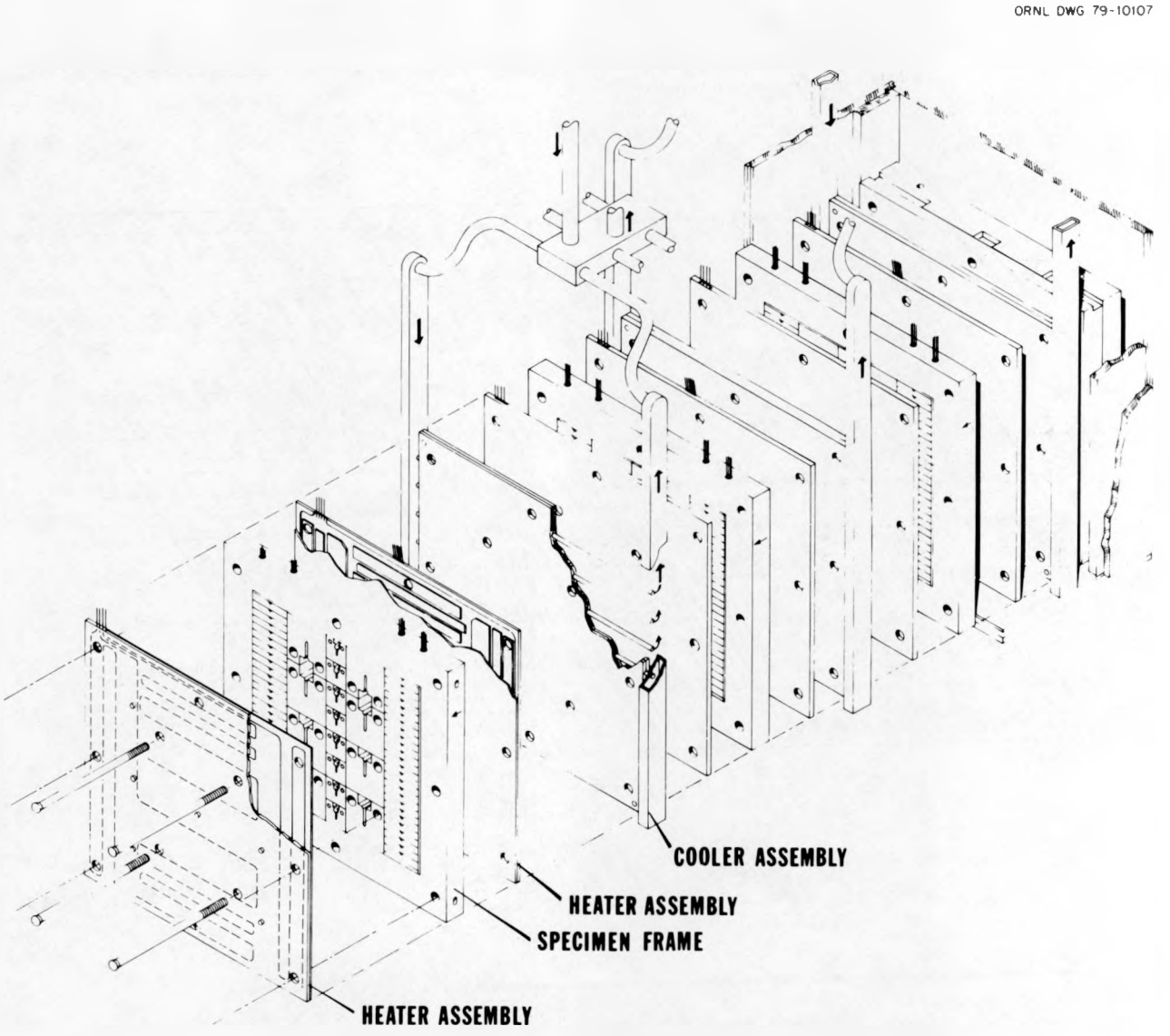

FIGURE 2.16. Exploded View of the SPVC. Neg 8010270-15

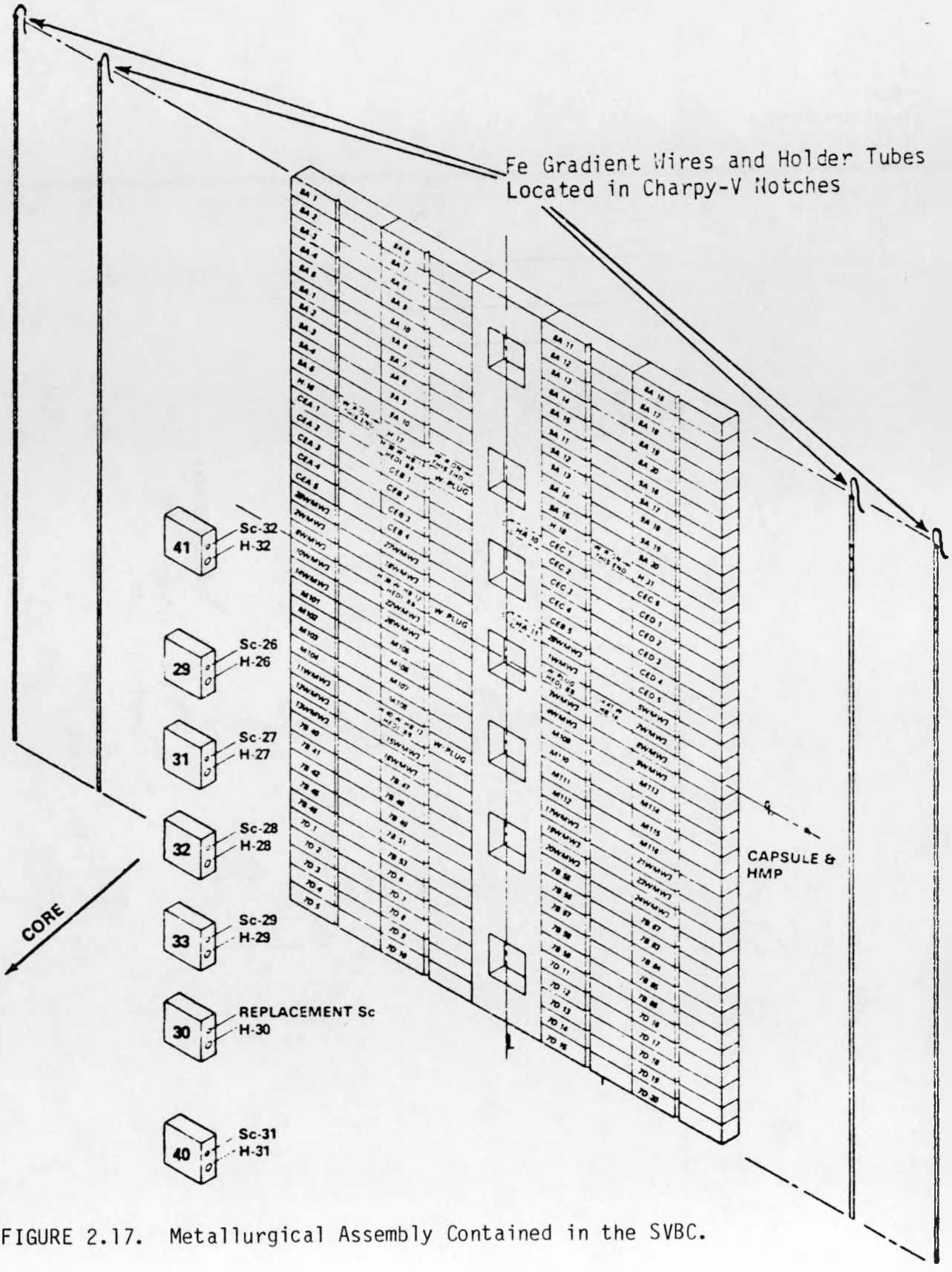

FIGURE 2.17. Metallurgical Assembly Contained in the SVBC.

Testing and confirmation of the accuracy of RM, SSTR, HAFM, and DM sensors for LWR surveillance programs is being accomplished in PSF and SDMF physics-dosimetry-metallurgy experiments. Application of SSTR, HAFM, and DM for neutron dosimetry in higher flux/fluence LWR-PV environments entails verification and/or extension of the overall existing experimental techniques. For instance, the need for automated SSTR track scanning systems of high quantitative accuracy has been recognized for some time. Since the availability of such systems is an overriding factor in cost-effective SSTR applications at high flux/fluence, the status of automated track scanning systems at HEDL in support of the PSF, SDMF, and PWR and BWR benchmark tests is reviewed in Section 2.5.2.1.

2.3.1.1 ORR-PSF

The 2-year physics-dosimetry-metallurgy irradiation experiment in the ORR-PSF was completed June 22, 1982. The simulated pressure vessel capsule (SPVC) and the simulated void box capsule (SVBC) were disassembled, and the dosimetry sensors and metallurgical specimens were shipped to the appropriate participants. The final physics-dosimetry-metallurgy irradiation and temperature distribution data and the reactor power time-history data for all these LWR-PV and support structure steel simulation experiments are or will be documented in LWR-PV-SDIP Quarterly Progress Reports and a series of NUREG reports, see Sections 2.1.2.1, 2.1.2.4, and 2.1.2.11.

FERRET-SAND physics-dosimetry results for SSC-1 have been provided to MEA and ORNL. These preliminary HEDL results have yet to be compared with those obtained by other participants (Belgium, UK, Germany, and US). Final exposure parameter values (fluence: total, thermal, E > 0.1 MeV, E > 1.0 MeV; and dpa maps) for SSC-1, SSC-2, SPVC, and SVBC must have the concurrence of all participants doing physics-dosimetry analysis. HEDL-RM results for SSC-1 have already been provided to PSF Blind Test participants. HEDL-RM results for SSC-2, SPVC, and SVBC have been provided to ORNL.

Preliminary physics-dosimetry-metallurgical results from the simulated surveillance capsules (SSC-1 and SSC-2) have been reported by several participants in the program (Fa82,Ha82a,Ke82,Mc82,To82a). Other than the rather large (up to 40%) cycle-to-cycle variation in saturated activities of RM dosimetry, no surprises have been observed in the SSC and SPVC data. The documentation of physics-dosimetry-metallurgical results for the SSC, SPVC, and SVBC is scheduled for FY 1984 through 1986 in a series of NUREG (HEDL, ORNL, MEA, and Mol) and EPRI (FCC-W-NTD) reports. More details on this planned documentation are given in Section 2.1.2.

2.3.1.1.1 PSF Dosimetry and Metallurgy

The dosimetry analysis for the PSF SSC, SPVC, and SVBC is still in progress at HEDL, Mol, Harwell, and Jülich. Interlaboratory comparisons of results with those of several US vendors and service laboratories have yet to be completed. Once this has been accomplished, consensus RM-reaction rate maps can be completed for the subsequent derivation of final exposure parameter

values and maps using ORNL and RRA physics results as input for the HEDL-FERRET, ORNL-LSL, and UK-CENSCK least-squares adjustment codes. This is expected to be completed and documented in NUREG/CR-3320, Vol. 2 by November 1984 for the SSC-1 and SSC-2 capsules. The corresponding work for the SPVC and SVBC is expected to be completed and documented in NUREG/CR-3320, Vol. 3 by January 1985.

The final SSC (SSC-1 and SSC-2) and SPVC/SVBC metallurgical data and results will be documented in NUREG/CR-3295, CR-3320, Vols. 4, 5, 7, and 8, and CR-3457. NUREG/CR-3295 and CR-3457 are MEA reports on the results of the SSC and SPVC Charpy, tensile, and CT specimen tests. Volumes 4 and 8 are HEDL reports, which include EPRI-HEDL space-compatible compression and hardness results. NUREG/CR-3320, Vol. 5 is a CEN/SCK metallurgy report for the SSC experiments, and NUREG/CR-3320, Vol. 7 is a EPRI/FCC/W-NTD report for the SVBC metallurgy. General distribution of these reports is expected in the period January 1984 through January 1986, depending on the subject matter, see Section 2.1.2.

The initial results of the Charpy and CT test results for the SSC-1 have been provided in a "PSF Blind Test Instructions and Data Packages." The information was sent to all "Blind Test" participants in April 1983.

The SSC-1 "Space Compatible" Compression Cylinder results are also given in the "Blind Test Instruction and Data Packages" referred to above. These results were previously reported in the LWR-PV-SDIP Quarterly Report for January 1981-March 1981 (NUREG/CR-2345, Vol. 1, HEDL-TME 81-33). Room-temperature Brinell hardness tests have been conducted on the SSC-2 hardness specimens, which were irradiated in a Charpy-shaped holder in the EPRI Charpy specimen group. In addition, room temperature compression testing has been conducted on compression specimens from SSC-2. The overall result of the hardness and compression tests is that the hardness and yield strength undergo an irradiation-induced increase that is proportional to the copper content. The results of the SSC-1 compression tests are shown in Figure 2.18. It appears from the figure that the copper effect has a partial saturation for copper content above 0.3 wt%.

2.3.1.1.2 PSF Blind Test

The following changes in dates, meetings, and publications concerning the PSF Blind Test have been agreed upon:

- Metallurgical and dosimetry test data for the PSF/SSC-2 and SPVC capsules will be released in April 1984.
- The Blind Test Workshop is now scheduled for April 9-10, 1984 at HEDL.
- All participants' PSF-SSC and -SPVC physics-dosimetry-metallurgy analysis and prediction results will be documented in NUREG/CR-3320, Volume 1, "PSF Blind Test," and Volume 6, "PSF Experiment - Recommended Physics-Dosimetry-Metallurgy Data Base and Blind Test Participant's Final Analyses." Current due dates for these publications are February 1985 and September 1986, respectively. As discussed in Section 2.3.1.1.1, the "PSF Experiments" final physics-dosimetry-metallurgy results will be documented in a series of NUREG reports.

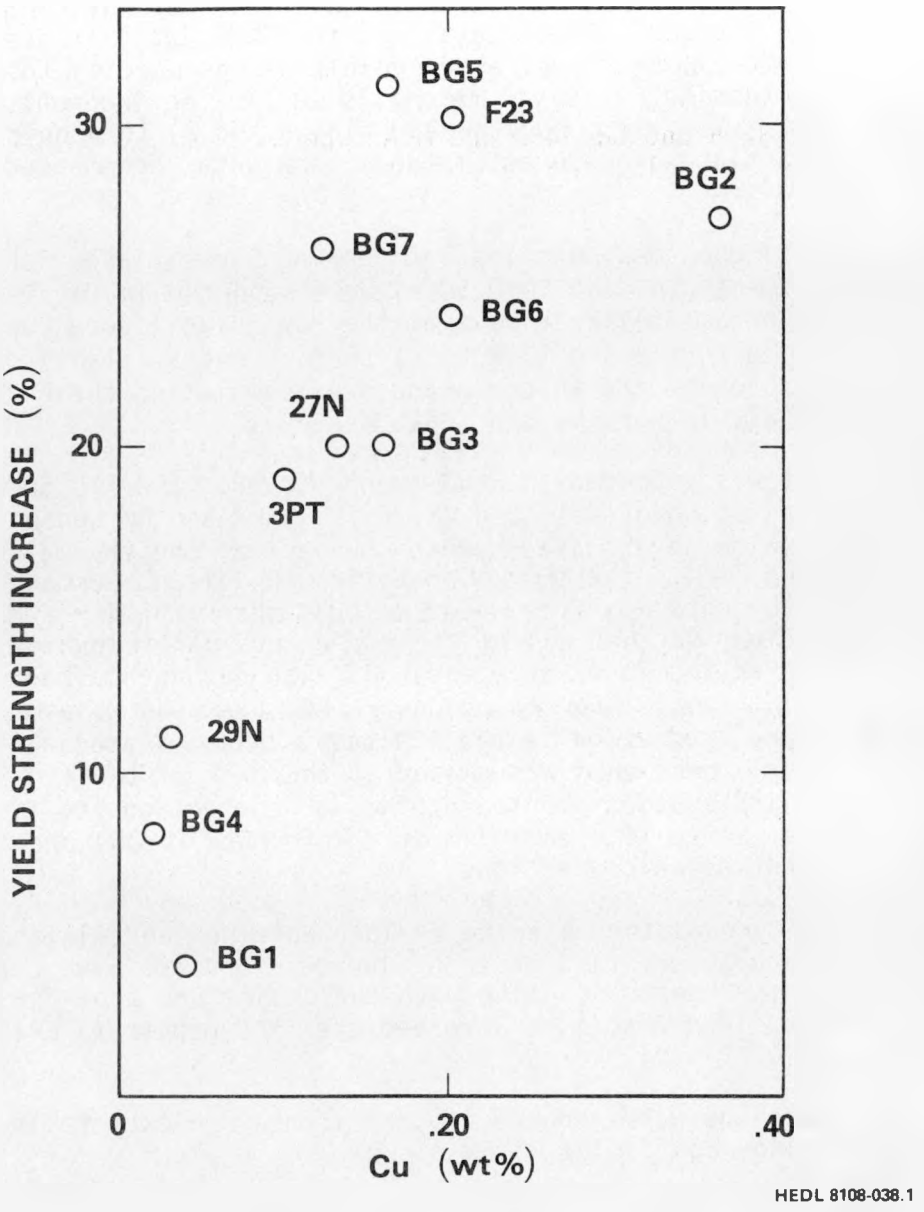

FIGURE 2.18. SSC-1 Compression Test Results.

2.3.1.2 ORR-SDMF

In addition to verification of surveillance capsule perturbation effects, the SDMF tests provide benchmark referencing of the primary neutron sensors used for irradiation surveillance of pressure vessels and their support structures. The SDMF tests are conducted in the high-flux environment of the PSF adjacent to the ORR. These tests and the SDMF Facility are an outgrowth of the LWR-PV-SDIP. They are a result of the need 1) to benchmark calculations and QA dosimetry sensor materials in flux environments more intense than are available in pure standard fields and 2) to acquire data to validate and substantiate procedures, methods, and data recommended for use in the ASTM standards.

Results of the Westinghouse-Combustion Engineering Surveillance Capsule Perturbation Experiment (the 2nd SDMF test) were reported in the 1982 Annual Report (Mc82a). Experimental results from the B&W Surveillance Capsule Perturbation Experiment (the 3rd SDMF test) are not yet available. HEDL and other program participants are in the process of completing their RM sensor measurements and analysis for the 3rd test.

Considerable effort was expended in FY83 to prepare for the 4th SDMF Test, a nominal 18-day irradiation of selected RM, SSTR, HAFM and DM sensors in the 4/12 configuration with an SSC attached to the back of the thermal shield, see Figures 2.19 and 2.20. The KFA Laboratories in Jülich, Germany provided two archive dosimetry capsules from their materials for the 4th SDMF Metallurgy Irradiation, so that all of their previous participation in the dosimetry efforts over the last few years will also be benchmarked. Section 2.4.3.2 provides additional information on the RM, SSTR, HAFM, and/or DM sensors selected for irradiation in the 4th test. Also, a special "tungsten photo-fraction gauge experiment" was placed at the back of the 4th SDMF void box to obtain some information about photofission corrections to fission reaction rates in a cavity-like environment. Reference (Ve80) provides more information on photofission corrections.

The actual 4th SDMF irradiation started in late November and finished on December 12, 1983. NBS-certified neutron fluence standards have been sent to HEDL and KFA for RM sensor counting with the dosimeters from the 4th SDMF irradiation. The nuclear reactions involved are $^{238}U(dep)(n,f)$ FP(Ba-La), $^{58}Ni(n,p)^{58}Co$, and $^{54}Fe(n,p)^{54}Mn$.

The latter two reactions were induced in pure iron and nickel foils as well as a nickel-iron alloy containing 33.6% nickel.

2.3.1.3 BSR-HSST

The metallurgical results of the 61W to 67W series have been reported in References (St82d and St82e) by ORNL. The original computer program for the

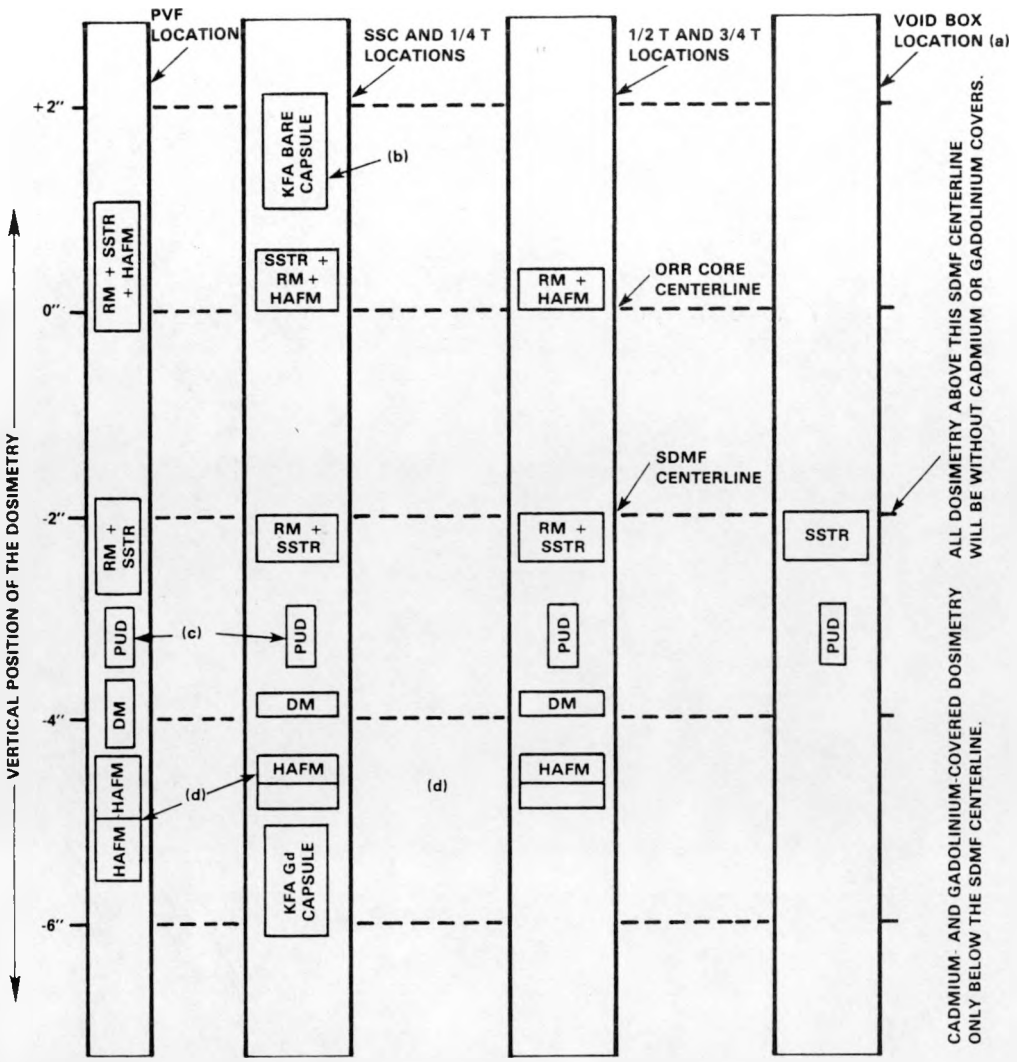

THE SIX VERTICAL TUBES WILL BE FABRICATED FROM 300-SERIES STAINLESS STEEL BY ORNL WITH THE FOLLOWING DIMENSIONS:

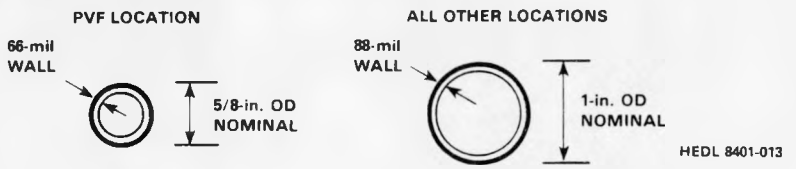

Footnotes:

[a]Dosimetry tube for the VB is located on the back of the box as opposed to through the center.

[b]KFA dosimetry will be described elsewhere. There are only two sets of capsules. One of each set is bare and 6.5 mm OD x 35 mm long. The other is gadolinium covered (0.45-mm wall thickness) and 8.5 mm OD x 42 mm long.

[c]NBS-supplied, pair uranium detectors; dimensions 670 mil OD x 150 mil thick.

[d]Plus iron gradient wires.

FIGURE 2.19. Diagram Showing the Six Vertical Tubes for Positioning Dosimetry in the SDMF and the Proposed Loading of Neutron Dosimetry for the 4th SDMF Test.

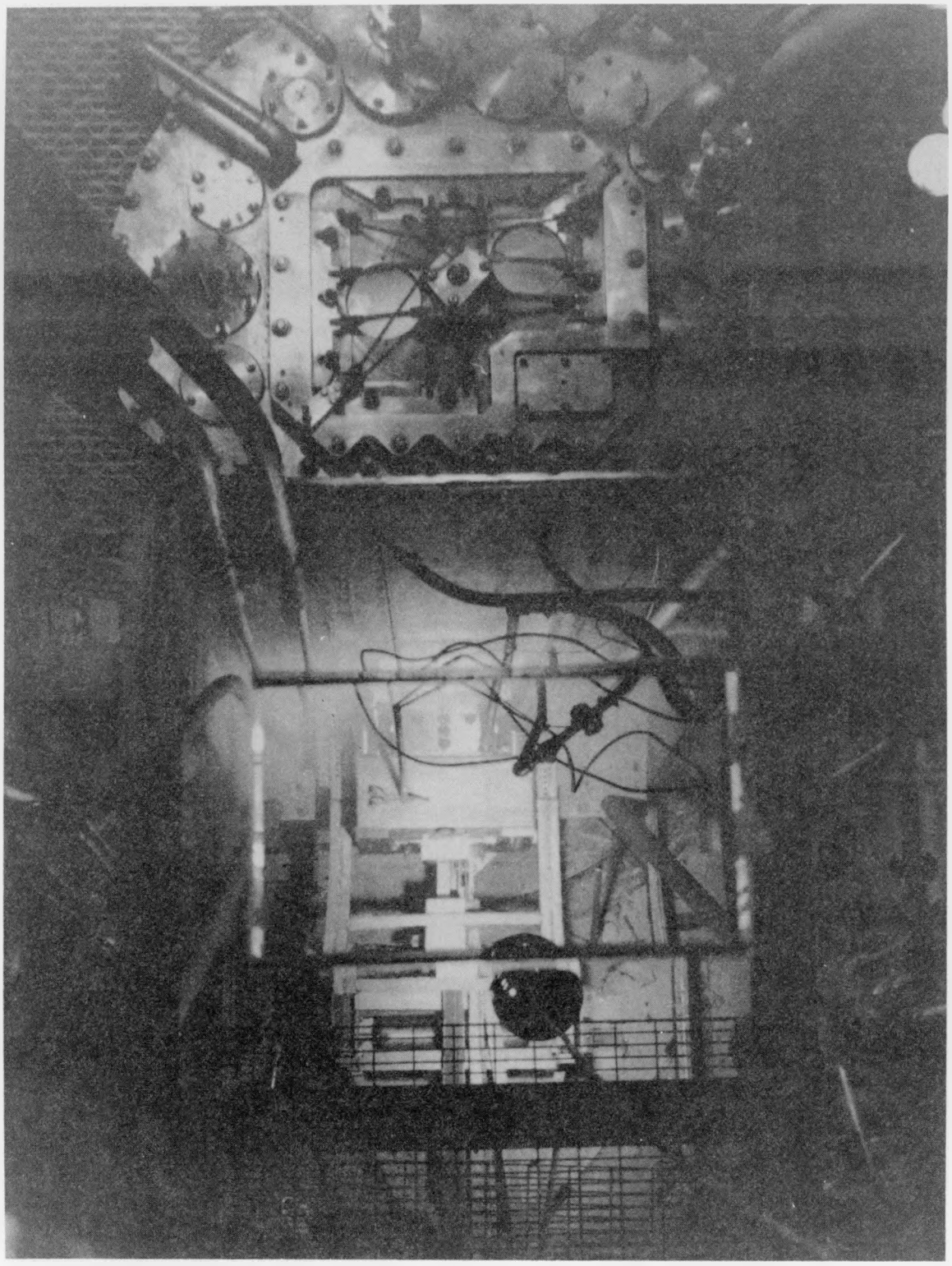

FIGURE 2.20. 4th SDMF Test with a SSC, PVB, and VB with a Tungsten Photofracture Gauge. Neg 8400017-1

statistical analysis has been modified and generalized to include nonlinear fitting. Additional information is provided in References (Fa80a,Ka82, Ka82a,Ka82b).

2.3.1.4 SUNY-NSTF

A joint MEA-ENSA-HEDL metallurgical irradiation study is underway with metallurgical specimens being irradiated at the State University of NY (SUNY) Nuclear Science and Technology Facilities (NSTF) at Buffalo, NY.

The purpose of the experiments is to determine the effect of variations of chemical composition on the irradiation embrittlement sensitivity of alloys having a composition typical of reactor PV steels. To determine the effects of the variations of the individual elements, a base composition has been selected and extra concentrations of particular elements have been added, one, two or three elements at a time.

MEA is responsible for melts, experiment design, construction, irradiation, and Charpy/tensile tests. HEDL is responsible for small specimen compression and hardness tests, fractography and computer analysis data/interactions and the physics dosimetry characterization program, see Section 2.3.2.4.

To date, 7 main melts have been prepared and split into 4 chemically different ingots in each main melt for a total of 28 separate ingot compositions. Specimens from 16 of the 28 ingots have been irradiated and tested (Charpy), and specimens from an additional 8 ingots have been irradiated but are at present untested. The results of the initial tests are available in (Ha83). The results identify phosphorous as a detrimental element. A phosphorous saturation phenomenon was observed.

2.3.2 Calculational Program

2.3.2.1 ORR-PSF

Flux, fluence, and dosimetry calculations were made of the 2-year metallurgical Blind Test irradiation experiment performed at the ORR-PSF during the period from April 1980 to June 1982.

Early in the calculations, it became apparent that significant cycle-to-cycle variations could exist in the ORR core neutron leakages among the 52 cycles in the irradiation. In order to compare dosimetry calculations with measurements, few short cuts could be employed. Nothing short of a complete analysis, taking into consideration the source distribution of each of the 52 cycles as well as their leakages, would suffice if an accurate comparison were desired. The calculations involved use of the 3D diffusion code VENTURE for the criticality and source distribution calculations, the 2D discrete ordinates transport code DOT4, the 1D discrete ordinates transport code ANISN for the flux calculations, and several other special purpose codes written to manipulate and combine the calculated data. The end result of these calculations was the generation of a tape that contains spectral fluence information for all the locations in the two SSCs, the SPVC, and the SVBC at which the

metallurgical specimens were irradiated. Initial comparisons of calculated results with HEDL dosimetry measurements have been performed for the experiment.

Table 2.6 illustrates the variation in some saturated activities at the 1/2 T location in the SPVC. It is to be observed that the variation is as much as 40%, with cycle groups 158C + 158D and 161C representing the extremes. In addition, the spectrum changes from cycle to cycle, since the last column represents the ratio of two sensor responses with markedly different thresholds (i.e., about 0.5 MeV for Np and 6 MeV for Cu); but this variation is much less than the absolute flux variation.

By decaying each calculated saturated activity to the end of irradiation and summing over all the cycles active during the irradiation, comparisons can be made with measured activities at the end of each irradiation. Table 2.7 illustrates some of these comparisons for the first simulated surveillance capsule (SSC-1). It can be seen that the absolute axial profiles agree to within about 10%. Other comparisons in the SSC-1 agree to within about 15%.

Table 2.8 illustrates a similar comparison with results for the second simulated surveillance capsule (SSC-2). Here the agreement is within about 5%. Other comparisons in the SSC-2 agree to within about 10%. Finally, comparisons are shown in Tables 2.9 and 2.10 for Fe and Ni activities in the simulated pressure vessel capsule (SPVC) after the full 2-year irradiation. No meaningful comparisons exist yet for the simulated void box capsule (SVBC) locations.

The comparisons in Tables 2.9 and 2.10 lie within 10%, but reaffirm slight deficiencies in the iron cross sections first brought to light by the PCA and PSF Startup experiment comparisons (Wi83), which show increasing disagreement the further into the pressure vessel one goes. Comparisons of Cu, Ti, and Np dosimetry data, similar to those shown in Tables 2.9 and 2.10, all lie within 15%; with the ^{238}U data, however, a significant disagreement exists that at this time is unresolved.* From all these dosimetry comparisons, it is expected that the calculated spectral fluences on which the metallurgical analyses will be based should be accurate to within about 10%. Documentation of this work will appear in a paper for the 5th ASTM-EURATOM Symposium and in the form of a NUREG-ORNL report by R. E. Maerker and B. A. Worley, as well as in the appropriate volumes of NUREG/CR-3320, Section 2.1.2.4.

2.3.2.2 ORR-SDMF

The calculational program to determine the energy-dependent flux distribution throughout the test region for the B&W surveillance capsule perturbation experiment has been started by C. Whitmarsh of B&W.

The cross-section library to be used by ORNL to compute the source distribution for the B&W perturbation experiment has been completed. The ORNL source distribution results are expected in the first quarter of FY 1984.

---

*This disagreement has since been resolved, see (St84). The HEDL analysis by Simons, Lippincott, and Kellogg of these same data had shown that when the fission from build-in of ^{239}Pu is acounted for, agreement within reasonable uncertainty is achieved.

TABLE 2.6

CYCLE GROUP-TO-CYCLE GROUP VARIATION OF SOME SATURATED ACTIVITIES AT THE 1/2 T LOCATION, X = -5.37, Z = 0

Cycles	$^{54}Fe(n,p)$	$^{63}Cu(n,\alpha)$	$^{237}Np(n,f)$	Np/Cu
153B+153C	7.59-15*	5.87-17*	6.17-13*	1.05+4
153D	7.58-15	5.87-17	6.16-13	1.05+4
153F	7.38-15	5.71-17	5.99-13	1.05+4
153G-154C	7.83-15	6.05-17	6.35-13	1.05+4
154D-154J	7.47-15	5.79-17	6.06-13	1.05+4
155B-155F	9.15-15	7.06-17	7.42-13	1.05+4
156C-157B	8.65-15	6.68-17	6.99-13	1.05+4
157C-157E	8.82-15	6.80-17	7.14-13	1.05+4
158C+158D	9.65-15	7.45-17	7.83-13	1.05+4
158E-158G	8.24-15	6.36-17	6.64-13	1.04+4
158H-158K	8.14-15	6.33-17	6.50-13	1.03+4
159A-159C	8.42-15	6.54-17	6.73-13	1.03+4
159D-160C	7.83-15	6.10-17	6.24-13	1.02+4
160D+160E	7.27-15	4.69-17	5.76-13	1.01+4
161B	7.14-15	5.62-17	5.65-13	1.01+4
161C	6.86-15	5.40-17	5.41-13	1.00+4

*Units are reactions per atom per second at 30 MW.

TABLE 2.7

CONTRIBUTIONS OF THE CYCLE GROUPS TO THE CALCULATED SSC-1 ACTIVITIES AT THE END OF IRRADIATION AND COMPARISON WITH HEDL MEASUREMENTS

	Axial profiles at x = 0, y = 131.5 mm*					
	E_{EOI}	153B+153C	153D	153F	C_{EOI}	C/E
$^{54}Fe(n,p)$:						
z = 96.9 mm	3.70-14**	1.37-14	1.20-14	0.85-14	3.43-14	0.93
z = 62.0	4.06-14	1.44-14	1.26-14	0.91-14	3.61-14	0.89
z = -1.5	4.01-14	1.46-14	1.29-14	0.93-14	3.68-14	0.92
z = -65.0	3.87-14	1.41-14	1.24-14	0.90-14	3.55-14	0.92
z = -100.0	3.36-14	1.33-14	1.17-14	0.85-14	3.35-14	1.00
$^{58}Ni(n,p)$:						
z = 96.9 mm	1.86-13	0.60-13	0.60-13	0.50-13	1.70-13	0.91
z = 62.0	2.01-13	0.63-13	0.64-13	0.53-13	1.80-13	0.90
z = -1.5	2.04-13	0.64-13	0.65-13	0.54-13	1.83-13	0.90
z = -65.0	1.95-13	0.61-13	0.62-13	0.52-13	1.75-13	0.90
z = -100.0	1.73-13	0.58-13	0.59-13	0.49-13	1.66-13	0.96
$^{46}Ti(n,p)$:						
z = 96.9 mm	1.51-14	0.48-14	0.47-14	0.38-14	1.33-14	0.88
z = 62.0	1.63-14	0.51-14	0.50-14	0.40-14	1.41-14	0.87
z = -1.5	1.68-14	0.51-14	0.51-14	0.41-14	1.43-14	0.85
z = -65.0	1.58-14	0.50-14	0.49-14	0.40-14	1.39-14	0.88
z = -100.0	1.35-14	0.46-14	0.46-14	0.37-14	1.29-14	0.96

*All locations are based on the coordinate system defined by HEDL.

**Units are disintegrations per second per atom. Read 3.70×10^{-14}.

TABLE 2.8

CONTRIBUTIONS OF THE CYCLE GROUPS TO THE CALCULATED SSC-2 ACTIVITIES AT THE END OF IRRADIATION AND COMPARISON WITH HEDL MEASUREMENTS

	Axial profiles at x = 0, y = 131.5 mm					
	E_{EOI}	157C-157E	158C+158D	158E-158G	C_{EOI}	C/E
$^{54}Fe(n,p)$:						
z = 96.9 mm	7.09-14	2.73-14	2.24-14	2.35-14	7.32-14	1.03
z = 62.0	7.74-14	2.90-14	2.36-14	2.52-14	7.78-14	1.01
z = -1.5	7.97-14	2.96-14	2.37-14	2.67-14	8.00-14	1.00
z = -65.0	7.63-14	2.86-14	2.27-14	2.62-14	7.75-14	1.02
z = -100.0	6.53-14	2.68-14	2.13-14	2.49-14	7.30-14	1.12
$^{58}Ni(n,p)$:						
z = 96.9 mm	2.89-13	0.80-13	0.92-13	1.24-13	2.96-13	1.02
z = 62.0	3.15-13	0.84-13	0.97-13	1.33-13	3.14-13	1.00
z = -1.5	3.24-13	0.84-13	0.98-13	1.41-13	3.25-13	1.00
z = -65.0	3.09-13	0.83-13	0.94-13	1.39-13	3.16-13	1.02
z = -100.0	2.73-13	0.78-13	0.88-13	1.32-13	2.98-13	1.09
$^{46}Ti(n,p)$:						
z = 96.9 mm	2.37-14	0.69-14	0.75-14	0.97-14	2.41-14	1.02
z = 62.0	2.80-14	0.73-14	0.79-14	1.04-14	2.56-14	0.91
z = -1.5	2.81-14	0.75-14	0.80-14	1.09-14	2.64-14	0.94
z = -65.0	2.71-14	0.72-14	0.76-14	1.08-14	2.56-14	0.94
z = -100.0	2.38-14	0.68-14	0.71-14	1.02-14	2.41-14	1.01

TABLE 2.9

CONTRIBUTIONS OF THE CYCLE GROUPS TO THE CALCULATED SPVC AND SVBC ACTIVITIES AT THE END OF IRRADIATION AND COMPARISON WITH HEDL MEASUREMENTS FOR $^{54}Fe(n,p)$

Cycle group	"OT"	T/4	T/2	VEPCO
153B+153C	3.65-16	1.53-16	5.59-17	3.07-18
153D	3.21-16	1.35-16	4.92-17	2.70-18
153F	2.32-16	9.73-17	3.55-17	1.93-18
153G-154C	1.53-16	3.57-16	1.30-16	7.09-18
154D-154J	1.81-15	7.58-16	2.77-16	1.54-17
155B-155F	1.44-15	6.02-16	2.20-16	1.22-17
155G-156B	2.81-15*	1.18-15*	4.29-16*	2.38-17*
156C-157B	2.87-15	1.20-15	4.40-16	2.42-17
157C-157E	2.04-15	8.53-16	3.12-16	1.71-17
158C+158D	1.65-15	6.91-16	2.52-16	1.43-17
158E-158G	1.83-15	7.64-16	2.79-16	1.42-17
158H-158K	3.29-15	1.38-15	5.02-16	1.43-17
159A-159C	3.75-15	1.57-15	5.71-16	3.03-17
159D-160C	4.75-15	1.98-15	7.22-16	3.89-17
160D+160E	1.78-15	7.45-16	2.72-16	1.48-17
161B	2.32-15	9.72-16	3.54-16	1.89-17
161C	2.53-15	1.06-15	3.87-16	2.10-17
Sum. Calc.	3.46-14	1.45-14	5.29-15	2.88-16
Measured	3.40-14	1.51-14	5.87-15	
C/E	1.02	0.96	0.90	

*Estimated.

TABLE 2.10

CONTRIBUTIONS OF THE CYCLE GROUPS TO THE CALCULATED SPVC AND SVBC ACTIVITIES AT THE END OF IRRADIATION AND COMPARISON WITH HEDL MEASUREMENTS FOR $^{58}Ni(n,p)$

Cycle group	"OT"	T/4	T/2	VEPCO
153B+153C	6.29-18	2.69-18	1.01-18	5.52-20
153D	6.40-18	2.75-18	1.02-18	5.62-20
153F	5.34-18	2.28-18	8.55-19	4.63-20
153G-154C	2.68-17	1.15-17	4.28-18	2.32-19
154D-154J	9.71-17	4.17-17	1.56-17	8.62-19
155B-155F	1.45-16	6.19-17	2.31-17	1.28-18
155G-156B	2.95-16*	1.27-16*	4.74-17*	2.60-18*
156C-157B	7.12-16	3.05-16	1.14-16	6.26-18
157C-157E	7.54-16	3.23-16	1.21-16	6.60-18
158C+158D	8.68-16	3.73-16	1.40-16	7.86-18
158E-158G	1.24-15	5.31-16	1.98-16	1.07-17
158H-158K	3.12-15	1.34-15	4.97-16	2.68-17
159A-159C	5.44-15	2.33-15	8.67-16	4.59-17
159D-160C	1.15-14	4.93-15	1.83-15	9.82-17
160D+160E	5.92-15	2.54-15	9.48-16	5.13-17
161B	1.00-14	4.33-15	1.62-15	8.57-17
161C	1.38-14	5.87-15	2.21-15	1.19-16
Sum. Calc.	4.39-14	2.31-14	8.64-15	4.64-16
Measured	5.44-14	2.45-14	9.61-15	
C/E	0.99	0.94	0.90	

*Estimated.

2.3.2.3 BSR-HSST

The BSR-HSST irradiation experiments have been completed and the results have been documented (Be83,St83).

2.3.2.4 SUNY-NSTF

HEDL will have the lead responsibility for modeling, completing, and documenting the results for the transport calculations for the SUNY-NSTF (Buffalo, NY) MEA-ENSA-HEDL chemistry-metallurgical tests. ORNL will provide technical assistance in the use of the DOT transport code and offer suggestions as to the modeling of the core and experiment. MEA-ENSA will provide detailed information on the Buffalo irradiation rigs and their operation (i.e., materials, geometries, dimensions, tolerances, water and air gap changes resulting from temperature control, thermocouple lead gaps, etc.). The calculations are scheduled to be completed in FY 1984. HEDL will use the FERRET code to obtain dosimetry-adjusted neutron exposure parameters for this important series of metallurgical irradiations. Both HEDL and MEA-ENSA dosimetry measurement results will be available for input to the FERRET adjustment code.

2.3.3 Documentation

The documentation plans for the PSF, ORR-SDMF, BSR-HSST, and SUNY-NSTF are discussed in Section 2.3.1 through 2.3.2.

2.4 ANALYSIS AND INTERPRETATION OF POWER REACTOR SURVEILLANCE AND RESEARCH REACTOR TEST RESULTS

A primary objective of this multilaboratory program is to help in the development of statistically valid neutron radiation embrittlement data bases (NRC-MPC-EPRI-ASTM and others) (Di82,Fr78,Gu80,Gu82b,Gu82c,Gu83,Gu83a,Gu83b, Gu83c,Gu84,Ho78,Mc82c,Mp79,Od78,Od79,Od83,Pe84,Ra79,Ra81b,Ra82a,Ra83,Re77, Sc80,St80,Va81,Va82,Va83) for use in the critical evaluation of the procedures and data used for predicting the fracture toughness and embrittlement of irradiated reactor pressure vessel and support structure steels.

Analysis of existing and new additions to these data bases (from test and power reactors) has revealed that the variance of test data does not arise entirely from material variability. A substantial portion stems from lack of consistency in the application and/or shortcomings in test methods and control of important variables associated with the "reactor systems analysis," "physics-dosimetry," "metallurgy," and "fracture mechanics" disciplines (Fa82,Ga83,Gu83,Gu83a,Gu83b,Gu83c,Gu84,Gu84a,Ha82a,Ka82b,Ma78b, Ma82h,Ma83,Mc84e,Od83,Pe84,Ra83,Sc80,St82a,St82b,St82c,St82e,Va83).

Analyses of PWR surveillance capsule and research reactor data indicate that long-term LWR power plant surveillance capsule and short-term research reactor (~228°C irradiation temperature) neutron-induced property change data for steel (base metal, heat-affected zone, and weld metal) can show significantly different neutron exposure dependencies (Di82,Gu83,Gu83a, Gu83b,Gu83c,Gu84,Ma82h,Mc82,Od83,Pe84,Ra83,Sc80,St83b,Ta82,Va83). For instance, for low-flux surveillance capsule irradiated materials, the neutron-induced damage may increase at a rate per unit fluence similar to that of high-flux test reactor irradiated materials, up to some level of exposure that appears to be a function of chemistry and microstructure. At exposures above this level, the rate of embrittlement is much reduced; and it appears that the embrittlement saturates (Ma82h,Ma83). Another and more recent development is the establishment of trend curves that contain a term to account for possible thermal neutron effects (Gu82a,Mc84e), see Sections 2.4.1.1.2 and 2.4.1.3.2.

The functional forms of the chemistry term A and the slope N, of the equation $\Delta NDTT = A(\phi t)^N$, are as yet not well defined; but recent studies suggest that these forms should show a Cu and Ni effect for the "A" term, with the exposure exponent "N" assumed to be either an adjustable constant or possibly a linear function of the $\log_e(\phi t)$ (Di82,Gu83,Gu84,Od83,Pe84, Od83,Ra83,Va83). It is further concluded, at least for the present, that research reactor and surveillance capsule irradiation effects data should not be combined to predict PV steel fracture toughness and embrittlement as a function of neutron exposure without having: 1) more precisely defined and representative physics-dosimetry-metallurgy data bases, 2) a better understanding of the mechansims causing neutron damage, and 3) tested and verified exposure data and physical damage correlation models; all of which are needed for the preparation and acceptance of the ASTM E706(IE) Damage Correlation, ASTM E706(IIF) ΔNDTT Versus Fluence, and other E706 standards (see Section 2.1.1).

Summary information is presented in Sections 2.4.1 and 2.4.2 on the results of recent LWR-PV-SDIP studies associated with physics-dosimetry-metallurgy data development and testing for power reactor surveillance and research reactor irradiation effects programs.

2.4.1 Surveillance Capsule Data Development and Testing

2.4.1.1 Trend Curve Data Development

2.4.1.1.1 Equations with a Fast Neutron Term

As part of the LWR-PV Program, statistically based data correlation studies have been made by HEDL and other program participants using existing metallurgical data banks in anticipation of the analysis of new fracture toughness and embrittlement data from the BSR-HSST, SUNY-NSTF, ORR-PSF and other experiments (Di82,Fa80a,Gu83,Gu83a,Gu83b,Gu83c,Gu84,Ka82,Ka82a,Ma82g,Ma83, Mc80,Mc82c,Od83,Pe84,Ra83,Sc80,Si82a,St82a,St82c,St82d,St82e,St83,St83a, St83b,Ta82,Va83).

Work has been conducted at NRC/HEDL by Randall/Guthrie to develop accurate formulas relating irradiating embrittlement (shift in 41-joule Charpy temperature) to the chemistry and neutron exposure of the Charpy specimens. The ultimate objective of the work is to provide a means for predicting embrittlement and fracture toughness at points in the PV wall, based on chemistry information and on information obtained from Charpy specimens and dosimeters exposed in surveillance capsules (Gu83,Gu83a,Gu83b,Gu83c,Gu84, Ra83).

The more recent trend curve work has been based on surveillance data originally supplied by Randall. The neutron exposure parameters have been corrected using the results of studies by Simons as these results have become available. The chemistry values have been improved by additional information obtained from Randall after the transmission of the original data base and by information obtained from Marston of EPRI (Ma83,Ta82). The original data base supplied by Randall has been enlarged using data from newly acquired surveillance reports, including reports from Switzerland supplied by Hegedus (U180). These additions have increased the data base from 147 points (106 plate and 41 weld points) to 126 plate and 51 weld points for a total of 177 data points (Gu84). Work with the 147-data point base resulted in Charpy trend curve equations having standard deviations of 26.4°F for weld and 16.6°F for plate specimens. Addition of the later data has increased the standard deviations to 28.2°F for welds and 17.2°F for plates. This may be due to lack of sufficient time to uncover improved values of the variables in the new data.

Several improvements in the HEDL data analysis approach have been made in the last year. The use of separate weld and plate equations has allowed the attainment of a lower standard deviation for the plate equation and a more realistic standard deviation for the weld equation. The computer programs have been improved so that weld and plate equations are derived simultaneously using least-squares techniques that still allow the consideration of errors in both Charpy measurements and fluence values. The simultaneous

computation allows the computer to constrain the fluence adjustments so that specimens (plate and weld) irradiated in a common capsule receive identical fluence adjustments. As has been reported previously, the use of fluence adjustments is a unique capability of the HEDL code and produces a realistic assessment of the saturation effect, which would be overestimated (non-conservatively) by other available computer codes. Recently, the HEDL computer code has been enlarged to calculate the covariance matrices for the parameters in the Charpy formulas. A report has been written on the use of these matrices in estimating the uncertainties in the calculated temperature shifts in any specific application. This formalism provides a means to account for the accuracy of chemistry and fluence information rather than simply assuming that the uncertainty in any given application is typical of the uncertainties found in the data base used to derive the trend curve formulas.

In conformance with the procedures and in (Mc82a), the least-square trend curve analysis adapted the general form

$$\Delta T = f(\text{chemistry}) \cdot (\phi t)^N \qquad (1)$$

for the equation giving the irradiation-induced increase in the 41-joule Charpy transition temperature. As before, N was allowed to be a slowly varying function of fluence, in the form

$$N = A + B \log_e(\phi t). \qquad (2)$$

The standard deviations stated above were achieved using only copper and nickel concentrations as independent chemistry variables in f(chemistry) in Eq. (1) above. Searches for additional significant chemical variables resulted in the discovery that the inclusion of a term of the type $Cu \cdot Ni \cdot \sqrt{Si}$ resulted in a slight reduction in the standard deviation of the weld relationship for some reduced data sets with high scatter points deleted. However, even for these sets the statistical F value was only 2.97, which is not completely conclusive, and the improvement was not apparent for the full data set.

The equations found using only Cu and Ni as independent variables are:

Weld, 147-point data set (41 welds),

$$\Delta T = (582.0\ Cu - 322.3\ \sqrt{Cu \cdot Ni} + 261.3 \cdot Ni) \cdot \left(\frac{\phi t}{10^{19}}\right)^N \qquad (3)$$

$$N = 0.2868 - 0.0472 \log_e \left(\frac{\phi t}{10^{19}}\right) \qquad (4)$$

$$\sigma = 26.42°F$$

Plate, 147-point data set (106 plates),

$$\Delta T = \left[-37.8 + 539.8\ Cu + 522.2 \cdot Cu \cdot \tanh\left(\frac{0.3042 \cdot Ni}{Cu}\right)\right] \cdot \left(\frac{\phi t}{10^{19}}\right)^{N} \quad (5)$$

$$N = 0.2718 - 0.0457 \log_e\left(\frac{\phi t}{10^{19}}\right) \quad (6)$$

$$\sigma = 15.56°F$$

For the expanded 177-point data set, (126 plates and 51 welds):

Weld, 177-point data set (51 welds),

$$\Delta T = (624.0 \cdot Cu - 333.1 \sqrt{Cu \cdot Ni} + 251.2\ Ni) \cdot \left(\frac{\phi t}{10^{19}}\right)^{N} \quad (7)$$

$$N = 0.2819 - 0.0409 \log_e\left(\frac{\phi t}{10^{19}}\right) \quad (8)$$

$$\sigma = 28.2°F$$

Plate, 177-point data set (126 plates),

$$\Delta T = \left[-38.4 + 555.6\ Cu + 480.1 \cdot Cu \cdot \tanh\left(\frac{0.353 \cdot Ni}{Cu}\right)\right] \cdot \left(\frac{\phi t}{10^{19}}\right)^{N} \quad (9)$$

$$N = 0.2661 - 0.0449 \log_e\left(\frac{\phi t}{10^{19}}\right) \quad (10)$$

$$\sigma = 17.2°F$$

2.4.1.1.2 Equations with Fast and Thermal Neutron Terms

During the last year, Simons continued to analyze the dosimetry information from surveillance capsules to obtain spectral information that was used to determine the fast fluence (n/cm², E > 1.0 MeV), the thermal fluence (n/cm², E < 0.414 eV), as well as the dpa exposure values, see Table 2.11. The study used information from 42 surveillance capsules and provided the exposure values of the above types for 91 plate data points and 31 welds. The study to determine the thermal fluence was initiated because of the results of previous work by Serpan, McElroy, Alberman, Lynch, and Varsik (Al82a,Mc69,Se69,Se71,Se72,Se72a,Se73b,Se75a,Va82). As discussed in (Va82 and Mc82a), Varsik used an adjustable linear combination of saturation activities of thermal and fast neutron sensitive dosimeters as an exposure parameter. He found that the best linear combination (lowest standard deviation) used a linear combination in which individual parameters indicated an increased importance of thermal neutrons; i.e., the importance was increased beyond that anticipated from existing damage function theory. Varsik stated that his results were similar to those noted in a previous

TABLE 2.11

RE-EVALUATED EXPOSURE VALUES AND THEIR UNCERTAINTIES FOR LWR-PV SURVEILLANCE CAPSULES
[Revision of Reference (Si82a) data]

Plant	Unit	Capsule	Service Lab*	Biblio Ref	Fluence (ϕt > 1 MeV) (n/cm^2) Old	Fluence (ϕt > 1 MeV) (n/cm^2) New [% (1σ)]***	New/Old	Fluence (E < 0.414 eV) (n/cm^2)	dpa [% (1σ)]	New dpa/ϕt	dpa/s	Exposure** Time (s)
Westinghouse												
Conn. Yankee		A	BMI	(Ir70)	2.08 E+18	3.16 E+18 (12)	1.53	2.54 E+18 (18)	0.00482 (12)	1.52 E-21	9.06 E-11	5.233 E+07
Conn. Yankee		F	BMI	(Pe72)	4.04 E+18	6.06 E+18 (24)	1.50	5.43 E+18 (32)	0.00949 (27)	1.56 E-21	1.24 E-10	7.651 E+07
Conn. Yankee		H	W	(Ya67)	1.79 E+19	2.00 E+19 (24)	1.12	2.33 E+19 (19)	0.0324 (27)	1.62 E-21	1.36 E-10	2.390 E+08
San Onofre		A	SwRI	(No71)	1.20 E+19	2.86 E+19 (22)	2.38	2.05 E+19 (23)	0.0486 (27)	1.70 E-21	8.35 E-10	5.824 E+07
San Onofre		D	SwRI	(No72)	2.36 E+19	5.62 E+19 (26)	2.38	3.76 E+19 (23)	0.0944 (29)	1.68 E-21	1.06 E-09	8.881 E+07
San Onofre		F	W	(Ya79)	5.14 E+19	5.73 E+19 (14)	1.11	2.99 E+19 (28)	0.0955 (20)	1.67 E-21	3.92 E-10	2.438 E+08
Turkey Point	3	S	SwRI	(No79)	1.41 E+19	1.62 E+19 (24)	1.15	1.34 E+19 (24)	0.0255 (27)	1.57 E-21	2.33 E-10	1.095 E+08
Turkey Point	3	T	W	(Ya75)	5.68 E+18	7.01 E+18 (10)	1.23	5.12 E+18 (58)	0.0109 (12)	1.55 E-21	4.73 E-10	2.302 E+07
Turkey Point	4	S	SwRI	(No76)	1.25 E+19	1.31 E+19 (25)	1.05	1.31 E+19 (25)	0.0213 (27)	1.63 E-21	1.97 E-10	1.079 E+08
Turkey Point	4	T	SwRI	(No76)	6.05 E+18	7.54 E+18 (13)	1.25	8.40 E+18 (21)	0.0130 (13)	1.72 E-21	3.48 E-10	3.728 E+07
H. B. Robinson	2	S	W	(Ya73)	3.02 E+18	3.91 E+18 (24)	1.29	8.81 E+18 (18)	0.00615 (27)	1.57 E-21	1.06 E-10	4.209 E+07
H. B. Robinson	2	V	SwRI	(No76b)	4.51 E+18	7.24 E+18 (22)	1.61	8.96 E+18 (20)	0.0115 (25)	1.59 E-21	1.09 E-10	1.050 E+08
Surry	1	T	BMI	(Pe75)	2.50 E+18	2.86 E+18 (9)	1.14	3.57 E+18 (20)	0.00449 (12)	1.57 E-21	1.33 E-10	3.378 E+07
Surry	2	X	BMI	(Pe75a)	3.02 E+18	3.03 E+18 (11)	1.00	3.64 E+18 (20)	0.00473 (13)	1.56 E-21	1.28 E-10	3.687 E+07
North Anna	1	V	B&W	(Lo81d)	2.49 E+18	2.72 E+18 (9)	1.09	5.80 E+18 (14)	0.00411 (11)	1.51 E-21	1.15 E-10	3.570 E+07
Pr. Island	1	V	W	(Da77)	5.21 E+18	6.03 E+18 (11)	1.16	9.21 E+18 (21)	0.0102 (16)	1.69 E-21	2.41 E-10	4.248 E+07
Pr. Island	2	V	W	(Ya81)	5.49 E+18	6.74 E+18 (10)	1.23	9.75 E+18 (26)	0.0117 (13)	1.74 E-21	2.67 E-10	4.394 E+07
R. E. Ginna	1	R	W	(Ya74)	7.60 E+18	1.17 E+19 (10)	1.54	1.84 E+19 (25)	0.0215 (14)	1.83 E-21	2.59 E-10	8.328 E+07
R. E. Ginna	1	V	W	(Ma73a)	4.90 E+18	5.93 E+18 (14)	1.21	1.37 E+19 (59)	0.0102 (22)	1.72 E-21	2.20 E-10	4.612 E+07
Kewaunee		V	W	(Ya77)	5.59 E+18	6.41 E+18 (10)	1.15	1.23 E+19 (23)	0.0114 (13)	1.78 E-21	2.82 E-10	4.057 E+07
Point Beach	1	S	W	(Ya76)	--	8.45 E+18 (10)	--	1.20 E+19 (19)	0.0146 (13)	1.73 E-21	1.25 E-10	1.163 E+08
Point Beach	1	R	W	(Ya78)	2.22 E+19	2.29 E+19 (10)	1.03	2.85 E+19 (22)	0.0408 (13)	1.78 E-21	2.50 E-10	1.632 E+08
Point Beach	2	V	BMI	(Pe75b)	4.74 E+18	7.28 E+18 (11)	1.54	1.09 E+19 (18)	0.0121 (13)	1.66 E-21	2.52 E-10	4.805 E+07
Point Beach	2	T	W	(Da78a)	9.45 E+18	9.40 E+18 (10)	0.99	1.48 E+19 (21)	0.0157 (12)	1.67 E-21	1.44 E-10	1.087 E+08
Point Beach	2	R	W	(Ya79a)	2.01 E+19	2.52 E+19 (10)	1.25	4.71 E+19 (26)	0.0460 (14)	1.83 E-21	2.81 E-10	1.640 E+08
D. C. Cook	1	T	SwRI	(No77b)	1.80 E+18	2.71 E+18 (22)	1.51	3.26 E+18 (19)	0.00445 (25)	1.64 E-21	1.12 E-10	3.991 E+07
Indian Point	2	T	SwRI	(No77a)	2.02 E+18	3.28 E+18 (22)	1.62	4.01 E+18 (44)	0.00537 (27)	1.64 E-21	1.20 E-10	4.473 E+07
Indian Point	3	T	W	(Da79)	2.92 E+18	3.23 E+18 (22)	1.11	3.13 E+18 (21)	0.00520 (25)	1.61 E-21	1.23 E-10	4.211 E+07
Zion	1	T	BMI	(Pe78)	1.80 E+18	3.04 E+18 (10)	1.69	3.17 E+18 (21)	0.00488 (12)	1.61 E-21	1.29 E-10	3.789 E+07
Zion	1	U	W	(Ya81a)	8.92 E+18	1.01 E+19 (10)	1.13	8.87 E+18 (24)	0.0166 (13)	1.64 E-21	1.47 E-10	1.123 E+08
Zion	2	U	BMI	(Pe78)	2.00 E+18	2.80 E+18 (9)	1.40	3.80 E+18 (15)	0.00446 (12)	1.59 E-21	1.11 E-10	4.007 E+07
Salem	1	T	W	(Ya80)	2.56 E+18	2.84 E+18 (22)	1.11	3.26 E+18 (19)	0.00460 (25)	1.62 E-21	1.34 E-10	3.426 E+07
Combustion Engineering												
Palisades		A240	BMI	(Pe79b)	4.40 E+19	6.06 E+19 (23)	1.38	7.26 E+19 (61)	0.0972 (28)	1.60 E-21	1.36 E-09	7.130 E+07
Fort Calhoun		W225	CE	(By80)	5.10 E+18	5.83 E+18 (14)	1.14	3.09 E+19 (60)	0.00879 (18)	1.51 E-21	1.07 E-10	8.191 E+07
Maine Yankee		1	ET	(Wu75)	1.30 E+19	1.76 E+19 (19)	1.35	3.00 E+19 (29)	0.0285 (23)	1.62 E-21	1.03 E-09	2.777 E+07
Maine Yankee		2	W	(Ya81b)	8.84 E+19	7.73 E+19 (13)	0.87	1.20 E+20 (23)	0.121 (18)	1.57 E-21	8.38 E-10	1.446 E+08
Maine Yankee		W263	BMI	(Pe80)	7.10 E+18	5.67 E+18 (12)	0.82	2.67 E+19 (21)	0.00843 (14)	1.49 E-21	5.83 E-11	1.446 E+08
Babcock & Wilcox												
Oconee	1	F	B&W	(Lo75)	8.70 E+17	6.98 E+17 (21)	0.80	1.00 E+18 (13)	0.000959 (19)	1.37 E-21	3.65 E-11	2.629 E+07
Oconee	1	E	B&W	(Lo77)	1.50 E+18	1.50 E+18 (10)	1.00	2.61 E+18 (15)	0.00208 (10)	1.39 E-21	4.01 E-11	5.186 E+07
Oconee	2	C	B&W	(Lo77a)	9.43 E+17	1.01 E+18 (10)	1.07	1.55 E+18 (15)	0.00148 (11)	1.47 E-21	3.88 E-11	3.802 E+07
Oconee	3	A	B&W	(Lo77b)	7.39 E+17	8.05 E+17 (10)	1.09	1.34 E+18 (11)	0.00113 (11)	1.40 E-21	3.79 E-11	2.983 E+07
Three Mile Is.	1	E	B&W	(Lo77c)	1.07 E+18	1.09 E+18 (9)	1.02	1.90 E+18 (11)	0.00151 (9)	1.39 E-21	3.75 E-11	4.036 E+07
							Avg 1.27					

*BMI = Battelle Memorial Institute; W = Westinghouse; SwRI = Southwest Research Institute; CE = Combustion Engineering; ET = Effects Technology; B&W = Babcock and Wilcox.

**Equivalent constant power level exposure time.

***3.16 E+18 (12) means 3.16×10^{18} with a 12% (1σ) uncertainty.

study by Lynch (Ly72) and both studies suggested the presence of a transition shift "saturation" effect associated with thermal neutrons and irradiation time. For his regression analysis study, Lynch used the physics-dosimetry-metallurgy results previously developed by Serpan and McElroy, but included temperature as one additional independent variable. For his study, Varsik used the EPRI PWR and BWR power plant surveillance capsule metallurgical data base (Fr78,Mc82c,Va81,Va82,Va83).

Guthrie used the Table 2.11 exposure parameters calculated by Simons to derive Charpy trend curve formulas using the thermal neutrons as part of the neutron "dose" variable (Gu84). The data were used to generate least-squares Charpy trend curve fits for the following cases: (1a) weld formula using only dpa as the exposure parameter; (1b) the same functional form for a weld formula, but with an additional contribution of thermal neutrons added into the exposure parameter (the ratio of the mixture was common to all data but was adjusted for a best fit); (2a) similar to (1a), but using fluence E > 1.0 MeV in place of dpa; (2b) similar to (1b), but using fluence E > 1.0 MeV in place of dpa. For the plates, four fitting cases were calculated in parallel with the weld study.

Statistical F tests failed to show significant benefit from the inclusion of thermal neutrons in the plate studies. For the welds, however, the best fits occurred for the cases in which the exposure parameter was a mixture of fast fluence (or dpa) (E > 1.0 MeV) and thermal fluence. The F tests showed a significant improvement over the case in which only fast fluence (E > 1.0 MeV) or dpa were used. The values were 5.5 for the addition of a thermal term to fast fluence and 6.6 for the addition to dpa. An improvement of this amount (or better) occurs at a frequency of ~4% by chance. The derived equation using fast and thermal fluence terms and for a 31-point weld data set was (Gu84):

$$\Delta T = (581.6\ Cu - 415.8\ \sqrt{Cu \cdot Ni} + 281.3\ Ni)(Dose)^{N} \qquad (11)$$

where

$$N = 0.3370 - 0.05243\ \log_e (Dose), \qquad (12a)$$

$$Dose = \frac{(\phi t)_F}{10^{19}} + 0.3744 \cdot \frac{(\phi t)_T}{10^{19}}, \qquad (12b)$$

and $(\phi t)_F$ is the fast fluence (E > 1.0 MeV) and $(\phi t)_T$ is the thermal fluence (E < 0.414 eV) and both terms are in n/cm².

The 31-point weld data set encompassed a range of fast fluences (E > 1.0 MeV) from ~1 x 10^{18} to ~8 x 10^{19} n/cm² and thermal fluences (E < 0.414) from ~1 x 10^{18} to ~9 x 10^{19} n/cm². Equations (11) and (12), therefore, should not be used outside these fluence ranges.

The application and implications of the use of Equations (11) and (12) are considered in (Mc84e) and are briefly summarized in Section 2.4.1.3.

2.4.1.2 Trend Curve Error and Uncertainties

The use of the Charpy trend curve standard deviation as a complete error indicator assumes that the expected error in an application is typical of the error in the data base used to develop the trend curve formula. It also assumes that the error is not dependent on the values of the independent variables in the trend curve application. In Reference (Gu83b), a covariance treatment is described that overcomes these shortcomings and takes into account the estimated errors in the independent variables in the application. The method is applied to several trend curve formulas developed recently at HEDL, sources and magnitudes of errors are discussed, and covariance matrices are supplied. Separate formulas are given for plate and weld specimens. The covariance treatment assumes that the errors in the fluence are log-normal while the errors in the chemical concentrations and in the Charpy measurements are normal.

Work is continuing on the study of the implications of changes in the amount and accuracy of data in the data base and of improvements in the accuracy of the independent variables in various applications. Further work on the treatment of errors for other HEDL and University of California at Santa Barbara (USCB) trend curve formulas has been started (Gu84).

2.4.1.3 Trend Curve Data Testing and Applications

2.4.1.3.1 Equations with a Fast Neutron Term

A brief review with references to the literature of the status of international work directed towards the establishment, testing, and application of physics-dosimetry-metallurgy data bases developed from both power (PWR and BWR) and test reactors was provided in the introductory part of Section 2.4. Progress in the US, UK, France, West Germany, and other countries associated with the IAEA Working Group on Reliability of Reactor Pressure Components, EURATOM, and ASTM Committee E-10 on Nuclear Technology and Applications is discussed in References (Sc80,St79,St80a,St83a,St83b) and in a series of invited papers presented at the June 1983, Detroit, MI, ANS meeting, see Section 2.4.2.

Section 2.4.1 presented the most recent results of the joint NRC (Randall) and HEDL (Guthrie) efforts to establish improved Charpy trend curves for use in the 1984 revision of Reg. Guide 1.99 (Re77). Randall anticipates that the 1984 revision will use Cu and Ni as independent chemical variables and the Charpy shift will be a product of a chemistry factor and a fluence factor (Ra83). The chemistry factor is expected to be presented both in tabular form and as a family of curves, derived partly from recent work by Perrin (Pe84), Odette (Od83), and Guthrie (Gu83,Gu83a,Gu83b,Gu83c,Gu84) with the actual values chosen by Randall. In regions of (Cu,Ni) space having adequate data, it is expected that the Odette, Guthrie, and final Randall chemistry factors will agree quite well. In regions of sparse or missing data, intuition and judgement will play an important role.

There has been considerable discussion of methods of error propagation, see Section 2.4.1.2, above. HEDL will continue to derive formal error propagation methods using covariance matrix methods for plate and weld formulas developed by Guthrie and Odette, including Fortran codes for the calculations. In addition, methods are to be developed to formalize possible error calculation methods applicable to the curves and tables of the 1984 Revision 2 of Reg. Guide 1.99.

It is anticipated that HEDL (Guthrie) will assist NRC (Randall) in the development of Charpy upper-shelf-reduction equations in late 1984 or early 1985. The HEDL (Simons) physics-dosimetry-derived exposure parameter values (Table 2.11) will be used for the HEDL upper-shelf-energy trend curve development work; see Sections 2.1.2.3, 2.1.2.6 and 2.1.2.10 for more information on planned supporting documentation for both power and test reactor physics-dosimetry-metallurgy data bases.

It is noted that the present Table 2.11 results are based primarily on PWR surveillance capsule results. Future additions to the table will involve information developed for a number of BWR surveillance capsules. The initial BWR power plants that have been selected for study by HEDL, Quad-Cities Unit 1 (Ya81c) and Unit 2 (Ya82a) and Dresden Unit 3 (Ya82), have already been analyzed by Anderson et al. of Westinghouse as a part of an existing EPRI "Structural Mechanics Program" (Ma78b,Ma82f,Ma82g,Ma83,Ta82). In regard to the testing and application of BWR physics-dosimetry-metallurgy data, Galliani has reported on recently derived physics-dosimetry exposure parameter values for the Caorso BWR. In his report, he states that available physics calculational predictions of the flux level and fluence ($E > 1.0$ MeV) appear to be considerably higher than the derived results based on $^{54}Fe(n,p)^{54}Mn$ and $^{63}Cu(n,\alpha)^{60}Co$ measured reaction rates. More specifically he and G. Martin state:

> "The fast neutron flux measurements performed at the end of the first cycle of operation of the Boiling Water Reactor of Caorso, gave a fast neutron flux of about 2×10^8 nv, at about 90% of the nominal thermal power (2410 MW), in the location where the flux monitors were irradiated. Likewise, the fast neutron fluence was about 1×10^{16} nvt.
>
> The maximum fast neutron flux and fluence, impinging on the inner vessel wall, were estimated to be of the order of 4×10^8 nv and 2×10^{16} nvt, respectively.
>
> The values both predicted for Caorso and measured at similar plants by General Electric were considerably higher. An additional effort should be made to better understand this discrepancy."

The main point to be made here is that self-consistent and verified neutron exposure parameters with assigned uncertainties for both PWR and BWR power plants must be available to help improve the predictive capabilities for estimating changes in fracture toughness and embrittlement as nuclear power plants began to approach their EOL conditions, be it in ~32 years or longer. It is apparent from the results presented in Table 2.11 and illustrated in Figure 2.21 that significant progress is being made; however, more effort is still required to meet the stated objectives of providing neutron exposure parameter values that are accurate at the 5 to 15% (1σ) level.

2.4.1.3.2 Equations with Fast and Thermal Neutron Terms

In the discussion of trend curves in the 1982 Annual Report (Mc82a) and in Equations (3) through (10), no provision was made for possible neutron damage caused by thermal and low-energy epithermal neutrons. The development of equations for trend curves that included the use of dpa and the effect of thermal neutrons was discussed in Section 2.4.1.1. Equations (11) and (12)

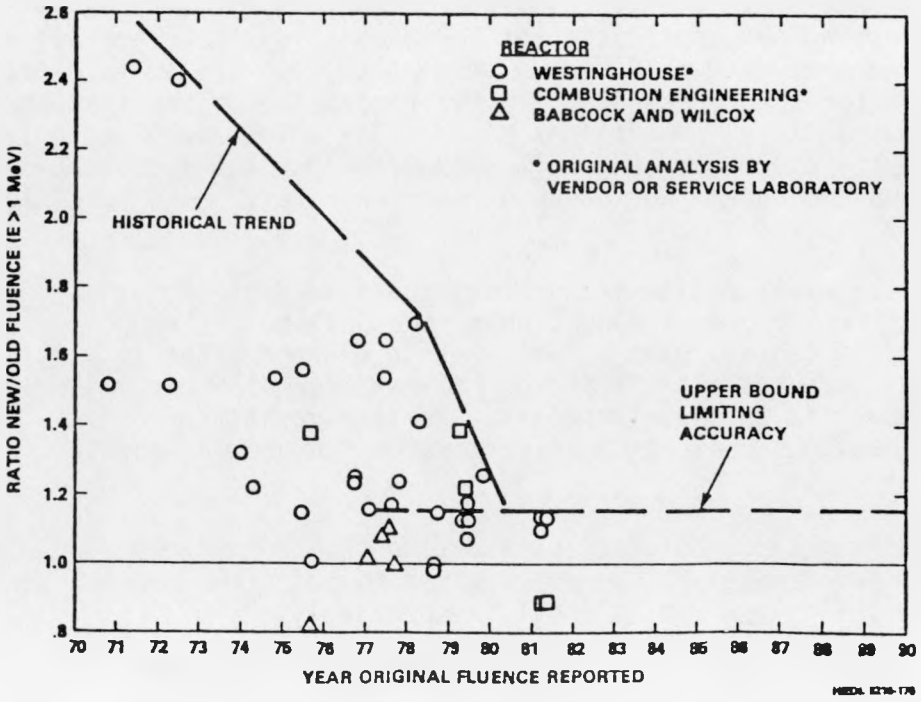

FIGURE 2.21. Ratio of New Fluence to Old Fluence as a Function of Reported Old Fluence Data [revision of Reference (Si81) data].

are examples of one type of relationship, (using fast and thermal fluence exposure parameters) that Guthrie (Gu84) generated by least-squares analysis for PWR surveillance capsule weld data on steels irradiated at ~288°C (550°F). A discussion of the application and implications of the use of Equations (11) and (12) follows. Additional and more detailed information is provided elsewhere (Mc84).

A parametric study of the application of Equations (11) and (12) for PWR and BWR surveillance capsule-derived values of the Charpy shift was completed by HEDL. The results are shown in Figure 2.22, where a lower bound for the thermal neutron relative to the fast neutron contribution to the Charpy shift (%) is given versus the fast fluence for fluence values between 10^{18} and 10^{20} n/cm². A set of curves is given for thermal-to-fast fluence ratios that vary from 0.1 up to 10, even though the data base used to generate Equations (11) and (12) was restricted to ratios between ~0.5 to ~5.

The results of the application of the Figure 2.22 set of curves to a selected number of surveillance capsules withdrawn from PWR and BWR power plants are shown in Table 2.12. The first two columns of the table give the name of the power plant and the surveillance capsule identification letter-number. Columns three, four, and five give the fast fluence, thermal fluence, and thermal/fast (T/F) ratio. The last column gives the percent thermal contribution to the Charpy shift based on the use of the Figure 2.22 set of curves. The thermal contribution to damage varies from a low of ~3% (San Onofre 1, Capsule F) to a maximum of 45% (Fort Calhoun Capsule W225). Furthermore, and as a result of the mathematical model [Equations (11) and (12)] and setting the thermal dose term to zero to obtain an estimate of its contribution to the measured Charpy shift, the thermal neutron contribution decreases dramatically and stays at or below ~15% for all values of fast fluence above ~5 x 10^{19} n/cm². Because of the non-linear form of Equations (11) and (12), the value of ~15% can only be considered as some type of lower bound for the predicted thermal neutron contribution to the measured shift. Stated another way, during the approach to saturation, when the slope N of Equation (11) is expected to possess a value near unity (Pe84), the percent contribution of the thermal fluence to the total value of the "Dose" term would also be its percent contribution to the shift. If this were the case, and for high T/F ratios, thermal neutrons could then be the dominant contributor to the measured charpy shift; i.e., at the front surface of the pressure vessel.

If Equations (11) and (12) represent a real effect and not just some combination of statistical behavior and uncertainties, it will become important to account for the effects of thermal neutrons* in establishing the present and EOL condition of PV steels because: 1) the shape of trend curves and PV wall embrittlement and toughness damage gradients recommended in future revisions of Regulatory Guide 1.99 (Re77) would be affected [as well as

---

*The possible contribution of intermediate energy neutrons to embrittlement is also discussed in Reference (Mc84).

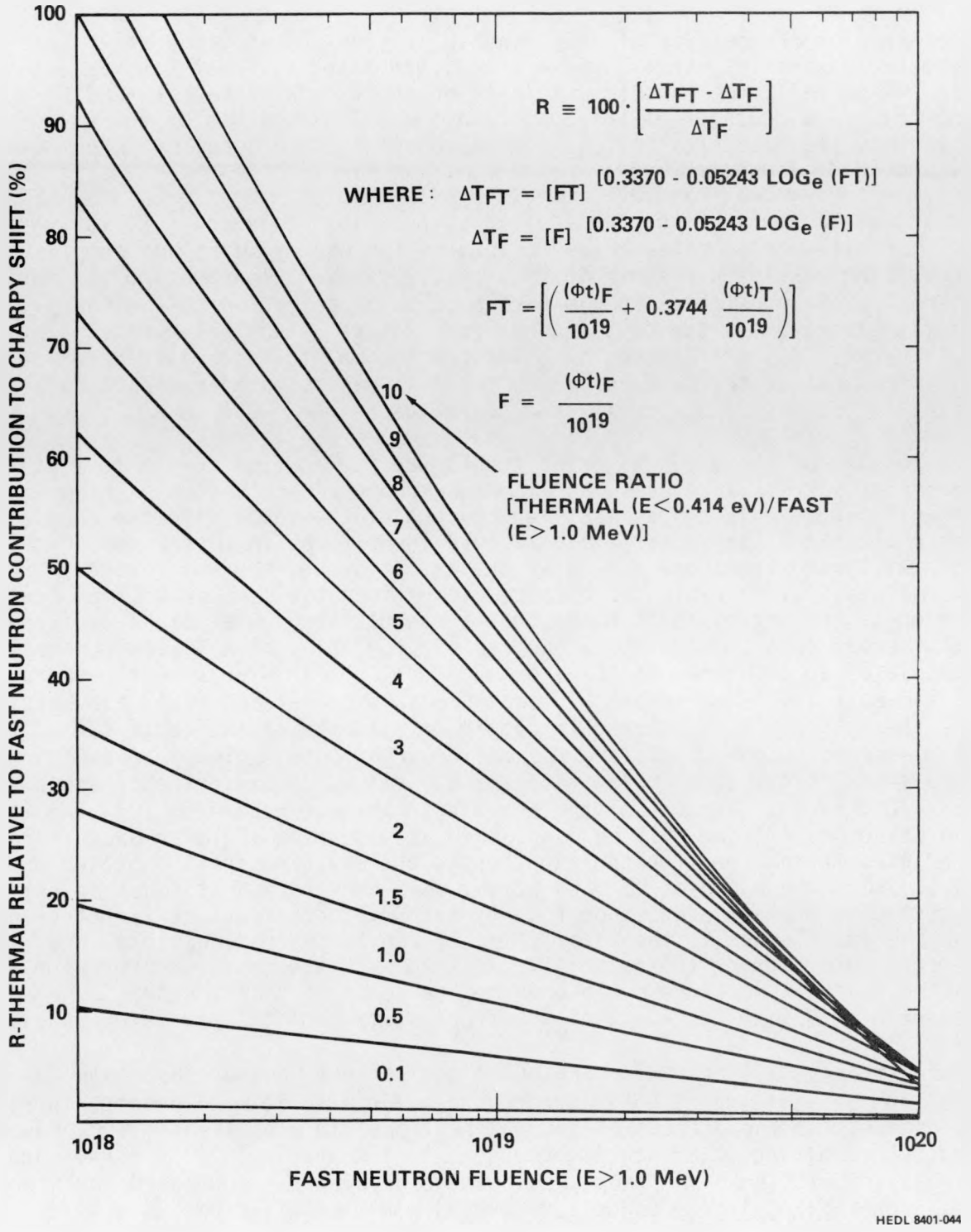

FIGURE 2.22. Thermal-Relative-to-Fast-Fluence (E > 1.0 MeV) Contribution to Charpy Shift.

TABLE 2.12

THERMAL NEUTRON CONTRIBUTION TO CHARPY SHIFT FOR SELECTED PWR AND BWR SURVEILLANCE CAPSULES

Power Plant	Type	Surveillance Capsule	Weld Material % Cu	Weld Material % Ni	Charpy Shift[a] (Predicted/ Measured)	(F) Fast Fluence 10^{19} n/cm², (E > 1.0 MeV)	(T) Thermal Fluence 10^{19} n/cm², (E < 0.414 eV)	Ratio T/F	Thermal Relative[b] to Fast Neutron Contribution (%) to Charpy Shift	Reference[c]
H. B. Robinson 2	PWR	S[d]	0.34	0.65	--	0.391	0.881	2.25	28.0	Table 2.11
H. B. Robinson 2	PWR	V	0.34	0.65	0.95	0.724	0.896	1.24	14.3	Table 2.11
Turkey Point 3	PWR	S[d]	0.31	0.57	--	1.62	1.34	0.83	7.6	Table 2.11
Turkey Point 3	PWR	T	0.31	0.57	0.99	0.701	0.512	0.73	9.1	Table 2.11
Turkey Point 4	PWR	S[d]	0.30	0.60	--	1.31	1.31	1.00	9.7	Table 2.11
Turkey Point 4	PWR	T	0.30	0.60	0.76	0.754	0.840	1.11	12.9	Table 2.11
Fort Calhoun	PWR	W225	0.35	0.60	0.91	0.583	3.09	5.31	44.5	Table 2.11
Maine Yankee	PWR	1	0.36	0.78	1.04	1.79	3.00	1.68	13.0	Table 2.11
Maine Yankee	PWR	2	0.36	0.78	1.01	7.73	12.0	1.55	4.6	Table 2.11
Maine Yankee	PWR	W263	0.36	0.78	1.08	0.567	2.67	4.71	41.7	Table 2.11
Oconee 1	PWR	F[d]	0.18	0.52	--	0.0698	0.100	1.43	29.0	Table 2.11
Oconee 1	PWR	E	0.32	0.58	1.20	0.150	0.262	1.75	29.2	Table 2.11
Oconee 2	PWR	C	0.30	0.48	1.71	0.101	0.155	1.53	28.4	Table 2.11
Point Beach 1	PWR	S	0.21	0.57	0.92	0.845	1.20	1.42	15.2	Table 2.11
Point Beach 1	PWR	R	0.21	0.57	1.17	2.29	2.85	1.24	9.2	Table 2.11
Point Beach 2	PWR	V	0.25	0.59	0.96	0.728	1.09	1.50	16.7	Table 2.11
Point Beach 2	PWR	T	0.25	0.59	1.19	0.940	1.48	1.57	15.9	Table 2.11
Point Beach 2	PWR	R	0.25	0.59	0.97	2.52	4.71	1.87	11.9	Table 2.11
Conn. Yankee	PWR	A	0.22	0.05	0.74	0.316	0.254	0.80	12.4	Table 2.11
Conn. Yankee	PWR	F[d]	0.22	0.05	--	0.606	0.543	0.90	11.4	Table 2.11
Conn. Yankee	PWR	H[d]	0.22	0.05	--	2.00	2.33	1.17	9.3	Table 2.11
Beznau II/2	PWR	R[d]	0.11	0.14	0.91	1.70	2.60	1.53	12.4	(Ul80)
Beznau II/1	PWR	V[d]	0.11	0.14	0.68	0.317	0.485[e]	1.53[e]	21.7	(Ul75)
Quad Cities 1	BWR	3[d]	0.31	0.65	0.97	2.37	4.74[e]	2.00[e]	12.9	(Ya81c)
Quad Cities 1	BWR	3[d]	0.17	0.28	0.77	3.56	7.12[e]	2.00[e]	10.2	(Ya81c)
Quad Cities 1	BWR	2[d]	0.31	0.65	1.23	0.720	1.44[e]	2.00[e]	21.1	(Ya81c)
Quad Cities 1	BWR	2[d]	0.17	0.28	1.25	0.890	1.78[e]	2.00[e]	19.6	(Ya81c)
Gundremmingen	BWR	A[d]	0.18	0.21	0.91	0.55	1.10[e]	2.00[e]	23.0	(Ei77)
Gundremmingen	BWR	B[d]	0.18	0.21	1.02	1.10	2.20[e]	2.00[e]	18.1	(Ei77)
Gundremmingen	BWR	C[d]	0.18	0.21	1.08	3.00	6.00[e]	2.00[e]	11.4	(Ei77)
Gundremmingen	BWR	D[d]	0.18	0.21	0.60	22.5	45.0[e]	2.00[e]	0.0	(Ei77)
San Onofre 1	PWR	A	0.19	0.08	1.45	2.87	2.05	0.72	5.2	Table 2.11
San Onofre 1	PWR	F	0.19	0.08	0.89	5.73	2.99	0.52	2.6	Table 2.11
Surry 1	PWR	T	0.25	0.68	0.72	0.286	0.357	1.25	18.7	Table 2.11
Surry 2	PWR	X	0.19	0.56	1.02	0.303	0.364	1.20	17.9	Table 2.11
Praire Island 1	PWR	V	0.13	0.17	2.42	0.603	0.921	1.53	18.0	Table 2.11
Praire Island 2	PWR	V	0.08	0.07	0.61	0.675	0.975	1.44	16.6	Table 2.11
R. E. Ginna 1	PWR	R	0.23	0.56	0.98	1.17	1.84	1.58	14.7	Table 2.11
R. E. Ginna 1	PWR	V	0.23	0.56	1.02	0.593	1.37	2.31	25.1	Table 2.11
Kewaunee	PWR	V	0.20	0.77	1.00	0.641	1.23	1.92	21.2	Table 2.11
D. C. Cook 1	PWR	T	0.27	0.74	1.47	0.271	0.326	1.20	18.4	Table 2.11
Indian Point 3	PWR	T	0.15	1.02	1.08	0.323	0.313	0.97	14.6	Table 2.11
Zion 1	PWR	T	0.35	0.57	1.22	0.304	0.317	1.04	15.8	Table 2.11
Zion 1	PWR	U	0.35	0.57	1.04	1.01	0.887	0.88	9.5	Table 2.11
Zion 2	PWR	U	0.28	0.55	0.87	0.280	0.380	1.36	20.3	Table 2.11
Palisades	PWR	A240	0.24	0.95	0.97	6.06	7.26	1.20	4.9	Table 2.11
Three Mile Is 1	PWR	E	0.34	0.71	0.79	0.109	0.190	1.75	31.5	Table 2.11

[a]Equation (11), prediction; "--" indicates that a measured value was not readily available.
[b]Using Figure 2.22 curves.
[c]Reference for fast and thermal fluence values.
[d]Data points not used to establish the values of the coefficients for the independent variables of Equations (5), (6), (7), and (8).
[e]Assumed value that gives relatively consistent calculated to measured Charpy shift values.

their application to the setting of NRC screening criteria associated with PV steel embrittlement and pressurized thermal shock (PTS)]; 2) an important reduction of scatter in the existing and future surveillance capsule physics-dosimetry-metallurgy data should result; 3) the thermal-to-fast-neutron-flux ratio is lowest (~0.5 to ~2.0) at accelerated surveillance capsule locations and peaks at the pressure vessel inner surface (~5.0 to 10, depending on the amount of water between the reactor core and the PV wall); 4) as a result of 3), existing trend curve formulas (based primarily on PWR surveillance capsule data) grossly under-predict the effect of thermal neutrons at the PV wall inner surface and seriously over-predict the effect at the 1/4-T, 1/2-T, etc. locations; and 5) as a result of 4), present predictions of the steel embrittlement gradient through the PV wall could be in serious error for PTS studies.

It is of interest to compare the results of Figure 2.22 with similar results obtained by Alberman (A177,A182a) for A537 steel irradiated at 60°C. Alberman found an experimental relationship between the thermal and fast (equivalent iron fission) fluences that indicated an 0.45% thermal relative to fast neutron contribution to the Charpy shift for a fast-to-thermal ratio of unity, or 4.5% for a ratio of 10. For the A537 steel used in his experiment, the derived Charpy shift equation was

$$\Delta T(°C) = 145\left[(\phi t)_{Fe} \times 10^{-19} + 4.5 \times 10^{-3} \cdot (\phi t)_T \times 10^{-19}\right]^{1/2} \quad (13)$$

where $(\phi t)_{Fe}$ is the equivalent iron fission and $(\phi t)_T$ is the thermal neutron fluence (n/cm^2). The fast, $(\phi t)_{Fe}$, and thermal, $(\phi t)_T$, fluence ranges for the irradiated Charpy specimens were from ~3 x 10^{17} to 2 x 10^{18} and ~9 x 10^{17} to 12 x 10^{20} n/cm^2, respectively.

With regard to the application and use of Equations (11), (12) and (13), it is noted that the A302B steel results of Serpan et al., for irradiation temperatures <116°C (240°F), supported a thermal neutron contribution to damage for research reactor test locations with high-thermal-to-fast (E > 1.0 MeV) neutron ratios ($\geq$ about 10); but the nonboron-containing A533B steel results of Alberman et al., did not for an irradiation temperature of ~100°C (212°F); see References (Se75a and A177). Alberman et al. did observe, however, a substantial thermal neutron effect at ~100°C for iron specimens with boron concentrations up to 5 ppm, irradiated in high-thermal to-fast-neutron flux ratios. Above the 5-ppm level, the increased boron content appeared to have little further influence on any increases in measured mechanical property. The boron content of the A302B steel used by Serpan et al. is estimated to be in the range of 1-6 ppm. Consequently (and depending on the boron content of the steel, the irradiation temperature and time at temperature, and the thermal flux levels encountered for individual surveillance or test reactor capsules), it appears that some, and perhaps a significant, contribution from thermal neutrons to the observed damage in PV steels should be anticipated.

Furthermore, if the thermal neutron contribution to the Charpy shift suggested by Equations (11) and (12) is shown to be real, a mechanism other

than just displaced atoms of iron must be contributing to the damage. For instance, such a mechansim might be associated with the interaction of thermal and epithermal neutrons with the boron in PV steels at the elevated temperature of ~288°C (550°F) encountered in most operating PWR surveillance capsules. That is, while Alberman et al. find <1% contribution from thermal neutrons to the damage in A537 steel irradiated at 60°C (with approximately equal thermal and fast fluxes), a greater relative amount of residual neutron damage might remain (after in-situ at temperature annealing) from boron (n,α) recoils and helium production than from dpa at 288°C.

The planned HEDL-RI use of the HAFM method to determine the helium content of selected irradiated Charpy specimens from SSC, SPVC, and a number of PWR surveillance capsules is expected to shed additional light on this matter; i.e., provide an estimate of the effective boron content by measurement of the helium content. This, in effect, would determine the value of the coefficient of the thermal neutron term for the different steels; i.e., provide a direct measure of any boron/helium-induced contribution to the neutron damage. RI results for the boron content of a number of PSF space-compatible compression steel specimens have been reported by Oliver and Farrar (0184). The measured boron contents are 0.65, 0.68, 0.54, 0.43, 0.52. 0.54, and 1.27 wt ppm, respectively, for the BG1 - BG7 specimens; see Figure 2.18 for the corresponding SSC-1 measured yield strength increases versus copper content. It is noted that the measurements of the helium produced in irradiated PV steel Charpy specimens is also being accomplished to determine if measured helium in scrapings from PWR pressure vessels might be used as HAFM dosimetry sensors.

Results from the above work are being used in studies associated with the verification of the procedures and data being recommended in new ASTM E706(IE) Damage Correlation, ASTM E706(IIF) ΔNDTT With Fluence, and other E706 standards.

2.4.2 Research Reactor Data Development and Testing

As part of the LWR Program, statistically based (as well as other) physics-dosimetry-metallurgy data analysis and correlation studies using research reactor data are being made by ORNL, MEA, HEDL, UCSB, and other program participants (Al82a,Au82a,Ca81,Fa80a,Fa82,Ha79,Ha82a,Ka82,Ka83,Lo82b,Ma82b, Ma82g,Ro82a,Sc80,St82a,St82c,St82d,St82e,St83,Wh83). The reader is referred to Sections 2.3.1 and 2.3.2 and the appropriate references given above for more information on the ORNL, MEA, HEDL, UCSB, and other studies. Of particular interest here is a series of invited papers presented at a special June 1983 session of the Detroit, MI, ANS Meeting (Be83,Gu83a,Lu83,Ma83, Od83,Pa83,Ra83,Va83,Wo83). Two other references of current interest are (Da83 and St83b). Summary information on the HEDL studies was provided in the 1982 Annual Report (Mc82a), and there are no new results to report at this time.

2.4.3 Benchmark Referencing Programs

Benchmark referencing studies on both the experimental and calculational aspects of the LWR-PV-SDIP are important program elements. The results of such studies are discussed and referenced throughout Sections 1.0 and 2.0. In subsequent subsections, the discussions will center on current or planned benchmark referencing studies involving NBS and other program participants.

2.4.3.1 Comparisons of Fission Rate Measurements and Fissionable Deposit Masses

Two separate experiments to compare NBS and HEDL results in the subject areas were completed in FY83 year. The first experiment, performed in the Standard ^{252}Cf Fission Spectrum at NBS, circumvented the absolute mass issue and was a blind test of fission rate measurement capability. R. Armani of ANL served as referee.

HEDL-SSTR Response Intercompared to NBS Active Fission Chamber Response

Two fission chambers were used simultaneously on either side of the ^{252}Cf source. This configuration reduces uncertainties in source-to-deposit distances and permits exposure of four deposits, each pair of which is in a back-to-back orientation separated only by 0.025 cm of stainless steel. Furthermore, a 180° rotation is made to compensate for this separation. Precise optical-bench measurements of the source-to-deposit distances are made before and after the rotation and are again checked after the experiment. In this manner, relative fission rates may be obtained to accuracies of several tenths of a percent.

To circumvent the mass issue, the relative fission rates of two HEDL and NBS deposits were actively measured in the two NBS fission chambers. This established a mass ratio. Subsequently, SSTRs were placed against one of the deposits in each chamber and were exposed to the ^{252}Cf standard neutron field. In this manner, the number of fission events seen by each SSTR was directly monitored by an active fission chamber. A total of twelve track recorders was irradiated in this manner.

Finally, as a quality control measure, the relative counting rates of the fissionable deposits were again compared to ensure that there was no loss of deposit material because of an SSTR being in contact with a deposit. The results are summarized in Table 2.2, Section 2.2.1.1. The agreement is excellent and demonstrates that the two techniques can provide absolute fission rate measurements that agree at the nominally 1% level.

Fissionable Deposit Mass Intercomparison

The fission rate comparison did not use deposits used at PCA and, as mentioned, did not compare absolute masses. Therefore, a second experiment was done that did address the masses of two HEDL and two NBS deposits. The HEDL materials were a ^{237}Np Deposit, identified now as ORNL Deposit 4, and a ^{238}U Deposit, identified as Harwell Deposit 4. The NBS materials were,

similary, a ^{237}Np Deposit 37K-5-1 and a ^{238}U Deposit 28S-4-3. Again, the comparison was accomplished by observing relative fission rates in NBS chambers of back-to-back NBS and HEDL deposits. NBS processed the data and derived masses for the HEDL deposits as shown in Tables 2.13 and 2.14. Table 2.15 gives the results of subsequent comparison reported by HEDL.

2.4.3.2 RM, SSTR, HAFM and DM Data Development and Testing

2.4.3.2.1 Certified Fluence Standards and Advanced Surveillance Dosimetry

NBS has been actively involved in supplying certified fluence standards for ex-vessel dosimetry in four commercial reactors: Maine Yankee, H. B. Robinson, ANO-1 and ANO-2, see Table 2.22. These standards tie RM and SSTR dosimetry measurements of fluence and dpa at commercial facilities to standard neutron fields, such as the ^{252}Cf and ^{235}U fission spectra at NBS and the ^{235}U fission spectrum at Mol, Belgium. Furthermore, NBS, RI and the HEDL National Reactor Dosimetry Center have been active in consulting the nuclear industry about commercial power reactor pressure vessel dosimetry and/or are participating in providing advanced RM, SSTR, HAFM, and/or DM dosimetry sensors for Maine Yankee, H. B. Robinson, Crystal River 3, Davis Besse-1, McGuire, Turkey Point 3, and Diablo Canyon Units 1 and 2. Figures 2.23 through 2.26 show a few examples of the application of advanced RM, SSTR, HAFM, and DM dosimetry sensors. As appropriate, NBS will continue to assist HEDL, RI, and other program participants in the calibration and data development and testing of advanced as well as existing state-of-the-art dosimetry measurement techniques discussed in Sections 2.2 through 2.6 and References (Gr81,Mc82a).

2.4.3.2.2 NBS and CEN/SCK Sensor Cross-Section Measurements

In the Standard ^{235}U Cavity Fission Spectrum of the BR-1 Reactor at the CEN/SCK, Mol, Belgium, a series of cross sections were measured to more closely relate this standard neutron facility to the US ^{235}U and ^{252}Cf standard neutron fission spectra at NBS. For these measurements, the neutron flux density in the Belgian facility was determined by a transfer measurement from an absolutely calibrated ^{252}Cf neutron field at NBS. The absolute calibration of the ^{252}Cf field was established by means of a manganese bath intercomparison of the ^{252}Cf neutron source and the International Standard Radium-Beryllium Neutron Source, NBS-1. The fission cross sections measured were ^{238}U, ^{235}U, ^{233}U, ^{239}Pu, ^{240}Pu, ^{237}Np, and ^{232}Th. Also included in the measurements were the $^{115}In(n,n')$ and $^{58}Ni(n,p)$ cross sections. The results of these measurements will be presented in September 1984 at the 5th ASTM-EURATOM Symposium.

2.4.3.2.3 New NBS Standard Reference Material

NBS is developing a standard iron-nickel reference material to be included in a package containing an iron-nickel alloy and pure iron and nickel foils, all irradiated in the ^{235}U standard fission spectrum to transform them into certified fluence standards. These fluence standards will assist the dosimetrist in properly counting iron in the presence of a substantial amount of nickel or nickel in the presence of unwanted iron.

TABLE 2.13

NBS DERIVATION OF MASS FOR HEDL ^{238}U FISSIONABLE DEPOSIT
USED IN PCA PHYSICS-DOSIMETRY MEASUREMENTS

1. Observed Lower- to Upper-Level Fission Chamber Discriminator Measurements*

Ratio S_l/S_u	Deposit Identification: HEDL Harwell 4	NBS 28S-4-3	Former 28S-4-3 Result
H4 Facing Source	1.0188**	1.0135	1.0137
28S Facing Source	1.0152	1.0165	1.0165

2. Ratio of Deposits Fission Rates Corrected per the Above Data***

	Harwell 4/28S-4-3
H4 Facing Source	0.8674 ± 0.85% (statistics)
28S Facing Source	0.8349 ± 0.78% (statistics)
Average Ratio:	0.8510 ± 0.60% (statistics) and 0.35% (ETZ)***

3. Self Absorption of Fissions Correction

Harwell 4: 1.03 ± 0.01
28S-4-3: 1.026 ± 0.002 (mass: 479.7 μg ± 1.1%)

4. Mass of HEDL Deposit "Harwell 4"

$$\text{Mass } (\mu g) = (0.8510 \pm 0.69\%)\left(\frac{1.03}{1.026} \pm 1\%\right)(479.7 \pm 1.1\%) = 409.6 \pm 1.6\%$$

*This ratio checks for proper fission chamber operation and indications of deposit surface roughness.
**This deposit has a 33% higher ratio than would be expected.
***Known as the Extrapolation-to-Zero (ETZ) correction for fission pulses, which occur below the discriminator setting.

TABLE 2.14

NBS DERIVATION OF MASS FOR HEDL ^{237}Np FISSIONABLE DEPOSIT
USED IN PCA PHYSICS-DOSIMETRY MEASUREMENTS

1. Observed Lower- to Upper-Level Fission Chamber Discriminator Measurements*

Ratio S_l/S_u	Deposit Identification HEDL ORNL 4	NBS 37K-5-1
04 Facing Source	1.0057	1.0171
37K Facing Source	1.0035	1.0178

2. Ratio of Deposits Fission Rates Corrected per the Above Data***

	Harwell 4/28S-4-3
04 Facing Source	0.2821 ± 0.6% (statistics)
37K Facing Source	0.2788 ± 1.2% (statistics)
Average Ratio:	0.2804 ± 0.8% (statistics) and 1.1% (ETZ)**

3. Self Absorption of Fissions Correction

ORNL 4: 1.0096 ± 0.002
37K-5-1: 1.0350 ± 0.007 (mass: 641.6 μg ± 1.4%)

4. Mass of HEDL Deposit "ORNL 4"

$$\text{Mass } (\mu g) = (0.2804 \pm 1.1\%) \left(\frac{1.0096}{1.0350} \pm 0.62\%\right) (641.6 \pm 1.4\%) = 175.5 \pm 2.0\%$$

*This ratio checks for proper fission chamber operation and indications of deposit surface roughness.
**Extrapolation-to-Zero (ETZ) uncertainty large here; statistical deviation not meaningful.
***Known as the ETZ correction for fission pulses, which occur below the discriminator setting.

TABLE 2.15

HARWELL-HEDL-NBS MASS INTERCOMPARISONS OF
^{238}U AND ^{237}Np FISSIONABLE DEPOSITS USED AT PCA

^{238}U Intercomparison (Harwell-HEDL): Activity Comparison

Deposit identification	Harwell (dpm)	HEDL (dpm)	Ratio (HEDL/Harewll)
H1	9.325 ± 1%	9.212 ± 0.99%	0.988 ± 0.013
H2	32.00 ± 1%	33.044 ± 0.83%	1.033 ± 0.013
H3	56.69 ± 1%	60.413 ± 0.50%	1.066 ± 0.011
H4	293.5 ± 5%	303.98 ± 0.89%	1.036 ± 0.013

^{238}U Intercomparison (NBS-HEDL) and (NBS-Harwell): Mass Comparison

Deposit identification	Mass NBS (μg)	Mass HEDL (μg)	Mass Ratio (NBS/HEDL)	Mass Ratio (NBS/Harwell)
H4	409.6 ± 1.6%	407.4 ± 0.8%	1.0055 ± 0.0180	1.041 ± 0.019

^{237}Np Intercomparison (NBS-HEDL): Mass Comparison

Deposit identification	Mass NBS (μg)	Mass HEDL* (μg)	Mass Ratio (NBS/HEDL)
ORNL-4	175.5 ± 2.0%	178.6 ± 0.5%	0.9835 ± 0.020

*141.01 μg/cm² x 1.2668 cm² = 178.6 μg ± 0.5%.

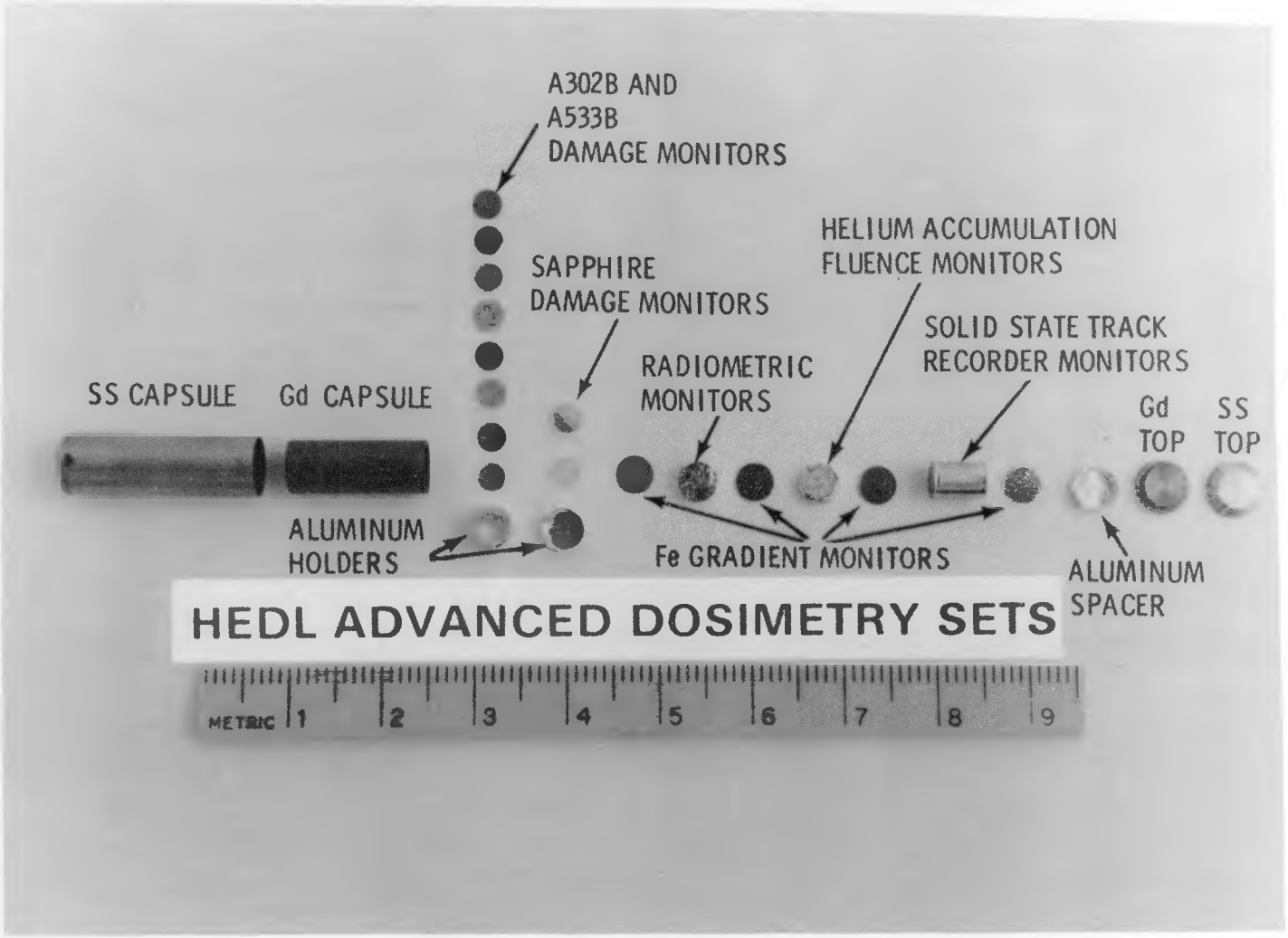

FIGURE 2.23. HEDL-RI Advanced Dosimetry Sets [taken from Reference (Mc80)]. Neg 7909355-2

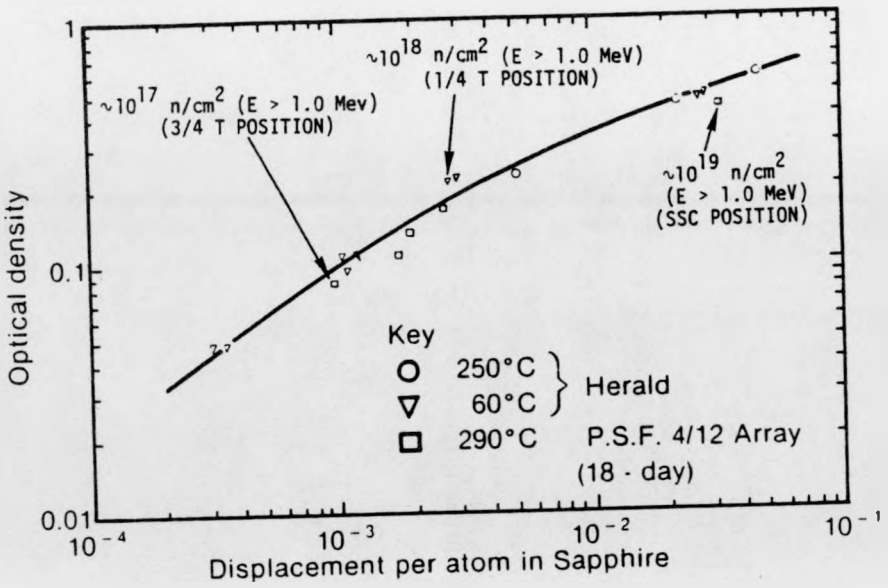

FIGURE 2.24. United Kingdom Advanced RM and DM Dosimetry Capsule and Sapphire Irradiation Damage Response [taken from Reference (Au82a)].

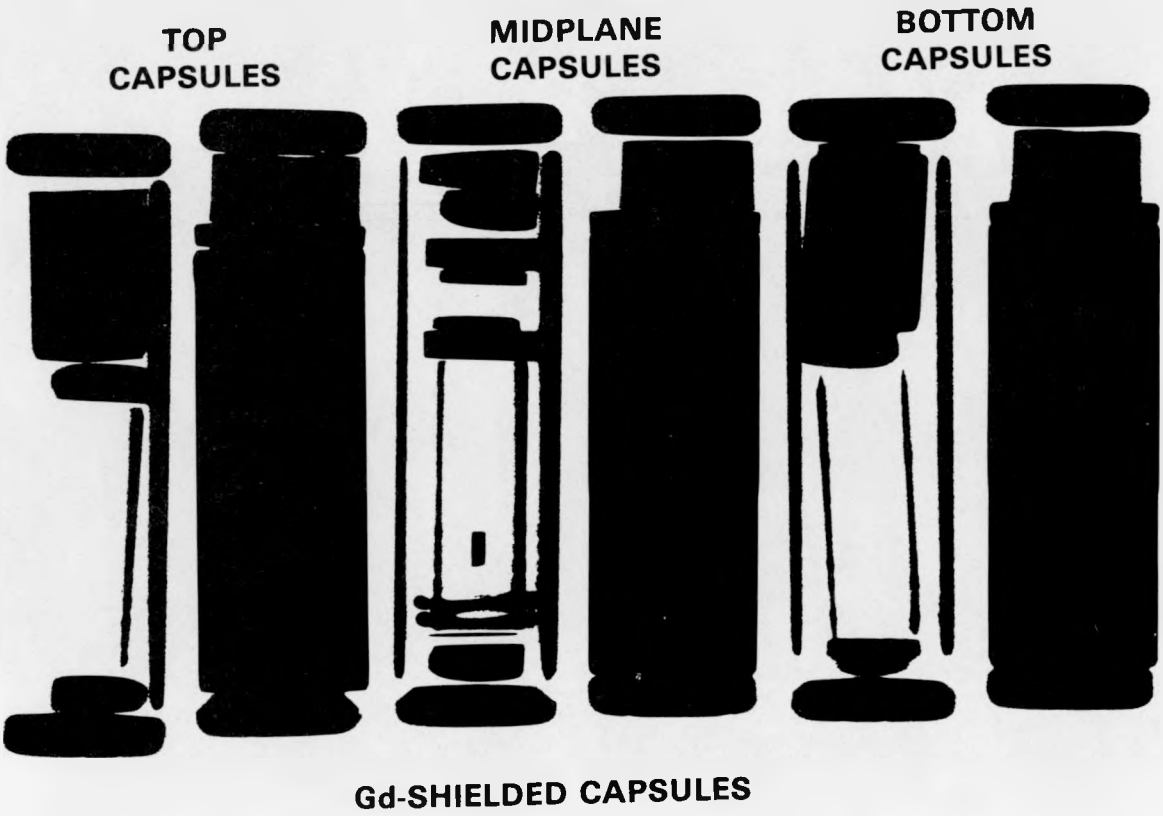

FIGURE 2.25. Quality Assurance Radiographs for Capsule Weld Integrity and Sensor Placement Verification in Maine Yankee Surveillance Capsules. Neg P17636-1

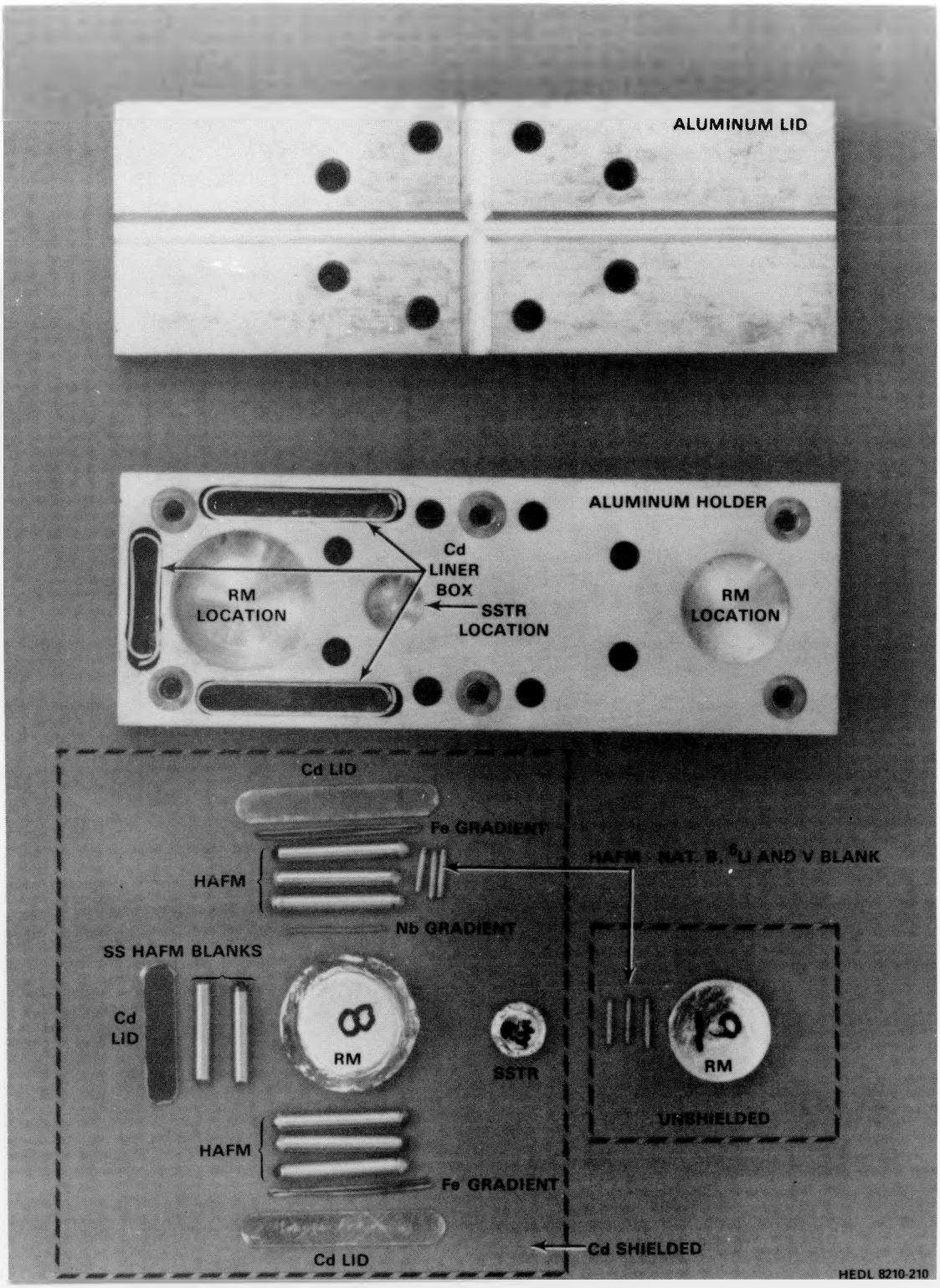

FIGURE 2.26. Maine Yankee 15° and 30° Cavity Dosimetry Holder with RM, SSTR, HAFM, and Gradient Wires Before Assembly [taken from Reference (Ma82a)]. Neg P14116-1

2.4.3.2.4 New NBS-Paired Uranium Detectors

In an attempt to offset current problems (expence and availability) of using highly depleted uranium for ^{238}U dosimetry of fast neutrons for pressure vessel and support structure surveillance, NBS has developed a paired-uranium detector system using less depleted (and much less expensive) uranium. A more cost effective and more readily available grade of ^{238}U is 200-ppm ^{235}U. It is irradiated together with a natural uranium foil which is used to determine the ^{235}U response; and therefore, the correction needed for the cheaper depleted uranium. It can be shown that for a typical ex-vessel spectrum in a commercial power plant, the ^{235}U to ^{238}U cross section ratio is ~400. Even at this level of sensitivity, the critical ^{238}U fast-neutron detector for RPV surveillance requires no more than a 10% correction for the 200-ppm ^{235}U content, and the error associated with this correction is essentially negligible. Such dosimeters will be offered for commercial use for future ex-vessel measurements in reactor power plants.

2.4.3.2.5 RM, SSTR, HAFM, and DM Sensors Irradiated in the 4th SDMF Test

Rockwell International (RI) supplied a total of 234 individual HAFM samples for the 4th SDMF Test. These consisted of 166 encapsulated HAFMs and 68 bare solid-wire HAFMs. The encapsulating material was 70% Au-30% Pt alloy material. Table 2.16 provides a summary of these materials and their planned irradiation locations during the subject test, see Figures 2.19, 2.20 and 2.23.

Harwell and RR&A supplied a total of 20 sapphire DM sensors for the 4th SDMF test, see Figures 2.19, 2.20, 2.23, and 2.25. The reader is referred to References (Au82a,Pe79,Pe79a,Pe82) for information on the current status of the development and testing of DM sensors for LWR surveillance dosimetry.

As discussed in Section 2.3.1.2, one of the main purposes of the 4th SDMF Test is to provide benchmark referencing of the primary neutron sensors used or planned for use in in-situ dosimetry for surveillance of pressure vessel and support structure steels. Table 2.17 provides a listing of HEDL and NBS nonfission and fission RM and SSTR sensors being used to benchmark the irradiation conditions for the 4th irradiation test; benchmarking will accurately define the environmental irradiation conditions for the NBS-paired uranium detectors, and the HAFM and the DM sensors.

2.4.4 VENUS, NESDIP, and DOMPAC Benchmark Experiments

2.4.4.1 VENUS PWR Core-Baffle-Barrel-Thermal Shield Benchmark

Dosimetry experiments in the PWR engineering mockup at the VENUS critical facility were carried out in the first half of 1983. A detailed description of the VENUS facility at CEN/SCK, Mol, Belgium, can be found in Section 2.5.1.1. This mockup was established to provide a relevant and practical reactor physics link between PCA/PSF tests and actual environments of PWR power plants. Indeed for actual power plants the azimuthal and vertical

TABLE 2.16

RI-HAFM SENSORS USED FOR THE 4TH SDMF TEST

Sensor Material Matrix	Physical Form	(n,He) HAFM Sensor	Approx. Mass (mg.)	Number of Capsules per Indicated SDMF Location						Thermal Neutron Shield
				SSC	PVF	1/4T	1/2T	3/4T	VB	
Al-0.7% ^{6}Li	0.5 mm-dia. wire X 1.3 cm long	^{6}Li	7	1	1	1	1	1	1	Gd + Bare
Al-0.5% B		^{10}B	7	1	1	1	1	1	1	
Al	0.50 or 0.76 mm dia. wire X 1.3 cm long	Al	7-15	1	1	1	1	1	0	(*) Gd
Fe		Fe	15-33	1	1	1	1	1	0	
Ni		Ni	18	1	1	1	1	1	1	
Cu		Cu	18-40	1	1	1	1	1	0	
Be	Sensors in Gold/Platinum Alloy** Capsules 1.27 mm dia. X 6.35 mm long	Be	1	3	3	3	3	3	3	(*) Gd
TiN		N	5	3	3	3	3	3	3	
GeO_2		O	3	3	3	3	3	3	0	
PbF_2		F	8	3	3	3	3	3	0	
PbS		S	6	3	3	3	3	3	0	
$PbCl_2$		Cl	6	3	3	3	3	3	0	
KI		K	4	3	3	3	3	3	0	
CaF_2		Ca	3	3	3	3	3	3	0	
empty	(same)	--	--	2	2	2	2	2	2	Gd

*One bare sample (capsule) at the SSC and PVF locations only.

**The 70% Au-30% Pt alloy.

TABLE 2.17

RM AND SSTR SENSORS USED FOR THE 4TH SDMF TEST

HEDL RM Sensors

The following sensors will be placed in the SSC, PVF, 1/4 T, 1/2 T and 3/4 T positions of the SDMF. The dosimetry position is behind, as opposed to in the middle center of the void box.There will be no HEDL RM sensors behind the void box.

Gadolinium-Covered Radiometric Sensors:
(One of each of the following will be in each position.) SSTRs and HAFMs will also be in these capsules.

Nonfissionable, Threshold Sensors: Ni, Ti, Cu, Nb, and Fe

Fissionable Sensors: ^{237}Np, ^{238}U, ^{235}U, and ^{232}Th

Epithermal Fluence Sensors: Co/Al and Sc

Bare Radiometric Sensors:
(One of each of the thermal and epithermal sensors, multiple Fe-flux gradient wires)

Thermal and Epithermal Fluence Sensors: Sc, Co/Asl, Ag/Al, ^{235}U

Flux Gradient Wires: Fe

NBS-Paired Uranium Detectors

	Foils per Location*	
	Cadmium-Covered**	
Position	Depleted***	Normal
SSC	1	1
PVF	1	1
1/4 T	1	1
1/2 T	1	1
3/4 T	1	1
VB	1	1
TOTAL	12 (6 pair)	

*All foils to be 1/2 in. diam. and 5 to 10 mil thick.
**All cadmium packages will be nominally 130-mil total thickness.
***Materials: Normal = 0.7% (+0.015%);
Depleted LANL 190 ppm ^{235}U (mass spec QA)

variation of the surveillance capsule lead factors can not be ignored. These variations, together with the core boundary fuel power distribution must be treated in detail, otherwise undetected biases may be entailed in calculations and prediction of EOL conditions. Such biases could even be further exacerbated by the use of advanced fuel and core management (low-leakage core) schemes where the effects of power level, fuel burnup and plutonium build-in must be handled properly to obtain reliable reactor transport physics calculational results.

2.4.4.1.1 Experimental Program

The interlaboratory experimental campaign in VENUS covered the period January to June 1983. It will be documented and fully analysed in two forthcoming NUREG/BLG reports, see Section 2.1.2.7. Within so short a time after termination of the measurements, it is not possible to present an interlaboratory synthesis. Consequently only a summary status of the present program is available from the host laboratory, CEN/SCK, at this time, and as reported at the 11th NRC WRSR Information Meeting (Fa82a).

Power Measurements and Data Normalization -- The absolute integral data compiled in the figures of Reference (Fa83a) are generally final and have been scaled to the VENUS maximum attainable core power, in terms of a NBS run-to-run monitor reading (consistent with reactor instrumentation and monitors, over ~6 decades). The corresponding absolute core power will be assessed as the best value from four independent techniques; at present, it is obtained by means of the uranium-235 fission chamber response as calibrated at NBS (E. D. McGarry) and used for definition of the PCA core power. Transport theory calculations have been normalized on the same basis.

The VENUS pin-to-pin relative fuel rating map, illustrated in (Fa83a) for the main corner assembly of interest, results from automatic ^{140}Ba-^{140}La gamma-scanning (L. Leenders); the precision is ±1.1%. Agreement with preliminary calculations and the "spot" fission chamber is excellent on the available relative scale.

Neutron Measurements -- The miniature fission chamber measurements and benchmark-field referencing of the neutronic integral data are a joint Mol-NBS undertaking (A. Fabry, E. D. McGarry et al.) but will be supplemented and confirmed by independent HEDL radiometric, Nuclear Emulsion and SSTR results (R. Gold, L. S. Kellogg et al.).

It is planned that gas-proton recoil neutron spectrometry in the three reference thimbles, V_1 to V_3 be confirmed and largely extended by $^6Li(n,\alpha)$ spectrometry (G. and S. De Leeuw, Mol); an additional thimble (at $\theta = 45°$, location of minimum azimuthal neutron flux) would be most helpful.

Gamma-Ray Measurements -- Thermoluminescent dosimetry (TLD) data by CEGB (T. Lewis) and Mol (R. Menil) will be extended and firmed-up by similar RR&A results (C. Wells-Barr; ^7LiF), by microcalorimetry (J. Mason, Imperial College, London) and by Compton-recoil gamma-ray spectroscopy (R. Gold,

J. McKnee, HEDL). Corrections for thermal neutron responses of gamma-ray sensors have been assessed carefully, but such is not yet the case for fast neutron responses.

Reference gamma-ray fields developed at BR-1 (A. Fabry) are used for validation and standardization of all these techniques.

2.4.4.1.2 Calculational Program

The design basis for the VENUS mockup is based upon two-dimensional transport theory calculations (G. Minsart) that used 6 energy groups, diagonal-transport approximation, non-final localization of core absorbers (Pyrex®), thermal shield not represented, and the old cross-section library (most data based on the 1970 KEDAK evaluation and some from the ABBN set).

State-of-the-art analyses are now in progress at Mol (G. Minsart), ORNL (M. Williams and F. B. K. Kam), and W-NTD (S. Anderson and A. Faro). A brief discussion of the recent ORNL results follows.

ORNL Calculational Program for VENUS -- A 10-group DOT-IV eigenvalue calculation of the VENUS core was performed to obtain space-dependent ^{235}U fission rate for comparison with CEN/SCK measurements. Preliminary calculation/experimental (C/E) ratios for each pin cell are shown in Figure 2.27. The normalization procedure for the calculations still requires verification of its consistency with measurements. The average disagreement between calculation and experiment is about 4%, with a measurement uncertainty of about 1%.

The worst disagreement is about 7% and tends to occur where expected (near the baffles and the Pyrex rods). There seems to be a slight power tilt in the calculations, relative to the experimental measurements. The C/Es are greater than unity near the boundary and less than one near the core center. Nevertheless, an accuracy of 5% to 6% in the relative power distribution near the core-baffle interface should be sufficient to ensure accurate pressure vessel fluence calculations. However, since these results were obtained with transport theory, an important question is how well does diffusion theory perform?

2.4.4.2 NESDIP Power-Reactor Ex-Vessel Cavity Configuration

The Nestor Shielding and Dosimetry Improvement Program (NESDIP) was successfully launched in 1983 (Au82,Au82a,Au83,Mc82a). A detailed description of the NESDIP facility at AEEW can be found in Section 2.5.1.2. NESDIP efforts have been divided into three formally scheduled phases that are discussed below.

Phase I (PCA 12/13 Replica Experiments) of the program has now been completed, and an AEEW report fully detailing the experiments will be published shortly, see Section 2.1.2.8. As reported elsewhere, calculational trends

®Pyrex is a registered trademark of Pittsburgh Corning, Pittsburgh, PA.

ORNL DWG 83-19026

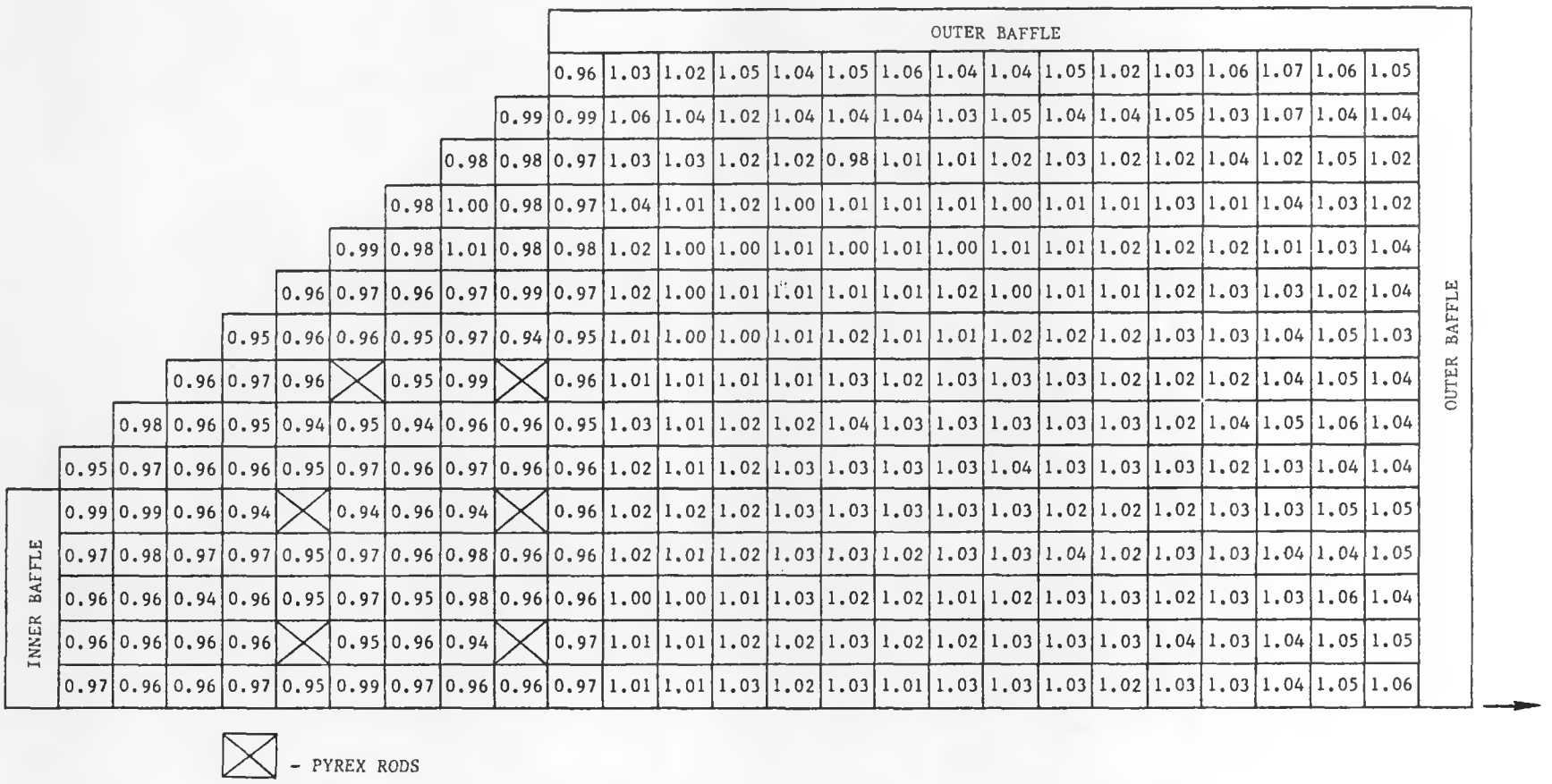

FIGURE 2.27. C/E Values for VENUS Relative Pin Power Distribution.

of the replica were at variance with those on the original ORNL PCA experiments. A joint RR&A/AEEW paper on the analysis of Phase I was presented at the 11th Water Reactor Safety Research (WRSR) Information Meeting (Au83).

Phase II of NESDIP, the lateral extension of PCA replica to 2-m^2 shields began in November 1983. This phase will be an AEEW responsibility in order to verify the extension of the original LWR-PV simulator assembly to this much larger size PV simulator.

Phase III of NESDIP, which involves the simulations of actual commercial LWR cavity configurations tailored to the requirements of the NRC and US utilities, and vendors, is scheduled to begin in Spring 1984. This will be the subject of formal agreement between NRC and AEEW since considerable US participation is entailed. In addition, timely exchange of AEEW data and analyis will be essential to meet NRC schedules. In return, AEEW has asked NRC to supply sufficient technical data including source terms to enable AEEW to calculate the γ and neutron fields within an actual PWR cavity (probably at H. B. Robinson, a Westinghouse plant operated by Carolina Power and Light Co.). Until this agreement is signed, specifics of Phase III experiments can not be further detailed.

2.4.4.2.1 Experimental Program

NRE Measurements -- Nuclear research emulsions (NRE) were exposed in February - March 1983 in the PCA replica (12/13 configuration) at NESDIP. Both Ilford and Fuji emulsions, 200 and 400-μm thick, were irradiated. A summary of these NRE irradiations can be found in Table 2.18.

All NRE have now been processed at HEDL. Adequate track density and good optical clarity were obtained in eight of the eleven irradiations. Run 4 at the 1/4-T location must be repeated as well as the A3 and 1/4 T locations of the background irradiation with the fission plate removed (Run 2). Arrangements have been made to repeat these specific exposures when the PCA replica is again available for irradiations.

SSTR Fission Rate Measurement -- Absolute ^{235}U, ^{238}U, and ^{237}Np fission rate measurements have been carried out with mica SSTR in the PCA replica at NESDIP during February - April 1983. A summary of these SSTR irradiations can be found in Table 2.19. All SSTR fission rate measurements were conducted under Cd covers except for the ^{235}U measurements performed in Run 8. Runs 4 through 11 were carried out at the calibration facility in the center of the NESTOR reactor, which is called NESSUS.

All these irradiated mica SSTR have now been processed. Most of the NESDIP/SSTR possess track densities too low for automatic scanning on the Hanford Optical Track Scanner (HOTS), i.e., less than 10^4 tracks/cm^2. Consequently, these SSTR will have to be scanned manually.

Janus Probe Gamma Spectrometry -- Continuous gamma-ray spectrometry was carried out in the PCA replica at NESDIP during February 1983. A summary of

TABLE 2.18

NRE IRRADIATIONS IN NESDIP

Date	Run No.	Locations	Power (kW)	Duration (min)	Fission Plate Status
2/25/83	1	VB	30	90	In
3/1/83	2	A3,1/4T,3/4T,VB	30	120	Out
3/1/83	3	A3	2.0	30	In
3/1/83	4	1/4T	5.6	30	In
3/1/83	5	3/4T	22.0	30	In
3/3/83	6	A3	2.0	30	In
3/3/83	7	1/4T	5.6	30	In
3/3/83	8	3/4T	22.0	30	In
3/3/83	9	A3	2.0	30	In
3/3/83	10	1/4T	5.6	30	In
3/3/83	11	VB	30	75	In

these gamma spectrometry efforts can be found in Table 2.20. Data analysis awaits completion of the high-energy Janus probe response matrix work now underway. It is anticipated that absolute spectral results will be reported up to ~6 MeV. The experimental uncertainty is ~10% (1σ) in the energy region below ~3 MeV, whereas from 3 to 6 MeV the anticipated uncertainty will be considerably higher.

Janus probe perturbation factors for the 12/13 configuration were measured by T. Lewis and P. Heffer (BNL, UK) using BeO-TLD. These results with important implications for both gamma and neutron measurements, are described and analyzed in Section 4.4 of NUREG/CR-3318.

2.4.4.2.2 Calculational Program

The design basis for the NESDIP mockups will be different than for the ORNL-PCA. The intended scope of the NESDIP effort is discussed in Section 2.5.1.2.2. In addition to the neutron studies, the NESDIP will place more emphasis on the evaluation of the gamma-ray environment within the chosen

TABLE 2.19

SSTR IRRADIATIONS IN NESDIP

Date	Run No.	Isotopes	Locations	Power (kW)	Duration (h)	Fission Plate Status
2/28/83	1	^{237}Np, ^{235}U	A3,T/V, 3/4T, VB	30	6.0	Out
3/2/83	2	^{237}Np, ^{235}U	A3,T/V, 3/4T, VB	30	7.0	In
3/4/83	3	^{237}Np, ^{235}U, ^{238}U	A3,T/V, 3/4T, VB	30	6.0	In
3/7/83	4	^{235}U	NESSUS	0.05	1.0	--
3/7/83	5	^{237}Np	NESSUS	0.44	1.0	--
3/7/83	6	^{238}U	NESSUS	0.60	1.0	--
3/15/83	8	^{235}U (bare)	NESSUS	3.3	0.5	--
3/15/83	9	^{237}Np	NESSUS	0.80	0.5	--
3/16/83	10	^{238}U	NESSUS	0.60	1.0	--
4/28/83	11	^{232}Th	NESSUS	2.0	1.0	--

experimental arrays. The results of current UK-Winfrith-RR&A calculational work are being documented, see Section 2.1.2.8. The exact involvement of LWR-PV-SDIP participants in the calculational program for NESDIP has, as yet, not been established.

2.4.4.3 DOMPAC PWR Pressure Vessel and Surveillance Capsule Benchmark

The DOMPAC dosimetry experiment is an irradiated PWR pressure vessel and surveillance capsule simulation performed in the pool of the TRITON reactor (Fortenay-aux-Roses). It was designed for radiation damage characterization inside the vessel (neutron spectrum variation) and a surveillance capsule located behind a simulated "thermal shield" of a reference PWR of the Fessenheim 1 (900-MW) type. A detailed description of the DOMPAC test facility can be found in Reference (A183). Figure 2.28 shows the DOMPAC position in relation to the overall French LWR-PV Surveillance Dosimetry Program.

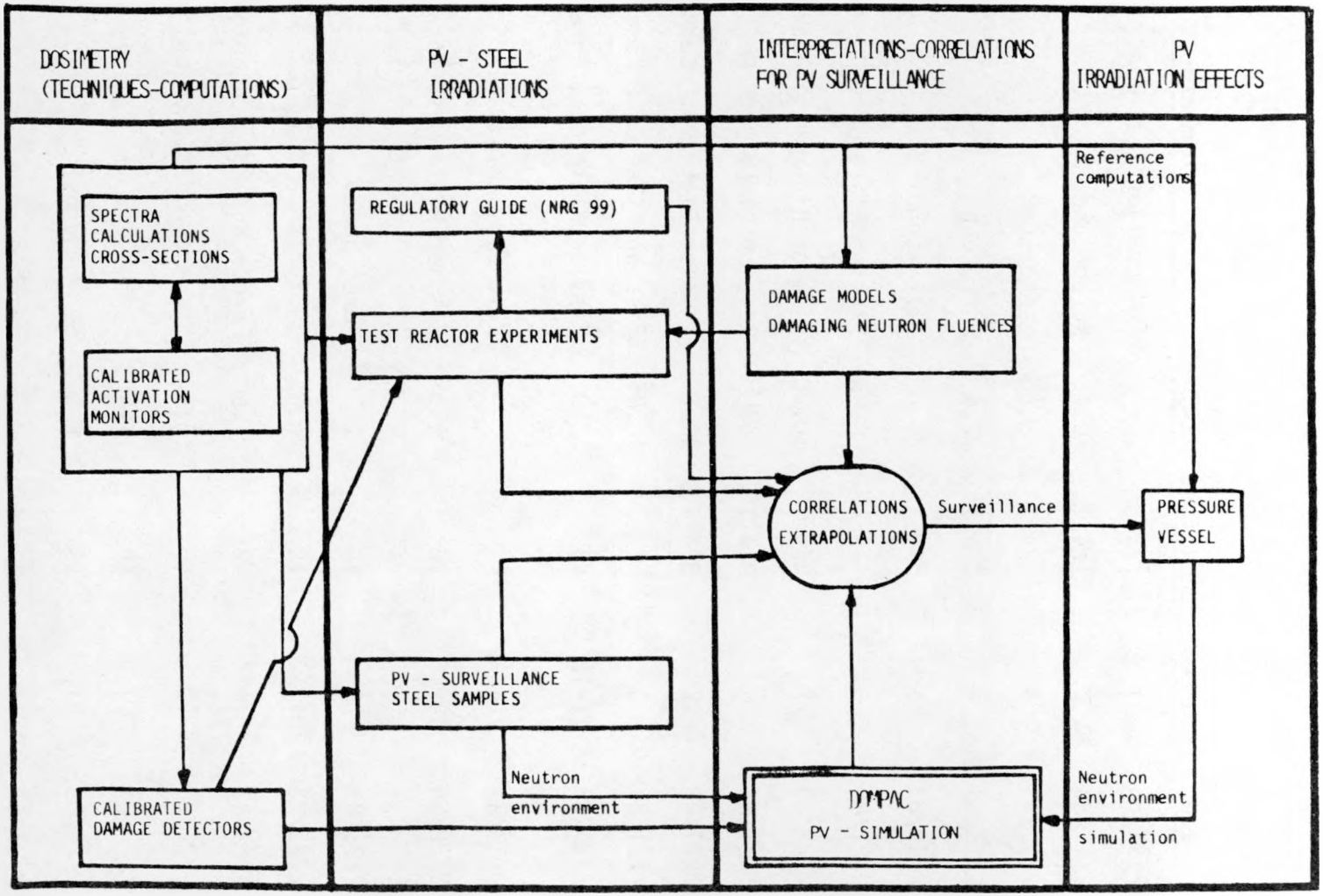

FIGURE 2.28. DOMPAC Position in LWR-PV Surveillance Dosimetry Programs.

TABLE 2.20

GAMMA-RAY SPECTROMETRY IN NESDIP

Date	Run No.	Location	Power (kW)	Comments
2/17/83	1	--	--	Calibration/Test Run
2/17/83	2	1/4 T	0.15	Foreground
2/17/83	3	1/4 T	0.60	Background
2/18/83	4	3/4 T	2.4	Foreground
2/18/83	5	3/4 T	10.0	Background
2/21/83	6	1/4 T	0.25	Fission Plate Out, Foreground
2/21/83	7	1/4 T	0.80	Fission Plate Out, Background
2/21/83	8	3/4 T	4.0	Fission Plate Out, Foreground
2/21/83	9	3/4 T	11.0	Fission Plate Out, Background
2/21/83	10	A2	0.05	Fission Plate Out, Foreground
2/21/83	11-12	VB	3.0	Fission Plate Out, Foreground CL and 28.5 cm below CL
2/22/83	13	--	--	Calibration/Test Run
2/22/83	14-15	VB	1.5	Fission Plate Out, Foreground 14 cm and 28.5 cm below CL
2/22/83	16	VB	2.5	Foreground
2/22/83	17	VB	8.0	Background
2/22/83	18	VB	1.5	Foreground 28.5 cm below CL
2/22/83	19	VB	5.0	Background 28.5 cm below CL
2/22/83	20	VB	2.5	Foreground 14 cm below CL
2/22/83	21	VB	8.0	Background 14 cm below CL
2/23/83	22	A2	0	Background
2/23/83	23	A2	0.15	Foreground
2/23/83	24	A2	0.15	Background

Passive $^{58}Ni(n,p)$, $^{54}Fe(n,p)$ and $^{63}Cu(n,\alpha)$ radiometric (RM) and graphite (GAMIN) and tungsten (W) damage monitor (DM) dosimetry measurements were performed in DOMPAC at ambient temperatures (50 to 100°C). ANISN (100-group) transport and SABINE (26-group) computations were performed for the design of DOMPAC, and the method of spectral indices was used to readjust the DOMPAC design to represent the actual water and steel configuration of Fessenheim.

The experimental RM Ni-derived flux level results were found, generally, to be in good agreement with calculated gradients inside the vessel. A 3D Monte-Carlo (TRIPOLI-code) computation has provided validation of the experimental GAMIN and W damage fluences. It also indicates a lower effective damage threshold (0.3 MeV) than expected from the theoretical iron displacement model (0.45 MeV), which also implies weaker neutron damage attenuation inside the vessel. The damage gradient in the PV wall, (evaluated experimentally by tungsten DM dosimetry), is, however, entirely consistent with that computed using steel damage models (iron dpa or probable zones).

2.4.4.3.1 Experimental Program

The DOMPAC experiment was performed in 1979 (A183). The description of the facility is given in Section 2.5.1.3. The main purpose of the experiment was the validation of the predicted damage fluences in the pressure vessel (PV) wall. The PV wall simulator was positioned in the periphery of the TRITON reactor (now shut down and replaced by OSIRIS for steel irradiation programs in Saclay) and equipped with graphite (G.A.M.I.N.) and tungsten (W) damage monitors (DM) (stack of 5 DM per location).

The DM results are based on the measurement of the electrical resistivity shift after irradiation and are correlated with nickel-activation foil measurements. Therefore, experimental damage/activation ratios are obtained. DM characteristics are given in Table 2.21.

G.A.M.I.N. and tungsten DM monitors have been routinely used for French steel irradiation programs; so damage parameter values obtained in DOMPAC must be considered as conservative reference data for damage analysis at various locations, as shown in Figure 2.28.

- Damage Detectors Results

Tungsten -- A new miniaturized tungsten (W) damage detector (Ø = 5 mm; L = 31 mm) has been developed for direct damaging neutron fluence measurements in metals without further neutron spectral computations. Further, there is a shape similarity between W and iron dpa theoretical cross sections:

$$\phi_W^f \simeq \phi_{Fe}^f$$

with the equivalent fission flux for reaction x defined as

TABLE 2.21

DAMAGE MONITOR CHARACTERISTICS

	G.A.M.I.N.	TUNGSTEN
Sample/Al container . Length	45 / 55 mm	31 / 39 mm
. Outer diameter	2.85 / 5 mm	5 / 6.5 mm
Resistor type	4 contacts	4 contacts
Typical resistance value at 25°C	40 mΩ	1 Ω
Temperature range	30°C - 180°C	30°C - 300°C
Temperature dependance	yes	no
ΔR/R min, max	1 % to 15 %	0.4% to 0,4 %
Damage fluence range ($n.cm^{-2}$)	$5.10^{15} < \phi_G < 10^{17}$	$7.10^{15} < \phi_W < 7.10^{16}$
Accuracy	1 σ < 3 % (5 samples)	1 σ < 5 % (6 samples)

$$\phi_x^f = \int_0^\infty \frac{\sigma_x}{\bar{\sigma}_x^f} (E)\ \phi(E)\ d\,E\ ,$$

where the differential neutron flux, $\phi(E)$, for cross section x averaged over the fission spectrum is given as

$$\bar{\sigma}_x^f = \int_0^\infty \sigma_x\ (E)\ \chi\ (E)\ d\,E\ .$$

Correlations obtained to date for the W response are given as

$$\rho W/Ni = \frac{\phi_W^f}{\phi_{Ni}^f} = \alpha\ s\ , \qquad \text{(spectrum index)}$$

where s is the W damage/Ni activation measured ratio. s is defined as

$$s \equiv \frac{10^{-5}\ \Delta R/R^r{}_{corr}}{A_{Ni}}\ ,$$

where $\Delta R/R^r$ is the saturation and "thermal damage" corrected relative electrical resistivity increase of irradiated W, and A_{Ni} is the number of ^{58}Ni (n,p) reactions per target atom. No temperature effect has been observed between 50°C and 300°C for the W damage monitor. An average value of $\alpha = 0.247$ ($\pm$ 0.006) is found through theoretical W dpa computations for different neutron spectra.

The important result is that the measured "s" variation in the simulator block gives the relative damage efficiency gradient.

In Table 2.22, W results per container (DM capsule) are tabulated for the simulator block midplane position; given are the: measured electrical resistivity change; cadmium ratio measured on ^{60}Co; thermal/nickel flux ratio; "fast" resistivity change (after "thermal damage" correction); saturation corrected resistivity change; S, the damage/activation ratio averaged over each container; δ relative error (1σ); and $\rho W/Ni$.

TABLE 2.22

W RESULTS PER CONTAINER

No cont	$\Delta R/R$ %	R_{Cd}	$\phi th/\phi^F_{Ni}$	$\Delta R/R^r$%	$\Delta R/R^r$ corr %	ϕ^F_{Ni} (n.cm^{-2})	s	δ	$\rho W/Ni$
1	0.214	4.1	0.69	0.190	0.195	$3.63\ 10^{16}$	5.45	2.3 %	1.35
2	0.238	5.9	0.51	0.227	0.237	$3.89\ 10^{16}$	5.98	3.4 %	1.48
4	0.129	7.1	0.43	0.125	0.125	$1.85\ 10^{16}$	7.15	3.8 %	1.77
5	0.189	12.2	0.24	0.187	0.192	$2.01\ 10^{16}$	8.53	9 %	2.11
7	0.071	7.5	0.43	0.070	0.070	$7.11\ 10^{15}$	10.22	2.9 %	2.52
Surv.	0.163	5.1	0.83	0.150	0.151	$2.42\ 10^{16}$	*6.29	2.8 %	1.55

Graphite (G.A.M.I.N.) -- Widely used for test reactor dosimetry (and especially for French PV steel irradiations since 1973), the G.A.M.I.N. detector has been fully calibrated and its response is matched to the Thompson-Wright damage function for graphite. Although spectrum analysis is needed for the determination of steel dpa from G.A.M.I.N. measurements, the two main reasons for using it were:

1) Validation/calibration of the computed graphite fluence, since

$$\rho\ G/Ni = 0.50\ (\pm 0.01)\ r$$

$$\text{with } r = \frac{10^{-7}\ \Delta R/R}{A_{Ni}}\ .$$

2) The previously established damage/activation ratio consistency of r versus s.

In Table 2.23, G.A.M.I.N. results are given per container. The following values are given for the midplane position: measured and corrected (saturation + 40°C linearization) electrtical resistivity change; temperature and Ni fluence; r, the damage/activation ratio averaged over each container; δ, the relative error (1σ); and $\rho G/Ni$.

TABLE 2.23

G.A.M.I.N. RESULTS PER CONTAINER

N° cont.	$\Delta R/R$ %	$\Delta R/R_{corr}$ %	$T_{irr.}$	Φ^{F}_{Ni} ($n.cm^{-2}$)	r	δ	$\rho G/Ni$
3	9.73	15.63	103°C	$3.95\ 10^{16}$	3.86	1.6 %	1.93
6	6.87	10.59	99°C	$2.01\ 10^{16}$	4.94	3.3 %	2.47
8	4.47	6.16	84°C	$7.62\ 10^{15}$	7.76	4.5 %	3.88
9	3.97	5.38	82°C	$7.66\ 10^{15}$	6.81	6.5 %	3.41
10	2.48	3.11	72°C	$2.94\ 10^{15}$	10.47	7 %	5.24
Surv.	7.05	7.97	58°C	$2.23\ 10^{16}$	3.40	2.6 %	1.70

"Surveillance" Radiometric Monitors -- The measured average spectrum indices are:

$$\rho^{54}Fe/^{58}Ni = 0.98 \quad (\pm 2\%), \text{ and}$$

$$\rho^{63}Cu/^{58}Ni = 1.21 \quad (\pm 2\%).$$

The cross sections used are:

$$\sigma^{f}_{Ni}\ (n/p) = 101 \text{ mbarn},$$

$$\sigma^{f}_{Fe}\ (n/p) = 73.5 \text{ mbarn, and}$$

$$\sigma^{f}_{Cu}\ (n,\alpha) = 0.44 \text{ mbarn}.$$

The damage spectrum indices measured in the steel block simulator are in good agreement with SABINE computations. The graphite response is close to

the "buckling" model; the tungsten response is close "without the buckling" model. Validation of experimental measurements will be obtained through TRIPOLI computations.

2.4.4.3.2 Calculational Program

- Optimazation of Core-Steel Simulator Block Water Gap

Neutron spectrum "softening" and consequently damaging attenuation in a steel block depends on the steel itself, of course, but also on the "incident" neutron spectrum. This last statement enables us to find a computational method; i.e., "realistic" spectrum indices in front of the block that can be matched to "standard" LWR-PV indices.

Optimization Method -- One expects to minimize calculational errors by using the same computational tools. This condition is partly met through the use of the ANISN 1-D transport code, which has been used as a reference for the Fessenheim-1 PWR calculations. This code was also used for the DOMPAC (spherical geometry) calculations in order to:

- Give a reference spectrum of neutrons leaving the TRITON-core
- Validate the SABINE removal diffusion code results used for the optimization of the water gap

SABINE - Results -- For each water gap, two SABINE runs were studied:

- "With buckling" neutron leakage through the finite lateral dimensions (except TRITON core)
- "Without buckling" infinite lateral dimensions

The reactions studied and reported relative to the ^{58}Ni (n,p) reaction are: ^{63}Cu (n,α), G (dpa), O > 1 MeV, and Fe (dpa). The results are given in Table 2.24.

Agreement for Fessenheim-1 PWR and DOMPAC could not be found for all spectral responses. Since the target was to obtain damage exposure parameters, and assuming that the DOMPAC geometry is actually between the extreme descriptions (with or without buckling), one may confidentially use the 3.65-cm water gap. This value also takes into account the "surveillance capsule" position, which is very close to the steel block; surveillance capsules are "developed" over the thermal shield, which is 2.65 cm thick in this last calculation. Hence, the actual thermal shield-block gap is 4.3 cm. Spectrum indices agreement is good for the damage "G" and "Fe" (Figure 2.29) responses in the first 1/4 T. Optimization for the exposure parameter, O > 1 MeV, would lead to a 6-cm water gap.

Comparison to W and G.A.M.I.N. damage detector measurement results, included between the two SABINE calculational descriptions, will give confidence to the Fessenheim damage computations.

TABLE 2.24

SPECTRUM INDICES OPTIMIZATION

			Cu 63			G dpa			Flux >1MeV			Fe dpa		
			Point 1	Point 2	Point 3	Point 1	Point 2	Point 3	Point 1	Point 2	Point 3	Point 1	Point 2	Point 3
P.W.R.			0.94	1.20	1.15	2.65	1.82	3.60	1.30	1.03	1.28	1.57	1.18	1.84
DOMPAC TRITON	Water gap 10cm	Buckling	0.54	0.73	0.73	1.61	1.15	1.92	1.11	0.902	1.04	1.18	0.96	1.23
		-	0.54	0.70	0.62	1.62	1.38	2.75	1.12	0.998	1.44	1.19	1.07	1.64
	Water gap 6cm	Buckling	0.54	0.65	0.64	1.62	1.35	2.25	1.12	0.986	1.13	1.19	1.06	1.36
		-	0.54	0.62	0.54	1.64	1.61	3.16	1.13	1.09	1.57	1.20	1.18	1.81
	Water gap 3,65 cm	Buckling	0.53	0.59	0.59	1.75	1.60	2.64	1.16	1.07	1.22	1.24	1.16	1.51
		-	0.52	0.56	0.48	1.82	1.91	3.66	1.19	1.20	1.71	1.27	1.30	2.02

	Point 1	Point 2	Point 3
P.W.R.	Thermal shield exit	PV entry	1/4 T PV
DOMPAC TRITON	Thermal shield exit	Steel block entry	1/4 T steel block

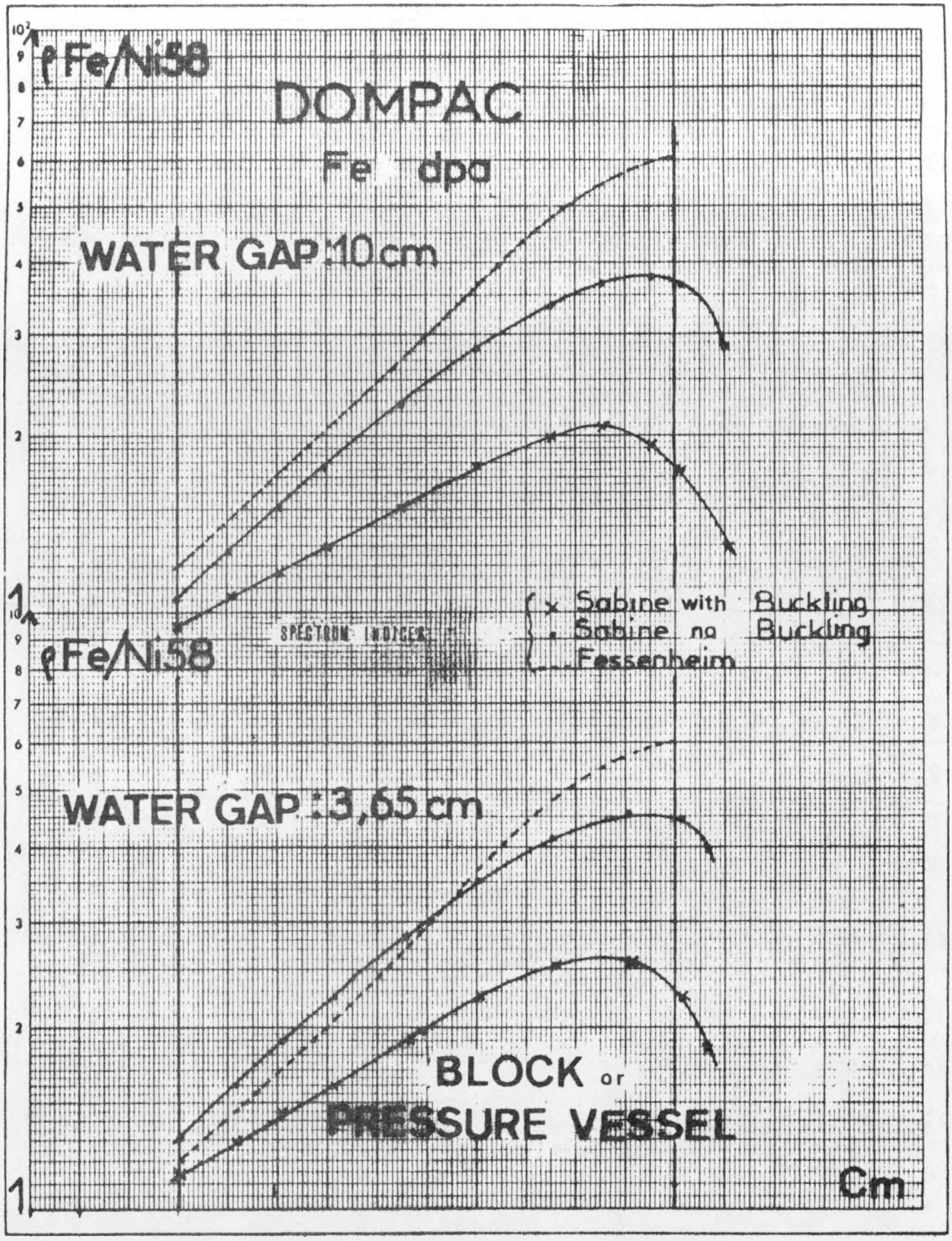

FIGURE 2.29. Iron dpa Optimization.

- TRIPOLI: Interpretation of the DOMPAC Dosimetry

Brief Description of the Method -- TRIPOLI is a 3-D Monte Carlo transport code. Volumes are homogeneous in space. Limit conditions are specified for each volume. Acceleration processes allow one to reduce statistical uncertainties. The steel block simulator has been divided into 5 x 3 x 4 volumes (Figure 2.30). Radial volumes are centered on measurement points.

UKNDL cross sections (n,n), (n,n'γ), (n,2n), (n,γ), (n,p), (n,α) are given in 155 energy groups from 14.8 MeV down to 3.5 keV (threshold for this problem). TRITON neutron sources were obtained by a diffusion code (Cranberg fission spectrum).

TRIPOLI Results -- The TRIPOLI computational results provide a good confirmation of the initial SABINE results. The TRIPOLI damaging flux (iron dpa) results fall between the SABINE extreme curves (with and without buckling). The computed spectrum indices are given in Table 2.25.

TABLE 2.25

PV TRIPOLI SPECTRUM INDICES

Axis B	Entry	1/4 T	1/2 T
$\phi > 0{,}1$ MeV / $\phi > 1$ MeV	1.52	2.26	2.63
ϕ^f_W / $\phi^f_{Fe\ d.p.a.}$	1.03	1.04	1.02
$\phi^f_{Fe\ d.p.a.}$ / $\phi > 1$ MeV	1.11	1.35	1.42

These computational results are validated by comparison to equivalent computed and measured (normalized to 6 MW) nickel fission flux values.

Good agreement is found for the graphite G.A.M.I.N. results. The tungsten dpa results are consistent for the first 1/4 wall thickness but are found to divert further in the wall.

Applicaton to Fessenheim Pressure Vessel -- Damage fluences (normalized to 1 at the PV entry) through the Fessenheim vessel wall, and calibrated by the DOMPAC assessment, are given in Figure 2.31.

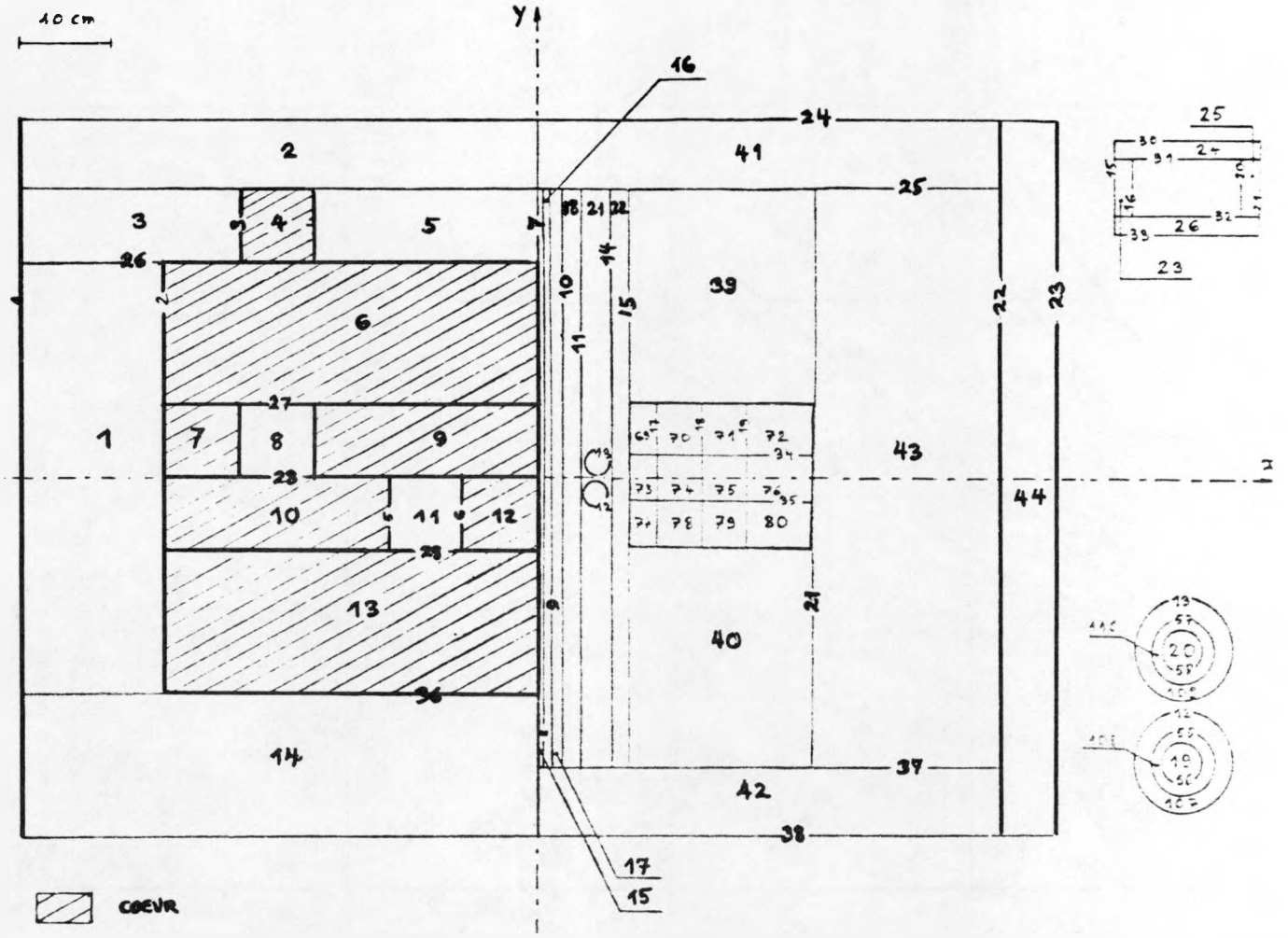

FIGURE 2.30. TRIPOLI (Monte Carlo) Description of DOMPAC.

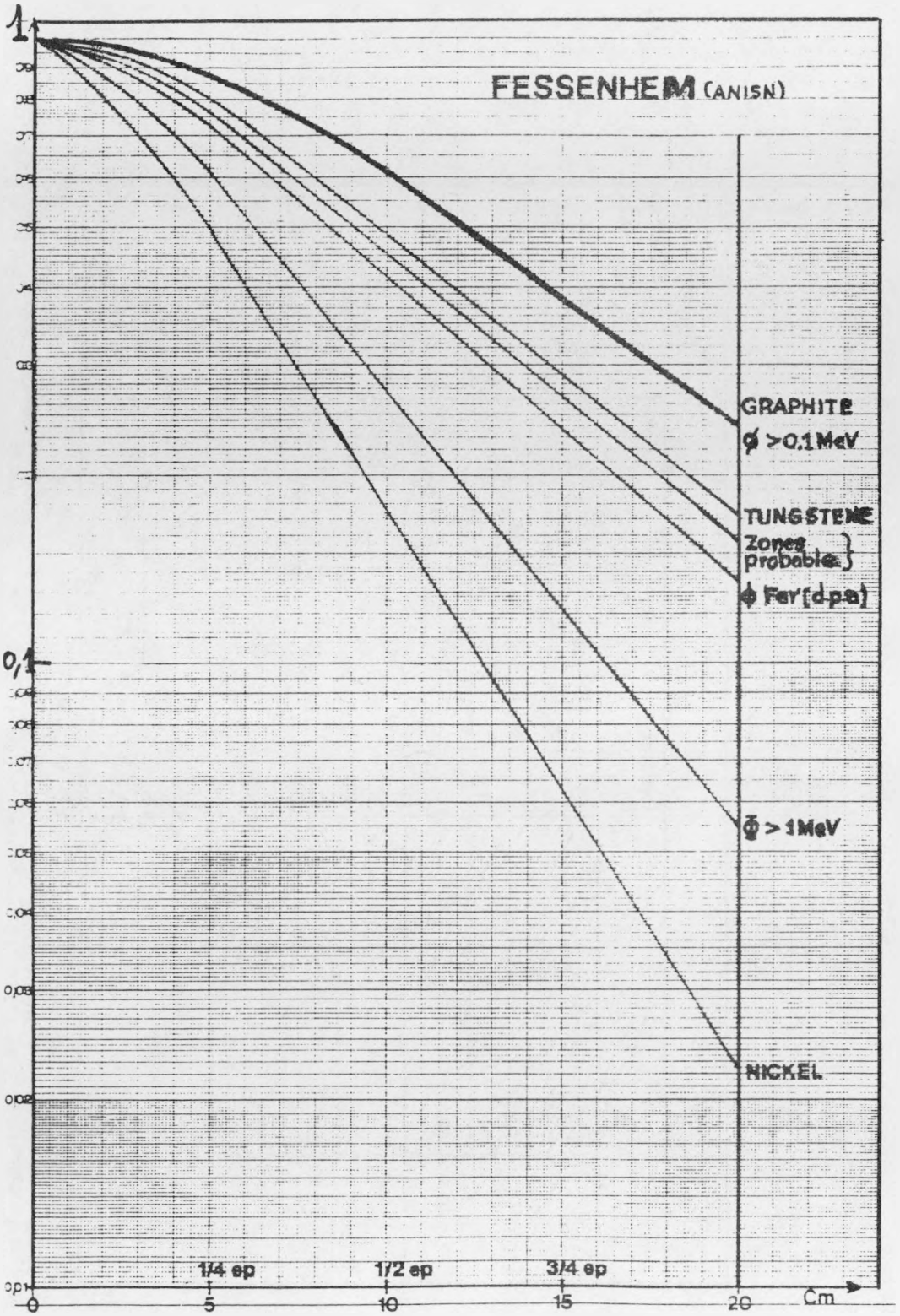

FIGURE 2.31. Damage Fluences in Fessenheim PWR-PV Wall.

Conclusions -- Damage monitor responses in the simulator block were found to be very consistent with computational predictions for the Fessenheim-1 PWR vessel. Damage fluences experimentally derived by the G.A.M.I.N. and W measurement techniques led to the following conclusions:

- Fast fluence (E > 1 MeV) is not a conservative neutron exposure parameter.
- 95% of the measured damage comes from neutrons with E > 0.1 MeV.
- The best damage correlation parameter is the damage fluence.
- The tungsten response, which theoretically is close to the steel dpa response, was found to have a somewhat lower threshold, 0.3 MeV, in the PV simulator geometry.
- The spectrum perturbation effect (dpa/fluence) in the simulated surveillance capsule was 10% at most with respect to the computed 1-D spectrum just behind the thermal shield.

2.4.5 Fifth ASTM-EURATOM International Symposium on Reactor Dosimetry

The EURATOM and ASTM program committees have completed the necessary FY83 planning for the Fifth Symposium to be held in Geesthacht, Federal Republic of Germany, September 24-28, 1984, see Reference (Mc84). An ASTM-EURATOM program committee meeting will be held in conjunction with the San Diego, CA ASTM meeting in January 1984 to establish a preliminary program based on available contributed and planned invited papers. A final program will be established in April 1984 during the 13th LWR-PV-SDIP meeting to be held at HEDL. At the request of European participants, a LWR-PV-SDIP review meeting will be held the week of October 1-5, 1984 in London, UK just after the symposium.

2.5 FACILITIES, EQUIPMENT, AND DOSIMETRY MATERIALS

2.5.1 Facilities and Programs

In order to meet the needs of the LWR-PV-SDIP, simulated LWR-PV environments have been established throughout the world. Tables 2.26 and 2.27 provide summary information on research reactor and commercial PWR and BWR neutron/gamma-ray benchmark field facilities, respectively. Each of the highly specialized research reactor and the commercial facilities has been established to address specific LWR-PV-SDIP problem areas of importance to PWR and BWR reactor design, operation, safety, and licensing and regulatory issues.

Description and use of these benchmark field facilities in the LWR-PV-SDIP have already been adequately described (Mc82a), with the exception of the three most recent facilities, namely VENUS, NESDIP, and DOMPAC. Consequently, descriptions of the VENUS, NESDIP, and DOMPAC benchmark field facilities are presented here to illustrate and highlight the very special nature of facility requirements in the LWR-PV-SDIP. Further details on the VENUS and NESDIP benchmark facilities were recently presented at the 11th WRSR Information Meeting, October 1983 [see (Fa83) and (Au83), respectively]. Detailed information on DOMPAC is provided in Reference (Al83).

TABLE 2.26

LWR-PV BENCHMARK FIELD FACILITIES*

Benchmark Field Facility	Location	Anticipated Operation Schedule	Main Purpose
$^{252}Cf/^{235}U$	NBS,US	1975-Open	Standard fields for cross-section testing and validation; emphasis is on equivalent fission flux calibrations and RM fluence counting standards.
PCA-PV	ORNL,US	1978-84	Data base for the "PCA Physics-Dosimetry Blind Test": Low-power experimental/calculational benchmark for different LWR-PV configurations; emphasis is on verification of radial neutron exposure gradients and lead factors; i.e., confirmation of radial through-wall fracture toughness and embrittlement predictions.
PSF-PV	ORNL,US	1980-84	Data base for the "PSF Physics-Dosimetry-Metallurgy Blind Test": High-power LWR-PV physics-dosimetry-metallurgical test; emphasis is on high-temperature and high-fluence simulation of PWR environmental conditions and verification of neutron damage gradients; i.e., confirmation of radial through-wall fracture toughness and embrittlement predictions.
PSF-SDMF	ORNL,US	1979-Open	High-power LWR-PV benchmark: Emphasis is on verification of surveillance capsule perturbations; specific RM, SSTR, HAFM, and DM verification tests, and quality assurance evaluations of commercial dosimetry materials and services; i.e., confirmation of the physics-dosimetry methods, procedures, and data recommended for in-situ in- and ex-vessel surveillance programs.
VENUS	CEN/SCK, Mol, Belgium	1982-Open	Low-power LWR-PV core source boundary benchmark: Emphasis is on verification of effects of new and old fuel management schemes and accuracy of azimuthal lead factors; i.e., confirmation of azimuthal PV-wall fracture toughness and embrittlement predictions.
NESDIP	AEEW, Winfrith, UK	1982-Open	Low-power LWR-PV cavity benchmark: Emphasis is on different PWR configurations and verification, via cavity measurements, of neutron exposure gradients and lead factors; i.e., confirmation of radial through-wall fracture toughness and embrittlement predictions.
DOMPAC	CEA, Fontenay, France,	1980-1983	Low-fluence experimental/calculational benchmark for a specific PWR configuration: Emphasis is on verification of surveillance capsule perturbations and PV-wall neutron exposure and damage gradients; i.e, confirmation of radial PV-wall fracture toughness and embrittlement predictions.

*Acronyms:
- AEEW - Atomic Energy Establishment (Winfrith, UK)
- CEA - Commissariat a l' Energie Atomique (France)
- CEN/SCK - Centre d' Etude de l'Energie Nucleaire-Studiecentrum voor Kernernergie (Mol, Belgium)
- DOMPAC - Triton Reactor Thermal Shield and Pressure Vessel Mockup (Fontenay-aux-Roses)
- UK - United Kingdom
- NBS - National Bureau of Standards, US
- PCA-PV - Pool Critical Assembly Physics-Dosimetry Pressure Vessel Mockup (ORNL)
- ORNL - Oak Ridge National Laboratory
- PSF-PV - Oak Ridge Research (ORR) Reactor Pool Side Facility Physics-Dosimetry-Metallurgy Pressure Vessel Mockup
- PSF-SDMF - PSF Simulated Dosimetry Measurement Facility at the ORR
- VENUS - Critical Facility (Mol, Belgium)
- NESDIP - NESTOR Reactor Surveillance Dosimetry Improvement Program Facility (Winfrith, UK)
- PWR - Pressurized Water Reactor

TABLE 2.27

POWER REACTORS BEING USED BY LWR-PV-SDIP PARTICIPANTS TO BENCHMARK PHYSICS-DOSIMETRY PROCEDURES AND DATA FOR PRESSURE VESSELS AND SUPPORT STRUCTURE SURVEILLANCE*

(Plant name; reactor type/supplier; reactor operator; ex-vessel cavity (C) and in-vessel (V) surveillance positions available)

Energy Range (MeV)	Type of Dosimeter	Dosimetry Reaction	Nuclear One-1 PWR/B&W Arkansas Power & Light		Nuclear One-2 PWR/CE Arkansas Power & Light		Brown's Ferry-3 BWR/GE Tennessee Valley Authority		H.B. Robinson PWR/WEC Carolina Power & Light		Maine Yankee PWR/CE Maine Yankee Atomic Power		Point Beach-2 PWR/WEC Wisconsin Electric Power		McGuire PWR/WEC Duke Power		CR or DB PWR/B&W		Oconee 1,2&3 PWR/B&W Duke Power [1]		BR-3 PWR/WEC Belgium	
			C	V	C	V	C	V	C	V	C	V	C	V	C	V	C	V	C	V	C	V
>1.5	RMs	$^{63}Cu(n,\alpha)^{60}Co$[f]	Y		Y	Y	Y	Y	Y	Y	Y	Y		Y	Y	Y	P	Y	P		Y	Y
		$^{46}Ti(n,p)^{46}Sc$[f]	Y		Y	Y	Y	Y	Y	Y	Y	Y			Y		P	P	PYJ		Y	Y
		$^{54}Fe(n,p)^{54}Mn$[f]	Y	Y	Y	Y	Y	Y	Y	Y	Y	Y		Y	Y	Y	P	Y	PY	Y	Y	Y
		$^{58}Ni(n,p)^{58}Co$[f]	Y	Y	Y	Y	Y	Y	Y	Y	Y	Y		Y	Y	Y	P	Y	PY	Y	Y	Y
		$^{238}U(n,f)^{140}Ba$-La	Y	(N)	Y	(N)	Y	Y	(N)	(N)	(N)	(N)	(N)	(N)	(N)	(N)	(N)	(N)	(N)	(N)	(N)	(N)
		$^{238}U(n,f)^{103}Ru$	(Y)	Y	(Y)	(Y)	Y	Y	Y	Y	Y	Y			Y	Y	P	Y	P	Y	Y	Y
		$^{238}U(n,f)^{95}Zr$-Nb	(Y)	Y	(Y)	(Y)	Y	Y	Y	Y	Y	Y			Y	Y	P	Y	P	Y	Y	Y
		$^{238}U(n,f)^{137}Cs$	(Y)	Y	(Y)	Y	Y	Y	Y	Y	Y	Y			Y	Y	P	Y	P	Y	Y	Y
		$^{232}Th(n,f)^{140}Ba$-La		(N)		(N)	(N)	(N)	(N)	(N)	(N)	(N)	(N)	(N)	(N)	(N)	(N)	(N)	(N)	(N)	(N)	
		$^{232}Th(n,f)^{95}Zr$-Nb					Y	Y									P	P				
		$^{232}Th(n,f)^{137}Cs$					Y	Y									P	P				
		$^{237}Np(n,f)^{140}Ba$-La	Y	(N)	Y	(N)	Y	Y	(N)	(N)	(N)	(N)	(N)	(N)	(N)	(N)	P	(N)	(N)	(N)		(N)
>0.4		$^{237}Np(n,f)^{103}Ru$	(Y)	Y	(Y)	(Y)	Y	Y	Y	Y	Y	Y			Y	Y	P	Y	P	Y		Y
		$^{237}NP(n,f)^{95}Zr$-Nb	(Y)	Y	(Y)	(Y)	Y	Y	Y	Y	Y	Y			Y	Y	P	Y	P	Y		Y
		$^{237}Np(n,f)^{137}Cs$	(Y)	Y	(Y)	Y	Y	Y	Y	Y	Y	Y		Y	Y	Y	P	Y	P	Y		Y
		$^{93}Nb(n,n')^{93m}Nb$								Y	Y	Y					P	P	P			Y
		$^{59}Co(n,\gamma)^{60}Co$[e]	Y	Y	Y	Y	Y	Y	Y	Y	Y	Y		Y	Y	Y	P	Y	PY	Y	Y	Y
		$^{109}Ag(n,\gamma)^{110m}Ag$[e]	Y		Y	Y	Y	Y	Y	Y	Y	Y			Y		P	P	P		Y	Y
		$^{58}Fe(n,\gamma)^{59}Fe$	Y	Y	Y	Y	Y	Y	Y	Y	Y	Y			Y		P	Y	PY	Y	Y	Y
5 x 10^{-7}		$^{45}Sc(n,\gamma)^{46}Sc$[e]	Y		Y	Y	Y	Y	Y		Y	Y			Y		P	P	PY		Y	Y
to 0.5[b]		$^{235}U(n,f)^{140}Ba$-La	Y	(N)	Y	(N)	Y	Y	(N)	(N)	(N)	(N)	(N)	(N)	(N)		(N)	(N)	(N)	(N)		(N)
		$^{235}U(n,f)^{103}Ru$	(Y)		(Y)		Y	Y	Y	Y	Y	Y			Y		P	P	P			Y
		$^{235}U(n,f)^{95}Zr$-Nb	(Y)		(Y)		Y	Y	Y	Y	Y	Y			Y		P	P	P			Y
		$^{235}U(n,f)^{137}Cs$	(Y)		(Y)		Y	Y	Y	Y	Y	Y			Y		P	P	P			Y
As Above[a]		$^{238}U(n,f)FP$					Y		Y	Y	Y	Y			Y		P	P	P			
		$^{232}Th(n,f)FP$					Y								Y		P	P	P			
		$^{237}Np(n,f)FP$					Y		Y	Y	Y	Y			Y		P	P	P			
		$^{235}U(n,f)FP$					Y		Y	Y	Y	Y			Y		P	P	P		Y	
	SSTRs[g]	$^{239}Pu(n,f)FP$					Y										P	P	P			
<0.1		$^{6}Li(n,\alpha)$															P	P	P			
		$^{10}B(n,\alpha)$															P	P	P			
>0.3		H(n,p) as CR-39		N		N		N		N		N	(N)	N		N	(P)	N	(P)			N
>4		Ni(n,He) as metal[f]							(Y)	Y	(Y)	Y		Y	(Y)	Y	(P)	P	(Y)		(Y)	(Y)
		Al(n,He) as metal[f]	N		N		N		N	Y	(N)	Y		Y	N	Y	N	P	N		N	(Y)
		Cu(n,He) as metal[f]	N		N		N		N	Y	(N)	Y		Y	N	Y	N	P	N		N	(Y)
		Fe(n,He) as metal[f,h]	N		N		N		N	Y	(N)	Y		Y	N	Y	N	P	N		N	(Y)
>0.1[b]	HAFMs[d]	$^{7}Li(n,He)$ as LiF															P	P				
		Be(n,He) as metal								Y	Y						P	P				(Y)
		S(n,He) as PbS									Y						P	P				
		F(n,He) as PbF_2									Y						P	P				
		Ca(n,He) as CaF_2									Y						P	P				
		N(n,He) as NbN or TiN									Y						P	P				(Y)
		Cl(n,He) as $PbCl_2$									Y						P	P				
		O(n,He) as GeO_2															P	P				
<0.1		$^{6}Li(n,He)$ as LiF or alloy								Y	Y						P	P				(Y)
		$^{10}B(n,He)$ nat. or alloy								Y	Y						P	P				(Y)
		Quartz															P	P				
		Sapphire								Y							P	P				
>0.1	DMs[c]	A302B[f,k]								Y				Y			P	P				
		A533B[f,k]								Y				(Y)		Y	P	P				
		Other Steel[f]								Y		Y				Y	P	P				P

FOOTNOTES* for Table 2.27:

[a]Energy ranges for the solid state track recorders (SSTRs) are the same as those given for the fissionable radiometric sensors.

[b]Generally these reactions are used with cadmium, cadmium-oxide or gadolinium filters to eliminate their sensitivity to neutrons having energies less than 0.5 eV. The cavity measurements in the Arkansas Power & Light reactors have also included intermediate-energy measurements using thick (1.65 g/cm^2) boron-10 filters (shells) for the ^{235}U, ^{238}U and ^{237}NP fission sensors.

[c]DM means damage monitors (damage to the sensor crystal lattice, such as A302B and A533B or other steels with high copper content and high sensitivity to damage).

[d]HAFM means helium accumulation fluence monitors.

[e]Generally cobalt and silver are included as dilute alloys with aluminum. Scandium is normally Sc_2O_3, and more recently as a ~0.1% Sc_2O_3-MgO ceramic wire.

[f]Frequently when there is no specific HAFM dosimetry package, some of the radiometric sensors and some of the steel damage monitors serve as HAFMs after they have been analyzed for their principal function.

[g]Ni and/or Fe gradient disks were also included in the SSTR capsule, as required.

[h]Iron from RM sensors or Charpy specimens.

[i]Note that power plant CR is Crystal River-3 (Florida Power Corp.) and DB is Davis Besse-1 (Toledo Edison Co.).

[j]The Y following the P refers to a previous Oconee 2 test.

[k]Surveillance capsule reference correlation material (ASTM reference steel plates).

[l]The determination (or feasibility) of using any of the Oconee plants for future benchmark studies has yet to be made.

GE - General Electric
WEC - Westinghouse Electric Company
B&W - Babcock and Wilcox
CE - Combustion Engineering

2.5.1.1 VENUS

A PWR engineering mockup has been designed and assembled in the VENUS critical facility of the CEN/SCK laboratory in Mol, Belgium to address the following LWR licensing and safety issues:

- Accuracy of LWR surveillance capsule lead factors (azimuthal effects), including effects of fuel burnup and plutonium build-in
- Optimization paths for LWR core management for mitigation of pressurized thermal shock
- Why damage to LWR core internals can exceed design predictions (gamma heating)

Detailed agreements and commitments have been established for experimental and theoretical work in an interlaboratory physics-dosimetry characterization program (US, UK, Belgium). Work will concentrate on a single representative PWR mockup using a 15 x 15 pin fuel cell with appropriate core baffles, core barrels, and a neutron pad (thermal shield). This VENUS mockup, shown in Figures 2.32 and 2.33, contains several experimental insert thimbles (V1 - V4) that are large enough for active dosimetry measurements as well as many smaller measurement points appropriate for passive dosimetry monitors.

The core-baffle water interface possesses a relatively flat fast flux gradient so that flux gradient effects can be separated from other sources of uncertainty that arise in model and synthesis core management calculations. On this basis, it is anticipated that VENUS will represent a LWR-PV benchmark that can be used to validate core physics analysis in which pin-to-pin core source contributions are tested in a generic sense without the need to study further variants.

The general specifications for the VENUS mockup are:

- Lattice pitch: 1.260 cm
- Nominal active fuel height: 50.0 cm
- Fuel inventory and specifications: See Table 2.28
- Pyrex rods: See Table 2.29
- Core baffle: 304 SS; thickness: 2.858 cm
- Core barrel simulator: 304 SS; thickness: 4.972 cm; inner radius: 48.283 cm
- VENUS vessel: SS 304; thickness: 0.5 cm; inner radius: 62.00 cm.

Core loading is not centered in the VENUS grid to increase the space available for the barrel and the pad. As a consequence, the indicated inner radius of the VENUS vessel (62.00 cm) is an average value corresponding to the quadrant where measurements are scheduled.

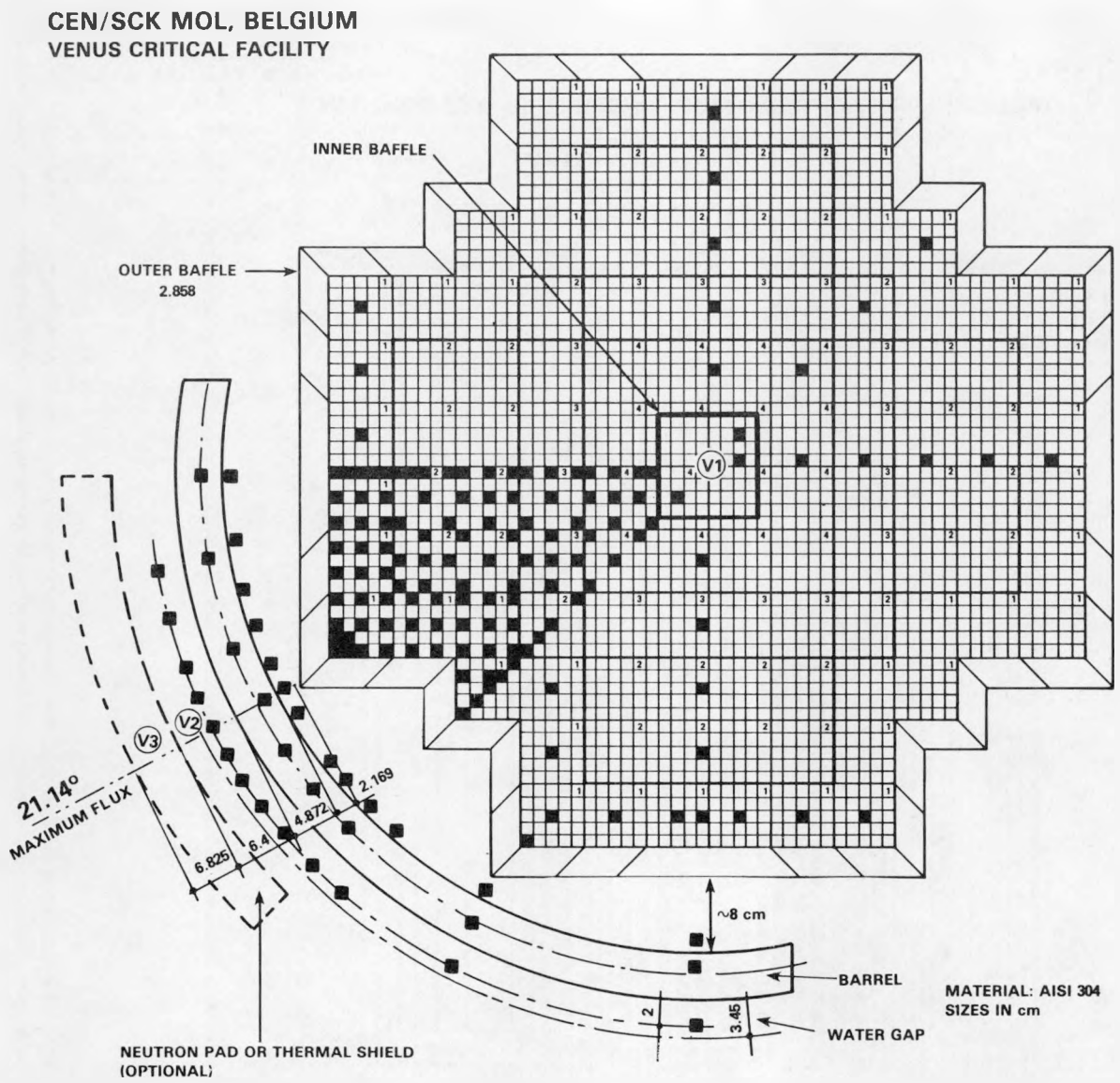

PWR — BENCHMARK

MOCKUP OF A 3-LOOP WESTINGHOUSE REACTOR

CORE CHARACTERISTICS

VARIANT 1 (V1)

SYMBOL	FUEL COMPOSITION $\%^{5}U/\%PuO_2$	ASSEMBLY AMOUNT	PIN AMOUNT	CLADDING
1	3.3/0	44	1100	Zr
2	4/0	36	900	SS
3	3/1	16	400	SS
4	2/2.7	16	400	SS
		TOTAL: 2800 PINS		

VARIANT 2 (V2)

SYMBOL	FUEL COMPOSITION $\%^{5}U/\%PuO_2$	ASSEMBLY AMOUNT	PIN AMOUNT	CLADDING
1	3.3/0	44	1100	Zr
2–3	4/0	52	1300	SS
4	3/1	16	400	SS
		TOTAL: 2800 PINS		

VARIANT 3 (V3)

SYMBOL	FUEL COMPOSITION $\%^{5}U/\%PuO_2$	ASSEMBLY AMOUNT	PIN AMOUNT	CLADDING
1	3.3/0	44	1100	Zr
2–3–4	4/0	68	1700	SS
		TOTAL: 2800 PINS		

PITCH: 1.26 cm (TYPICAL OF 17 × 17 ASSEMBLY)

MODERATOR: H_2O, AMBIENT TEMPERATURE, ~1000 ppm BORON

EXPERIMENTAL FACILITIES

■ MEASUREMENT POINTS: FUEL γ—SCANNING
FOIL ACTIVATION
FISSION CHAMBER
INNER THIMBLE DIAMETER: (0.902 ± 0.002) cm

○ MEASUREMENT POINT: NEUTRON SPECTROMETRY
INNER THIMBLE DIAMETER: (4.7 ± 0.05) cm

HEDL 8312-015

FIGURE 2.32. Mockup of a 3-Loop PWR-PV Benchmark in VENUS.

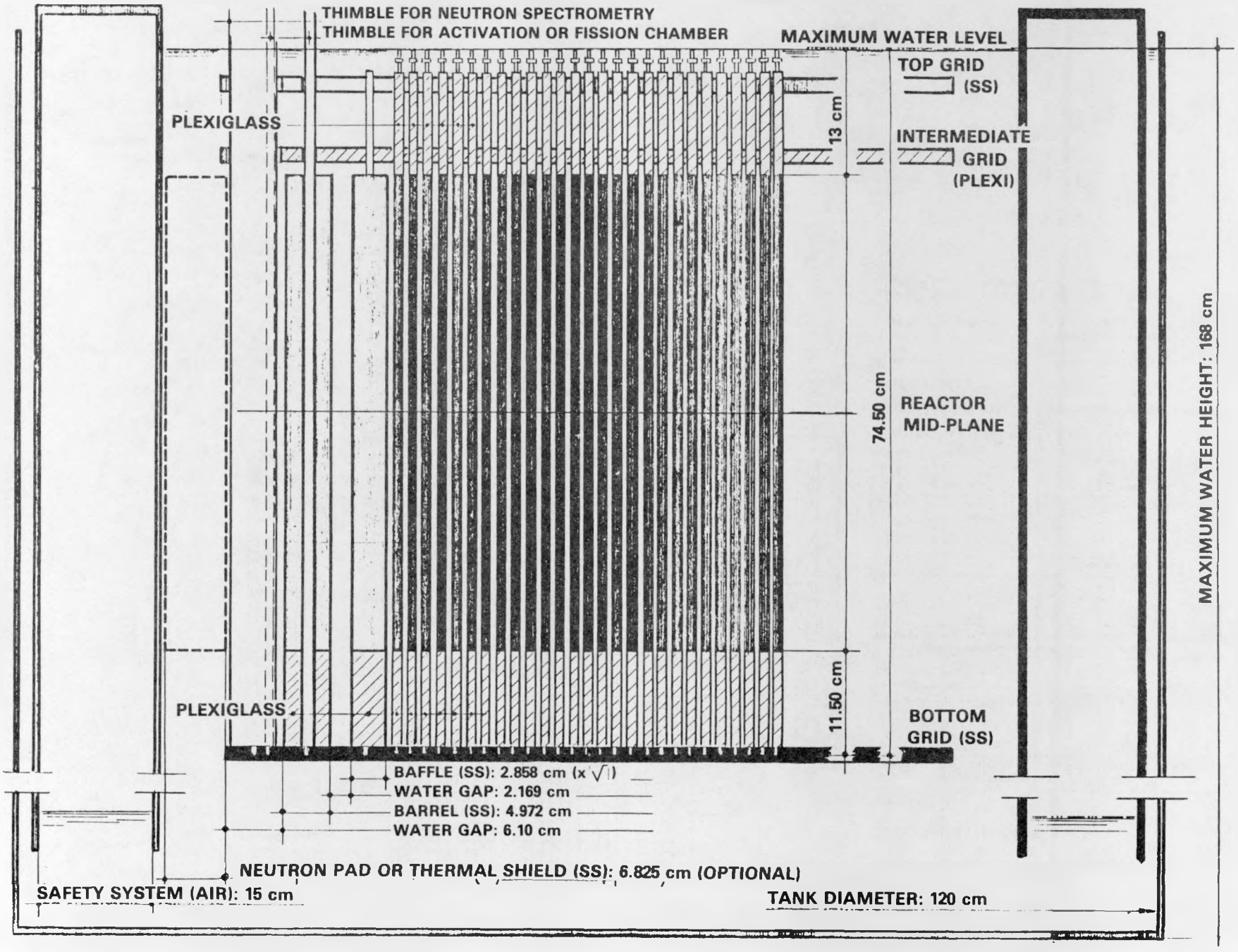

FIGURE 2.33. VENUS Critical Facility.

TABLE 2.28

CHARACTERISTICS OF FUEL PINS USED
IN THE VENUS LWR-PV BENCHMARK

Characteristic		4/0 Type Fuel Pelleted MMN	3.3/0 Type Fuel Pelleted FBFC
Stoichiometry (O/U + Pu)		$2.00 \pm \begin{matrix}0.02\\0.00\end{matrix}$	1.997 ± 0.010
Chemical composition (wt%)	UO_2	100	100
	PuO_2	0	0
Isotopic composition (wt%)	^{234}U	0.022	0.0293
	^{235}U	3.971 ± 0.01	3.3105 ± 0.015
	^{236}U	0.030	0.0165
	^{238}U	95.976	96.6437
Isotopic composition (wt%)	^{238}Pu	--	--
	^{239}Pu	--	--
	^{240}Pu	--	--
	^{241}Pu	--	--
	^{242}Pu	--	--
^{241}Am in Pu (wt%)		--	--
Reference date for Pu & ^{241}Am isotopic composition		--	--
Linear specific weight (g/cm)	Pellet	--	--
	Fuel pin	6.400 ± 0.096	5.40 ± 0.06
Fuel diameter (cm)		0.890 ± 0.001	0.819 ± 0.002
Pellet length (cm)		--	1.0 ± 0.1
Fuel length (cm)		49.90 ± 0.50	50.0 ± 0.1
Cladding composition		304 SS	Zircaloy® 4
Cladding outer diameter (cm)		0.978 ± 0.005	0.950 ± 0.004
Cladding thickness (cm)		0.038 ± 0.002	0.057 ± 0.004
Number of available fuel pins		1750	1200
H_2O content (ppm)		-	<1

®Zircaloy is a registered trademark of Westinghouse Electric Corp., Pittsburgh, PA.

TABLE 2.29

CHARACTERISTICS OF PYREX RODS USED IN THE VENUS LWR-PV BENCHMARK

Material		Corning Glass Code 7740
Chemical composition (wt%)	SiO_2	80
	B_2O_3	13
	Al_2O_3	2.25
	Fe_2O_3	0.05*
	Na_2O	3.5
	K_2O	1.15
Isotopic composition of boron		Natural*
Linear specific weight (g/cm)		0.773 ± 0.003
Pyrex inner diameter (cm)		0.605 ± 0.005
Pyrex outer diameter (cm)		0.905 ± 0.005
Pyrex length (cm)		50.0 ± 0.1
Cladding composition		304 SS
Cladding outer diameter (cm)		0.978 ± 0.005
Cladding thickness (cm)		0.019 ± 0.001
Number of available Pyrex rods		58

*To be analyzed.

Measurements to be Performed in the VENUS -- Scheduled milestones for the interlaboratory physics-dosimetry characterization program in VENUS are shown in Table 2.30. All milestones were completed on schedule. Data reduction and analyses are already underway on these VENUS experiments.

TABLE 2.30

VENUS PROGRAM

Date	Milestone
October 15, 1982	- Final Program Plan - Facility Loading and Quality Assurance - Core Criticality
January 1, 1983	- Gamma-Heating (Thermoluminescent Dosimetry) - Gamma-Spectroscopy (Janus) - Proton-Recoil Spectroscopy (Emulsions and Chambers, as appropriate)
February 15, 1983	- Core Power Distribution and Absolute Normalization - ^{237}Np, ^{238}U, ^{235}U Fission Flux Distributions (Fission Chambers and SSTR)
March 31, 1983	- Radiometric Dosimetry - $^{6}Li(n,\alpha)$ Spectrometry - Experimental and Theoretical Analysis

2.5.1.2 NESTOR Dosimetry Improvement Program (NESDIP)

NESDIP comprises a series of experiments in which some outstanding problems of PV dosimetry and monitoring can be explored under conditions broadly representative of current LWR designs. The objectives of the program are:

- To provide benchmark-quality measurements of neutron and gamma-ray fields against which calculational methods for predicting damage to PV and reactor internals can be validated and provide for further development or refinement of necessary dosimetry measurement techniques.
- To ensure that the program complements and, where necessary, extends the scope of other international programs in the PV dosimetry area (e.g., the USNRC/LWR-PV-SDIP and the VENUS programs).
- To incorporate, as part of this complementary role, requirements of external calculational and experimental groups in the development of the NESDIP (conforming the overall level of time and resources available to the program).
- To provide reports of calculational and experimental data derived as part of the program in an available form similar to reports provided as part of the USNRC/LWR-PV-SDIP.

The NESDIP is being carried out on the ASPIS Facility of the NESTOR reactor situated at the United Kingdom Atomic Energy Authority Establishment, Winfrith, UK. The main difference between the UK facility and its US counterpart at ORNL (PCA-PV) is, in essence, that the radiation source for ASPIS is a fission-plate rather than a volume-distributed core thereby ensuring a precise definition of source terms in experiment and calculation. In addition, the cave facilities of ASPIS provide a convenient environment for the proposed experiments, thus facilitating mounting and disassembly. It is also possible to extend the ASPIS cave facility to mockup features such as the PV cavity, which have not to date been amenable to benchmark-quality experimental investigation. As mentioned, program development depends to a large extend on the input from interested parties, so that at present, three broad phases of the NESDIP have been identified:

- Phase 1 - Replica Experiment
- Phase 2 - PV Cavity Simulation Studies
- Phase 3 - PV Support Structure and Streaming Studies

Of these, Phase 1 has been started and is initially supporting UK methods developmental work in the dosimetry area and measurements to aid the evaluation of UK specimens irradiated in the PSF-PV experiment. Detailed work for Phases 2 and 3 has not yet been agreed upon, and input from groups other than the UK participants is now being examined. It is hoped that an official

UK-US agreement can be endorsed for the work within the near future. However, it is possible to briefly describe the work envisaged under the phases given above, and reference should be made to the accompanying Figures 2.34 through 2.39.

Phase 1 - Replica Experiment -- As is evident from Figures 2.34, 2.37, 2.38 and 2.39, the purpose of this phase is to essentially reproduce the features of the ORNL PCA measurement arrays with the important difference that the core source of radiation is replaced by a fission plate. In addition, full use will be made of the Winfrith experience in active neutron spectrometry to derive full range-of-interest (0.1 to 10 MeV) neutron spectra in measurement positions of interest. (It is possible within this arrangement to produce any of the arrays used for the US PCA measurements.) In the initial experiments, attention will be concentrated on the 12/13 configuration. The UK program planned for this phase will aim at providing detailed neutron measurements for the development and validation of adjustment techniques currently under investigation in the UK and linked to PV cavity measurements. Some work in the 4/12 array will be carried out to facilitate the analysis of the UK metallurgical specimens irradiated in off-axis positions of the ORNL/PSF experiment.

Phase 2 - PV Cavity Simulation Studies -- It is possible to provide, in the ASPIS cave, a "roof slot" facility that may be used very effectively to simulate PV cavity arrangements, representative of LWR plants (see Figure 2.35). In this phase, it will be possible to measure not only relevant reaction rates and spectra in the cavity, but also to investigate the effect of varying associated design parameters, such as a range of cavity dimensions and structural materials, in validating calculational and measurement techniques. This is an ideal experimental arrangement for investigating the application of cavity-monitoring techniques to the prediction of damage rates within the PV itself.

Phase 3 - PV Support Structures and Streaming Studies -- This phase may be seen as an extension of the investigation into the practical problems of carrying out cavity-monitoring measurements with high accuracy, but further, as a means of investigating the effects of neutron spectrum and streaming upon the other features to which attention has been drawn as part of the USNRC/LWR-PV-SDIP (e.g., the reactor pressure vessel support structure). Figure 2.36 indicates the potential present in the ASPIS Facility to mockup such support structure arrangements.

Current progress and proposed future activity at NESDIP are discussed below, but it should be stressed that the detailed planning of later phases of the NESDIP are intended to reflect as wide a range of design and analysis requirements as possible, and that early input is sought from interested groups who may intend to participate.

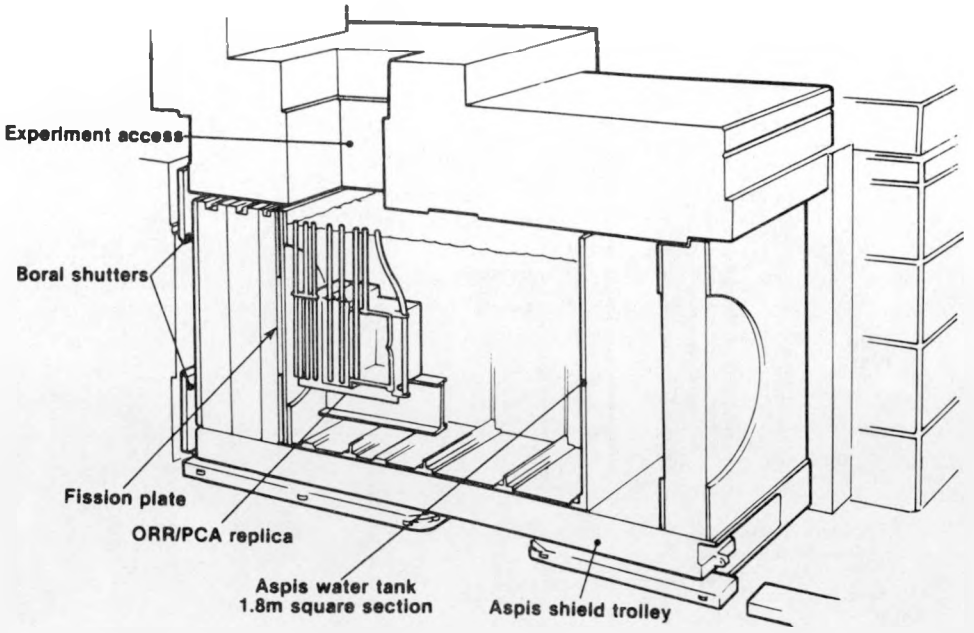

FIGURE 2.34. ASPIS Replica of PCA/PSF Configuration.

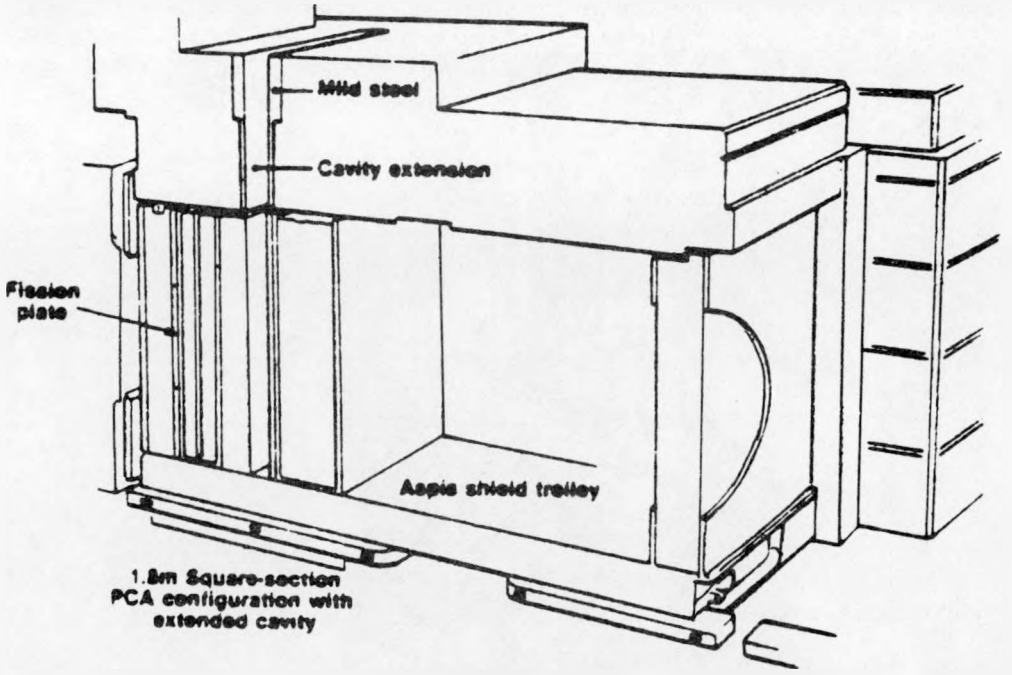

FIGURE 2.35. ASPIS PCA/PSF Cavity Streaming Benchmark.

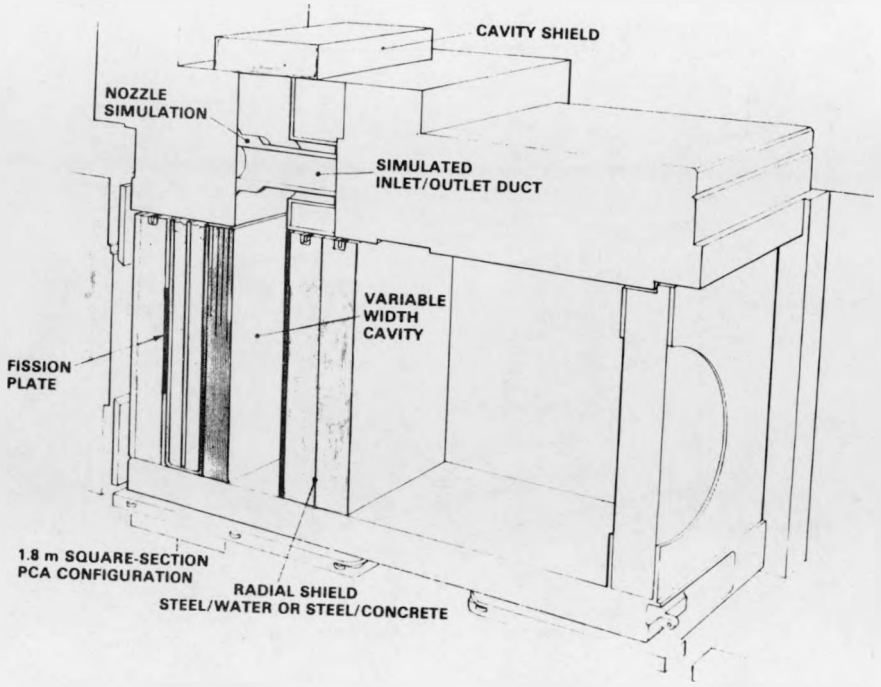

FIGURE 2.36. ASPIS Generic LWR Engineering Benchmark with PCA/PSF Thermal Shield/RPV Configuration.

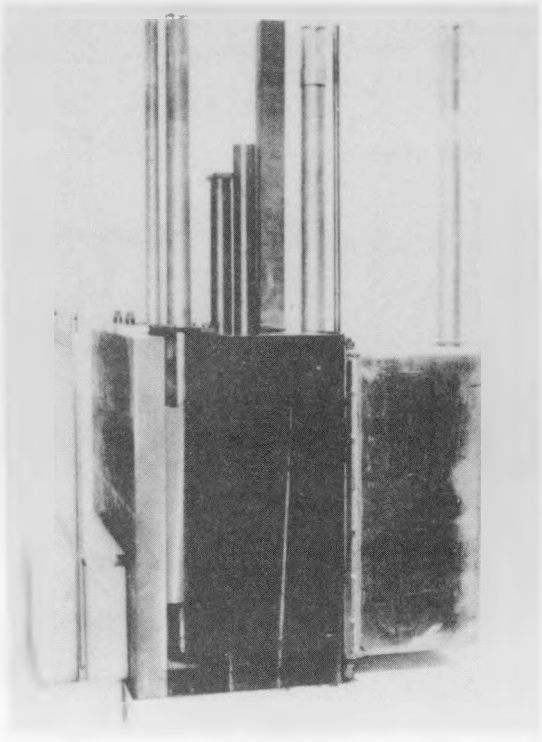

FIGURE 2.37. Side View of ASPIS Replica.

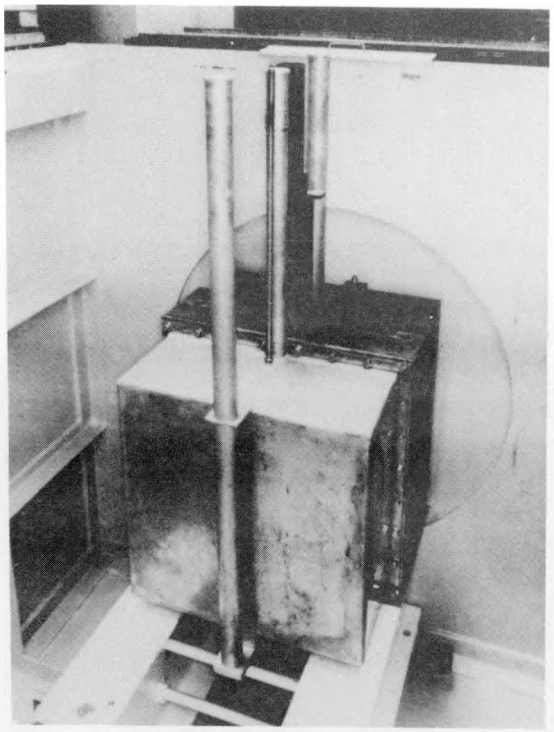

FIGURE 2.38. Back View of ASPIS Replica.

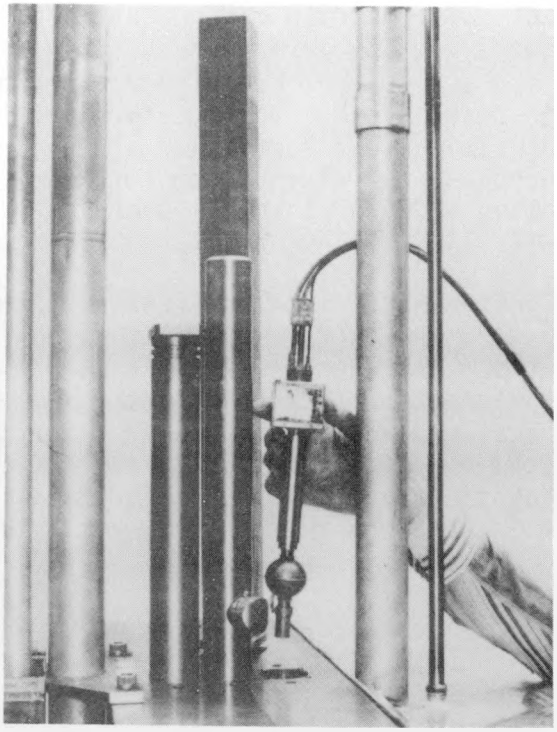

FIGURE 2.39. Spherical Proton Recoil Spectrometer Being Inserted into PCA Replica.

Measurements to be Performed in the NESDIP -- ASPIS is a penetration-benchmark facility in which the power is restricted to reduce background activation and maintain a clean environment for spectrometry measurements. Thus, reaction-rate measurements will be obtained in indium, rhodium, sulphur, and nickel foils at a representative range of positions throughout the arrays studied. These results will be supplemented by active spectrometry measurements using the well-established Winfrith hydrogen proportional-counter techniques (covering the energy range 0.1 to 2 MeV) and the NE213 spectrometer (covering the range 2 to 10 MeV). Experience has demonstrated the feasibility of using individual proportional counters as "integral detectors" in their own right in regions where low sensitivity precludes the use of activation monitors. Moreover consistency between spectrum measurements and activation techniques is always sought by predicting reaction rates from the measured spectrum and the activation cross sections. In addition to the neutron measurements, the NESDIP will place more emphasis on the evaluation of the gamma-ray environment within the chosen experimental arrays. These measurements will include the estimation of integral quantities using thermoluminescent dosimeter (TLD) techniques and, it is hoped, assessment of the gamma-spectra at key positions. The environment and access would be very suitable for such a characterization using the HEDL Janus probe.

It is intended to reference the measurement techniques (both neutron and gamma-ray) by making use of the NESSUS Facility of the NESTOR reactor (see Figure 2.40), although such benchmark referencing can be usefully extended in principle to include any other benchmark field that may be suggested by participants. Particular attention is being paid to the development of niobium as a fluence monitor. Measurements of the niobium cross section are being made and integral checks carried out by irradiation in NESSUS, British materials testing reactors, and other standard fields.

Current NESDIP Status -- As mentioned above, only Phase 1 was planned in detail and carried out from September 1982 to March 1983. Significant effort has been invested in careful characterization of the source distribution in the fission plate and this is now substantially complete. First measurements in Phase 1 concentrated on the 12/13 array. In this configuration, foil measurements have been carried out at all centerline locations and spectral information obtained at the 1/4 T and cavity positions using the hydrogen proportional counters. The remainder of the

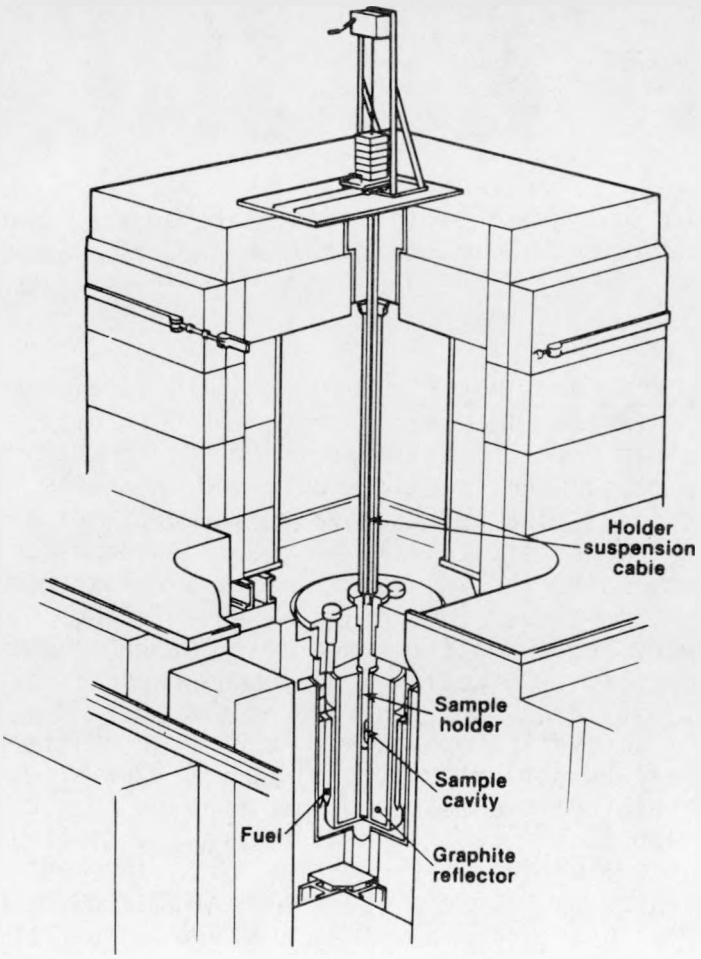

FIGURE 2.40. NESTOR Calibration Facility NESSUS.

period was devoted to completing centerline activation foil measurements, checking off-axis locations, and performing first irradiations of gamma-ray detectors.

As mentioned, a real advantage of the ASPIS Facility is the ease with which experiments can be mounted and dismantled. Thus, although it was necessary to re-assemble the replica experiment during 1983 for further measurements, this posed no difficulties in terms of run-to-run reproducibility. During this operating period, the first opportunity will be taken to irradiate detectors from other participating groups, principally Mol and HEDL.

NESDIP: The Complementary Context -- As explained above, NESDIP is seen as part of a complementary cycle of benchmark experiments that includes the PCA program at ORNL and the VENUS program at Mol, Belgium. These are aimed, in their entirety, at a comprehensive investigation of current problems and techniques for PV physics-dosimetry (see Figure 2.41). It should be noted that each program possesses its own independent features. Thus, the PCA was able to present an extended core source and pressure vessel array capable of a wide dynamic range in terms of activation and fission-foil measurements.

As a result of this program, the importance of calculation and representation of core sources was recognized together with some features of the transport calculation of penetrating neutrons within the PV array. The purpose of NESDIP, therefore, is 1) to provide a replica of the PCA PV array driven by a fission plate in which source representation uncertainties were reduced to a minimum (by virtue of the thin plate source) and 2) to extend the PCA cavity box concept to include a full-range, full-depth cavity facility. In the VENUS program, the cycle will be completed by an experimental array that will concentrate heavily upon the representation of a typical LWR core in which core physics calculations and fuel-management strategies can, in principle, be investigated.

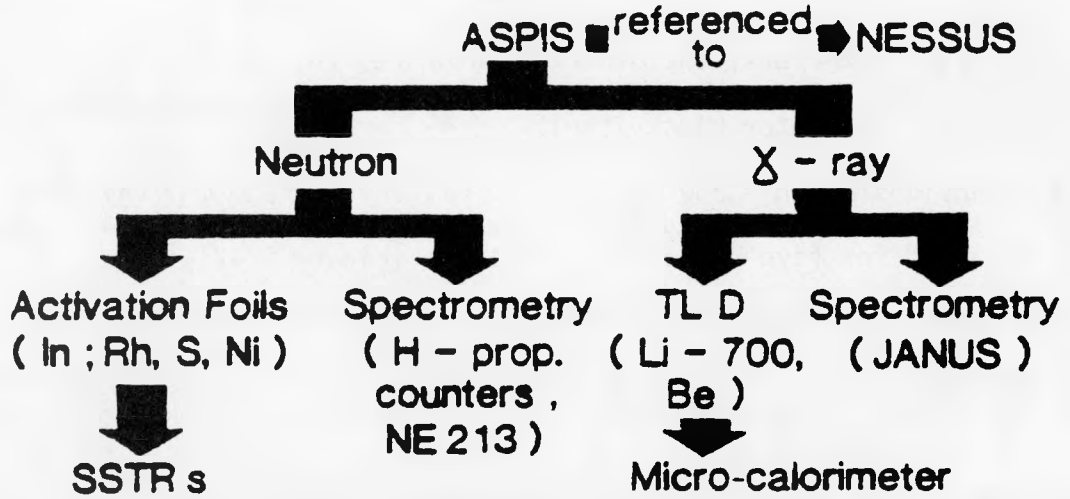

FIGURE 2.41. NESDIP-Proposed Measurement Techniques.

By means of such a cyclic program and the international collaboration that typified the US NRC/LWR-PV-SDIP, it is hoped that these new projects (VENUS and NESDIP) will achieve their common goal of resolving outstanding PV physics-dosimetry problems and of standardizing the solution techniques.

2.5.1.3 DOMPAC

Damaging neutron fluence determination to commercial LWR pressure vessels is of main importance for both safety and economical purposes: design and end-of-life condition of the PV. Another question is: to what extent are mechanical tests on surveillance samples reliable for PV-damage predictions? Design and implementation of the DOMPAC dosimetry experiment are based on the following considerations: simulation in a test reactor (TRITON - Fontenay aux Roses) of a commercial LWR-PV neutron environment and a large ferritic steel block should be representative of irradiated PV as long as two conditions are met:

1) Similar fast neutron flux gradient

2) Similar neutron spectrum incident on the steel surface

The steel block, 20 cm thick, is instrumented with Saclay's damage dosimeters (spectrum sensitive) in the front, 1/4 and 1/2 thickness positions. Validity of condition (1) has been proven in light water pool test reactors, but condition (2) requires optimization of the simulator block location in the test reactor water reflector region.

Commerical PWR-type surveillance capsules were mocked up by an equivalent steel loading (and damage dosimeters) attached to a simulated "Thermal Shield." Starting from the TRITON core, there is a thin aluminum plate to ensure cooling of fuel elements. Beyond this is a 30-mm water gap and a 20-mm thick stainless steel thermal shield equipped with two ferritic steel tubes 25 mm in diameter. One of these simulated "surveillance capsules" is filled with damage detectors, the other one with Fe, Cu, and Ni activation foils. Following this is another water gap (thickness to be determined) in front of the steel simulator block itself.

The block dimensions are h = 300 mm, l = 150 mm, and L = 200 mm (thickness) with 2 mm of stainless steel cladding. Experimental holes are Ø 9 mm. The height is designed for five detectors/containers (Figure 2.42).

The lateral dimensions were limited mainly for three reasons:

1) Basically, the mean free path for fast flux in iron is <5 cm; so the B axis should be sufficiently representative of the spectrum radial evolution.

2) The A and C axes, loaded respectively with W and G.A.M.I.N. dosimeters, are assumed to integrate equal damaging fluences in an equivalent neutron environment.

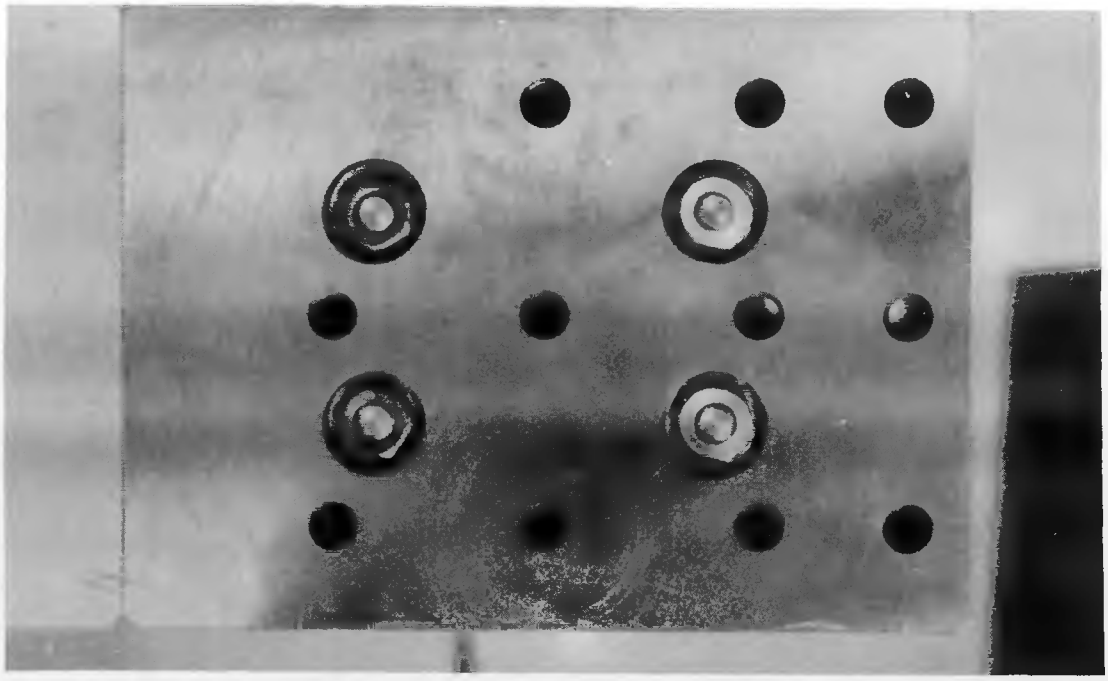

FIGURE 2.42. Steel Block for PV Simulation.

3) The validation of damage detector response versus neutron spectrum in the B axis shall be ensured if somewhat lower damage/activation ratios are measured in the A and C axes ("harder" spectrum).

These considerations led to damage dosimeter loadings as indicated on Figure 2.43.

The DOMPAC experimental device is shown in Figures 2.44 and 2.45. Shown on top of steel block are the 2-m long tubes for detector recovery (and thermocouple plugs) when the device is immersed in water.

To avoid excessive heating in G.A.M.I.N. detectors, the TRITON power was limited to 2 MW (6 MW full power). The irradiations took place on January 2, 1979. The actual duration (9 h-10 min) was optimized so that each detector integrates convenient fluences. The "surveillance" damage dosimeter plug was taken up after 2 h-20 min and then replaced with a dummy aluminum loading.

Since 1979, no other DOMPAC experiment reactor irradiations have been performed on this facility. The program's main objectives were successfully achieved (as damage fluence attenuation inside the simulated vessel) during the January 1979 irradiations. As stated previously, full validation of DM responses were successfully computed by the TRIPOLI (Monte-Carlo) transport code.

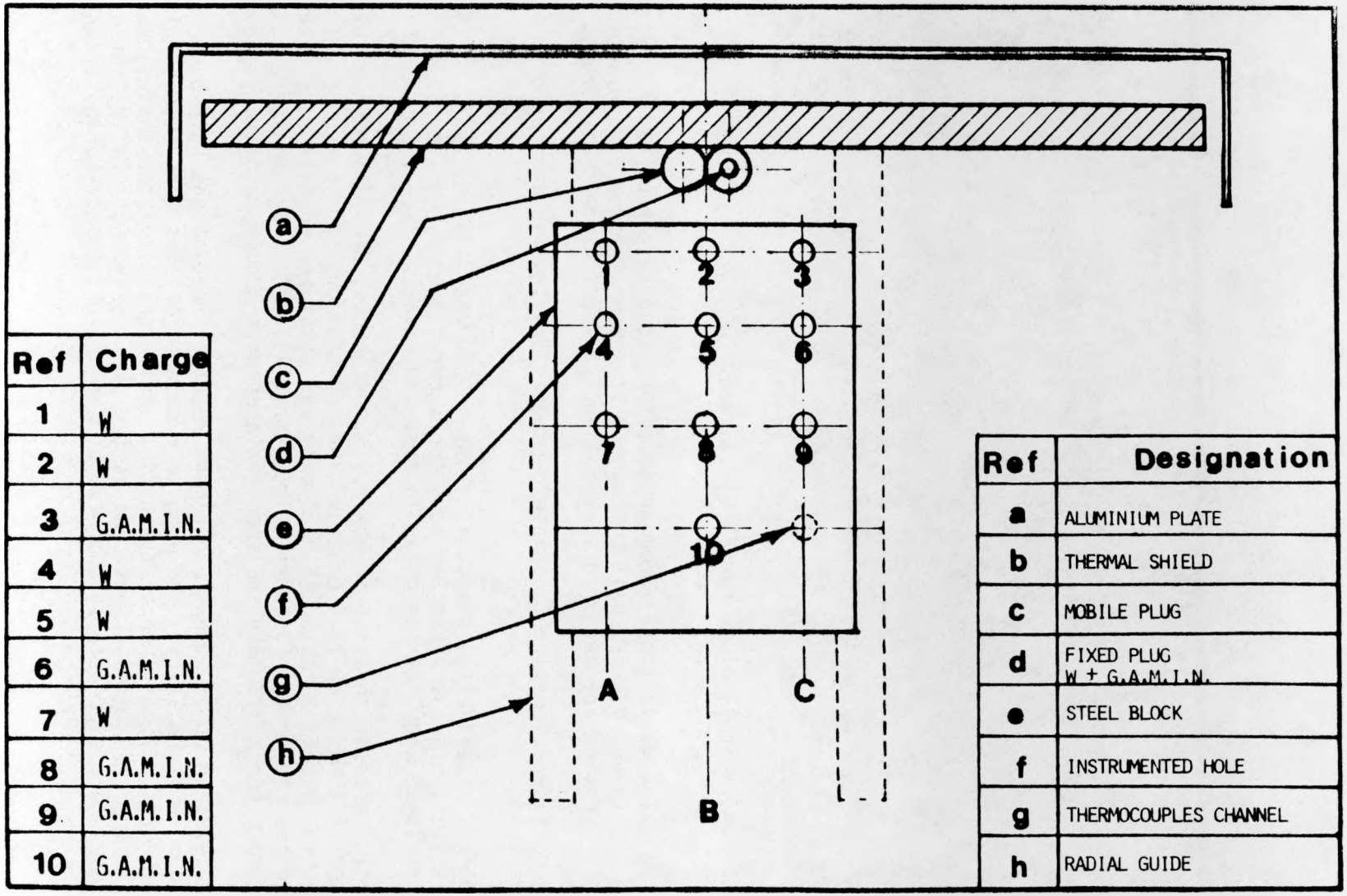

Ref	Charge
1	W
2	W
3	G.A.M.I.N.
4	W
5	W
6	G.A.M.I.N.
7	W
8	G.A.M.I.N.
9	G.A.M.I.N.
10	G.A.M.I.N.

Ref	Designation
a	ALUMINIUM PLATE
b	THERMAL SHIELD
c	MOBILE PLUG
d	FIXED PLUG W + G.A.M.I.N.
e	STEEL BLOCK
f	INSTRUMENTED HOLE
g	THERMOCOUPLES CHANNEL
h	RADIAL GUIDE

FIGURE 2.43. DOMPAC Design.

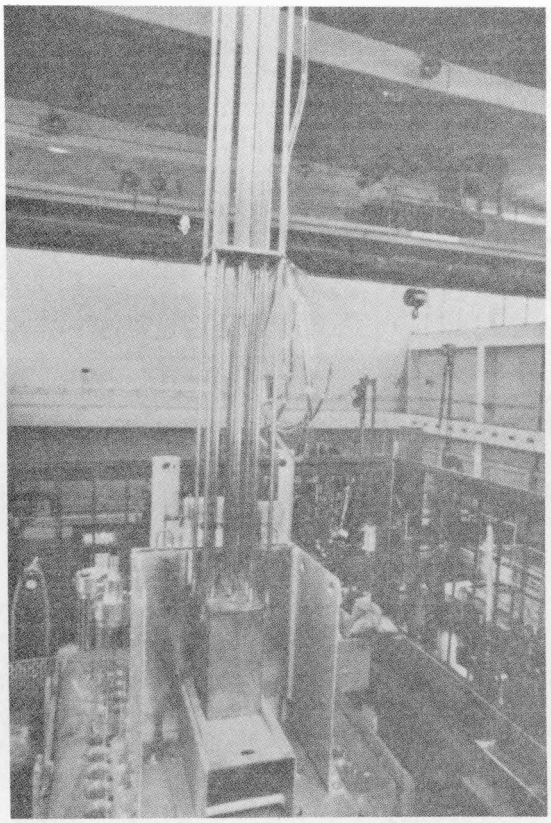

FIGURE 2.44. DOMPAC Out-of-Pile Device.

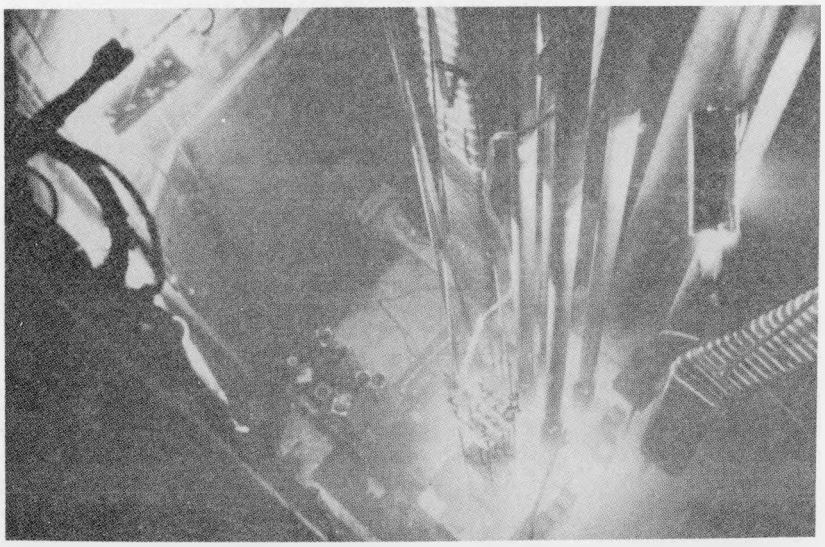

FIGURE 2.45. Irradiation in TRITON.

As a matter of general interest, the TRITON reactor has been shut down. It is presently being decommissioned. The whole DOMPAC experiment device has been dismantled and all steel irradiation programs are now performed in the OSIRIS (Saclay) 70 MW pool-type reactor. For on-going programs, the neutron damaging fluence are routinely qualified by the same DM techniques as described here. Studies that involve advanced and/or up-dated surveillance program analysis may lead to further dosimetry mock-up experiments.

2.5.2 Equipment

Two areas of experimental effort have been selected in order to illustrate the advanced nature of equipment required in LWR-PV-SDIP, namely computer-controlled nuclear track scanning systems and continuous gamma-ray spectrometry. However, many other specialized experimental methods have also been applied for LWR-PV-SDIP neutron dosimetry, such as radiometric (RM) dosimeters, helium accumulation fluence monitors (HAFM), and absolute NBS fission chambers. For a general discussion of all LWR-PV-SDIP experimental techniques, consult the NUREG reports on the PCA Experiments and Blind Test (Mc81).

2.5.2.1 Computer-Controlled Nuclear Track Scanning Systems

Instrumentation systems are required for quantitative scanning of solid state track recorders (SSTR) and nuclear research emulsions (NRE) irradiated in LWR-PV environments. SSTR and NRE are applied in LWR-PV neutron dosimetry over an enormous range of flux/fluence from low-power benchmark mockups to high-power actual on-line LWR commercial power plants. See for example, ASTM E854-81, "Standard Method for Application and Analysis of Solid State Track Recorder (SSTR) Monitors for Reactor Surveillance," (As82b) which was prepared within the "Master Matrix for LWR-PV Surveillance Standards," ASTM E706-81a (As82). Cost-effective dosimetry for the LWR-PV-SDIP requires automation of different NRE and SSTR scanning tasks to the fullest possible extent.

2.5.2.1.1 Hanford Optical Track Scanner (HOTS)

Although considerable effort has been expended by many groups in attempts to automate track scanning, overall progress has been slow. A spark counting method applicable with plastic SSTR such as Makrofol or Lexan has been successfully demonstrated (Cr69,La69) but possesses severe limitations for precision work. Detailed investigations (Co70,Co72a) reveal accuracy of roughly 10% to 20% for this technique, provided track density is limited to $<10^3/cm^2$.

A more sophisticated automation system, using an optical microscope under computer control, was developed at Argonne National Laboratory (Co69,Co72, Go71). This Argonne optical track scanner (AOTS) system has demonstrated comparable accuracy to manual scanning for plastic SSTR of the polycarbonate resin variety such as Makrofol, Lexan, etc. (Co72,Go72).

Although this AOTS system did establish that SSTR automation was possible at an accuracy level comparable with human observations, severe limitations

arose. Extreme difficulty was originally encountered using mineral track recorder materials, such as mica, with any degree of reliability or reproducibility. Subsequent efforts by (Co75) have overcome these difficulties in scanning mica SSTR. A track density limit of roughly 10^5 tracks/cm^2 was established, beyond which SSTR accuracy could be seriously compromised. System speed was ~10 h/cm^2, which provides a relatively slow processing rate of 1 to 2 SSTR/day.

The AOTS system was the first microscope system ever built that possessed automatic focussing capability. It was transferred to HEDL to meet the overall dosimetry needs of the US fast breeder reactor (FBR), light water reactor (LWR), and magnetic fusion reactor (MFR) energy programs. During the past two years, major hardware modifications have been undertaken to improve the utility of this system, which is now called the Hanford optical track sensor (HOTS).

While the microscope remains little changed from the original AOTS, major improvements have been made in both the imaging system and computer-control modules (Mc83). Figure 2.46 is a photograph delineating the components of the HOTS system. The specimen stage moves on linear ball bearings. Movements of the stage in the X and Y directions are made by two independent stepping motors of 800 steps/revolution coupled to a micrometer screw of 40 threads/inch. Positioning accuracy is a $\pm$1 motor step. A third stepping motor having 200 steps/revolution provides focus control.

A major improvement in converting the optical image into a digital format for computer analysis is the use of a high-resolution videcon camera. The camera replaces the original photomultiplier tube imaging system. Conversion of the optical image to digital format is accomplished with the internal high-speed digitizer of the camera controller. The maximum resolution of the videcon system is 1024 x 1024 pixels per frame. Current computer memory capacity limits the resolution to 256 x 512 pixels per frame.

Each pixel is converted to a digital value over the range from zero (a completely dark image) to 255. An entire frame can be digitized and stored in the computer memory in ~250 ms. Once the frame image is stored, high-speed data analysis begins, and the stage moves to the next location. Control of the entire system as well as data analysis is accomplished with the LSI 11/23 computer. The lower 32K words of memory are used for program storage, and upper 64K words are used to store a digitized frame image. In addition to controlling the automatic scan operation, a stepping motor interface provides for inputs from two joysticks. The joysticks allow for manual operation of the stage for initial alignment and setup of the SSTR specimen.

Control of the entire system is accomplished with a program written in FORTRAN and DEC assembly language. All data analysis routines are written in assembly language due to the speed-intensive nature of this task. The control program consists of six basic modules that provide for initial setup and alignment, input of required parameters, image digitizing, stage movement, autofocusing, and track correlation.

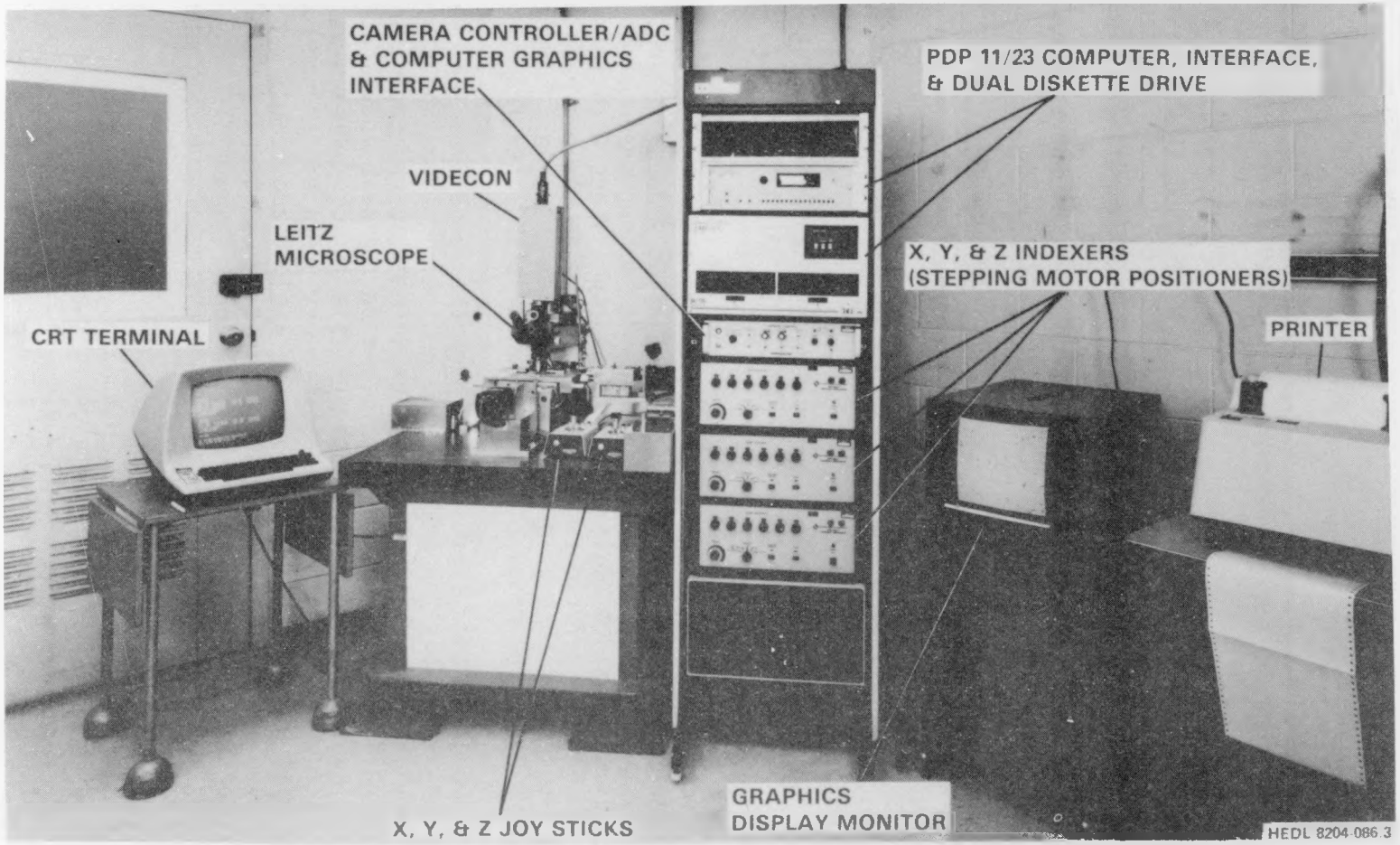

FIGURE 2.46. Hanford Optical Track Scanner (HOTS) System. Neg 8202689-4

Before the control program begins, the user inputs the event detection threshold, the focus check frequency, and the diameter of the SSTR area to be scanned. The event detection threshold is based on a user input multiplier (0-1) and the average pixel intensity (0-255). The average pixel intensity is computed by averaging 8192 randomly selected pixels whose intensity exceeds the event threshold. The threshold for event detection is then recomputed as the product of the average value and the user input multiplier. A user input of 0.9 is most commonly used. Periodically during the scan, an autofocus routine is used to optimize the image contrast. The routine is based on the maximum opacity criterion introduced by Cohn and Gold (Co72).

The most time-consuming operation performed by the control program is the correlation of the events into tracks. It is for this reason that all correlation routines are written in assembly language. The correlation routines are based on the technique described in (Co72). This technique can be extended to the present system because the frame image can be reconstructed into single-line scan images. An additional routine correctly accounts for tracks that continue into one or more frames.

After the scan is completed, tracks are grouped by area (pixels) so that a track size histogram can be produced. These histograms are similar to those obtained with the AOTS system. A nonlinear regression analysis program is used to fit the histogram data to an equation of the form

$$F(x) = ae^{-bx} + \frac{c}{(x - d)^2 + e} + \frac{f}{(x - g)^2 + h} \qquad (1)$$

where x is the track area in pixels, a, b, c, d, e, f, and h are parameters to be determined, and F(x) is the number of tracks for each x. For low-track density, $\sim 10^5$ tracks/cm^2, the third term can be omitted.

The first term represents the decreasing exponential function that is characteristic of the background seen on unexposed mica samples. The second and third terms represent the track area distribution. Figure 2.47 illustrates a typical track size histogram obtained from the HOTS and the excellent fit provided by Eq. (1).

The HOTS system has been calibrated using procedures completely analogous to the earlier calibration work carried out for the AOTS system (Go72). If one plots N, the fissions/cm^2 against the average values of N_0, the tracks/cm^2, for each sample, the data is found to give a good fit to the paralyzable counter model. This model predicts the relationship where $\langle\alpha\rangle$ is the average area for pile-up of tracks in the sample. By using a nonlinear

$$N_0 = N\, e^{-\langle\alpha\rangle N} \quad , \qquad (2)$$

regression analysis code, the value of $\langle\alpha\rangle$ was found to be 1.5592×10^{-6} cm^2, with a relative sigma of 0.014. The excellent fit to the paralyzable

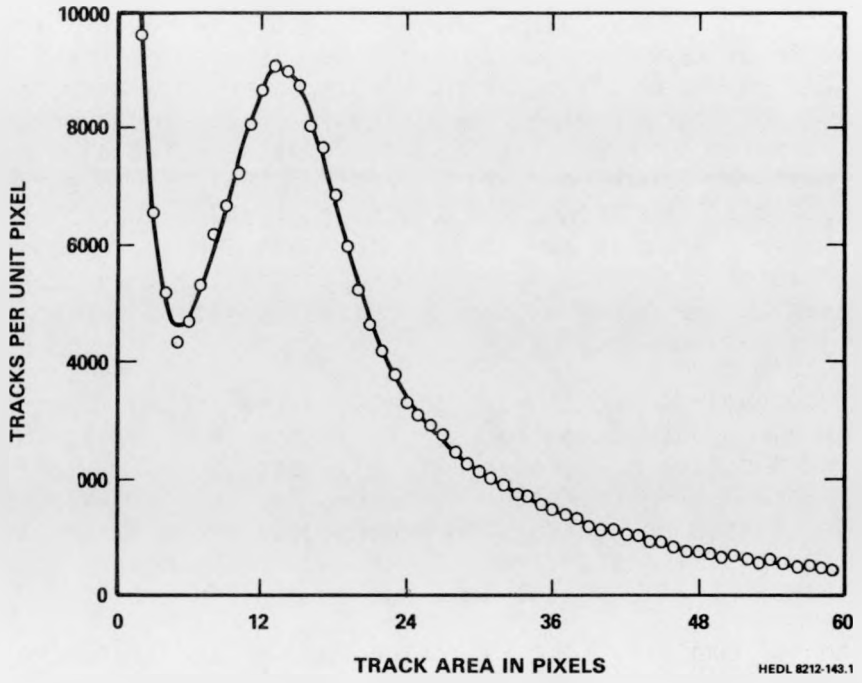

FIGURE 2.47. Typical Track Area Distribution for a Mica SSTR Sample Exposed to a Thin Deposit of an Actinide Element and Etched in 40% HF for 45 min at 22 ± 0.2°C. The data were fit to the functions given in Eq. (1).

counter model is shown in Figure 2.48. Considerably greater detail on the HOTS system operation (Mc83) and calibration (Ro83) is now available in a special issue of Nucl. Tracks.

The processing time on the HOTS varies with track density from about 45 minutes for a density of ~4 x 10^4 tracks/cm² up to about 150 minutes for a density of ~7 x 10^5 tracks/cm². The increased time for higher track densities follows from the need to correlate more events into tracks. The reproducibility for repeated scans of SSTR on the HOTS system is at the 2% (1σ) level. These enhanced features greatly increase the cost effectiveness of SSTR applications in reactor dosimetry. Consequently, when sufficient tracks are available for counting, statistics are no longer a problem; other sources of uncertainty will then dominate the overall experimental error.

2.5.2.1.2 Automated Scanning Electron Microscope (ASEM)

A block diagram of the ASEM system in current use at HEDL is shown in Figure 2.49. The system is essentially a video digitizer with a programmable trigger circuit. The computer can instruct the trigger circuit to store data from any selected video line. Data are stored in the buffer memory

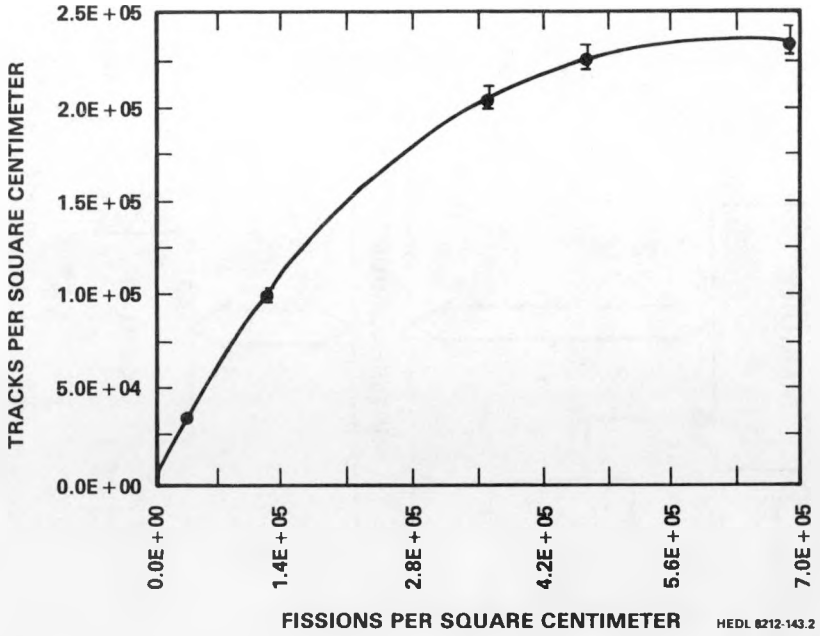

FIGURE 2.48. Track Densities Obtained from Fitting the Track Area Distribution to Eq. (1) Plotted Against the Known Fission Densities for Mica Samples Exposed to a Calibrated Fission Source. [The data have been fit to the paralyzable counter model expressed by Eq. (2)].

and may, in turn, be read into the PDP 11/03 at a slower rate. The data acquired by the PDP 11/03 can then be transmitted to a larger computer for storage on disk or magnetic tape for analysis. A PE3220 computer is utilized for this task. The major components of the ASEM system are shown in Figures 2.50 and 2.51.

Automation of a scanning electron microscope (SEM) for track scanning eliminates the mechanical motion inherent in the stage of an automated optical microscope, yielding improved speed. Since the electron beam is scanned across the SSTR surface in TV raster fashion, reproducibility and reliability are vastly improved by elimination of any mechanical motion.

In addition to improved reproducibility and reliability, a SEM offers a much higher magnification range and, hence, covers a much greater dynamic range of track density than is possible in optical microscopy. These two factors together with the much greater depth of focus of a SEM should provide quantitative data of greater accuracy, especially for high-flux or high-fluence neutron dosimetry experiments in power reactors.

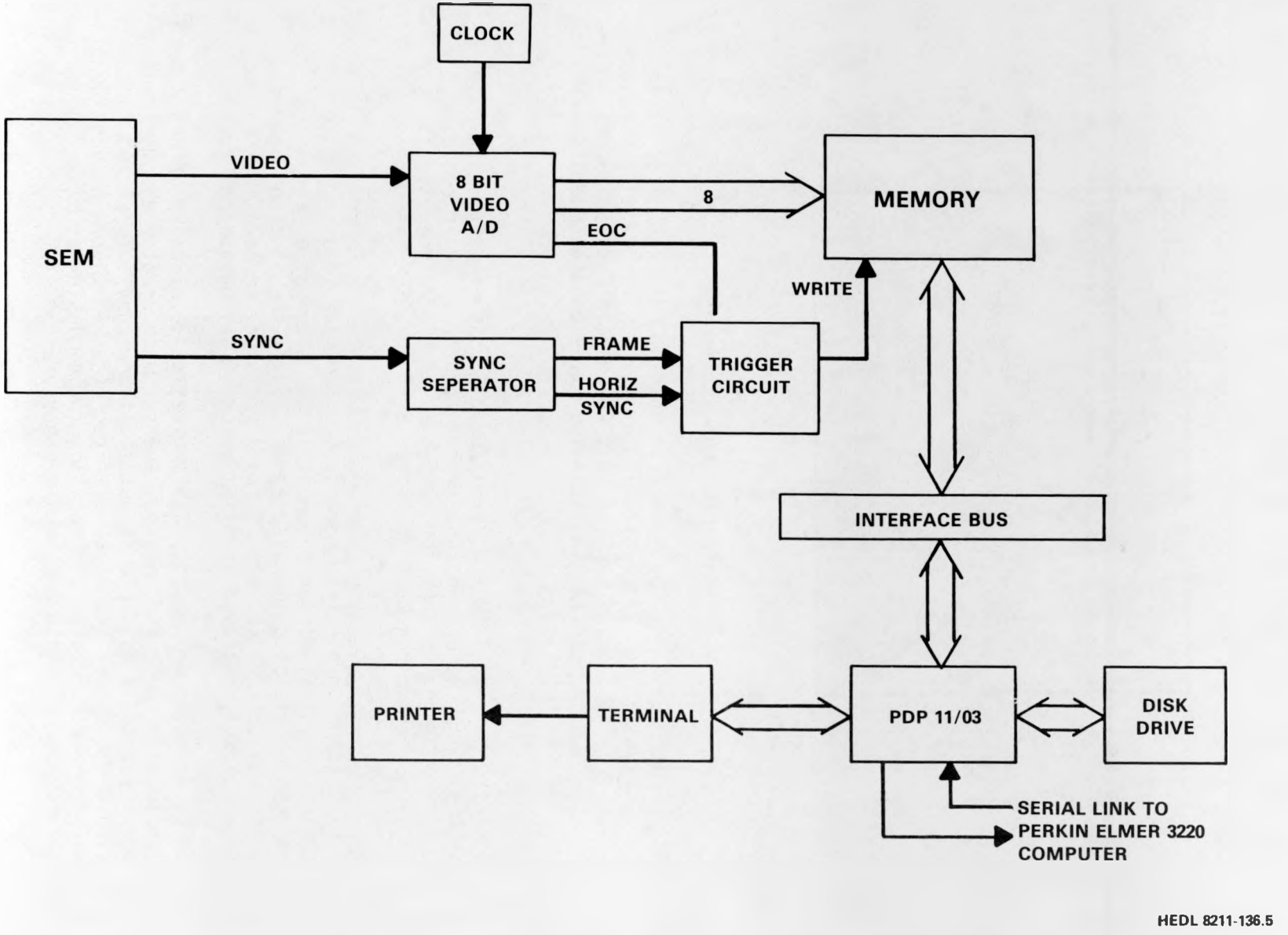

FIGURE 2.49. Block Diagram of the Automated Scanning Electron Microscope (ASEM) System.

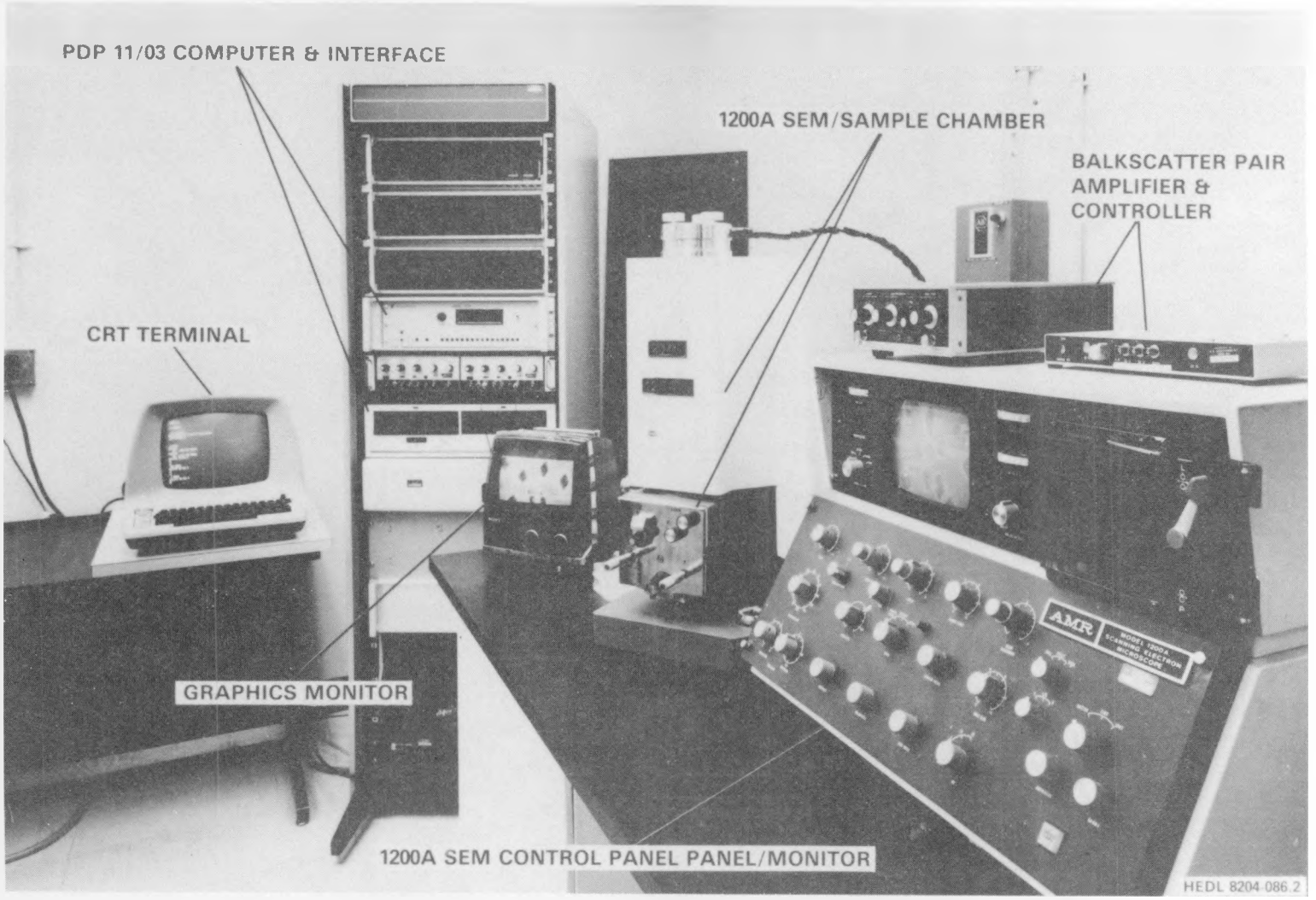

FIGURE 2.50. View of ASEM System Showing SEM and Controls. Neg 8202689-3

FIGURE 2.51. PE3220 Computer System Used to Control and Receive Data for the ASEM System. Neg 8102282-3

In contrast with the HOTS and ESP systems, which are in routine use, the ASEM is still under development. A more detailed description of progress with the ASEM system can be found in the special issue of Nucl. Tracks (Pr83). Software algorithms have been developed for control of the SEM. For example, a code named BUFFON is being developed to take advantage of the Buffon Needle method. Preliminary results indicate the Buffon Needle method of track scanning has significant potential, but further work is necessary before routine operation can be established.

Current development plans to enhance the operation of the ASEM are illustrated in Figure 2.52. Key improvements will be:

- Programmable read-only memory (PROM)-based sequencer to control all logic in the system
- 14-bit precision D/A conversion to generate sweep signals for the SEM
- A/D comparator for data reduction so only significant information need be recorded
- Complete video frame digitized to allow detailed analysis of video information by the computer
- Computer interface protocol to ensure reliable transfer of data
- Built-in diagnostics to verify proper system operation and allow identification of improperly operating components

The key component in the system is the PROM-based sequencer. This unit completely controls and synchronizes all system operations. Its use greatly simplifies the design process and increases reliability because a much smaller number of integrated circuits are required for implementation. The circuit is customized for a particular application by programming a PROM memory. An added advantage is that any future modification desired may be made by simply reprogramming the PROM memory.

The sweep generating circuit is the other significant feature. A 14-bit precision D/A is used to provide precise, externally controlled positioning of the SEM beam. Because the central signal for beam positioning starts as a digital count and is available in the system, there is no difficulty providing an accurate position count to the computer.

Diagnostic software programs on the DEC 1103, which would fully exercise the signal processing system to verify correct operation and identify any malfunction, is also planned.

Emulsion Scanning Processor (ESP) System

Because of the diverse utility of NRE in scientific research, many groups have developed special instrumentation systems to aid in the task of emulsion scanning. A review text (Ba63) on NRE summarizes earlier NRE-instrumentation activities. More recently, a Russian group has developed an emulsion scanning instrumentation system for fast neutron measurements (Be72).

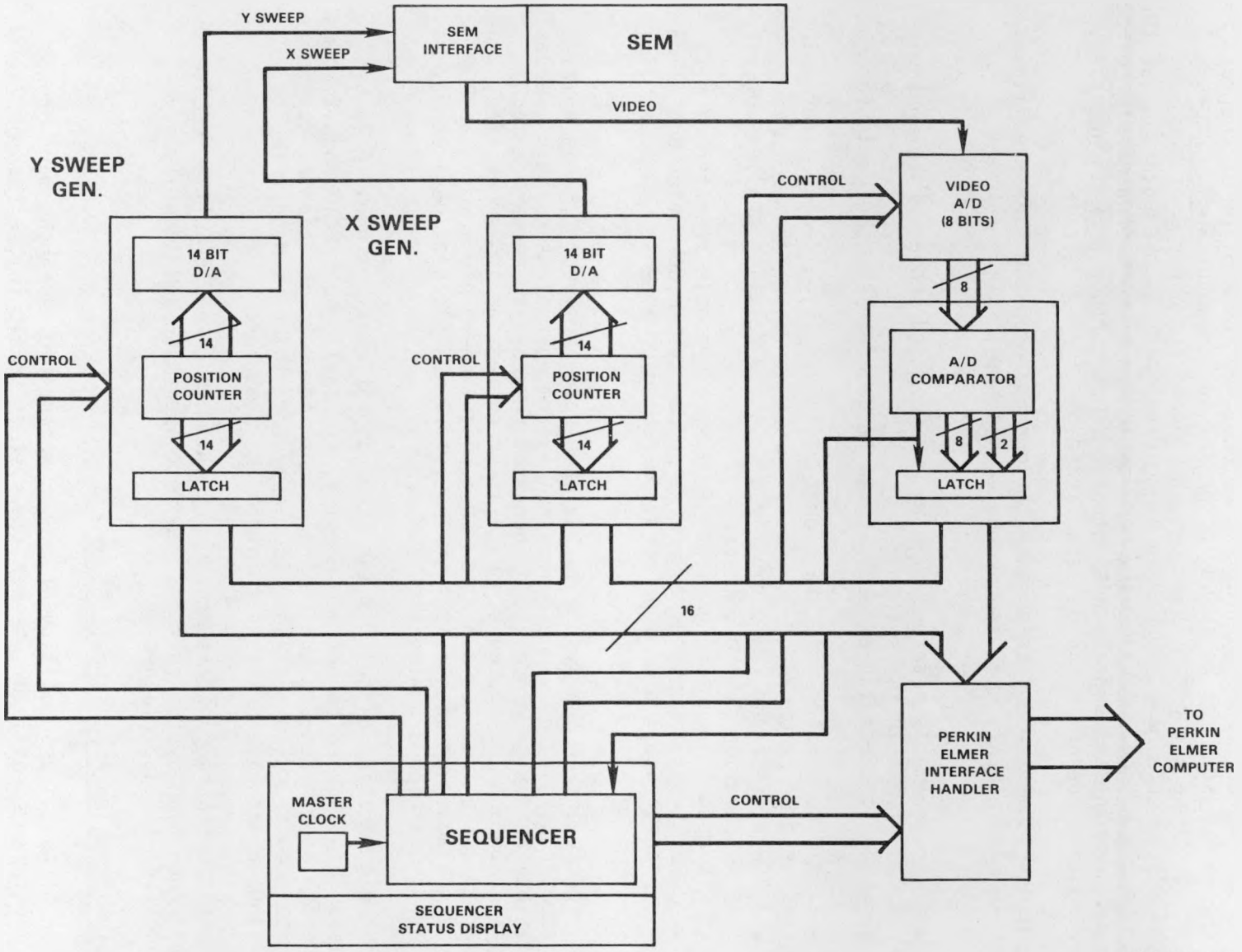

FIGURE 2.52. Block Diagram of the ASEM System Under Development.

Applications of NRE in neutron dosimetry and spectrometry have motivated the development of a computer-based interactive system for scanning emulsions. This system, the Emulsion Scanning Processor (ESP), has been developed to measure the lengths of proton-recoil tracks in NRE as well as to store, process, and analyze track data so obtained. To date, this system has been successfully used for neutron dosimetry and spectrometry in FBR and LWR environments as well as in the standard ^{252}Cf neutron field at the NBS.

In the ESP system (shown in Figure 2.53) the X, Y, and Z (focus) stage motion of a motorized Universal Zeiss microscope is controlled by a PDP 11/03-L computer. The computer receives all operator instructions, moves the stage as directed, and stores positional information on command. Software programs, stored on floppy disks, provide the flexibility needed to conveniently tailor operating, storage, and data presentation formats to fit different scanning situations. The motorized stage possesses a travel of 75 mm in the X-direction, 25 mm in the Y-direction, and 4 mm in the Z (focus) direction. Digital motion step size is 0.25 μm in the X and Y directions, whereas the Z-direction step size 0.05 μm. An operator must interact with the system to obtain the desired results. The joystick and push button controls are used to set parameters and boundaries, focus, locate tracks, measure track lengths, categorize, and store track data.

To our knowledge, the ESP system is the first truly interactive system developed and used for emulsion scanning. This system possesses interfaces between all three fundamental constituent elements, namely man, microscope, and computer. Of equal significance is the reliance upon computer control to the maximum extent possible. For these reasons, the ESP system provides a substantial advance in the state-of-the-art of emulsion scanning systems in terms of both accuracy and cost-effectiveness. Since space limitations preclude an in-depth description of the ESP system here, the reader should consult a recent publication (Go83) for greater details.

To date, the ESP system has been used exclusively for observation of proton-recoil tracks in neutron dosimetry measurements. Based on these efforts, the power and flexibility of this system have been demonstrated by the development of computer codes to handle three completely different scanning tasks:

- Track length measurements in 4π irradiated emulsions for differential neutron spectrometry
- Track length measurements in 4π irradiated emulsions for integral neutron dosimetry
- Track length measurements in emulsions irradiated in collimated or undirectional neutron beams for differential neutron spectrometry

These scanning tasks correspond to operation of the ESP system in different modes, namely differential mode scanning, integral mode scanning, and end-on scanning, respectively. Differential mode scanning has been used for NRE

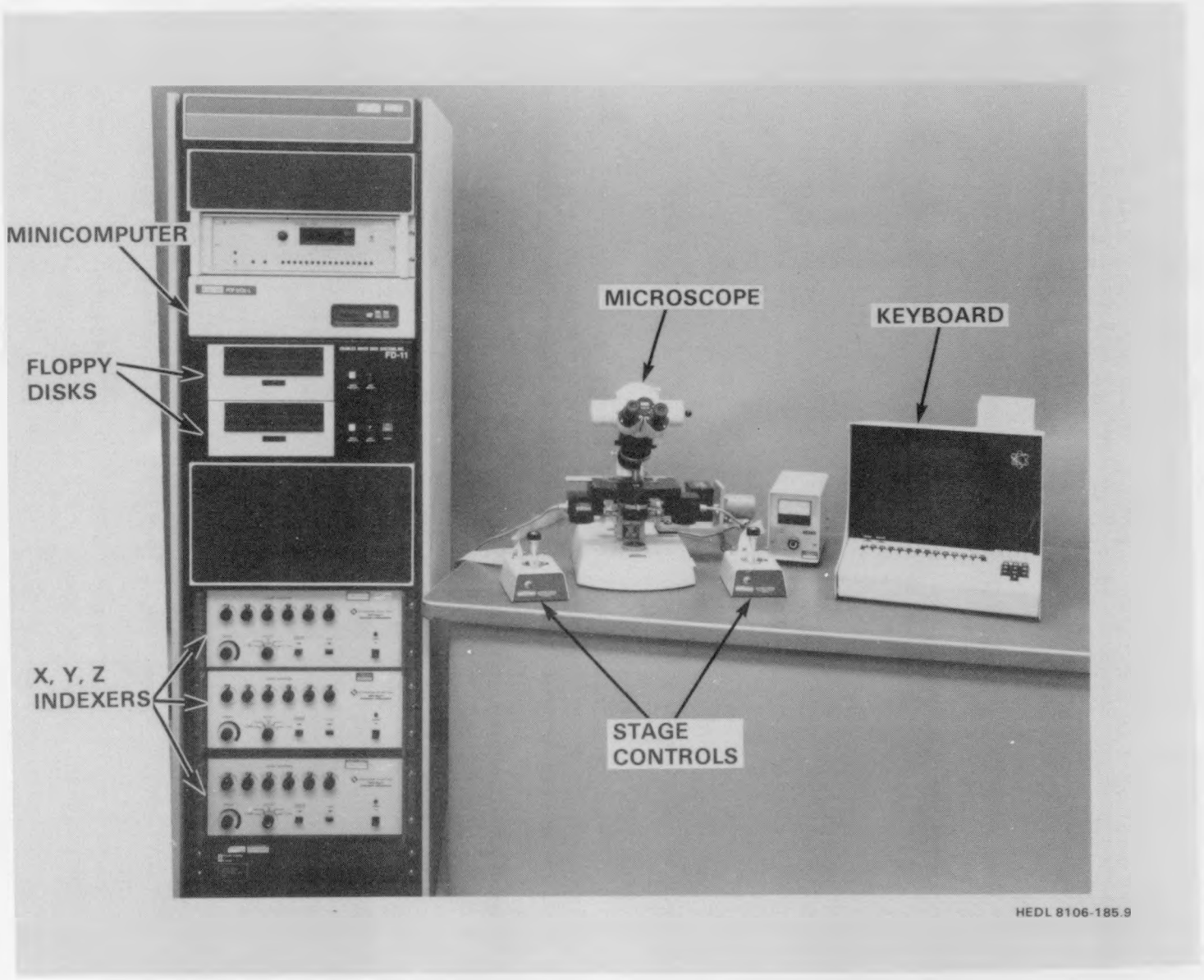

FIGURE 2.53. Interactive Emulsion Scanning Processor (ESP) System. Neg 8105389-3

differential neutron spectrum measurements in the FFTF at startup (Go81). Indeed, these efforts led to the first experimental confirmation of the existence of angular anisotropy in the neutron field within a reactor core. Integral mode scanning has been used for NRE integral proton-recoil reaction rate measurements in the LWR-PV mockup at the ORNL PCA (Go81d,Go81e). The end-on scanning mode has been applied with NRE exposed in the NBS Standard ^{252}Cf fission neutron benchmark field. End-on irradiations can be conveniently carried out in this point source ^{252}Cf neutron field. Figure 2.46 displays results obtained from scanning ~2 x 10^3 tracks in the end-on mode. The comparison presented in Figure 2.54 with the recommended ^{252}Cf spectrum is absolute. Over the energy range of these NRE measurements (~0.8 MeV to 10 MeV), the NRE-observed ^{252}Cf neutron spectrum is within experimental uncertainty of the absolute neutron intensity claimed for this neutron standard benchmark field (Gr75b,Gr78). This agreement in absolute neutron flux intensity is particularly significant since the NBS ^{252}Cf neutron field has been calibrated independently using the manganese bath method (Gr77b).

Sources of uncertainty arising in absolute NRE neutron spectrometry are summarized in Table 2.31. In contrast with the first five sources of

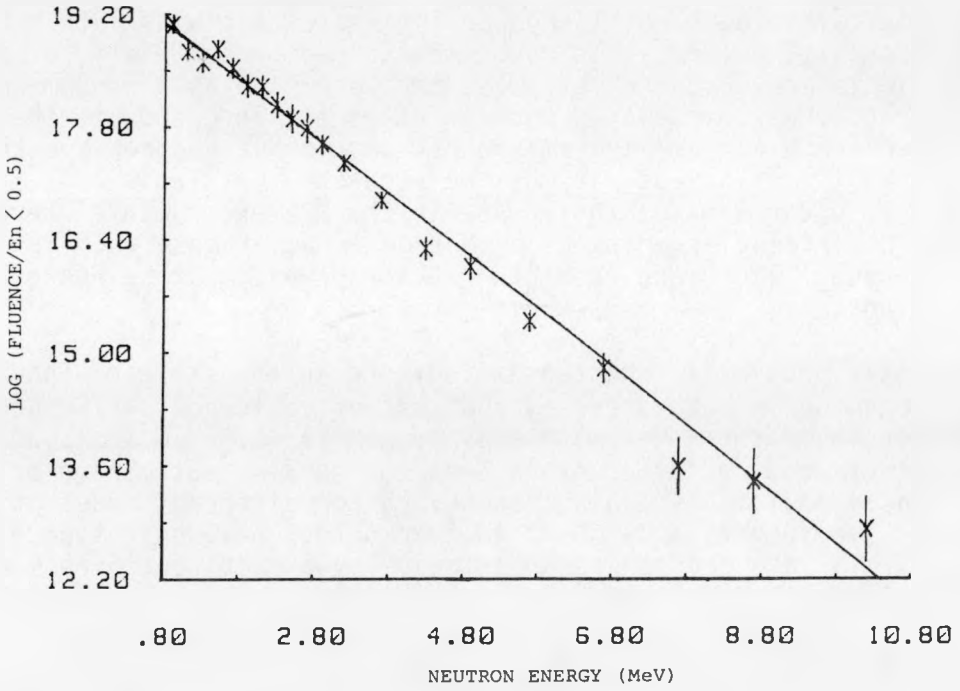

FIGURE 2.54. End-On Scanning Mode Results Obtained from NRE Irradiated in the Reference ^{252}Cf Fission Neutron Field at NBS. [The smooth curve is the NBS-recommended segmented representation of the ^{252}Cf spectrum (Gr75,Gr78). The comparison is absolute.]

TABLE 2.31

UNCERTAINTY ESTIMATES FOR ABSOLUTE NEUTRON SPECTROMETRY WITH NRE

Source of Uncertainty	Approximate Uncertainty (1σ)
Proton range straggling	2%
Proton energy based on range-energy relation	2%
Hydrogen density in the emulsion	3%
Elastic scattering cross section σ_{np} (E)	1%
Volume of emulsion scanning with ESP system	2%
Range measurements with the ESP system	0.5 μ

uncertainty listed in Table 2.31, which are systematic, the range measurement uncertainty does not introduce any systematic bias into NRE neutron spectrometry. Hence, this range measurement uncertainty, or the corresponding energy uncertainty, must be classified as a random uncertainty. Since these systematic uncertainties are independent, the quadrature uncertainty for all systematic effects in NRE neutron spectrometry comes to ∿5%. Nevertheless, it must be stressed that Table 2.31 is restricted to uncertainties that arise in the NRE experimental technique. Additional uncertainties arising in neutron irradiations, such as in irradiation exposure time t and absolute reactor power, must be recognized and treated separately.

The ESP system provides a substantial advance in the state-of-the-art of emulsion scanning in both accuracy and cost-effectiveness. The uncertainty in track length measurements with this system is ∿0.52 μm (1σ), an improvement of about a factor of ∿4 over the earlier automation efforts of (Be72). While emulsion scanning rates vary for different modes of system operation, scanning rates of 30 to 40 tracks/hour have been typically obtained. This rate represents an increase by a factor of 3 to 4 over the scanning rates attained in earlier work (Be72).

Current Efforts

HOTS -- A number of improvements are currently being implemented on the HOTS system. Methods for improving reproducibility are being implemented. Finer control of focus as well as improved autofocusing will be incorporated to improve discrimination between tracks and imperfections in both mineral and plastic SSTR. Imperfections in mica present problems in accurate track counting at low-track densities. Methods of alleviating this problem, such

as software routines for track shape discrimination, will be explored. Preliminary studies of track diameter measurements in CR-39® polymer show promise, but finer focus control is necessary to attain accurate results. Software improvements currently underway are frame-by-frame correction for track pile-up (for SSTR possessing non-uniform track density) and subframe corrections for variations in frame (videcon) illumination.

ASEM -- The ASEM will be applied in scanning high-track density SSTR, and the limitations of the Buffon Needle method (Go82) and alternative sampling methods will be established.

ESP -- Design plans to convert the interactive ESP system to a fully automated system will be initiated. The highest priority of this new design will be to fully automate integral mode scanning.

2.5.2.2 Continuous Gamma-Ray Spectrometry

To meet the needs of the LWR-PV-SDIP, continuous gamma-ray spectrometry has been carried out in simulated LWR-PV environments. These in-situ observations provide gamma-ray spectra, dose, and heating rates that are needed to:

- Assess the radial, azimuthal, and axial contributions of gamma heating to the temperature attained within the PV wall and other components of commercial LWR power reactors
- Design and analyze high-power LWR irradiation tests, such as the PSF metallurgical test
- Test a new and novel nondestructive method for the direct determination of PV neutron exposure based on in-situ observation of continuous gamma-ray spectra.

Independently, these measurements provide absolute data that can be used for comparison with calculations. In particular, gamma-ray flux spectral data are needed and are used to assess photofission background in LWR-PV passive neutron fission dosimetry and gamma heating in reactor components.

Experimental Technique

The basic principles underlying Compton recoil gamma-ray spectroscopy have been adequately documented (Go68a,Go70a,Go70b,Ji78,Ko75,Si68,Si69). Since its inception, however, this method has undergone continuous improvement. Advances in this technique were reviewed at the last two international ASTM-EURATOM Symposia on reactor dosimetry (Go80d,Go82b). Further developments as well as applications in breeder reactor environments have also been reported (Go79b,Go80b). This method continues to evolve so that even the most recently reported efforts (Go82b) require updating. Consequently, improvements incorporated into the Janus spectrometer for the 1981 PCA experiments are explained below.

®CR-39 is a registered trademark of PPG Industries, Pittsburgh, PA.

Janus Spectrometer -- The basic elements that comprise the Si(Li) gamma spectrometer Janus probe system are displayed in Figure 2.55. This optimized system differs from that previously reported in four important ways:

- Two separate, identical, cooled, 1-cm³ Si(Li) detectors are placed face-to-face as shown in Figure 2.56.
- Each detector output is fed into a reconfigured version of the ORTEC 142A preamplifier, in which the front end FET stage is cooled.
- Pulse processing instrumentation has been altered from the original Janus probe electronics. Coincident counting between Si(Li) detectors is still possible, but no pulse shape discrimination is used.
- The detector vacuum enclosure has also been modified, as shown in Figure 2.57, to reduce the probe perturbation on the LWR-PVS gamma field. Specifically, the detectors are now separated from the electronics below by a 0.254-cm steel plate. Steel plates have also been used to reduce the vacuum voids beside and above the detector to 0.254 cm.

These modifications provide the following capabilities:

- Two complementary modes of operation:
  - -- Noncoincidence mode for low-energy spectrometry ($\lesssim$3 MeV).
  - -- Coincidence mode for high-energy spectrometry ($\gtrsim$3 MeV).
- Improved discrimination against neutron-induced events, since neutron interactions produce short-range events that are excluded in the coincidence-mode operation.
- Improved high-energy coincidence-mode response for unfolding analyses.
- Lower common mode noise and better resolution by utilizing a differential shaping amplifier in place of the cascaded differential and linear amplifiers used previously.
- Single-parameter, rather than dual-parameter analysis, reduces the complexity of the pulse processing instrumentation as well as the procedures necessary for data collection and unfolding.

The recent change from dual- to single-parameter pulse analysis was based upon a careful study of Si(Li) energy and rise-time spectra as a function of gamma-ray energy, using monoenergetic gamma-ray sources in the 0.1 to 7.0 MeV energy region. Two significant observations were generated in this study:

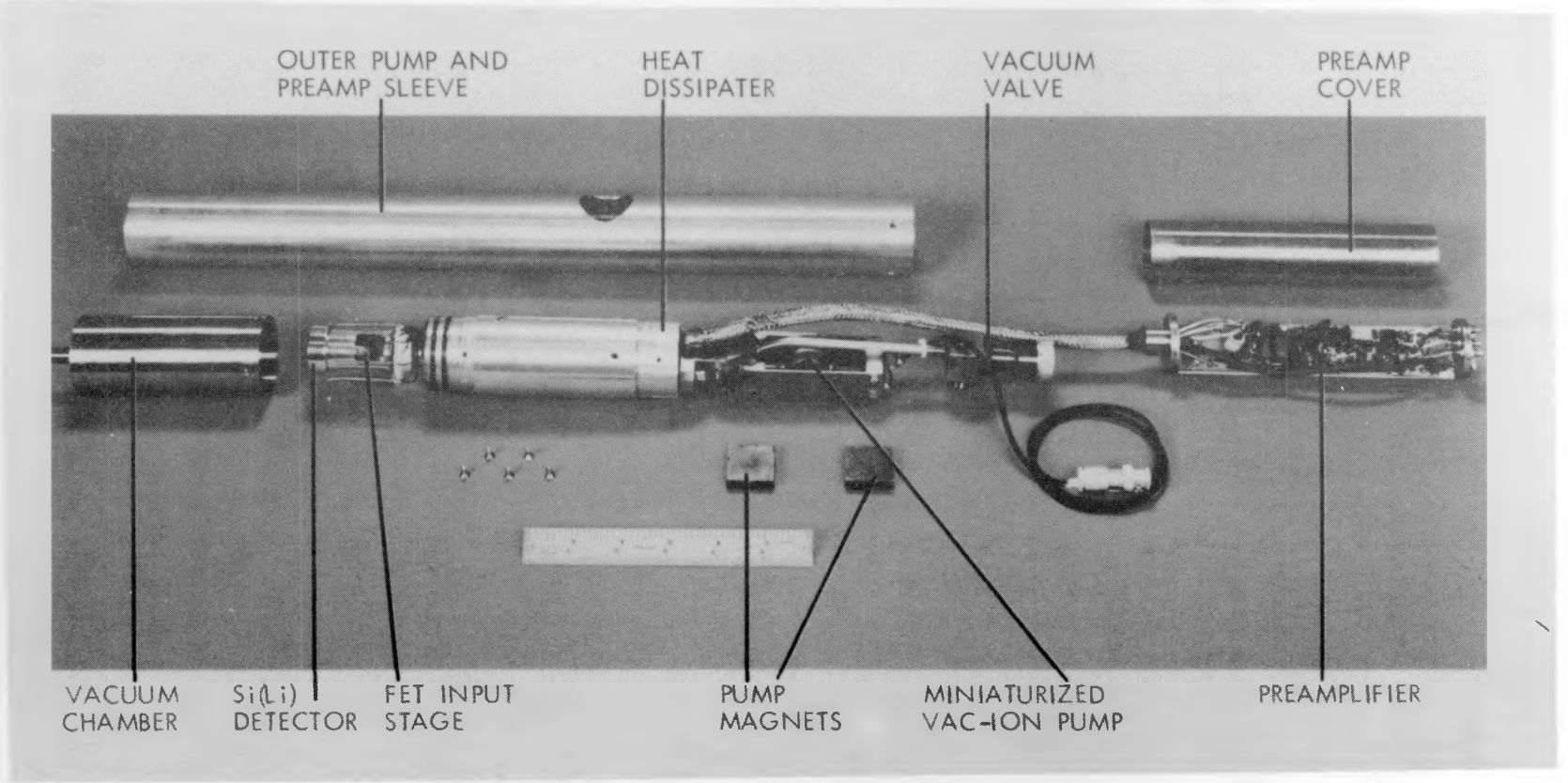

FIGURE 2.55. Components That Comprise the Janus Probe Used for Continuous Compton Recoil Gamma-Ray Spectroscopy. Neg 7908303-4

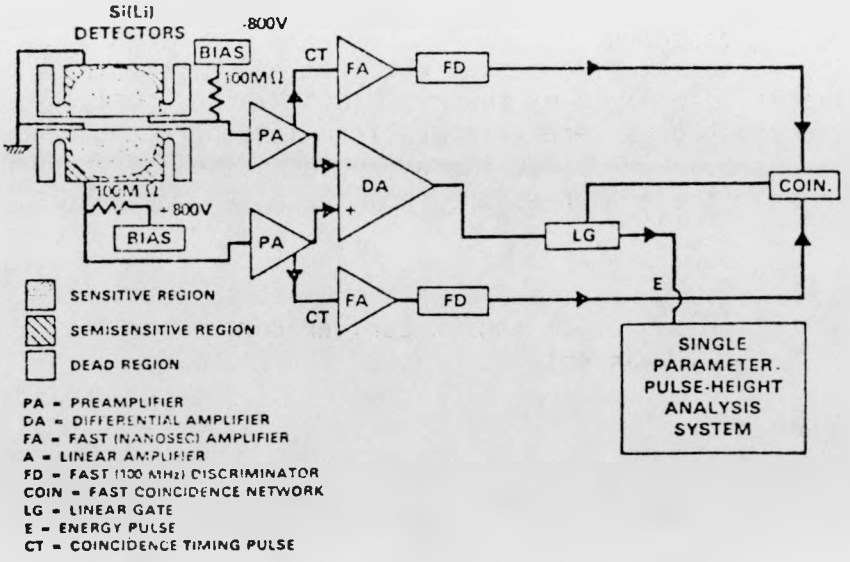

FIGURE 2.56. Cross Section of the Janus Detector Configuration and Block Diagram of the Pulse Processing Instrumentation.

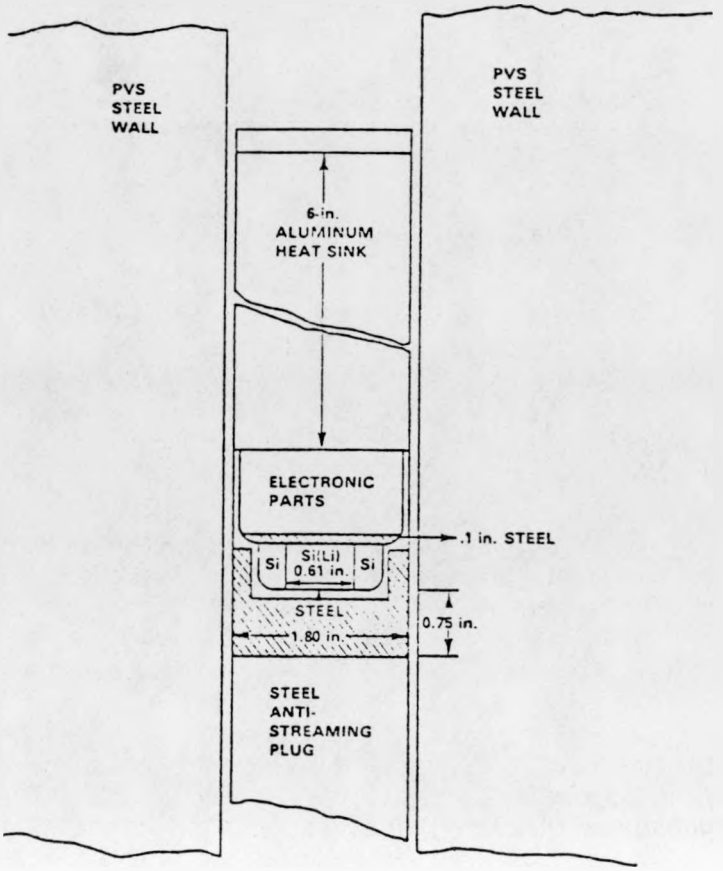

FIGURE 2.57. In-Situ Irradiation Environment of the Si(Li) Janus Probe in the LWR-PVS.

- Rise-time spectra were found to be electron (hence gamma-ray) energy-dependent.
- The variation of observed electron energy spectra was not adequately described by theory (Klein-Nishina formula). [These energy spectra were obtained from monoenergetic gamma-ray sources in the 0.1 to 7.0 MeV energy region using rise-time discrimination to reject electron escape from the Si(Li) detectors.]

As a result of this study, the use of theory as the basis for response matrix construction, as practiced in earlier continuous gamma-ray spectrometry efforts (Go70), was not appropriate for the Janus probe. Under these conditions, empirical response matrix construction affords greater accuracy, since systematic effects are automatically included in the observed monoenergetic responses that are used, in turn, to construct the response matrix. Moreover, the experimental technique is simplified considerably by use of single-parameter as opposed to dual-parameter pulse analysis. The success of this single-parameter, empirical response matrix approach has already been demonstrated through the satisfactory comparison of Janus probe results with a Ge(Li) spectrometer observation of a line spectrum from a ^{226}Ra source (Go81c,Go82b).

Data Analysis -- Empirical response matrix construction to date has only been performed in the low-energy (noncoincidence) region. Hence, results reported here are necessarily confined to the energy region $\lesssim$3 MeV.

The empirical response matrix was constructed from the measured responses of eight monoenergetic gamma-ray sources. Monoenergetic gamma-ray energies ranged from 0.3208 to 2.754 MeV. Table 2.32 lists the sources used. The following sections describe data preparation and response matrix construction in detail.

Initial Data Preparation -- The first step in preparing the eight measured monoenergetic responses is to normalize each response to a fixed fluence at the center of the detector. Using absolute source strength together with geometric correction factors, each monoenergetic Compton recoil spectrum is normalized to 10^6 γ/cm^2 at the detector center. In addition, the ^{22}Na and ^{24}Na spectra are corrected to remove secondary gamma (0.511 MeV for ^{22}Na and 1.3686 MeV for ^{24}Na).

Response Matrix Generation -- An empirical response matrix (256 x 256) is constructed for the Janus probe. Each column, j, of the matrix represents the response of the detector for a gamma-ray fluence of 10^6 γ/cm^2 at the detector center. The gamma-ray energy of each column is that energy having its Compton edge at row i=j. Rows of the matrix possess a 10-keV electron energy width.

Construction of the matrix is accomplished by the use of an analytical expression having parameters computed from the eight measured monoenergetic gamma-ray responses. The analytical expression contains terms to account for

TABLE 2.32

MONOENERGETIC SOURCES USED IN RESPONSE MATRIX CONSTRUCTION

Radioisotope	Photon Energy (MeV)	Compton Edge Energy (MeV)
^{51}Cr	0.3208	0.1779
^{198}Au	0.4118	0.2541
^{64}Cu	0.511	0.3407
^{137}Cs	0.6616	0.4773
^{54}Mn	0.8348	0.6394
^{65}Zn	1.115	0.9071
^{22}Na	1.275	1.0618
^{24}Na	2.754	2.5201

the basic Gaussian broadened theoretical Compton recoil spectrum, low-energy tails due to escape and electronic noise, photopeaks, pair production peaks, and multiple-scattering effects. To more clearly explain how these parameters are computed, the analysis of the ^{137}Cs will be shown in detail.

The measured response (electron spectrum) for ^{137}Cs is shown in Figure 2.58. The first step in the analysis is to define the Gaussian broadened theoretical Compton spectrum portion of the measured response. Figure 2.59 shows the theoretical Compton recoil spectrum for a 0.662-MeV gamma ray. A trial-and-error method is used to define a broadening term that, when applied to the theoretical spectrum, will produce a spectrum having a shape at the Compton edge comparable to the measured response.

The Gaussian-broadened spectrum is then normalized to the measured response magnitude at the Compton edge. Figure 2.60 shows the normalized, Gaussian-broadened spectrum. The broadening factor and the magnitude of the response at the Compton edge are two terms used in the final expression.

Parameters for the other components of the spectrum are determined from the result of subtracting the broadened, theoretical spectrum from the measured response. This result is shown in Figure 2.61. Three of the four possible components are shown: the low-energy tail, the multiple-scattering peak, and the photopeak. The pair production peak is not a part of the ^{137}Cs response since the gamma-ray energy is below the threshold for pair production ($\sim$1.02 MeV).

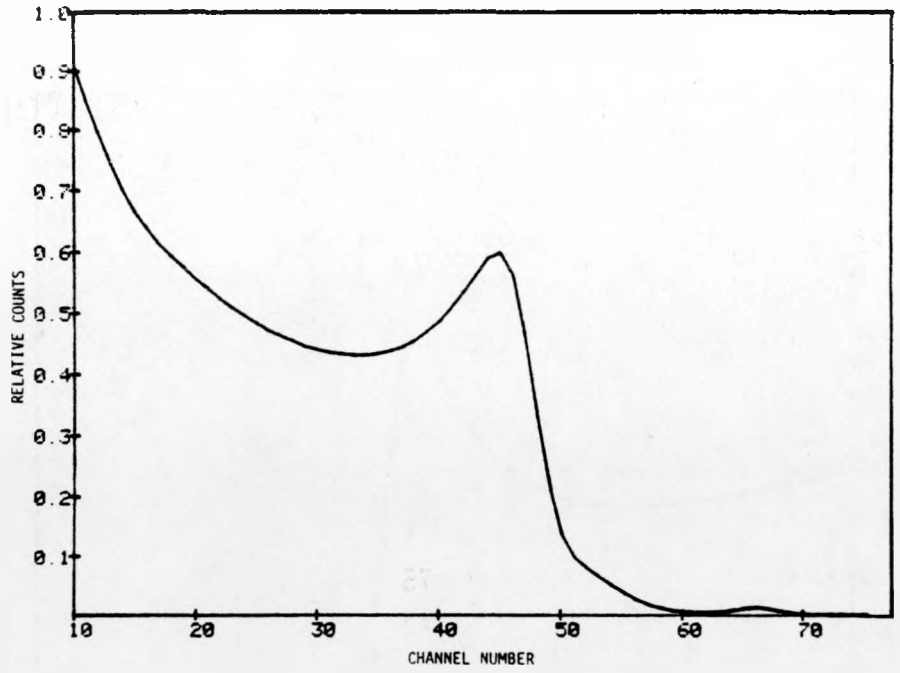

FIGURE 2.58. Measured Electron Spectrum for ^{137}Cs.

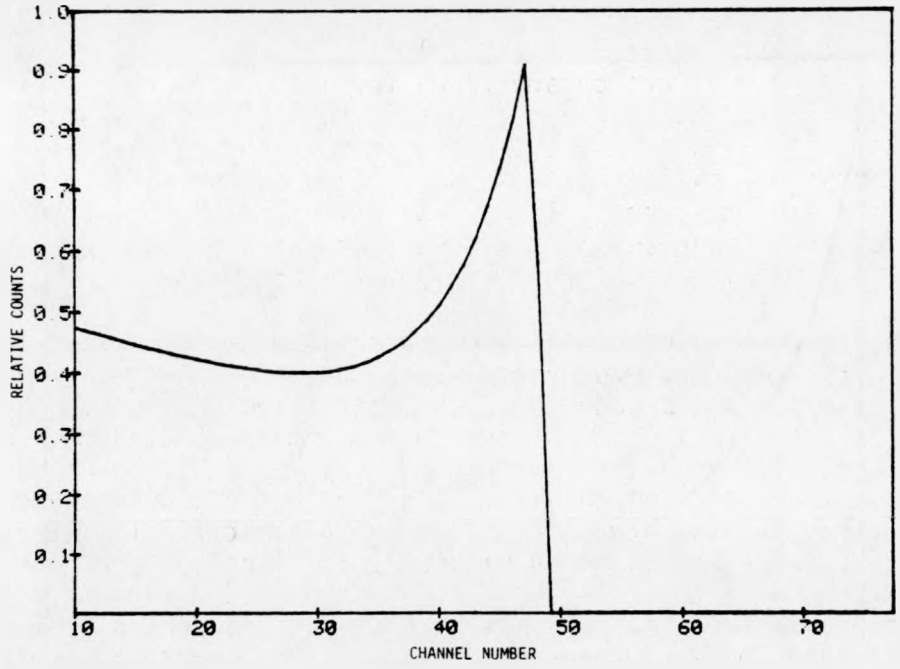

FIGURE 2.59. Theoretical Compton Recoil Spectrum for the 0.662-MeV Gamma Ray.

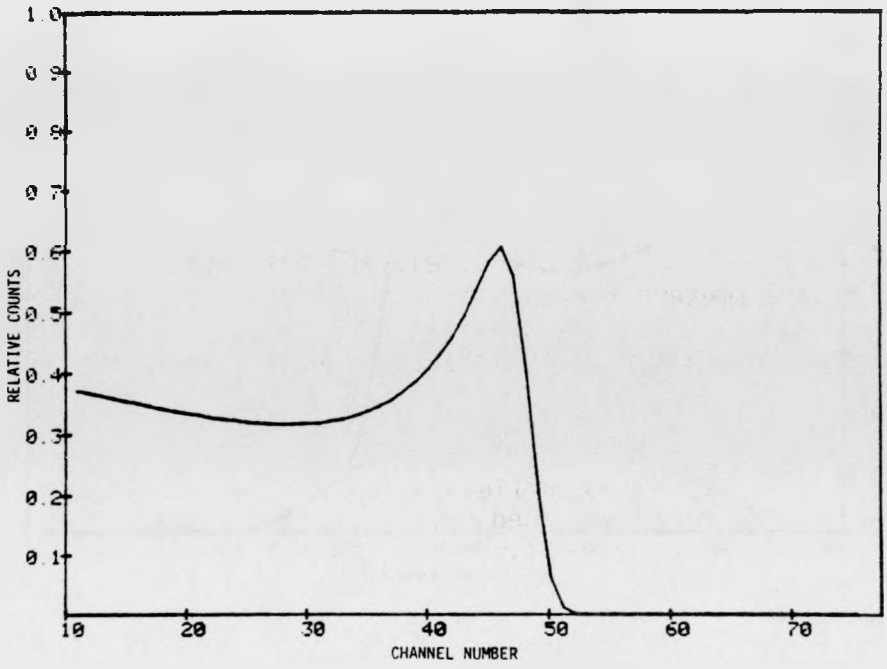

FIGURE 2.60. Normalized Gaussian-Broadened Spectrum for ^{137}Cs.

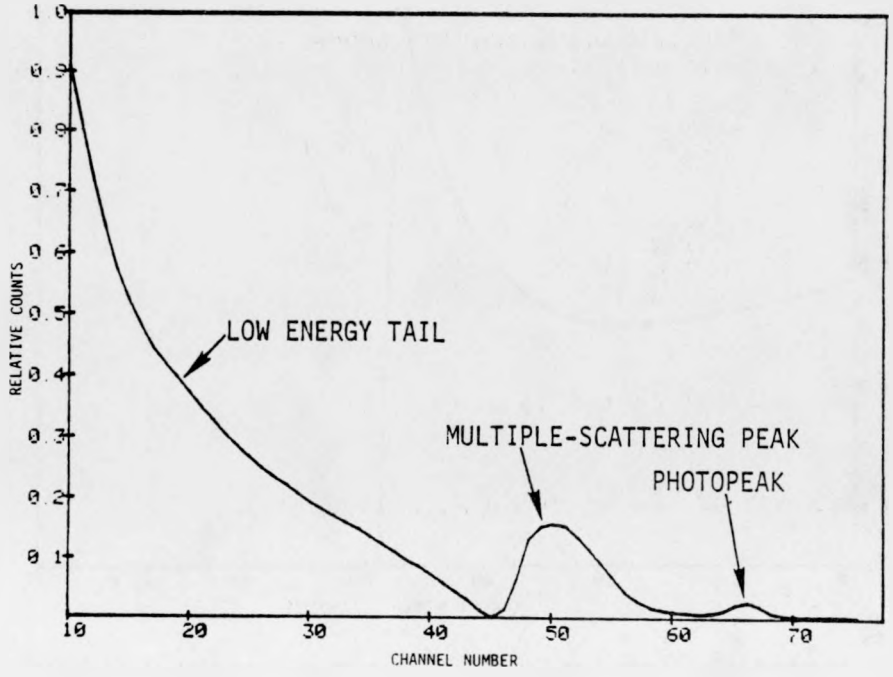

FIGURE 2.61. Results of Subtracting the Broadened, Theoretical Spectrum from the Measured Spectrum for ^{137}Cs.

The low-energy tail is fit to a sum of two decaying exponentials using a nonlinear least-squares fitting routine. Four parameters are generated from this fitting process. The multiple-scattering peak is represented by the coupling of two Gaussians, both having the same height but different widths. Figure 2.62 shows the result for the ^{137}Cs spectrum. Three parameters are generated from this fit. The photopeak is treated as a single Gaussian. A least-squares fit is made to calculate the height and width parameters. Pair production peaks are treated in the same manner as photopeaks.

The result of the analysis is a set of eleven (thirteen, if there is a pair production peak) parameters for each of the monoenergetic gamma-ray sources. Each of these parameters is, in turn, fit to a smooth curve in gamma-ray energy space. Thirty values are tabulated between 0.32 MeV and 2.75 MeV for each parameter.

The response matrix is generated column by column. The gamma energy is chosen such that its Compton edge lies in row i=j, and the parameters for this gamma-ray energy are determined by interpolation in the parameter tables. Figure 2.63 shows the calculated response for ^{137}Cs, and Table 2.33 presents a comparison between the calculated and measured ^{137}Cs responses. The deviation between parametric and observed responses can exceed 10%. However, these larger deviations arise in regions where the response is relatively small. In regions where the response is substantial, the deviation between parametric and observed responses is generally <5%.

Unfolding -- Gamma continua are obtained with iterative unfolding (Go70c). The arresting criterion for the iteration process was modified to account for not only the statistical fluctuation in the data, but also for the error, σ_E, in energy calibration. Hence, the standard deviation at each channel σ_i was computed as:

$$\sigma_i^2 = N_i + \left(\frac{\partial W}{\partial E}\right)_i^2 (\sigma_E)_i^2 \qquad (1)$$

where:

N_i = Number of counts in channel i

$\left(\frac{\partial W}{\partial E}\right)_i$ = Slope of the spectrum at channel i

$\left(\sigma_E\right)_i$ = Error in electron energy at channel i

Iterative unfolding is arrested when the sum of the residuals decreases below a prescribed bound A. The initial estimate for A is taken as:

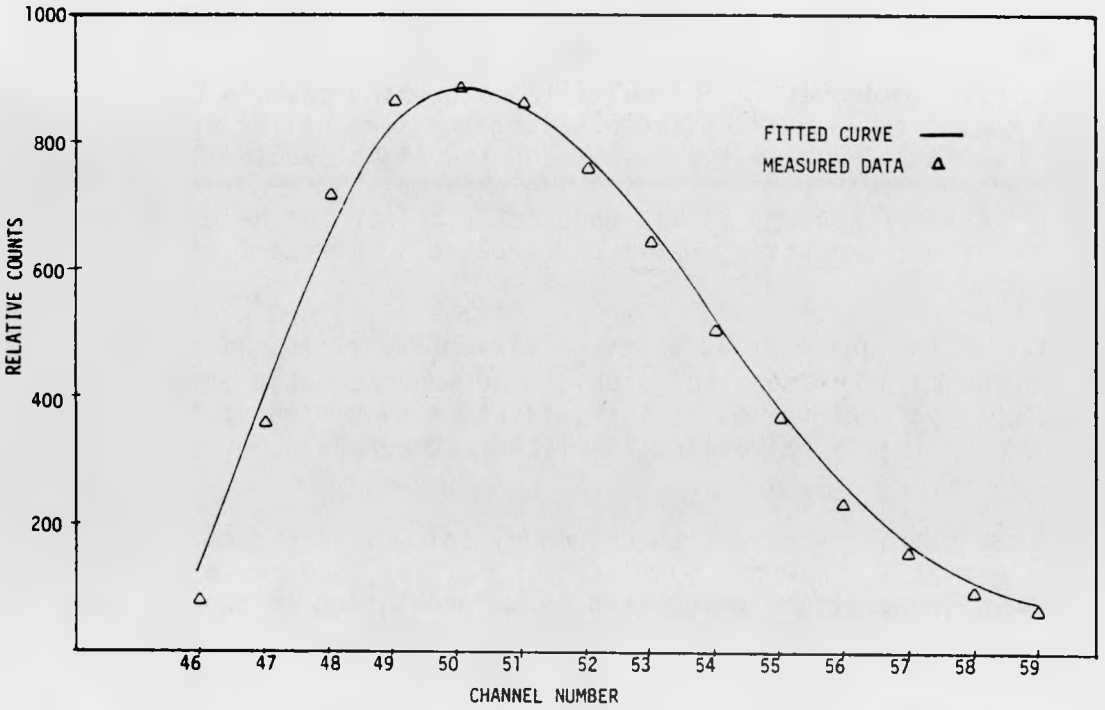

FIGURE 2.62. Result of Nonlinear Least-Squares Fit of the Multiple-Scatter Peak for the ^{137}Cs Spectrum.

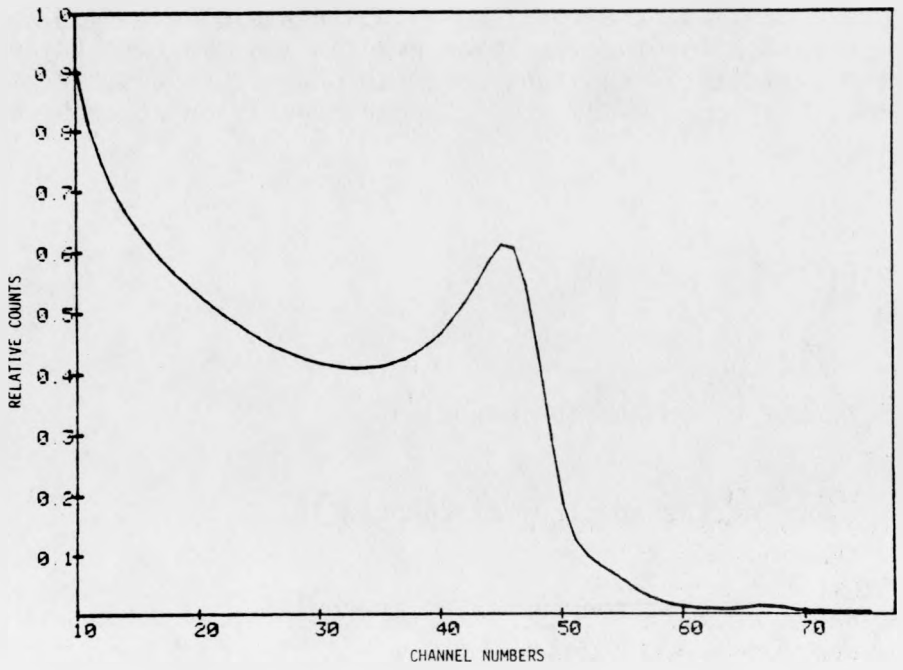

FIGURE 2.63. ^{137}Cs Response Calculated from the Empirical Response Matrix.

TABLE 2.33

COMPARISON BETWEEN CALCULATED AND MEASURED
COMPTON RECOIL SPECTRA FOR ^{137}Cs

Channel No.	Calc/ Meas	Channel No.	Calc/ Meas	Channel No.	Calc/ Meas
10	0.987	32	0.947	54	1.060
11	0.956	33	0.947	55	1.087
12	0.947	34	0.948	56	1.102
13	0.948	35	0.950	57	1.140
14	0.954	36	0.950	58	1.022
15	0.958	37	0.951	59	1.136
16	0.960	38	0.953	60	1.131
17	0.959	39	0.955	61	1.128
18	0.956	40	0.957	62	1.128
19	0.953	41	0.960	63	1.125
20	0.951	42	0.965	64	1.116
21	0.951	43	0.973	65	1.093
22	0.951	44	0.988	66	1.026
23	0.951	45	1.019	67	1.091
24	0.950	46	1.080	68	1.128
25	0.950	47	0.970	69	1.118
26	0.949	48	0.921	70	1.116
27	0.948	49	0.900	71	1.096
28	0.948	50	0.932	72	1.110
29	0.948	51	0.990	73	1.130
30	0.948	52	1.047	74	1.146
31	0.947	53	1.063	75	1.138

$$A = \sum \sigma_i^2 \qquad (2)$$

The arresting criterion is empirically refined by observing the results of unfolding a known gamma-ray line spectrum, such as ^{226}Ra.

The adequacy of using single-parameter data acquisition together with empirical response matrix unfolding has already been demonstrated through comparison with a Ge(Li) spectrometer using the line spectrum from a ^{226}Ra source (Go81b,Go82b). Obviously, unfolding a line spectrum, such as ^{226}Ra, is a very rigorous test for a continuum spectrometry method. Nonetheless, the unfolded gamma-ray continuum is indeed a line spectrum, and the energy of the unfolded peaks agrees with known ^{226}Ra energy peaks to an uncertainty of <1%. Of equal significance was the fact that the absolute peak intensities of the Janus and Ge(Li) spectrometers agreed to within ~10% over the low-energy region (i.e., $\lesssim$3 MeV).

2.5.2.3 Instrumentation

The computer-based pulse height analyzer system, shown in Figure 2.64, serves as the main instrumentation system for in-situ gamma spectrometry in LWR-PV environments. As such, it must be readily transportable to different sites throughout the world without adverse effects. It is capable of routine use in the following configurations:

- Low-resolution (256 x 256), high-speed (10^5 cps) data acquisition for Compton recoil gamma-ray spectrometry with up to 8×10^6 counts/channel.
- High-resolution (8192 x 8192 x 8192 x 8192 or any subset), low-speed (10^4 cps) data acquisition for proton-recoil and ^6Li fast neutron spectrometry.
- Data processing and analysis of spectra using complex unfolding codes.

Other operating modes are readily programmed into the special analog-to-digital converter (ADC) microprocessor, such as the input from four ADC with a 256-channel resolution. For example, this special microprocessor can operate on the ADC signal to produce a two-parameter direct memory access (DMA) input to the DEC 11/34 computer of

$$\text{Parameter 1} = \frac{\text{ADC1 + ADC2}}{\text{Sum of all ADC}}$$

$$\text{Parameter 2} = \frac{\text{ADC1 + ADC4}}{\text{Sum of all ADC}}$$

Table 2.34 lists the specific components of the system. Figure 2.64 is a photograph of this system, as well as the "front-end" NIM electronics used for Compton recoil gamma-ray spectrometry measurements.

To gain greater system flexibility and to eliminate the need for interchanging ADC boards to go from the list mode to the DMA mode of operation, a microprocessor-controlled ADC interface for the DEC Q-bus was designed. Versatility has been emphasized in the design of this ADC interface. It will be possible to use this interface with any DEC 11/34 system. More significantly, it will provide the capability of DMA in any two-parameter configuration up to 256 by 256 and any list mode acquisition up to four parameters with a resolution fo 8192. Moreover, being microprocessor based, a great number of other ADC configurations can be programmed.

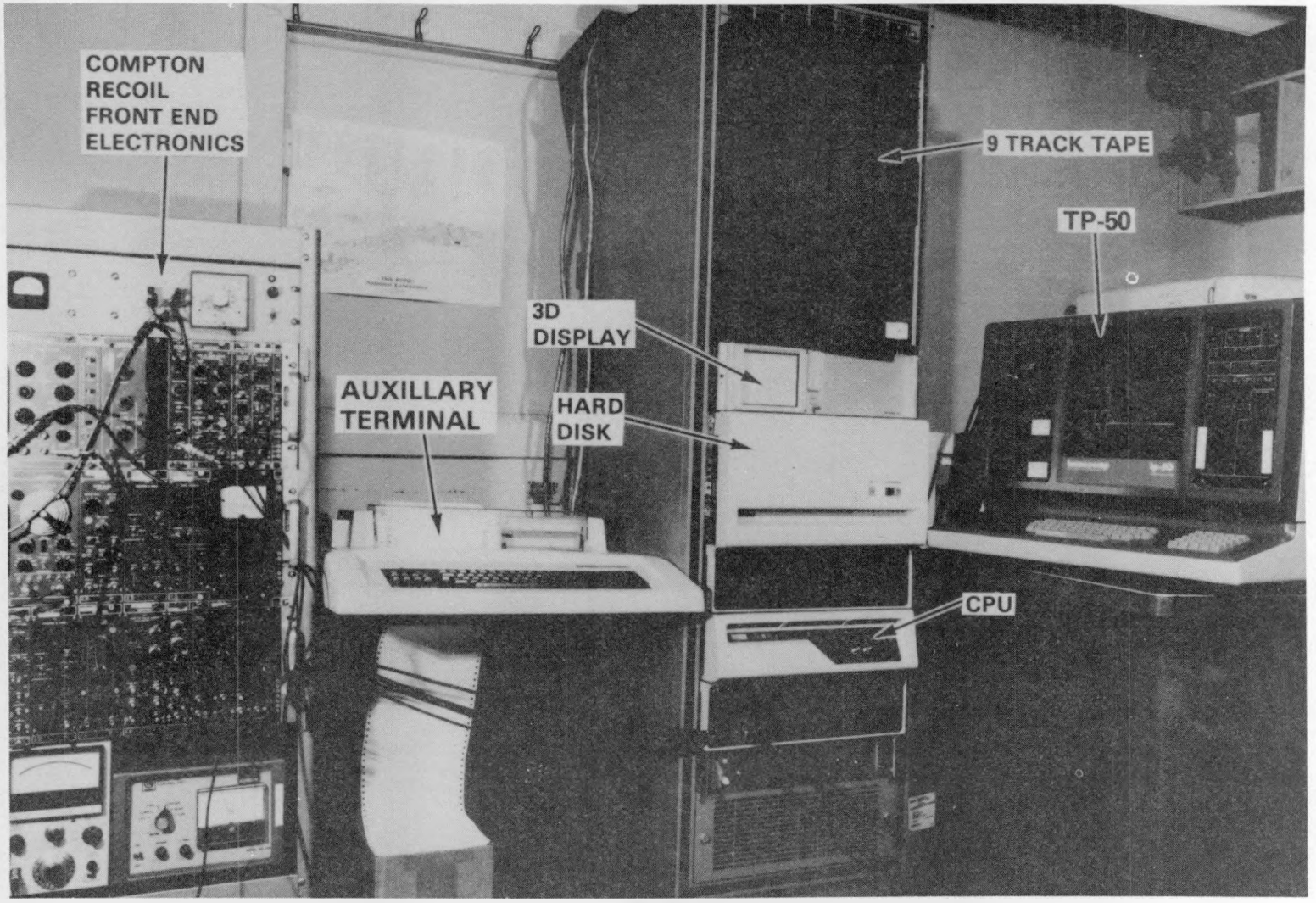

FIGURE 2.64. HEDL Computer-Based Multiparameter Data Acquisition System. Neg 8102095-1

TABLE 2.34

COMPONENTS OF THE LWR-PV DATA ACQUISITION SYSTEM

Component	Manufacturer and Model
Central processing unit with 128K core memory	DEC 11/34
Industry compatible 9-track magnetic tape drive	Cipher/Datum
2 mini-floppy disk drives	Shugart
5 megabite hard disk drives	DEC RL01
3 two-dimensional monitors	Tektronix 604 oscilloscope
Spectra display and analysis terminal including: Functional control panel ADC interface control	Tennecomp TP5000
High-speed multi- and single-parameter DMA interface	Motorola 68000 microprocessor
Auxillary control terminals	DECwriter II/Tektronix 4010
High-speed portable line printer	Data Products M200
Thermal plotter	Gould 5000

2.5.3 Dosimetry Materials

An inventory of dosimeter materials has been established at the HEDL National Reactor Dosimetry Center to provide a source of high-quality materials for LWR applications. Included in the inventory are individual dosimetry wires and foils and bulk material fission deposits for use with solid state track recorder (SSTR), and also high-purity evaporating materials, capsules, and neutron shielding materials (Cd and Gd). Applications are routinely made for reactor cavity measurements [10^{15} to 10^{7} ϕt ($E > 1$)], but measurements can be made in fluences ranging from 10^{8} to 10^{23} n/cm^2.

Materials in the inventory must meet rigorous specifications, which are checked by extensive Quality Assurance (QA) work at HEDL, ORNL, NBS, and RI. The QA checks verify vendor results and enable accurate determination of the mass of the element or isotope to be activated and any critical impurities,

together with uncertainties. Impurities often present particular problems in LWR environments where thermal cross sections can be several orders of magnitude higher than cross sections of fast reactions of interest.

A listing of dosimeters included in a typical basic LWR cavity set is given in Table 2.35. The fission dosimeters are selected to have relatively long half-life products to enable integration of the neutron fluence over times to several years. These dosimeters are in the form of wires or foils and typically are used in quantities of 0.1 to 2 grams to obtain adequate response to high-energy reactions. Co alloy wires (0.1% to 0.5% Co) are used to determine thermal and epithermal neutrons. Fission reactions are measured using both RM and SSTR sensors. The SSTR deposits are prepared by electroplating at HEDL. HEDL calibrations of these deposits are confirmed by intercalibrations with deposits produced elsewhere (including GEEL and Harwell) and are also calibrated by irradiation at NBS in a standard field. The reader is referred to Section 2.4.3.2.4 for more information on the RM-^{238}U metal detectors.

The present status of the dosimeter inventory is:

TABLE 2.35

TYPICAL LWR DOSIMETRY MONITORS

Element or Isotope	Form	Reaction(s) Measured
Ti	RM-Metal Foil*	^{46}Ti(n,p)
Fe	RM-Metal Foil*	^{54}Fe(n,p), ^{58}Fe(n,γ)
Co	RM-Al Alloy Wire*	^{59}Co(n,γ)
Ni	RM-Metal Foil*	^{58}Ni(n,p)
Cu	RM-Metal Wire*	^{63}Cu(n,γ)
^{238}U	RM-Natural Metal Foil	^{235}(n,f)**
^{238}U	RM-Depleted Metal Foil (~200 ppm of ^{235}U)	^{238}(n,f)
^{235}U	SSTR-Deposit on Ni Foil	^{235}U(n,f)
^{237}Np	SSTR-Deposit on Ni Foil	^{237}Np(n,f)
^{238}U	SSTR-Deposit on Ni Foil	^{238}U(n,f)
^{239}Pu	SSTR-Deposit on Ni Foil	^{239}Pu(n,f)

*Material may be analyzed as a HAFM for helium, as required.
**The infinitely dilute measured ^{235}U reaction rate is used to correct for the same reaction rate in the depleted ^{238}U.

Metal Foils and Wires -- A large supply of 0.020-in. diameter wire is available, but the supply of thick metal foils is limited. Additional metal foil materials will be provided and assayed.

Co Alloy -- A quantity of NBS 0.116% Co/Al alloy wire is in inventory, but use in the amounts necessary for LWR cavity dosimetry would rapidly deplete this supply. An alternate material of nominal 0.5% and 0.1% Co/Al alloy wire is on hand from Sigmund Vohm. This Co/Al wire will be irradiated to obtain an accurate assay by comparison with the NBS reference material.

SSTR Deposits -- A small quantity of SSTR deposits has been fabricated for LWR applications. Additional deposits will be fabricated at HEDL as needed with about a 90-day lead time.

Mica -- A sufficient quantity of mica and quartz is on hand to enable selection for all SSTR applications. The quartz would be used for higher temperature applications, such as for LWR-surveillance capsules.

In addition to the above, other materials are in inventory or being considered for purchase. These other dosimeters include advanced helium accumulation fluence monitors (HAFM) (B, Li, and theshold monitors) and damage monitors (sapphire and A302B and A533B reference steels).

2.6 TECHNOLOGY TRANSFER

A crucial outgrowth of the LWR-PV-SDIP is the adaptation of advanced dosimetry methods and capabilities by the private sector for commercial activities in the US LWR nuclear industry. This transfer of technology from the LWR-PV-SDIP is being accomplished in many different ways; and each may, in turn, require transfer at many different levels. Two mechanisms have been and will be particularly effective in the transfer of technology from the LWR-PV-SDIP to the private sector, namely the establishment of ASTM standards and the initiation of specific dosimetry experiments in commercially operated LWR power plants.

2.6.1 ASTM Standards

Figures 1.2 and 1.3 summarize the status of the preparation of LWR-ASTM standards and their supporting documentation. Additional and more detailed information is provided in Sections 2.1.1 and 2.1.2.

2.6.2 Commercial Dosimetry Activities

Considerable effort has been expended throughout the world to understand and quantify the radiation induced damage of LWR-PV steels. These efforts are justified by the impact that pressure vessel integrity has upon power plant operation, safety, and licensing issues as exemplified by pressurized thermal stock (PTS) scenarios. This particular work underscores the need to accurately characterize LWR radiation environments and thereby generate a more general basis of support and understanding for problems encountered in the US nuclear power industry.

The status of joint NRC-EPRI-industry-wide LWR-PV-SDIP-related commercial dosimetry activities in the US is summarized in Table 2.27. It is anticipated that the main work will be completed and the results of these joint activities will be documented and published by the end of CY 1988. During the same period and particularly after 1988, however, it is expected that there will be a significant increase in similarity directed and utility-supported activities; both for PTS and other problems involving the characterization of plant specific neutron and gamma radiation fields.

4.0 BIBLIOGRAPHY

(A177) A. A. Alberman et al., "Damage Function for the Mechanical Properties of Steels, "Nucl. Technol. 36, p. 336, 1977.

(A182) A. A. Alberman et al., "Nouveaux Developpements de la Dosimetrie des Dommages par Technique Tungstene," Proc. of the 4th ASTM-EURATOM Symposium on Reactor Dosimetry, Gaithersburg, MD, March 22-26, 1982, NUREG/CP-0029, NRC, Washington, DC, Vol. 1, pp. 321-329, July 1982.

(A182a) A. A. Alberman et al., "Influence des Neutrons Thermiques sur la Fragilisation de l'Acier de Peau d'Etancheite des Reacteurs a Haute Temperature (H.T.R.)," Proc. of the 4th ASTM-EURATOM Symposium on Reactor Dosimetry, Gaithersburg, MD, March 22-26, 1982, NUREG/CP-0029, NRC, Washington, DC, Vol. 2, p. 839, July 1982.

(A183) A. A. Alberman et al., DOMPAC Dosimetry Experiment Neutron Simulation of the Pressure Vessel of a Pressurized-Water Reactor, Characterization of Irradiation Damage, CEA-R-5217, Centre d'Etudes Nucleaires de Saclay, France, May 1983.

(As82) ASTM E706-81a, "Master Matrix for LWR Pressure Vessel Surveillance Standards," 1982 Annual Book of ASTM Standards, Part 45, "Nuclear Standards," American Society for Testing and Materials, Philadelphia, PA, 1982.

(As82b) ASTM E854-81, "Standard Method for Application and Analysis of Solid State Track Recorder (SSTR) Monitors for Reactor Surveillance," 1982 Annual Book of ASTM Standards, Part 45, "Nuclear Standards," American Society for Testing and Materials, Philadelphia, PA, 1982.

(As83) 1983 Annual Book of ASTM Standards, Section 12, Volume 12.02, "Nuclear (II), Solar, and Geothermal Energy," American Society for Testing and Materials, Philadelphia, PA, 1983.

(Au82) M. Austin, "Description and Status of the NESTOR Dosimetry Improvement Programme (NESDIP)," Proc. of the 10th WRSR Information Meeting, Gaithersburg, MD, October 12-15, 1982, NUREG/CP-0041, Vol. 4, NRC, Washington, DC, pp. 228-231, January 1983.

(Au82a) M. Austin, "Sense of Direction: An Observation of Trends in Materials Dosimetry in the United Kingdom," Proc. of the 4th ASTM-EURATOM Symposium on Reactor Dosimetry, Gaithersburg, MD, March 22-26, 1982, NUREG/CP-0029, NRC, Washington, DC, Vol. 1, p. 461-469, July 1982.

(Au83) M. Austin et al., "The NESTOR Shielding and Dosimetry Improvement Programme (NESDIP): The Replica Experiment (Phase 1)," Proc. of the 11th WRSR Information Meeting, National Bureau of Standards, Washington, DC, October 1983.

(Ba63) W. H. Barkas, "Techniques and Theories," Nuclear Research Emulsions, Vol. I, Academic Press, New York, NY, 1963.

(Be72) G. E. Belovitiskii et al., "Measurement of the Spectra of Fast Neutrons (~14 MeV) with High-Energy Resolution with the Aid of Nuclear Emulsions - Automation of the Measurements," Proc. (Trudy) of the P. N. Lebedev Physics Institute, Nuclear Reactions and Interaction of Neutrons and Matter, Vol. 63, pp. 109-119, Nanka Press, Moscow, USSR, 1972.

(Be83) R. G. Berggren and F. W. Stallmann, "Statistical Analysis of Pressure Vessel Steel Embrittlement Data," from the ANS Special Session on Correlations and Implications of Neutron Irradiation Embrittlement of Pressure Vessel Steels, Detroit, MI, June 12-16, 1983, Trans. Am. Nucl. Soc. 44, p. 225, 1983.

(By80) S. T. Byrne, Omaha Public Power District Fort Calhoun Station Unit No. 1: Post-Irradiation Evaluation of Reactor Vessel Surveillance Capsule W-225, TR-0-MCM-001, Rev. 1, Combustion Engineering Inc., August 1980.

(Ca81) K. Carlson, G. Guthrie and G. R. Odette, "Embrittlement of Compression Specimens in the PSF," LWR-PV-SDIP, Quarterly Progress Report, NUREG/CR-2345, Vol. 1, HEDL-TME 81-33, Hanford Engineering Development Laboratory, Richland, WA, October 1981.

(Cf83) Code of Federal Regulations, 10CFR50, "Domestic Licensing of Production and Utilization Facilities," "General Design Criteria for Nuclear Power Plants," Appendix A; "Fracture Toughness Requirements," Appendix G; "Reactor Vessel Material Surveillance Program Requirements," Appendix H; US Government Printing Office, Washington, DC, current edition.

(Ch82) R. D. Cheverton, "A Brief Account of the Effect of Overcooling Accidents on the Integrity of PWR Pressure Vessels," Proc. of the 4th ASTM-EURATOM Symposium on Reactor Dosimetry, NUREG/CP-0029, NRC, Washington, DC, Vol. 2, pp. 1061-1070, July 1982.

(Ch83) R. D. Cheverton, S. K. Iskander and G. D. Whitman, "The Integrity of PWR Pressure Vessels During Overcooling Accidents," Proc. of the 10th WRSR Information Meeting, Gaithersburg, MD, October 12-15, 1982, NUREG/CP-0041, Vol. 4, NRC, Washington, DC, pp. 232-241, January 1983.

(Co69) C. E. Cohn, R. Gold and T. W. Pienias, "Computer-Controlled Microscope for Scanning Fission Track Plates," Trans., Am. Nucl. Soc. 12, p. 68, 1969.

(Co70) F. J. Congel et al., "Automatic System for Counting Etched Holes in Thin Dielectric Plastics," Trans. Am. Nucl. Soc. 13, p. 419, 1970.

(Co72) C. E. Cohn and R. Gold, "Computer-Controlled Microscope for Automatic Scanning of Solid-State Nuclear Track Recorders," Rev. Sci. Instrum. 42, pp. 12-17, 1972.

(Co72a) F. J. Congel et al., "Automatic System for Counting Etched Holes in Thin Dielectric Plastics, Nucl. Instrum. Methods 100, pp. 247-252, 1972.

(Co75) C. E. Cohn and R. J. Armani, "Automatic Scanning of Mica Track Recorders," Rev. Sci. Instrum. 46, pp. 18-19, 1975.

(Cr69) N. G. Cross and L. Tommasino, Proc. of the International Topical Conf. on Nuclear Track Registration in Insulating Solids and Applications, Univ. of Clermont, Clermont-Ferrand, France, Vol. I, p. 73, 1969.

(Da77) J. A. Davidson, S. L. Anderson and K. V. Scott, Analysis of Capsule V from Northern States Power Company Prairie Island Unit No. 1 Reactor Vessel Radiation Surveillance Program, WCAP-8916, Westinghouse Electric Corp., Pittsburgh, PA, August 1977.

(Da78a) J. A. Davidson, S. L. Anderson and R. P. Shogan, Analysis of Capsule T from the Wisconsin Electric Power Company Point Beach Nuclear Plant Unit No. 2 Reactor Vessel Radiation Surveillance Program, WCAP-9331, Westinghouse Electric Corp., Pittsburgh, PA, August 1978.

(Da79) J. A. Davidson, S. L. Anderson and W. T. Kaiser, Analysis of Capsule T from the Indian Point Unit 3 Reactor Vessel Radiation Surveillance Program, WCAP-9491, Westinghouse Electric Corp., Pittsburgh, PA, April 1979.

(Da83) L. M. Davies et al., "Analysis of the Behavior of Advanced Reactor Pressure Vessel Steels Under Neutron Irradiation - The UK Programme," Report from the UK for the IAEA Coordinated Research Programme on the Analysis of the Behavior of Advanced Reactor Pressure Vessel Steels Under Neutron Irradiations," Unnumbered UKAEA-Harwell Report, Harwell, UK, April 1983.

(De82) S. De Leeuw and R. Menil, "Silicon P.I.N. Diode Neutron Damage Monitors," Proc. of the 4th ASTM-EURATOM Symposium on Reactor Dosimetry, Gaithersburg, MD, March 22-26, 1982, NUREG/CP-0029, NRC, Washington, DC, Vol. 1, pp. 387-412, July 1982.

(Di82) W. J. Dircks, Pressurized Thermal Shock (PTS), and Enclosure A, "NRC Staff Evaluation of PTS," SECY-82-465, NRC, Washington, DC, November 1982.

(Ei77) N. Von Eichselpasch and R. Seepolt, "Experimentelle Ermittung der Neutronendosis des KRB - Druckgefässes und deren Betriebliche Bedeutung," Atomkernenergie 29, 1977.

(Fa80a) A. Fabry et al., "Results and Implications of the Initial Neutronic Characterization of Two HSST Irradiation Capsules and the PSF Simulated LWR Pressure Vessel Irradiation Facility," Proc. of the 8th WRSR Information Meeting, Gaithersburg, MD, October 27-31, 1980, NUREG/CP-0023, NRC, Washington, DC, March 1982.

(Fa82) A. Fabry et al., "Improvement of LWR Pressure Vessel Steel Embrittlement Surveillance: Progress Report on Belgian Activities in Cooperation with the USNRC and other R&D Programs," Proc. of the 4th ASTM-EURATOM Symposium on Reactor Dosimetry, Gaithersburg, MD, March 22-26, 1982, NUREG/CP-0029, NRC, Washington, DC, Vol. 1, pp. 45-77, July 1982.

(Fa82a) A. Fabry et al., "The Mol Cavity Fission Spectrum Standard Neutron Field and Its Applications," Proc. of the 4th ASTM-EURATOM Symposium on Reactor Dosimetry, Gaithersburg, MD, March 22-26, 1982, NUREG/CP-0029, NRC, Washington, DC, Vol. 2, pp. 665-687, July 1982.

(Fa83) A. Fabry et al., "VENUS Dosimetry Program," Paper presented at the 10th WRSR Information Meeting, Gaithersburg, MD, October 12-15, 1982, preprint available.

(Fa83a) A. Fabry et al., "The Belgium Characterization Program and the Venus Program for Core Source to PV Wall Fluence Verification," Proc. of the 11th WRSR Information Meeting, National Bureau of Standards, Washington, DC, October 1983.

(Fr78) Fracture Control Corp., Nuclear Pressure Vessel Steel Data Base, EPRI NP-933, Electric Power Research Institute, Palo Alto, CA, December 1978.

(Ga83) D. M. Galliani, Nuclear Power Plant of Caorso Pressure Vessel Surveillance Program: Fast Neutron Flux Measurement, Performed at the End of the First Operating Cycle (January 1983), DPT/SN-158/R/83, ENEL - Italian Atomic Power Authority, National Electric Energy Agency, Rome, Italy, July 1983.

(Go68a) R. Gold, "Compton Continuum Measurements for Continuous Gamma-Ray Spectroscopy," Bull. Am. Phys. Soc. 13, p. 1405, 1968.

(Go70) R. Gold and I. K. Olson, Analysis of Compton Continuum Measurements, ANL-7611, Argonne National Laboratory, Argonne, IL, 1970.

(Go70a) R. Gold, "Compton Recoil Gamma-Ray Spectroscopy," Nucl. Instrum. Methods 84, p. 173, 1970.

(Go70b) R. Gold, "Compton Recoil Measurements of Continuous Gamma-Ray Spectra," Trans. Am. Nucl. Soc. 13, p. 421, 1970.

(Go70c) R. Gold, R. J. Armani and J. H. Roberts, "Spontaneous-Fission Decay Constants of ^{241}Am," Phys. Rec. C, I, p. 738, 1970.

(Go71) R. Gold and C. E. Cohn, "Analysis of Automatic Fission Track Scanning Data, Trans. Am. Nucl. Soc. 14, p. 500, 1971.

(Go72) R. Gold and C. E. Cohn, "Analysis of Automatic Fission Track Scanning in Solid-State Nuclear Track Recorders," Rev. Sci. Instrum. 43, pp. 18-28, 1972.

(Go79b) R. Gold and B. J. Kaiser, "Status of Compton Recoil Gamma-Ray Spectroscopy," Trans. Am. Nucl. Soc. 33, p. 692, 1979.

(Go80b) R. Gold, R. B. Kaiser, F. S. Moore, Jr., W. L. Bunch, W. M. McElroy and E. M. Sheen, "Continuous Gamma-Ray Spectrometry in the Fast Flux Test Facility," HEDL-SA-2166, Proc. of the ANS Topical Meeting on 1980 Advances in Reactor Physics and Shielding, Sun Valley, ID, September 14-17, 1980, ISDN 0-89448-107-X, p. 803, 1980.

(Go80d) R. Gold and B. J. Kaiser, "Reactor Gamma-Ray Spectrometry: Status," Proc. of the 3rd ASTM-EURATOM Symposium on Reactor Dosimetry, Ispra, Italy, October 1-5, 1979, EUR 6813, Commission of the European Communities, Vol. II, pp. 1160-1171, 1980.

(Go81) R. Gold and J. H. Roberts, "Nuclear Emulsion Neutron Spectrometry in FFTF," Trans. Am. Nucl. Soc. 39, p. 896, December 1981.

(Go81b) R. Gold, "Gamma-Ray Data," LWR-PV-SDIP: PCA Experiments and Blind Test, NUREG/CR-1861, HEDL-TME 80-87, Chap. 5, NRC, Washington, DC, July 1981.

(Go81c) R. Gold and B. J. Kaiser, "Gamma-Ray Spectrometry," LWR Pressure Vessel Surveillance Dosimetry Improvement Program: PCA Experiments and Blind Test, NUREG/CR-1861, HEDL-TME 80-87, Sec. 5.3, NRC, Washington, DC, July 1981.

(Go81d) R. Gold, J. H. Roberts, F. H. Ruddy, C. C. Preston and C. A. Hendricks, "Proton-Recoil Observations for Integral Neutron Dosimetry," Proc. of the IAEA Advisory Group Meeting on Nuclear Data for Radiation Damage and Safety, IAEA-TEC DOC-263, International Atomic Energy Agency, Vienna, Austria, pp. 115-121, 1981.

(Go81e) R. Gold, J. H. Roberts, C. C. Preston, and F. H. Ruddy, "Neutron Spectrometry with Nuclear Research Emulsions," LWR-PV-SDIP: PCA Experiments and Blind Test, NUREG/CR-1861, HEDL-TME 80-87, Sec. 3.3, NRC, Washington, DC, July 1981.

(Go82) R. Gold, J. H. Roberts and F. H. Ruddy, "Buffon Needle Method of Track Counting," Proc. of the 11th International Conference on Solid-State Nuclear Track Detectors, Bristol, UK, 1981, Pergamon Press, Oxford, UK, pp. 891-897, 1982.

(Go82b) R. Gold, B. J. Kaiser and J. P. McNeece, "Gamma-Ray Spectrometry in Light Water Reactor Environments," Proc. of the 4th ASTM-EURATOM Symposium on Reactor Dosimetry, Gaithersburg, MD, March 22-26, 1982, NUREG/CR-0029, NRC, Washington, DC, Vol. I, pp. 267-279, July 1982.

(Go83) R. Gold et al., "Interactive System for Scanning Tracks in Nuclear Research Emulsions," Rev. Sci. Instrum. 54, pp. 183-192, 1983.

(Gr75) R. C. Greenwood, R. G. Helmer, J. W. Rogers, N. D. Dudey, R. J. Popek, L. S. Kellogg and W. H. Zimmer, "Nonfission Reaction Rate Measurements," Nucl. Technol. 25, (2), p. 274, February 1975.

(Gr75b) J. A. Grundl and C. M. Eisenhauer, "Fission Spectrum Neutrons for Cross-Section Validation and Neutron Flux Transfer," Proc. of a Conference on Nuclear Cross Sections and Technology, NBS Special Publication 425, Vol. 1, National Bureau of Standards, Washington, DC, pp. 250-257, 1975.

(Gr77b) J. A. Grundl, V. Spiegel, C. M. Eisenhauer, H. T. Heaton, D. M. Gilliam and J. Bigelow, "A Californium-252 Fission Spectrum Irradiation Facility for Neutron Reaction Rate Measurements," Nucl. Technol. 32, p. 315, 1977.

(Gr78) J. A. Grundl and C. M. Eisenhauer, "Benchmark Neutron Fields for Reactor Dosimetry," Neutron Cross Sections for Reactor Dosimetry, IAEA-208, International Atomic Energy Agency, Vienna, Austria, Vol. I, pp. 53-104, 1978.

(Gr81) J. A. Grundl et al., "NRC-EPRI Studies of Pressure-Vessel-Cavity Neutron Fields," Proc. of the 9th Water Reactor Safety Information Meeting, Gaithersburg, MD, October 26-30, 1981, NUREG/CP-0024, Vol. 1-3, NRC, Washington, DC, March 1982.

(Gu80) G. L. Guthrie, "Reanalysis of the Existing Data Base Relating Irradiation Embrittlement and Neutron Exposure of Pressure Vessel Steels," LWR-PV-SDIP Quarterly Progress Report, January 1980 - March 1980, NUREG/CR-1241, Vol. 1, HEDL-TME 80-4, Hanford Engineering Development Laboratory, Richland, WA, December 1980.

(Gu82) G. L. Guthrie, W. N. McElroy and S. L. Anderson, "A Preliminary Study of the Use of Fuel Management Techniques for Slowing Pressure Vessel Embrittlement," Proc. of the 4th ASTM-EURATOM Symposium on Reactor Dosimetry, Gaithersburg, MD, March 22-26, 1982, NUREG/CP-0029, NRC, Washington, DC, Vol. 1, pp. 111-120, July 1982.

(Gu82a) G. L. Guthrie, W. N. McElroy and S. L. Anderson, "Investigations of Effects of Reactor Core Loadings on PV Neutron Exposure," LWR-PV-SDIP Quarterly Progress Report, October 1981 - December 1981, NUREG/CR-2345, Vol. 4, HEDL-TME 81-36, Section E and Appendix, pp. HEDL-35 - HEDL-36 & HEDL-A1 - HEDL-A46, Hanford Engineering Development Laboratory, Richland, WA, October 1982.

(Gu82b) G. L. Guthrie, "Development of Trend Curve Formulas Using Surveillance Data," LWR-PV-SDIP Quarterly Progress Report, January 1982 - March 1982, NUREG/CR-2805, Vol. 1, HEDL-TME 82-18, Hanford Engineering Development Laboratory, Richland, WA, pp. HEDL-3 - HEDL-18, December 1982.

(Gu82c) G. L. Guthrie, "Development of Trend Curve Formulas Using Surveillance Data-II," LWR-PV-SDIP Quarterly Progress Report, April - June 1982, NUREG/CR-2805, Vol. 2, HEDL-TME 82-19, Hanford Engineering Development Laboratory, Richland, WA, pp. HEDL-3 - HEDL-13, December 1982.

(Gu83) G. L. Guthrie, "Charpy Trend Curve Formulas Derived from an Expanded Surveillance Data Base," LWR-PV-SDIP Quarterly Progress Report, October 1982 - December 1982, NUREG/CR-2805, Vol. 4, HEDL-TME 82-21, Hanford Engineering Development Laboratory, Richland, WA, pp. HEDL-3 - HEDL-13, July 1983.

(Gu83a) G. L. Guthrie, "Pressure Vessel Steel Irradiation Embrittlement Formulas Derived from PWR Surveillance Data," from the ANS Special Session on Correlations and Implications of Neutron Irradiation Embrittlement of Pressure Vessel Steels, Detroit, MI, June 12-16, 1983, Trans. Am. Nucl. Soc. 44, p. 222, January 1983.

(Gu83b) G. L. Guthrie, "Error Estimations in Applications of Charpy Trend Curve Formulas," LWR-PV-SDIP Quarterly Progress Report, January 1983 - March 1983, NUREG/CR-3391, Vol. 1, HEDL-TME 83-21, Hanford Engineering Development Laboratory, Richland, WA, pp. HEDL-3 - HEDL-13, November 1983.

(Gu83c) G. L. Guthrie, "Charpy Trend-Curve Development Based on PWR Surveillance Data," Proc. of the 11th WRSR Information Meeting, Gaithersburg, MD, October 24-28, 1983, NUREG/CP-0048, NRC, Washington, DC.

(Gu84) G. L. Guthrie, "Charpy Trend Curves Based on 177 PWR Data Points," LWR-PV-SDIP Quarterly Progress Report, April 1983 - June 1983, NUREG/CR-3391, Vol. 2, HEDL-TME 83-22, Hanford Engineering Development Laboratory, Richland, WA, HEDL-3 - HEDL-15, April 1984.

(Gu84a) G. L. Guthrie, W. N. McElroy and R. L. Simons, "Effect of Thermal Neutrons in Irradiation Embrittlement of PWR Pressure Vessel Plates and Welds," LWR-PV-SDIP Quarterly Progress Report, April 1983 - June 1983, NUREG/CR-3391, Vol. 2, HEDL-TME 83-22, Hanford Engineering Development Laboratory, Richland, WA, HEDL-16 - HEDL-21, April 1984.

(Ha79) J. R. Hawthorne and J. A. Sprague, Radiation Effects to Reactor Vessel Support Structures, Report by Task C of Interagency Agreement NRC-03-79-148, NRC, Washington, DC, October 22, 1979.

(Ha82a) J. R. Hawthorne, "Irradiation and Annealing Sensitivity Studies," MEA-2009, Materials Engineering Associates, Inc., Oxen Hill, MD, October 1982, and Proc. of the 10th WRSR Information Meeting, Gaithersburg, MD, October 12-15, 1982, NUREG/CR-0041, Vol. 4, NRC, Washington, DC, January 1983.

(Ha83) J. R. Hawthorne, "Evaluation of Reimbrittlement Rate Following Annealing and Related Investigations on RPV Steels," MEA-2032, Materials Engineering Associates, Inc., Oxen Hill, MD, and Proc. of the 11th WRSR Information Meeting, Gaithersburg, MD, October 24-28, 1983, NUREG/CP-0048, NRC, Washington, DC.

(He82) P. D. Hedgecock and J. S. Perrin, "Standards for Materials Behavior Under Neutron Irradiation," Proc. of the 4th ASTM-EURATOM Symposium on Reactor Dosimetry, Gaithersburg, MD, March 22-26, 1982, NUREG/CP-0029, p. 829, NRC, Washington, DC, July 1982.

(Ho78) W. C. Hopkins, "Suggested Approach for Fracture-Safe RPV Support Structure Design in Neutron Environments," Trans. Am. Nucl. Soc. 30, p. 187, November 1978.

(Ir70) D. R. Ireland and V. G. Scotti, Examination and Evaluation of Capsule A for the Connecticut Yankee Reactor Pressure Vessel Surveillance Program, Battelle Memorial Institute, Columbus Laboratories, Columbus, OH, October 30, 1970.

(Ji78) S. H. Jiang and H. Werle, "Fission Neutron-Induced Gamma Fields in Iron," Nucl. Sci. Eng. 66, p. 354, 1978.

(Ka82) F. B. K. Kam, Ed., Proc. of the 4th ASTM-EURATOM Symposium on Reactor Dosimetry, Gaithersburg, MD, March 22-26, 1982, NUREG/CP-0029, NRC, Washington, DC, Vols. 1 and 2, July 1982.

(Ka82a) F. B. K. Kam, "Characterization of the Fourth HSST Series of Neutron Spectral Metallurgical Irradiation Capsules," Paper presented at the 4th ASTM-EURATOM Symposium on Reactor Dosimetry, Gaithersburg, MD, March 22-26, 1982, preprints available.

(Ka82b) F. B. K. Kam et al., "Neutron Exposure Parameters for the Fourth HSST Series of Metallurgical Irradiation Capsules," Proc. of the 4th ASTM-EURATOM Symposium on Reactor Dosimetry, Gaithersburg, MD, March 22-26, 1982, NUREG/CP-0029, NRC, Washington, DC, Vol. 2, pp. 1023-1033, July 1982.

(Ka83) F. B. K. Kam, F. W. Stallmann, R. E. Maerker and M. L. Williams, "Light Water Reactor Pressure Vessel (LWR-PV) Benchmark Facilities (PCA, ORR-PSF, ORR-SDMF) at ORNL," LWR-PV-SDIP Quarterly Progress Report, April 1982 - June 1982, HEDL-TME 82-19, Hanford Engineering Development Laboratory, Richland, WA, pp. ORNL-1 - ORNL-19, January 1983.

(Ke82) L. S. Kellogg and E. P. Lippincott, "PSF Interlaboratory Comparison," Proc. of the 4th ASTM-EURATOM Symposium on Reactor Dosimetry, Gaithersburg, MD, March 22-26, 1982, NUREG/CP-0029, NRC, Washington, DC, Vol. 1, pp. 929-945, July 1982.

(Ko75) H. E. Korn, Measurement of the Energy Distribution of the Gamma Field in a Fast Reactor, KFK 2211, Karlsruhe Nuclear Research Center, Karlsruhe, Federal Republic of Germany, 1975.

(La69) N. L. Lark, "Spark Scanning for Fission Fragment Tracks in Plastic Foils," Nucl. Instrum. Methods 67, pp. 137-140, 1969.

(Li82) E. P. Lippincott and W. N. McElroy, "ASTM Standard Recommended Guide on Application of ENDF/A Cross Section and Uncertainty File: Establishment of the File," Proc. of the 4th ASTM-EURATOM Symposium on Reactor Dosimetry, Gaithersburg, MD, March 22-26, 1982, NUREG/CP-0029, NRC, Washington, DC, Vol. 2, pp. 705-710, July 1982.

(Lo75) A. L. Lowe Jr et al., Analysis of Capsule OCI-F from Duke Power Company, Oconee Unit No. 1 Reactor Vessel Materials Surveillance Program, BAW-1421, Babcock & Wilcox, Lynchburg, VA, August 1975.

(Lo77) A. L. Lowe Jr et al., Analysis of Capsule OCI-E from Duke Power Company, Oconee Nuclear Station - Unit 1, BAW-1436, Babcock & Wilcox, Lynchburg, VA, September 1977.

(Lo77a) A. L. Lowe Jr et al., Analysis of Capsule OCII-C from Duke Power Company, Oconee Nuclear Station - Unit 2, BAW-1437, Babcock & Wilcox, Lynchburg, VA, May 1977.

(Lo77b) A. L. Lowe Jr et al., Analysis of Capsule OCII-A from Duke Power Company, Oconee Nuclear Station - Unit 3, BAW-1438, Babcock & Wilcox, Lynchburg, VA, July 1977.

(Lo77c) A. L. Lowe Jr et al., Analysis of Capsule TMI-1E from Metropolitan Edison Company, Three Mile Island Nuclear Station - Unit 1, BAW-1439, Babcock & Wilcox, Lynchburg, VA, January 1977.

(Lo81a) A. L. Lowe Jr et al., Analysis of Capsule V Virginia Electric and Power Company, North Anna Unit No. 1 Reactor Vessel Materials Surveillance Program, BAW-1638, Babcock & Wilcox, Lynchburg, VA, March 1981.

(Lo82b) F. J. Loss, B. H. Menke and A. L. Hiser, "Fracture Toughness Characterization of Irradiated, Low-Upper Shelf Welds," Proc. of the 10th WRSR Information Meeting, Gaithersburg, MD, October 12-15, 1982, NUREG/CP-0041, Vol. 4, NRC, Washington, DC, pp. 168-183, January 1983.

(Lu83) G. E. Lucas et al., "Preliminary Observations of the Chemistry and Temperature Dependence of Radiation Hardening in Pressure Vessel Steels," from the ANS Special Session on Correlations and Implications of Neutron Irradiation Embrittlement of Pressure Vessel Steels, Detroit, MI, June 12-16, 1983, Trans. Am. Nucl. Soc. 44, p. 231, 1983.

(Ly72) J. H. Lynch, "Correlation of Irradiation Data Using Activation Fluences and Irradiation Temperatures," Nucl. Technol. 3, pp. 411-421, September 1972.

(Ma73a) T. R. Mager et al., Analysis of Capsule V from the Rochester Gas and Electric Company, R. E. Ginna Unit No. 1 Reactor Vessel Radiation Surveillance Program, FP-RA-1, Westinghouse Electric Corp., Pittsburgh, PA, April 1973.

(Ma78b) T. U. Marston and K. E. Stahlkopf, "Radiation Embrittlement: Significance of Its Effects on Integrity and Operation of LWR Pressure Vessels," Nuclear Safety 2, (6), p. 724, November - December 1978.

(Ma82) N. Maene, R. Menit and G. Minsart, "Gamma Dosimetry and Calculations," Proc. of the 4th ASTM-EURATOM Symposium on Reactor Dosimetry, Gaithersburg, MD, March 22-26, 1982, NUREG/CP-0029, NRC, Washington, DC, Vol. 1, pp. 355-363, July 1982.

(Ma82b) P. Mas and R. Perdreau, "Caracterisation d' Emplacements d'Irradiation en Spectres Neutroniques et en Dommages," Proc. of the 4th ASTM-EURATOM Symposium on Reactor Dosimetry, Gaithersburg, MD, March 22-26, 1982, NUREG/CP-0029, NRC, Washington, DC, Vol. 2, pp. 847-854, July 1982.

(Ma82e) R. E. Maerker and M. L. Williams, "Calculations of the Westinghouse Perturbation Experiment at the Poolside Facility," Proc. of the 4th ASTM-EURATOM Symposium on Reactor Dosimetry, Gaithersburg, MD, March 22-26, 1982, NUREG/CP-0029, NRC, Washington, DC, Vol. 1, pp. 131-141, July 1982.

(Ma82f) P. J. Maudlin and R. E. Maerker, "Supplementary Neutron Flux Calculations for the ORNL PCA-PV Facility," Proc. of the 4th ASTM-EURATOM Symposium on Reactor Dosimetry, Gaithersburg, MD, March 22-26, 1982, NUREG/CP-0029, NRC, Washington, DC, Vol. 2, pp. 689-698, July 1982.

(Ma82g) T. R. Mager et al., Feasibility of and Methodology for Thermal Annealing of Embrittled Reactor Vessel - Vol. 2: Detailed Technical Description of the Work, EPRI NP-2712, (Final Report, Project 1021-1), Electric Power Research Institute, Palo Alto, CA, November 1982.

(Ma82h) T. U. Marston and T. R. Mager, "EPRI Thermal Anneal Program RP1021-1," Report to ASME Section XI Subcommittee on Repairs and Replacements and to NRC, February 1982.

(Ma83) T. U. Marston, "A Brief on the Assessment of Relative Uncertainties," from the ANS Special Session on Correlations and Implications of Neutron Irradiation Embrittlement of Pressure Vessel Steels, Detroit, MI, June 12-16, 1983, Trans. Am. Nucl. Soc. 44, p. 221, 1983.

(Mc69) W. N. McElroy, R. E. Dahl Jr and C. Z. Serpan Jr, "Damage Functions and Data Correlation," Nucl. Appl. Technol. 7, (6), pp. 561-571, December 1969.

(Mc80) W. N. McElroy et al., LWR-PV-SDIP: 1979 Annual Report, NUREG/CR-1291, HEDL-SA-1949, NRC, Washington, DC, February 1980.

(Mc81) W. N. McElroy, Ed., LWR-PV-SDIP: PCA Experiments and Blind Test, NUREG/CR-1861, HEDL-TME 80-87, NRC, Washington, DC, July 1981.

(Mc82) W. N. McElroy et al., "Surveillance Dosimetry of Operating Power Plants," Proc. of the 4th ASTM-EURATOM Symposium on Reactor Dosimetry, Gaithersburg, MD, March 22-26, 1982, NUREG/CP-0029, NRC, Washington, DC, pp. 3-43, July 1982. (Serves as the LWR-PV-SDIP 1981 Annual Report.)

(Mc82a) W. N. McElroy et al., LWR-PV-SDIP: 1982 Annual Report, NUREG/CR-2805, Vol. 3, HEDL-TME 82-20, NRC, Washington, DC, December 1982.

(Mc82a) W. N. McElroy et al., LWR-PV-SDIP: 1982 Annual Report, NUREG/CR-2805, Vol. 3, HEDL-TME 82-20, NRC, Washington, DC, December 1982.

(Mc82c) P. McConnell et al., Irradiated Nuclear Pressure Vessel Steel Data Base, EPRI NP-2428, Electric Power Research Institute, Palo Alto, CA, June 1982.

(Mc83) J. P. McNeece, R. Gold, C. C. Preston and J. H. Roberts, "Automated Scanning of Solid-State Track Recorders: Computer-Controlled Microscope," Nucl. Tracks 7, pp. 39-45, 1983.

(Mc84) W. N. McElroy et al., LWR-PV-SDIP 1983 Annual Report, NUREG/CR-3391, Vol. 3, HEDL-TME 83-23, NRC, Washington, DC, January 1984.

(Mc84e) W. N. McElroy, G. L. Guthrie and R. L. Simons, "Thermal-Relative-to-Fast-Neutron Contribution to Charpy Shift for PWR and BWR Surveillance Capsule Weld Materials," LWR-PV-SDIP Quarterly Progress Report, April 1983 - June 1983, NUREG/CR-3391, Vol. 2, HEDL-TME 83-22, Hanford Engineering Development Laboratory, Richland, WA, HEDL-22 - HEDL-33, April 1984.

(Mp79) MPC Subcommittee 6 on Nuclear Materials, "Prediction of the Shift in the Brittle-Ductile Transition Temperature of LWR Pressure Vessel Materials," Final Report to ASTM Subcommittee E10.02, June 1979.

(No71) E. B. Norris, Analysis of First Surveillance Material Capsule from San Onofre Unit 1, SwRI Project 07-2892, Southwest Research Institute, San Antonio, TX, May 1971.

(No72) E. B. Norris, Analysis of Second Surveillance Material Capsule from San Onofre Unit 1, Final Report, SwRI Project 07-2892, Southwest Research Institute, San Antonio, TX, June 1972.

(No76) E. B. Norris, Reactor Vessel Material Surveillance Program for Turkey Point Unit No. 4 -- Analysis of Capsule T, Final Report, SwRI Project 02-4221, Southwest Research Institute, San Antonio, TX, June 1976.

(No76b) E. B. Norris, Reactor Vessel Material Surveillance Program for H. B. Robinson Unit No. 2 -- Analysis of Capsule V, Final Report, SwRI Project 02-4397, Southwest Research Institute, San Antonio, TX, October 1976.

(No77a) E. B. Norris, Reactor Vessel Material Surveillance Program for Indian Point Unit No. 2 -- Analysis of Capsule T, Final Report, SwRI Project 02-4531, Southwest Research Institute, San Antonio, TX, June 1977.

(No77b) E. B. Norris, Reactor Vessel Material Surveillance Program for Donald C. Cook Unit No. 1 -- Analysis of Capsule T, Final Report, SwRI Project 02-4770, Southwest Research Institute, San Antonio, TX, December 1977.

(No79) E. B. Norris, Reactor Vessel Material Surveillance Program for Capsule S -- Turkey Point Unit No. 3; Capsule S -- Turkey Point Unit No. 4, Final Report, SwRI Projects 02-5131 and 02-5380, Southwest Research Institute, San Antonio, TX, May 1979.

(Nr80) NRC Staff, Presentation to Advisory Committee on Reactor Safeguards, Metal Components Subcommittee, Transcribed Proceedings of Meeting, Washington, DC, January 24, 1980.

(Nr82) NRC Staff, Presentation to Advisory Committee on Reactor Safeguards, Metal Components Subcommittee, Meeting on Reactor Vessel Integrity (RVI), Washington, DC, May 11-12, 1982.

(Od78) G. R. Odette, W. L. Server, W. Oldfield, R. O. Ritchie and R. A. Wullaert, Analysis of Radiation Embrittlement Reference Toughness Curves, FCC 78-11, Fracture Control Corp., Goleta, CA, November 14, 1978.

(Od79) G. R. Odette, "Neutron Exposure Dependence of the Embrittlement of Reactor Pressure Vessel Steels: Correlation Models and Parameters," Proc. of an IAEA Specialists' Meeting on Z Accuracies in Correlation Between Property Change and Exposure Data from Reactor Pressure Vessel Steel Irradiations, Jülich, Federal Republic of Germany, September 24-27, 1979, ISSN0344-5798, p. 310, May 1980.

(Od83) G. R. Odette and P. Lombrozo, "A Physically Statistically Based Correlation for Transition Temperature Shifts in Pressure Vessel Steel Surveillance Welds," from the ANS Special Session on Correlations and Implications of Neutron Irradiation Embrittlement of Pressure Vessel Steels, Detroit, MI, June 12-16, 1983, Trans. Am. Nucl. Soc. 44, p. 224, 1983.

(Ol84) B. M. Oliver and H. Farrar, "Application of Helium Accumulation Fluence Monitors (HAFM) to LWR Surveillance, LWR-PV-SDIP Quarterly Progress Report, April 1983 - June 1983, NUREG/CR-3391, Vol. 2, HEDL-TME 83-22, Hanford Engineering Development Laboratory, Richland, WA, pp. RI-3 - RI-5, April 1984.

(Pa83) D. Pachur, "Mechanical Properties of Neutron-Irradiated Reactor Pressure Vessel Steel Dependent on Radiation Mechanisms," from the ANS Special Session on Correlations and Implications of Neutron Irradiation Embrittlement of Pressure Vessel Steels, Detroit, MI, June 12-16, 1983, Trans. Am. Nucl. Soc. 44, p. 229, 1983.

(Pe72) J. S. Perrin, J. W. Sheckherd and V. G. Scotti, Examination and Evaluation of Capsule F for the Connecticut Yankee Reactor Pressure Vessel Surveillance Program, NRC, Public Document Room, Washington, DC, March 30, 1972.

(Pe75) J. S. Perrin et al., Surry Unit No. 1 Pressure Vessel Irradiation Capsule Program: Examination and Analysis of Capsule T, Docket 50280-462, NRC, Public Document Room, Washington, DC, June 24, 1975.

(Pe75a) J. S. Perrin et al., Surry Unit No. 2 Pressure Vessel Irradiation Capsule Program: Examination and Analysis of Capsule X, NRC, Public Document Room, Washington, DC, September 2, 1975.

(Pe75b) J. S. Perrin et al., Point Beach Unit No. 2 Pressure Vessel Surveillance Program: Evaluation of Capsule V, NRC, Public Document Room, Washington, DC, June 10, 1975.

(Pe78) J. S. Perrin et al., Zion Nuclear Plant Reactor Pressure Vessel Surveillance Program: Unit No. 1 Capsule T and Unit No. 2 Capsule U, BCL-585-4, Battelle Memorial Institute, Columbus Laboratories, Columbus, OH, March 1978.

(Pe79) G. P. Pells and D. C. Phillips, "Radiation Damage of α-Al_2O_3 in the HVEM: I. Temperature Dependence of the Displacement Threshold," J. Nucl. Mater. 80, p. 207, 1979.

(Pe79a) G. P. Pells and D. C. Phillips, "Radiation Damage of α-Al_2O_3 in the HVEM: II. Radiation Damage at High Temperature and High Dose," J. Nucl. Mater. 80, p. 215, 1979.

(Pe79b) J. S. Perrin et al., Palisades Nuclear Plant Reactor Pressure Vessel Surveillance Program: Capsule A-240, BCL-585-12, Battelle Memorial Institute, Columbus Laboratories, Columbus, OH, March 13, 1979.

(Pe80) J. S. Perrin et al., Maine Yankee Nuclear Plant Reactor Pressure Vessel Surveillance Program: Capsule 263, BCL-585-21, Battelle Memorial Institute, Columbus Laboratories, Columbus, OH, December 21, 1980.

(Pe82) G. P. Pells, A. J. Fudge, M. J. Murphy and M. Wilkins, "An Investigation into the Use of Sapphire as a Fast Neutron Damage Monitor," Proc. of the 4th ASTM-EURATOM Symposium on Reactor Dosimetry, Gaithersburg, MD, March 22-26, 1982, NUREG/CP-0029, NRC, Washington, DC, Vol. 1, pp. 331-344, July 1982.

(Pe84) J. S. Perrin, R. A. Wullaert, G. R. Odette and M. P. Lombroso, Physically Based Regression Correlations of Embrittlement Data from Reactor PV Surveillance Programs, EPRI NP-3319, Electric Power Research Institute, Palo Alto, CA, January 1984.

(Pr83) C. C. Preston, R. Gold, J. P. McNeece, J. H. Roberts and F. H. Ruddy, "Progress in Automated Scanning Electron Microscopy for Track Counting," Nucl. Tracks 7, pp. 53-61, 1983.

(Ra79) P. N. Randall, "Regulatory Aspects of Radiation Embrittlement of Reactor Vessel Steels," Proc. of an IAEA Specialists' Meeting on Irradiation Embrittlement, Thermal Annealing, and Surveillance of Reactor Pressure Vessels, Vienna, Austria, February 26 - March 1, 1979, IWG-RRPC-79/2, December 1979.

(Ra81b) P. N. Randall, "The Status of Trend Curves and Surveillance Results in USNRC Regulatory Activities," Proc. of an IAEA Specialists' Meeting, Vienna, Austria, October 20, 1981.

(Ra82a) P. N. Randall, "Status of Regulatory Demands in the U.S. on the Application of Pressure Vessel Dosimetry," Proc. of the 4th ASTM-EURATOM Symposium on Reactor Dosimetry, Gaithersburg, MD, March 22-26, 1982, NUREG/CP-0029, NRC, Washington, DC, Vol. 2, pp. 1011-1022, July 1982.

(Ra83) P. N. Randall, "NRC Perspective of Safety and Licensing Issues Regarding Reactor Vessel Steel Embrittlement," from the ANS Special Session on Correlations and Implications of Neutron Irradiation Embrittlement of Pressure Vessel Steels, Detroit, MI, June 12-16, 1983, Trans. Am. Nucl. Soc. 44, p. 220, 1983.

(Re77) Regulatory Guide 1.99, Effects of Residual Elements on Predicted Radiation Damage to Reactor Vessel Materials, Rev. 1, NRC, Washington, DC, April 1977.

(Rh79) W. A. Rhoades, D. B. Simpson, R. L. Childs and W. W. Engle, The DOT-IV Two-Dimensional Discrete Ordinates Transport Code with Space-Dependent Mesh and Quadrature, ORNL/TM-6529, Oak Ridge National Laboratory, Oak Ridge, TN, 1979.

(Ro82) R. W. Roussin et al., VITAMIN-C: 171 Neutron, 36 Gamma-Ray Group Cross Sections in AMPX and CCCC Interface Formats for Fusion and LMFBR Neutronics, ORNL/RSIC-37, Radiation Shielding Information Center, Oak Ridge, TN, 1982.

(Ro82a) G. C. Robinson, "Small-Scale Clad Effects Study," Proc. of the 10th WRSR Information Meeting, Gaithersburg, MD, Octo- ber 12-15, 1982, NUREG/CP-0041, Vol. 4, NRC, Washington, DC, pp. 272-281, January 1983.

(Ro83) J. H. Roberts, F. H. Ruddy, J. P. McNeece and R. Gold, "Automatic Scanning of Solid-State Track Recorders: Calibration," Nucl. Tracks 7, pp. 47-52, 1983.

(Sc80) W. Schneider, Ed., "CAPRICE 79: Correlation Accuracy in Pressure Vessel Steel as Reactor Component Investigation of Change of Material Properties with Exposure Data," Proc. of the IAEA Technical Committee Meeting, Jülich, Federal Republic of Germany, Jul-CONF-37, International Atomic Energy Agency, Vienna, Austria, May 1980.

(Sc83) F. A. Schmittroth and E. P. Lippincott, "Adjusted Cross Sections in Neutron Spectrum Unfolding," Trans. Am. Nucl. Soc., p. 606, November 1983.

(Se69) C. Z. Serpan Jr and W. N. McElroy, Damage Function Analysis of Neutron Energy and Spectrum Effects Upon the Radiation Embrittlement of Steels, NRL 6925, Naval Research Laboratory, Washington, DC, July 1969.

(Se71) C. Z. Serpan Jr, "Reliability of Fluence-Embrittlement Projections for Pressure Vessel Surveillance Analysis," Nucl. Technol. 12, pp. 108-118, September 1971.

(Se72) C. Z. Serpan Jr, Ed., Proc. of the IAEA Specialists' Meeting on Radiation Damage Units for Ferritic and Stainless Steels, Seattle, WA, October 31 - November 1, 1972, Unnumbered IAEA Report, International Atomic Energy Agency, Vienna, Austria, 1972.

(Se72a) C. Z. Serpan Jr and W. N. McElroy, "Elevated-Temperature Damage Functions for Neutron Embrittlement in Pressure Vessel Steels," Nucl. Technol. 13, February 1972.

(Se73b) C. Z. Serpan Jr, "Damage Function Analysis of Neutron-Induced Embrittlement in A302-B Steel at 550°F (288°C)," Effects of Radiation on Substructure and Mechanical Properties of Metals and Alloys, ASTM STP 529, American Society for Testing and Materials, Philadelphia, PA, pp. 92-106, 1973.

(Se75a) C. Z. Serpan Jr, "Engineering Damage Cross Sections for Neutron Embrittlement of A302B Pressure Vessel Steel," Nucl. Eng. Design 33, pp. 19-29, 1975.

(Si68) M. G. Silk, Iteractive Unfolding of Compton Spectra, AERE-R-5653, Atomic Energy Research Establishment, Harwell, UK, 1968.

(Si69) M. G. Silk, "Energy Spectrum of the Gamma Radiation in the DAPHINE Core," J. Nucl. Energy 23, p. 308, 1969.

(Si81) R. L. Simons, "Re-evaluation of Dosimetry for 19 PWR Surveillance Capsules - II," LWR-PV-SDIP Quarterly Progress Report, October 1980 - December 1980, NUREG/CR-1241, Vol. 4, HEDL-TME 80-6, Hanford Engineering Development Laboratory, Richland, WA, pp. HEDL-3 - HEDL-8, November 1981.

(Si82a) R. L. Simons et al., "Re-evaluation of the Dosimetry for Reactor Pressure Vessel Surveillance Capsules," Proc. of the 4th ASTM-EURATOM Symposium on Reactor Dosimetry, Gaithersburg, MD, March 22-26, 1982, NUREG/CP-0029, NRC, Washington, DC, Vol. 2, pp. 903-916, July 1982.

(St79) L. E. Steele, "Review of the IAEA Specialists' Meeting," Proc. of IAEA Specialist's Meeting on Irradiation Embrittlement, Thermal Annealing and Surveillance of Reactor Pressure Vessels, Vienna, Austria, February 26 - March 1, 1979, IWG-RRPC-79/2, International Atomic Energy Agency, December 1979.

(St80) J. Strosnider and C. Monseprate, with Appendix Prepared by L. D. Kenworthy and C. D. Tether, MATSURV -- Computerized Reactor Pressure Vessel Materials Information System, NUREG-0688, NRC, Washington, DC, October 1980.

(St80a) L. E. Steele, "Review of IAEA Specialists' Meeting on Irradiation Embrittlement, Thermal Annealing and Surveillance of Reactor Vessels," Proc. of the 3rd ASTM-EURATOM Symposium on Reactor Dosimetry, Ispra, Italy, October 1-5, 1979, EUR 6813, Commission of the European Communities, Vol. I, pp. 476-481, 1980.

(St82a) F. W. Stallmann, Curve Fitting and Uncertainty Analysis of Charpy Impact Data, NUREG/CR-2408, NRC, Washington, DC, 1982.

(St82b) F. W. Stallmann, "LSL - A Logarithmic Least Squares Adjustment Method," Proc. of the 4th ASTM-EURATOM Symposium on Reactor Dosimetry, Gaithersburg, MD, March 22-26, 1982, NUREG/CP-0029, NRC, Washington, DC, Vol. 2, pp. 1123-1128, July 1982.

(St82c) F. W. Stallmann, "Uncertainties in the Estimation of Radiation Damage Parameters," Proc. of the 4th ASTM-ERATOM Syumposium on Reactor Dosimetry, Gaithersburg, MD, March 22-26, 1982, NUREG/CP-0029, NRC, Washington, DC, Vol. 2, pp. 1155-1163, July 1982.

(St82d) F. W. Stallmann, "Evaluation and Uncertainty Estimates of Charpy Impact Data," Proc. of the 4th ASTM-EURATOM Symposium on Reactor Dosimetry, Gaithersburg, MD, March 22-26, 1982, NUREG/CP-0029, NRC, Washington, DC, Vol. 2, pp. 855-859, July 1982.

(St82e) F. W. Stallmann, "Pressure Vessel Benchmark Facility to Study Fracture Toughness of Irradiated Pressure Vessel Materials (BSR-HSST)," LWR-PV-SDIP Quarterly Progress Report, April 1982 - June 1982, NUREG/CR-2805, Vol. 2, HEDL-TME 82-19, Hanford Engineering Development Laboratory, Richland, WA, p. ORNL-17, December 1982.

(St83) F. W. Stallmann, C. A. Baldwin and F. B. K. Kam, Neutron Spectral Characterization of the 4th Nuclear Regulatory Commission Heavy Section Steel Technology 1T-CT Irradiation Experiment: Dosimetry and Uncertainty Analysis, NUREG/CR-3333, ORNL/TM-8789, Oak Ridge National Laboratory, Oak Ridge, TN, July 1983.

(St83a) L. E. Steele, Ed., Status of USA Nuclear Reactor Pressure Vessel Surveillance for Radiation Effects, ASTM STP 784, American Society for Testing and Materials, Philadelphia, PA, January 1983.

(St83b) L. E. Steele, Ed., Radiation Embrittlement and Surveillance of Nuclear Reactor Pressure Vessels: An International Study, ASTM STP 819, American Society for Testing and Materials, Philadelphia, PA, November 1983.

(St84) F. W. Stallmann, Determination of Damage Exposure Parameter Values in the PSF Metallurgical Irradiation Experiment, ORNL/TM-9166, Oak Ridge National Laboratory, Oak Ridge, TN, 1984.

(Ta82) S. W. Tagert et al., Structural Mechanics Program: Progress in 1981, EPRI NP-2705-SR, Electric Power Research Institute, Palo Alto, CA, October 1982.

(To82) H. Tourwé and G. Minsart, "Surveillance Capsule Perturbation Studies in the PSF 4/12 Configuration," Proc. of the 4th ASTM- EURATOM Symposium on Reactor Dosimetry, Gaithersburg, MD, March 22-26, 1982, NUREG/CR-0029, NRC, Washington, DC, Vol. 1, pp. 471-480, July 1982.

(To82a) H. Tourwé et al., "Interlaboratory Comparison of Fluence Neutron Dosimeters in the Frame of the PSF Start-Up Measurement Programme," Proc. of the 4th ASTM-EURATOM Symposium on Reactor Dosimetry, Gaithersburg, MD, March 22-26, 1982, NUREG/CP-0029, Vol. 1, pp. 159-168, NRC, Washington, DC, July 1982.

(Ul75) G. Ullrich and B. Bürgisser, Nachbestrahlungsuntersuchungen an NOK-Reaktordruckgefäss Material der Kernkraftwerke Beznau II/1, Kapsel V, PB-ME-75/01, Nordostschweizerische Kraftwerke AG (NOK), Baden, Switzerland, October 1975.

(Ul80) G. Ullrich, B. Bürgisser and F. Hegedüs, Nachbestrahlungsuntersuchungen an NOK-Reaktordruckgefäss Material der Kernkraftwerke Beznau II/2, Kapsel R, PB-ME-80/5, Nordostschweizerische Kraftwerke AG (NOK), Baden, Switzerland, April 1980.

(Va81) J. D. Varsik, "Evaluation of Irradiation Response of Reactor Pressure Vessel Materials," Semi-Annual Progress Report No. 3, July - December 1980, EPRI RP-1553-1, TR-MCM-110, Combustion Engineering Inc., Windsor, CT, 1981.

(Va82) J. D. Varsik, S. M. Schloss and J. M. Koziol, Evaluation of Irradiation Response of Reactor Pressure Vessel Materials, EPRI NP-2720, Electric Power Research Institute, Palo Alto, CA, 1982.

(Va83) J. D. Varsik, "An Empirical Evaluation of a Transition Temperature Shift in LWR-PV-SDIP Steels," from the ANS Special Session on Correlations and Implications of Neutron Irradiation Embrittlement of Pressure Vessel Steels, Detroit, MI, June 12-16, 1983, Trans. Am. Nucl. Soc. 44, p. 223, 1983.

(Ve80) V. V. Verbinski, C. G. Cassapakis, W. K. Hagen and G. L. Simmons, "Photointerference Corrections in Neutron Dosimetry for Reactor Pressure Vessel Lifetime Studies," Nucl. Sci. & Eng. 75, p. 159, 1980.

(Wh83) G. D. Whitman and R. W. McCulloch, "Pressurized-Thermal-Shock Experiments," Proc. of the 10th WRSR Information Meeting, Gaithersburg, MD, October 12-15, 1982, NUREG/CP-0041, NRC, Washington, DC, Vol. 4, pp. 262-271, January 1983.

(Wi83) M. L. Williams et al., "Validation of Neutron Transport Calculations in Benchmark Facilities for Improved Damage Fluence Predictions," Proc. of the 11th WRSR Information Meeting, Gaithersburg, MD, October 24-28, 1983, NUREG/CP-0048, Vol. 1-6, NRC, Washington, DC.

(Wo83) S. Wood et al., "Microstructural and Microchemical Characterization of Irradiated Pressure Vessel Steels," from the ANS Special Session on Correlations and Implications of Neutron Irradiation Embrittlement of Pressure Vessel Steels, Detroit, MI, June 12-16, 1983, Trans. Am. Nucl. Soc. 44, p. 228, 1983.

(Wu75) R. A. Wullaert and J. W. Shuckherd, Evaluation of the First Maine Yankee Accelerated Surveillance Capsule, CR75-317, Effects Technology, Inc., Goleta Heights, CA, August 15, 1975.

(Ya67) S. E. Yanichko, Connecticut Yankee Reactor Vessel Radiation Surveillance Program, WCAP-7036, Westinghouse Electric Corp., Pittsburgh, PA, April 1967.

(Ya73) S. E. Yanichko et al., Analysis of Capsule S from Carolina Power and Light Company, H. B. Robinson Unit No. 2 Reactor Vessel Radiation Surveillance Program, WCAP-8249, Westinghouse Electric Corp., Pittsburgh, PA, December 18, 1973.

(Ya74) S. E. Yanichko, T. R. Mager and S. Kang, Analysis of Capsule R from the Rochester Gas and Electric Corporation, R. E. Ginna Unit No. 1 Reactor Vessel Radiation Surveillance Program, WCAP-8421, Westinghouse Electric Corp., Pittsburgh, PA, November 1974.

(Ya75) S. E. Yanichko, J. H. Phillips and S. L. Anderson, Analysis of Capsule T from the Florida Power and Light Company, Turkey Point Unit No. 3 Reactor Vessel Radiation Surveillance Program, WCAP-8631, Westinghouse Electric Corp., Pittsburgh, PA, December 1975.

(Ya76) S. E. Yanichko and S. L. Anderson, Analysis of Capsule S from the Wisconsin Electric Power Company and Wisconsin-Michigan Power Company, Point Beach Nuclear Plant Unit No. 1 Reactor Vessel Radiation Surveillance Program, WCAP-8739, Westinghouse Electric Corp., Pittsburgh, PA, 1976.

(Ya77) S. E. Yanichko, S. L. Anderson and K. V. Scott, Analysis of Capsule V from the Wisconsin Public Service Corporation, Kewaunee Nuclear Plant Reactor Vessel Radiation Surveillance Program, WCAP-8908, Westinghouse Electric Corp., Pittsburgh, PA, January 1977.

(Ya78) S. E. Yanichko and S. L. Anderson, Analysis of Capsule R from the Wisconsin Electric Power Company, Point Beach Nuclear Plant Unit No. 1 Reactor Vessel Radiation Surveillance Program, WCAP-9357, Westinghouse Electric Corp., Pittsburgh, PA, August 1978.

(Ya79) S. E. Yanichko, S. L. Anderson and W. T. Kaiser, Analysis of Capsule F from the Southern California Edison Company, San Onofre Reactor Vessel Radiation Surveillance Program, WCAP-9520, Westinghouse Electric Corp., Pittsburgh, PA, May 1979.

(Ya79a) S. E. Yanichko et al., Analysis of Capsule R from the Wisconsin Electric Power Company, Point Beach Nuclear Plant Unit No. 2 Reactor Vessel Radiation Surveillance Program, WCAP-9635, Westinghouse Electric Corp., Pittsburgh, PA, December 1975.

(Ya80) S. E. Yanichko et al., Analysis of Capsule T from the Salem Unit 1 Reactor Vessel Surveillance Program, WCAP-9678, Westinghouse Electric Corp., Pittsburgh, PA, February 1980.

(Ya81) S. E. Yanichko, S. L. Anderson and W. T. Kaiser, Analysis of Capsule V from Northern States Power Company, Prairie Island Unit No. 2 Reactor Vessel Radiation Surveillance Program, WCAP-9877, Westinghouse Electric Corp., Pittsburgh, PA, March 1981.

(Ya81a) S. E. Yanichko et al., Analysis of Capsule U from the Commonwealth Edison Company, Zion Nuclear Plant Unit No. 1 Reactor Vessel Radiation Surveillance Program, WCAP-9890, Westinghouse Electric Corp., Pittsburgh, PA, March 1981.

(Ya81b) S. E. Yanichko et al., Analysis of the Maine Yankee Reactor Vessel Second Accelerated Surveillance Capsule, WCAP-9875, Westinghouse Electric Corp., Pittsburgh, PA, March 1981.

(Ya81c) S. E. Yanichko et al., Analysis of the Third Capsule from the Commonwealth Edison Company, Quad-Cities Unit 1 Nuclear Plant Reactor Vessel Radiation Surveillance Program, WCAP-9920, Westinghouse Electric Corp., Pittsburgh, PA, August 1981.

(Ya82) S. E. Yanichko et al., Analysis of the Fourth Capsule from the Commonwealth Edison Company, Dresden Unit 3 Nuclear Plant Reactor Vessel Radiation Surveillance Program, WCAP-10030, Westinghouse Electric Corporation, Pittsburgh, PA, January 1982.

(Ya82a) S. E. Yanichko et al., Analysis of the Third Capsule from the Commonwealth Edison Company, Quad Cities Unit 2 Nuclear Plant Reactor Vessel Radiation Surveillance Program, WCAP-10064, Westinghouse Electric Corporation, Pittsburgh, PA, April 1982.

DISTRIBUTION

R5

DOE-HQ/Office of Converter
Reactor Deployment
Nuclear Regulation & Safety Division
NE-12
Washington, DC 20545

JD Griffith, Deputy Director

DOE-HQ/Office of Breeder
Technology Projects (8)
NE-53
Washington, DC 20545

H. Alter, Asst Director, Safety
PB Hemmig, Asst Director,
Reactor Physics Technology
JW Lewellen, Manager,
Core Analysis Technology
DK Magnus, Director,
Fuels & Core Materials
WA Nelson, Director, Office of
Breeder Technology Projects
RJ Neuhold, Director,
Safety & Physics
CM Purdy, Asst Director,
Materials & Structures Tech
A. Van Echo, Manager, Metallurgy,
Absorbers & Standards

DOE-RL/AME
Breeder Technology Division
Technology Development Branch
P.O. Box 550, FED/242
Richland, WA 99352

KR Absher, Chief

Arizona State University (2)
College of Eng & Appl Sciences
Tempe, AZ 85287

JW McKlveen
B. Stewart

Argonne National Laboratory (2)
9700 South Cass Avenue
Argonne, IL 60439

RJ Armani
RR Heinrich, Bldg 316

Babcock & Wilcox Co.
Lynchburg Research Center (4)
P.O. Box 1260
Lynchburg, VA 24505

RH Lewis AA Lowe Jr
LB Gross CL Whitmarsh

Battelle
Pacific Northwest Laboratory
P.O. Box 999
Richland, WA 99352

EP Simonen

Battelle Memorial Institute
505 King Avenue
Columbus, OH 43201

MP Manahan

Bechtel Power Corporation
15740 Shady Grove Road
Gaithersburg, MD 20760

WC Hopkins

Brookhaven National Laboratory (3)
National Neutron Cross Section Center
Upton, Long Island, NY 11973

JF Carew BA Magurno
S. Pearlstein, Bldg T-197

Burns & Roe, Inc.
633 Industrial Avenue
Paramus, NJ 07672

J. Celnik

DISTRIBUTION (Cont'd)

Carolina Power & Light Co.
P.O. Box 1551
Raleigh, SC 27602

SP Grant

Centre d'Etude de l'Energie Nucléaire
Studiecentrum voor Kernenergie (7)
Boeretang 200
B-2400 Mol, Belgium

J. Debrue
G. DeLeeuw
S. DeLeeuw
PJ D'hondt
A. Fabry
G. Minsart
Ph. Van Asbroeck

Combustion Engineering Inc. (5)
1000 Prospect Hill Road
Windsor, CT 06095

ST Byrne
GP Cavanaugh
JJ Koziol
RG Shimko
D. Stephen

Comitato Nazional per Energia Nucléare
Centro di Studi Nucleari della Casaccia
Casella Postale 2400
Santa Maria di Galeria
I-00060 Rome, Italy

U. Farinelli

Commissariat a l'Energie Atomique
Centre d'Etudes Nucleaires de Saclay (6)
Boite Postale 2
91190 Gif-sur-Yvette, France

AA Alberman
C. Buchalet (Framatome)
JM Cerles
JP Genthon
P. Mas (Grenoble)
P. Petrequin

Commonwealth Edison
P.O. Box 767
Chicago, IL 60690

E. Steeve

EG&G Idaho, Inc. (3)
P.O. Box 1625
Idaho Falls, ID 83415

RC Greenwood
Y. Harker
JW Rogers

EG&G Ortec, Inc.
100 Midland Road
Oak Ridge, TN 37830

WH Zimmer

Electric Power Research Institute (7)
3412 Hillview Avenue
P.O. Box 10412
Palo Alto, CA 94304

TU Marston
O. Ozer
T. Passell
AD Rossin
R. Shaw
K. Stahlkopf
JJ Taylor

Energieonderzoek Centrum Nederland
Westerdionweg 3
NL-1755 ZG, Petten, The Netherlands

WL Zijp

Engineering Services Associates
3320 Bailey
Buffalo, NY 14215

M. Haas

EURATOM
Joint Research Center Ispra (2)
I-21020 Ispra, Varese, Italy

R. Dierckx
H. Rief

DISTRIBUTION (Cont'd)

Fracture Control Corporation
5951 Encina Road, No. 105
Goleta, CA 93117

P. McConnell

Fracture Control Corporation
2041 Willowick Drive
Columbus, OH 43229

JS Perrin

GE/Vallecitos Nuclear Center
P.O. Box 460
Pleasanton, CA 94566

GC Martin

IKE-Stuttgart (2)
Pfaffenwaldring 31
Postfach 801140
D-7000 Stuttgart 80 (Vaihingen),
Federal Republic of Germany

G. Hehn
G. Prillinger

International Atomic Energy Agency (2)
Wagramerstrasse 5
Postfach 100
A-1400 Vienna, Austria

A. Sinev
JJ Schmidt

IRT Corporation (3)
P.O. Box 80817
San Diego, CA 92183

NA Lurie WE Selph
C. Preskitt

Italian Atomic Power Authority
National Electric Energy Agency (2)
Viale Regina Margherita 137
Rome, Italy

M. Galliani
F. Remondino

Japan Atomic Energy Research Institute (2)
Tokai-mura, Naka-gun
Ibaraki-ken, Japan

S. Mizazono
K. Sakurai

Kernforschungsanlage Jülich GmbH (3)
Postfach 1913
D-517 Jülich 1,
Federal Republic of Germany

D. Pachur L. Weise
W. Schneider

Kraftwerk Union Aktiengesellschaft (3)
Postfach 3220
D-8520 Erlangen,
Federal Republic of Germany

A. Gerscha C. Leitz
J. Koban

Los Alamos National Laboratory (2)
P.O. Box 1663
Los Alamos, NM 87545

GE Hansen, Group N-2
L. Stewart

Maine Yankee Atomic Power Co.
Edison Drive
Augusta, MA 04336

HF Jones Jr

DISTRIBUTION (Cont'd)

Materials Engineering Associates
111 Mel-Mara Drive
Oxen Hill, MD 20021

JR Hawthorne

Max-Planck-Institüt
für Plasma Physik
The NET Team
D-8046 Garching bei München,
Federal Republic of Germany

DR Harries, Technology

National Bureau of Standards
Center of Radiation Research (6)
Washington, DC 20234

RS Caswell
CM Eisenhauer
DM Gilliam
JA Grundl
G. Lamaze
ED McGarry

Naval Research Laboratory
Engineering Materials Division
Thermostructural Materials Branch
Code 6390
Washington, DC 20375

LE Steele

Nuclear Regulatory Commission (17)
Office of Nuclear Regulatory Research
Division of Engineering Technology
Materials Engineering Branch
NL-5650
Washington, DC 20555

Chief
Public Doc Rm (3)
M. Bolotski
M. Dunenseld
R. Gamble
W. Hazelton
KG Hoge
RE Johnson
L. Lois
S. Pawlicki
PN Randall
CZ Serpan
D. Sieno
A. Taboada
M. Vagin

Oak Ridge National Laboratory (8)
P.O. Box X
Oak Ridge, TN 37830

CA Baldwin
RG Berggren
FBK Kam
AL Lotts
RE Maerker
LS Miller
R. Nanstad
FW Stallmann

Radiation Research Associates (2)
3550 Hulen Street
Fort Worth, TX 76107

RM Rubin
MB Wells

Rockwell International
Energy Systems Group (2)
P.O. Box 309
Canoga Park, CA 91304

H. Farrar IV
BM Oliver

Rolls-Royce & Associates Ltd. (4)
P.O. Box 31
Derby DE2 8BJ, UK

M. Austin
P. Burch
AF Thomas
TJ Williams

S.A. Cockerill-Ougree
Recherches et Developments
Division de la Construction Mecanique
B-4100 Seraing, Belgium

J. Widart

Science Applications Inc. (3)
P.O. Box 2325
La Jolla, CA 92037

W. Hagan
GL Simmons
VV Verbinski

DISTRIBUTION (Cont'd)

Ship Research Institute
Tokai Branch Office
Tokai-mura, Naka-gun
Ibaraki-ken, Japan

K. Takeuchi

Southwest Research Institute
8500 Calebra Road
P.O. Box 28510
San Antonio, TX 78284

EB Norris

Swiss Federal Institute
for Reactor Research
CH-5303 Würenlingen, Switzerland

F. Hegedus

United Kingdom Atomic Energy Authority
Atomic Energy Research Establishment (2)
Harwell, Oxon OX11 ORA, UK

LM Davies
AJ Fudge

United Kingdom Atomic Energy Authority
Atomic Energy Establishment (3)
Winfrith, Dorchester, Dorset, UK

J. Askew AK McCracken
J. Butler

University of Arkansas (2)
Dept of Mechanical Engineering
Fayetteville, AR 72701

CO Cogburn
L. West

University of California
at Santa Barbara (2)
Dept of Chem & Nucl Engineering
Santa Barbara, CA 93106

G. Lucas
GR Odette

Univ of London Reactor Center
Silwood Park, Sunnyhill
Ascot, Berkshire SL5 7PY, UK

JA Mason

University of Tokyo (2)
Dept of Nuclear Engineering
7-3-1, Hongo
Bunkyo-ku, Tokyo, 113 Japan

M. Nakazawa
J. Sekiguchi

Westinghouse
Nuclear Energy Systems (4)
P.O. Box 355
Pittsburgh, PA 15230

SL Anderson RC Shank
TR Mager SE Yanichko

Westinghouse
Research and Development Center
1310 Beulah Road
Pittsburgh, PA 15235

JA Spitznagel

University of Missouri (2)
at Rolla
Dept of Nucl Engineering
Building C
Rolla, MO 65401

DR Edwards
N. Tsoulfanidis

DISTRIBUTION

HEDL (46)
c/o Document Processing Supervisor
P.O. Box 1970, W/C-123
Richland, WA 99352

HJ Anderson	W/C-28	JP McNeece	W/A-56
RA Bennett	W/D-3	JE Nolan	W/B-65
LD Blackburn	W/A-40	RE Peterson	W/B-66
DG Doran	W/A-57	CC Preston	W/C-39
EA Evans	W/C-23	JH Roberts	W/C-39
DS Gelles	W/A-64	FH Ruddy	W/C-39
R. Gold	W/C-39	JM Ruggles	W/C-33
GL Guthrie	W/A-40	RE Schenter	W/A-58
BR Hayward	W/C-44	FA Schmittroth	W/A-58
LA James	W/A-40	WF Sheely	W/C-44
LS Kellogg	W/C-39	FR Shober	W/E-3
NE Kenny	W/C-115	RL Simons	W/A-57
RL Knecht	W/A-40	HH Yoshikawa	W/C-44
JJ Laidler	W/B-107	Program Files (10)	W/C-39
EP Lippincott (2)	W/C-39	Central Files (3)	W/C-110
WY Matsumoto	W/C-33	Publ Services	W/C-115
WN McElroy (2)	W/C-39		

NRC FORM 335 (7-77) U.S. NUCLEAR REGULATORY COMMISSION

BIBLIOGRAPHIC DATA SHEET

1. REPORT NUMBER *(Assigned by DDC)*
NUREG/CR-3391 VOL. 3
HEDL-TME 83-23

4. TITLE AND SUBTITLE *(Add Volume No., if appropriate)*
LWR Pressure Vessel Surveillance Dosimetry Improvement Program
1983 Annual Report- (October 1, 1982-September 30,1983).

2. *(Leave blank)*

3. RECIPIENT'S ACCESSION NO.

7. AUTHOR(S)
W.M. McElroy, F.B.K. Kam, J.A. Grundl, E.D. McGarry,A.Fabry

5. DATE REPORT COMPLETED
MONTH: December YEAR: 1983

9. PERFORMING ORGANIZATION NAME AND MAILING ADDRESS *(Include Zip Code)*
Hanford Engineering Development Laboratory
P.O. Box 1970
Richland, WA 99352

DATE REPORT ISSUED
MONTH: June YEAR: 1984

6. *(Leave blank)*

8. *(Leave blank)*

12. SPONSORING ORGANIZATION NAME AND MAILING ADDRESS *(Include Zip Code)*
Division of Engineering Technology
Office of Nuclear Regulatory Research
US Nuclear Regulatory Commission
Washington, DC 20555

10. PROJECT/TASK/WORK UNIT NO.

11. CONTRACT NO.
B5988

13. TYPE OF REPORT
Annual Progress Report

PERIOD COVERED *(Inclusive dates)*
October 1, 1982 - September 30, 1983

15. SUPPLEMENTARY NOTES

14. *(Leave blank)*

16. ABSTRACT *(200 words or less)*

The Light Water Reactor Pressure Vessel Surveillance Dosimetry Improvement Program (LWR-PV-SDIP) has been established by NRC to improve, test, verify, and standardize the physics-dosimetry-metallurgy, damage correlation, and the associated reactor analysis methods, procedures and data used to predict the integrated effect of neutron exposure to LWR pressure vessels and their support structures. A vigorous research effort attacking the same measurement and analysis problems exists worldwide, and strong cooperative links between the US NRC-supported activities at HEDL, ORNL, NBS, and MEA-ENSA and those supported by CEN/SCK (Mol, Belgium), EPRI (Palo Alto, USA), KFA (Jülich, Germany), and several UK laboratories have been extended to a number of other countries and laboratories. These cooperative links are strengthened by the active membership of the scientific staff from many participating countries and laboratories in the ASTM E10 Committee on Nuclear Technology and Applications. Several subcommittees of ASTM E10 are responsible for the preparation of LWR surveillance standards.

17. KEY WORDS AND DOCUMENT ANALYSIS

17a. DESCRIPTORS

17b. IDENTIFIERS/OPEN-ENDED TERMS

18. AVAILABILITY STATEMENT
Unlimited

19. SECURITY CLASS *(This report)*
Unclassified

21. NO. OF PAGES

20. SECURITY CLASS *(This page)*
Unclassified

22. PRICE
$

NRC FORM 335 (7-77)